UNIVERSIDAD COMPLUTENSE DE MADRID

FACULTAD DE CIENCIAS MATEMÁTICAS

TESIS DOCTORAL

Moving frames in Lorentzian manifolds R1,3 and their symmetry generators

MEMORIA PARA OPTAR AL GRADO DE DOCTOR

PRESENTADA POR

Robert Monjo Agut

Director

Rutwig Campoamor-Stursberg

Madrid

Universidad Complutense de Madrid

Facultad de Ciencias Matemáticas

TESIS DOCTORAL

Moving frames in Lorentzian manifolds $\mathbb{R}^{1,3}$ and their symmetry generators

Referencias móviles en variedades Lorentzianas $\mathbb{R}^{1,3}$ y sus generadores de simetría

Memoria para optar al grado de doctor presentada por

Robert Monjo Agut

Director/a/es:

Rutwig Campoamor-Stursberg

Universidad Complutense de Madrid

Facultad de Ciencias Matemáticas
Programa de Doctorado en Investigación Matemática

TESIS DOCTORAL

Moving frames in Lorentzian manifolds $\mathbb{R}^{1,3}$ and their symmetry generators

Referencias móviles en variedades Lorentzianas $\mathbb{R}^{1,3}$ y sus generadores de simetría

Memoria para optar al grado de doctor presentada por

Robert Monjo Agut

Director/a/es:

Rutwig Campoamor-Stursberg

Acknowledgements

This thesis has been developed in the Department of Algebra, Geometry and Topology of the Complutense University of Madrid between 2020 and 2023, and it is mainly based on the results of four papers:

- [Monjo and Campoamor-Stursberg 2020]: Monjo R, Campoamor-Stursberg R 2020 Lagrangian density and local symmetries of inhomogeneous hyperconical universes. *Class. Quantum Grav.* **37** 205015. `https://doi.org/10.1088/1361-6382/abadaf`

- [Monjo and Campoamor-Stursberg 2023]: Monjo R, Campoamor-Stursberg R 2023 Geometric perspective for explaining Hubble tension: theoretical and observational aspects. *Class. Quantum Grav.* **40**, 195006. `https://doi.org/10.1088/1361-6382/aceacc`

- [Monjo 2023]: Monjo R 2023 Galaxy rotation curve in hyperconical universes: a natural relativistic MOND. *Class. Quantum Grav.* **40**, 235002. `https://doi.org/10.1088/10.1088/1361-6382/ad0422`

- [Monjo et al. 2024]: Monjo R., Rodríguez-Abella Á, Campoamor-Stursberg R 2024 From coloured gravity to electromagnetism. *Class. Quantum Grav.* **CQG-110751** (under review). arXiv: `https://arxiv.org/abs/1012.4730`

However, other two previous papers were elaborated during earlier scientific training in mathematical physics, as master's theses of the master's degrees in Theoretical physics (Faculty of Physics) and Advanced Mathematics (Faculty of Mathematical Sciences); so they were partially considered here:

- [Monjo 2017]: Monjo R 2017 Study of the observational compatibility of an inhomogeneous cosmology with linear expansion according to SNe Ia. *Phys. Rev. D* **96** 103505. `https://doi.org/10.1103/PhysRevD.96.103505` arXiv:1710.09697

- [Monjo 2018]: Monjo R 2018 Geometric interpretation of the dark energy from projected hyperconical universes. *Phys. Rev. D* **98** 043508 (LS16206D). `https://doi.org/10.1103/PhysRevD.98.043508.arXiv:1808.09793`

The present work would not have been possible without the incalculable support of my director, Otto Rutwig Campoamor-Stursberg who, from the very beginning, trusted my career towards a doctorate in mathematics. His encouragement and technical advice have

been key in this Thesis. Additionally, it is very fair to appreciate all the great suggestions of my colleague Á. Rodríguez-Abella throughout the process, as well as to acknowledge the advice of professors Antonio L. Maroto and Luis J. Garay during the developing of the two early papers. Thanks also to all the reviewers and referees, especially professors M. Logares and Á. González-Prieto, as well as the external evaluators of my Thesis for their very valuable comments.

Of course, it is worth noting the unconditional support of all my family, and especially from Darío, who has always been by my side. We have learned a lot together about life.

Worth mentioning as a curiosity, the initial seed of this work was born over 20 years ago, in a talk with my bachelor's teacher on physics, Pep Martí (I.E.S. Tirant lo Blanc of Gandia, València). We were discussing on the amazing similarity between the Coulomb and the Newton's gravity laws, then I suggested to him the following relationship to be explored:

$$q \simeq \mathrm{i}\, m \sqrt{\frac{2\mathrm{G}}{\mathrm{k}}} \implies \mathrm{k}q^2 = -2\mathrm{G}m^2\,,$$

where i is the imaginary unity, q is the electric charge, m is the mass, G is the Newton's constant and k is the Coulomb constant. This equation is alike the Eq. 6.3.24 except for the '2' (red colour), which was missing in my original formulation. Furthermore, I found another 'easy equation' for cosmology by using a simple analogy with a bloating balloon:

$$H = \frac{1}{t}\,,$$

where H is the Hubble parameter and t is the age of the universe, as I shared with my friend Conrad a year later, at the beginning of the career. These two *toy equations*, emerged from simple intuition, have become a reality today, 20 years later. Due to life circumstances, it has had to take a long time until I was able to employ leisure to these issues. In fact, the first part of my career was oriented to other passion, *meteorology and climatology*, influenced by the typical *cut-off lows* that impact on my País Valencià. Consequently, I studied physics mixing lines of meteorology and theoretical physics, then choosing one of these passions to run the path to the first doctorate:

- Monjo R 2012 New probability models for precipitation: Application to Spain, and particularly to the Basque Country. PhD Thesis, Facultat de Física, Universitat de València, Spain. `https://doi.org/10.5281/zenodo.5810921`

Thanks to this, and especially to my first co-directors Vicente Caselles and Guillem Chust, I was able to develop my career as a climatologist, working and saving for years to pay for my latest studies.

Finally, I would like to thank all readers for their attention and interest in this subject, and for their patience in assimilating so many acronyms (see **Glossary** in page xiv). Please notice that we use natural units for the speed of the light ($c \equiv 1$) to put together spatial and temporal coordinates in our default spacetime.

Contents

Resumen

La geometrización es una forma natural de resolver algunos problemas de física, y podría ser clave para explicar las inconsistencias observadas recientemente en la dinámica espacio-temporal, tales como la llamada "tensión de Hubble" y las "galaxias tempranas imposibles". Para abordar el problema, esta Tesis propone una *técnica de incrustación dinámica* que construye variedades Lorentzianas $\mathbb{R}^{1,3} \subset \mathbb{R}^{1,4}_{flat}$ (espacio-tiempos) de manera natural, usando marcos de referencia con movimiento lineal y secciones espaciales homogéneas de curvatura espacial positiva ($k > 0$), nula ($k = 0$) o negativa ($k < 0$). La consistencia del enfoque se probó para tres escalas: (1) la cuatro-variedad Lorentziana incrustada, (2) objetos a gran escala y (3) campos de partículas. Los **principales resultados** son:

- **Variedad incrustada**. El análisis hamiltoniano (ADM) garantiza una dinámica consistente para el ($k = 1$)–hipercono $\mathcal{H}^4 \subset \mathbb{R}^{1,4}_{flat}$, mientras que la densidad lagrangiana de la *relatividad general* necesita extraer la curvatura escalar de fondo. Las referencias móviles conducen a una inhomogeneidad radial en la variedad, pero el valor de $k = 1$ produce un escalar de Ricci que es localmente equivalente al de la métrica FLRW estándar con sección espacial plana. El análisis de las propiedades de simetría indican que sólo los momentos angulares son simetrías globales. La inhomogeneidad radial rompe toda simetría local irrotacional a grandes distancias.
- **Objetos a gran escala**. Con proyecciones distorsionantes, la inhomogeneidad se asimila como una aceleración ficticia compatible con el modelo estándar, prediciendo los valores observados. Esta proyección también es un punto clave en la dinámica de objetos (por ejemplo, curvas de rotación de galaxias): La aceleración centrífuga presenta una pequeña contribución temporal en la dinámica a gran escala debido a la curvatura de la variedad, y la proyección distorsionante transfiere la aceleración ficticia a las curvas de rotación a escalas mayores, imitando a las borrascas.
- **Campos de partículas**. Para referencias móviles en partículas (p.e. espinores), esta Tesis explora pequeñas perturbaciones de la descomposición métrica relacionadas con la línea de Wilson y la métrica de Kaluza-Klein, pero en cuatro dimensiones. Las referencias son ahora matrices constituidas por generadores del álgebra de Lie $\mathfrak{su}(1,3)$. Bajo este marco de *color*, el electromagnetismo estándar se puede obtener como un caso abeliano particular. En términos generales, las referencias móviles perturban localmente la métrica plana η como $\eta \rightarrow \eta + u \otimes u$, donde u representa la velocidad en las tres escalas analizadas: la expansión del espacio-tiempo, las curvas de rotación de galaxias y la dinámica de partículas con sus generadores

de simetría.

Palabras clave: Variedades lorentzianas, incrustración dinámica, referencias móviles, simetrías

Abstract

Geometrization is a natural way to solve some physical issues, and could be key to explaining recent problems observed on spacetime dynamics, such as the so-called 'Hubble tension' and 'impossible early galaxies'. To face this challenge, the present Thesis proposes a *dynamical embedding technique* that builds Lorentzian manifolds $\mathbb{R}^{1,3} \subset \mathbb{R}^{1,4}_{flat}$ (spacetimes) in a natural manner by using linearly moving frames and homogeneous spatial sections of positive ($k > 0$), null ($k = 0$) or negative ($k < 0$) curvature. Self-consistency of the approach was proved at three scales: (1) The embedded Lorentzian four-manifold, (2) large-scale objects and (3) particle fields. **Main results** are the following:

- **Embedded manifold**. Hamiltonian (ADM) analysis only guarantees consistent dynamics for the ($k = 1$)–hypercone $\mathcal{H}^4 \subset \mathbb{R}^{1,4}_{flat}$, while Lagrangian density of *general relativity* needs subtracting the background scalar curvature. Moving frames lead to a fictitious radial inhomogeneity in the manifold, but the value of $k = 1$ displays a scalar curvature that, for every point, is equivalent to that of the standard flat-space FLRW metric. Results on symmetry properties show that only the angular momenta are global symmetries. The radial inhomogeneity breaks all the non-rotational local symmetries at large distances.
- **Large-scale objects**. A distorted projection is used to assimilate the inhomogeneity as a fictitious acceleration compatible with the standard model, predicting observed values. This projection is also a key point in object dynamics (e.g. galaxy rotation curves). Specifically, centrifugal acceleration presents a small time-like contribution at large-scale dynamics due to curvature of the manifold, and the distorted projection transfers the fictitious acceleration to the rotation curves at larger scales, imitating the extratropical cyclones.
- **Particle fields**. For particle moving frames (e.g. for spinors), we explore small perturbations of the metric decomposition related to the Wilson line and the Kaluza–Klein metric, but in four dimensions. Coordinates are now matrices consisting of generators of the $\mathfrak{su}(1,3)$ Lie algebra. Under this *coloured gravity* framework, standard electromagnetism is obtained as a particular abelian case. In general terms, moving frames locally perturb the flat metric η as follows: $\eta \to \eta + u \otimes u$, where u represent the velocity at the three scales analyzed: the manifold expansion, the galaxy rotation curves and the particle dynamics with their symmetry generators.

Keywords: Lorentzian manifolds, dynamical embedding, moving frames, symmetries

Glossary

ΛCDM	dark energy and cold dark matter
ΛLTB	dark energy in Lemâitre-Tolman-Bondi metric
ADM	Arnowitt-Deser-Misner
BAO	baryonic acoustic oscillation
BAO-Gal	baryonic acoustic oscillation - galaxy distribution
BTFR	baryonic Tully–Fisher relation
CC	cosmic chronometers
CMB	cosmic Microwave Background
CMD	cold dark matter
DE	dark energy
EFE	external field effects
ETG	extended teleparallel gauge
FLRW	Friedmann–Lemaître–Robertson–Walker
GR	general relativity
KΛCDM	curvature, dark energy and cold dark matter
LMC	Large Magellanic Cloud
LMC-CS	Large Magellanic Cloud - central star
LQG	loop quantum gravity
LTB	Lemâitre-Tolman-Bondi metric
Lyα	Lyman-alpha spectral absorption lines ("forest spectum"') in a quasar.
MDAR	mass-discrepancy acceleration relation
MOG	Moffat's modified gravtiy
MOND	modified Newtonian dynamics
OHD	observational Hubble parameter data
PL18	Planck Legacy 2018
PPN	parameterized post-Newtonian
QCD	quantum chromodynamics
QED	quantum electrodynamics
QSO	quasar - quasi stellar object
RMOND	relativistic MOND theory
SEP	strong equivalence principle

SH0ES	Supernovae H0 for Equation of State of DE
SNe	Supernovae
SPARC	Spitzer Photometry and Accurate Rotation Curves
SR	Special relativity
STEGR	symmetric teleparallel equivalent of general relativity
STVG	scalar–tensor–vector gravity
TEGR	teleparallel equivalent of general relativity
TeVeS	tensor–vector-scalar gravity
TRF	thermal recoil force
TRGB	Tip of the Red Giant Branch
TRP	thermal radiation pressure
WEP	weak equivalence principle
WMAP	Wilkinson Microwave Anisotropy Probe

Initial notes

Pseudo-Riemannian manifold

Some previous concepts are required to initiate or remind readers, fix notation, or facilitate reading itself. Firstly, we need to highlight one of the most important concepts in geometry, the **metric**, which generalizes the idea of measuring *tangential distances* or *lengths* over smooth objects, usually referred to manifolds or *hypersurfaces* embedded into other manifolds [Sharpe 1997]. From the Greek word $\mu\epsilon\tau\rho\sigma\nu/metron$ (meaning "*measure*"), the *metric* informs how to calculate distances; that is, in a similar way to how the *first fundamental form* does for regular *surfaces* defined into the Euclidean space $\mathbb{R}^3$, which aimed to describe our *world* (or *Earth*, from the Greek word "geo" in *geometry*)[1]. The notion of *metric* is closely linked to other abstract ideas: the Riemannian and pseudo-Riemannian (or semi-Riemannian) manifolds [O'Neill 1983], which are only distinguished in the signature (signs) of the diagonalized matricial representation of the *metric*, so these notions can be described in a compact way as "(pseudo-)Riemannian".

Definition 0.1 (**(pseudo-)Riemannian**)**.** A n-dimensional (pseudo-)Riemannian manifold is a *real differentiable manifold* $\mathscr{N} \subset \mathbb{R}^m$, with $m \geq n \in \mathbb{N}$, that generalizes the concept of Euclidean space so that, at each point $q \in \mathscr{N}$, there exists a tangent space $E_q := \mathrm{T}_q\mathscr{N}$ such that $E_q \cong \mathbb{R}^n$. Thus, for every open neighborhood $U_q \subset \mathbb{R}^m$ with $\hat{U}_q = U_q \cap \mathscr{N}$, it is possible to define a local **coordinate chart** $\{\hat{U}_q, \phi\}$ near q, with a parameterization $\phi : \mathbb{R}^n \to \hat{U}_q$ and a non-degenerate symmetric bilinear operation $g : \mathrm{T}_q\mathscr{N} \times \mathrm{T}_q\mathscr{N} \to \mathbb{R}$ so-called **(pseudo-)Riemannian metric**, which defines a **scalar product**. As for Euclidean affine space occurs, we will say that $q \in \mathscr{N}$ is a **point** of the manifold and $v \in \mathrm{T}_q\mathscr{N}$ is a "direction", a "tangential vector" o simply a **vector**.

Remark 0.1 (**Language abuse I, for points**)**.** Let $q \in \mathscr{N} \subset \mathbb{R}^m$ be any point of the manifold parameterized by $\phi : V_x \subset \mathbb{R}^n \to U_q \subset \mathbb{R}^m$ where $x = (x^1, \ldots, x^n) = \phi^{-1}(q) \in V_x$ are the so-called coordinates of q. The image of the parameterization can be noted as $q = \phi(x^1, \ldots, x^n) = (\phi^1(x^1, \ldots, x^n), \ldots, \phi^m(x^1, \ldots, x^n)) \in U_q$, but also as $q = (q^1, \ldots, q^m) \in U_q$. For simplicity, sometimes it is used that $q = q(x^1, \ldots, x^n) \in U_q$ to refer an implicit dependency of q with respect to the coordinates x^i, but the first q is a

[1] The idea of Euclidean space was introduced by ancient Greek mathematicians (s. IV BC) as an abstraction of our physical space by using the Euclid's Elements, that is a few very basic properties derived from our physical world.

m-dimensional (constant) point and the second q plays the role of the parameterization, $\phi : \mathbb{R}^n \to \mathscr{N} \subset \mathbb{R}^m$.

Remark 0.2 (**Language abuse II, for vectors**). Let $w \in \mathrm{T}_q\mathscr{N}$ be any tangent vector over $\mathscr{N}$ at q. This means that there exists a curve $\alpha : I \subset \mathbb{R} \to \mathscr{N}$ such that $\alpha(0) = q$ and $\alpha'(0) = w$. Moreover, another curve $\gamma : I \subset \mathbb{R} \to \mathbb{R}^n$ represents the coordinates of $\alpha = \phi \circ \gamma$ such that $\gamma'(0) = (x^{1\prime}(0), \ldots, x^{n\prime}(0)) = v \in \mathbb{R}^n$ and $\gamma(0) = (x^1(0), \ldots, x^n(0)) = p$ with $q = \phi(p)$. Therefore, $w = \alpha'(0) = \sum_{i=1}^n \partial_i\phi|_q \, x^{i\prime}(0) = \sum_i \partial_i\phi|_q \, v^i$. As for $\{x^i\}_{i=1}^n$, coordinates $\{v^i\}_{i=1}^n$ of the vector $v \in \mathbb{R}^n$ can be interpreted as n real parameters, or as a set of n specific real values that define any vector $v = \sum_{i=1}^n v^i e_i \in \mathbb{R}^n = (v^1, \ldots, v^n)_\varepsilon$, where $\varepsilon = \{e_i\}_{i=1}^n$ is the canonical basis of $\mathbb{R}^n$. Considering the basis $\beta = \{b_i := \partial_i\phi|_q = \partial\phi/\partial x^i|_q\}_{i=1}^n$, any vector $w \in \mathrm{T}_q\mathscr{N}$ can be expressed as $w = \sum_{i=1}^n v^i b_i = (v^1, \ldots, v^n)_\beta$, and therefore the components of w are the same that the components of $v = (v^1, \ldots, v^n)_\varepsilon$ but with different basis (ε or β). The language abuse for vectors $v \cong w$ is commonly applied by omitting these bases.

Therefore, the linear isomorphism ($\cong$) of each space $E_q := \mathrm{T}_q\mathscr{N}$ with the real hyperplane $\mathbb{R}^n$ provides $\mathscr{N}$ with the possibility of defining a **scalar product**, *inner product* or *dot product* $\langle \cdot | \cdot \rangle := g(\cdot, \cdot) \in \mathbb{R}$ in each tangent space $\mathrm{T}_q\mathscr{N}$, which in turn allows defining *measurements* such as angles, length of curves, d-volumes and curvature (intrinsic and extrinsic), as well as the exterior product and exterior derivative (over each tangent space).

In Riemannian spaces, the dot product is a **positive definite symmetric bilinear form** such that $\langle \cdot | \cdot \rangle : \mathbb{R}^n \times \mathbb{R}^n \to \mathbb{R}$. This implies that it can be represented by a non-degenerate symmetric matrix, but also with a tensor $g_q : \mathrm{T}_q\mathscr{N} \times \mathrm{T}_q\mathscr{N} \to \mathbb{R}$ at each point $q \in \mathscr{N}$. Thus, we can define our tensor field g of type $(0, 2)$, that is, 0-contravariant and 2-covariant (Table 2). For conveniently abbreviated notation, the quadratic norm is usually denoted by $||v||_g^2 := g(v, v)$. In contracst, for pseudo-Riemannian spaces, a (non-degenerate) metric can produce negative quadratic forms.

Definition 0.2 (**Embedding**). Let $\mathscr{N}$ and $\mathscr{M}$ be smooth manifolds and $\boldsymbol{\iota} : \mathscr{N} \to \mathscr{M}$ be a smooth map. Then, $\boldsymbol{\iota}$ is called an **immersion** if its derivative is everywhere injective. Moreover, an immersion is an **embedding** if it induces a homeomorphism of $\mathscr{N}$ onto its image $\boldsymbol{\iota}(\mathscr{N})$. The manifold $\mathscr{M}$, with $\dim(\mathscr{M}) \geq \dim(\mathscr{N})$, is so-called *ambient space* or *support space*. We will say that an embedding is minimal if $\dim(\mathscr{M})$ is the minimum possible (see for instance Nash 1956 and Sharpe 1997).

For instance, let $\boldsymbol{\iota} : \mathscr{N} \to \mathscr{M}$ be an embedding of $\mathscr{N}$ into a manifold $\mathscr{M} \cong \mathbb{R}^m$, with $\dim(\mathscr{M}) = m > n = \dim(\mathscr{N})$ and (pseudo-)Euclidean metric $\eta = \mathrm{diag}(\pm 1, \pm 1, \ldots, \pm 1)$[2]. Thus, the metric g of $\mathscr{N}$ is induced by the metric η of $\mathscr{M}$. The induced metric g is formally defined by $g := \boldsymbol{\iota}^*\eta$, which is the pullback ($*$) of η via the natural inclusion $\boldsymbol{\iota} : \mathscr{N} \to \mathbb{R}^m$. Using local coordinates $\phi : V_x \subset \mathbb{R}^n \to \mathscr{N} \subset \mathbb{R}^m$ at $x \in \mathbb{R}^n$ with

[2]We will say that η is a flat metric because the scalar curvature is zero according to the Riemann formalism.

$q = \phi(x) \in \mathscr{N} \subset \mathbb{R}^m$, the inclusion of $\mathscr{N} \cong (\mathbb{R}^n, g)$ in $\mathscr{M} \cong (\mathbb{R}^m, \eta)$ can be expressed by the same parameterization $\phi : \mathbb{R}^n \to \mathbb{R}^m$. Therefore, in this case, the inclusion is locally given by $\boldsymbol{\iota} = \phi$ and the induced metric is $(\boldsymbol{\iota}^*\eta)_x(u, v) = \eta_{\boldsymbol{\iota}(x)}\big(d\boldsymbol{\iota}_x(u), d\boldsymbol{\iota}_x(v)\big)$ for every pair $u, v \in \mathrm{T}_x\mathbb{R}^n$ where $d\boldsymbol{\iota}_x(e_j)$ is the pushforward of e_j by $\boldsymbol{\iota}$. For example, using the canonical base $\varepsilon = \{e_i\}_{i=1}^n$ of $\mathrm{T}_x\mathbb{R}^n$, it is $(\boldsymbol{\iota}^*\eta)_x(e_i, e_j) = \eta_{\boldsymbol{\iota}(x)}\big(d\boldsymbol{\iota}_x(e_i), d\boldsymbol{\iota}_x(e_j)\big)$.

In other words, the metric g of $\mathscr{N}$ can be expressed in local coordinates from any parameterization $\phi : V_x \subset \mathbb{R}^n \to \mathscr{N} \subset \mathscr{M}$, by using the basis $\beta = \{b_i := \partial_i\phi|_q\}_{i=1}^n$ of $\mathrm{T}_q\mathscr{N}$ that provides its components $g_{ij} := g_{(x)}(e_i, e_j) = \eta_{(q)}(b_i, b_j)$, where $b_i = \partial_i\phi|_q = d\phi_x(e_i)$.

Notice that the n-dimensional canonical basis formed by the n fields $\{e_i := \partial_i := \partial/\partial x^i\}_{i=1}^n$ is diffeomorphic to the basis β of the tangent space $\mathrm{T}_q\mathscr{N}$. At the same time, we can define the canonical **dual basis** as a set of contravariant 1-form elements $\{e^i := dx^i\}_{i=1}^n$ such that $\langle dx^i|\partial_j\rangle = \delta^i_j$, where $\delta^i_j = 1$ if $i = j$, and $\delta^i_j = 0$ if $i \neq j$. With this, the metric is written in local coordinates as follows:

$$g = \sum_{i,j=1}^{n} g_{ij} dx^i \otimes dx^j \quad \underbrace{:\equiv}_{\substack{\textit{summation}\\ \textit{convention}}} \quad g_{ij} dx^i \otimes dx^j$$

On the other hand, the *cometric* or inverse of the metric acts as $g_q^{-1} : \mathrm{T}^*_q\mathscr{N} \times \mathrm{T}^*_q\mathscr{N} \to \mathbb{R}$, where $*$ represents the dual space. Informally, it is often said that vectors "eat" covectors and vice versa. Thus, a tensor $T^{j_1\ldots j_r}_{i_1\ldots i_s} \in \mathscr{T}^{r,s}$ of type (r, s) (r-contravariant and s-covariant) is a **multilinear application** that "eats" r covectors and s vectors to obtain a scalar in $\mathbb{R}$.

Therefore, given a vector $v \in \mathrm{T}_q\mathscr{N}$, a quadratic **norm** can be defined by $||v||^2_g = \langle v|g|v\rangle = g(v, v) = g_{ij}v^iv^j =: v_jv^i$, thanks to the *non-degenerate symmetric bilinear form* or metric, g. Since it is symmetric, g is diagonalizable by some orthonormal basis, obtaining a number of positive elements γ and negative elements ν on the diagonal, which add up to $n = \gamma + \nu$ because it is "no degenerate". The well-known Sylvester rigidity theorem () ensures that, in a metric vector space, the numbers γ and ν of the metric do not depend on the orthonormal basis chosen [Sylvester 1852].

Definition 0.3 (**Metric signature**)**.** When the metric is **positive definite** ($\gamma = n$), it is known as **Riemannian metric**, while in any other case it is a **pseudo-Riemannian metric**, which gives the same name to its variety. In any case, we will say that the **signature of the metric is the pair** (γ, ν) formed by the number of positive elements γ and negative elements ν of its diagonalized matrix (eigenvalues). Therefore, a semi-Riemannian manifold of signature (γ, ν) and metric g can be compactly represented by $\mathbb{R}^{\gamma,\nu}_g \equiv (\mathbb{R}^{\gamma,\nu}, g)$.

[3]Subscript on the basis and superscript on the coordinates denote (contravariant) vectorial elements, while superscript on the basis and subscript on the coordinates denote (covariant) dual elements

[4]Notice that "exterior product" is different that "outer product", which is defined by the matricial product of two vectors, $u \otimes v = u\,v^{\mathrm{T}} = |u\rangle\langle v|$

[5]As an example of matricial representation for *outer products*, let us consider the ordinary Euclidean space with $n = 3$, in which it is isomorphic to the well-known *cross product*.

Table 2: Comparison of notations and representations of some geometric objects defined over a n-dimensional manifold $\mathscr{N}$, over its tangent space $\mathrm{T}_{q}\mathscr{N} \cong \mathbb{R}^n$ at a point $q \in \mathscr{N}$, over its dual or for tensorial products.

Object	**bra-ket**	**matrix**	**tensorial**[3]
Vector (contravariant with respect to the base)	$\|v\rangle \in V := \mathrm{T}_{q}\mathscr{N}$ $\|v\rangle = v^i \|e_i\rangle$	$v = \begin{pmatrix} v^1 \\ ... \\ v^n \end{pmatrix} = v^1 \begin{pmatrix} 1 \\ 0 \\ ... \end{pmatrix} + ...$ $\vec{v} = v^1\vec{i} + v^2\vec{j} + ...$ $\vec{v} = v^1\vec{e}_1 + v^2\vec{e}_2 + ...$	$v = v^i e_i = v^i \partial_i \in \mathscr{T}^{1,0}$
Covector, dual vector, linear form, differential form	$\langle u\| \in V^* := \mathrm{T}^*_{q}\mathscr{N}$ $\langle u\| = u_i \langle e^i\|$ $\langle v^*\| = \|v\rangle^T g$	$u = \begin{pmatrix} u_1 & ... & u_n \end{pmatrix}.$ $v^* = \begin{pmatrix} v_1 & ... & v_n \end{pmatrix}$	$u = u_i e^i = u_i dx^i \in \mathscr{T}^{0,1}$ $df = f_i dx^i$ (1-form)
Metric (non-degenerate) $g(\partial_i, \partial_j) =: g_{ij}$	$g = g_{ij} \|e^i\rangle \langle e^j\|$	$g = \begin{pmatrix} g_{11} & ... & g_{1n} \\ ... & ... & ... \\ g_{1n} & ... & g_{nn} \end{pmatrix}$	$g = g_{ij} e^i \otimes e^j \in \mathscr{T}^{0,2}$ $ds^2 = g_{ij} dx^i \otimes dx^j$ (bilinear form)
Cometric (non-degenerate) $g^*(dx^i, dx^j) =: g^{ij}$	$g^* = g^{ij} \|e_i\rangle \langle e_j\|$	$g^{-1} = \dfrac{1}{\det g} \mathrm{adj}(g^T)$	$g^{-1} = g^{ij} e_i \otimes e_j \in \mathscr{T}^{2,0}$ $g^* = g^{ij} \partial_i \otimes \partial_j$
2-form symplectic	$\omega = \omega_{ij} \langle e^j\| \wedge \langle e^j\|$	$\begin{pmatrix} 0 & ... & -\omega_{1n} \\ ... & ... & ... \\ \omega_{1n} & ... & 0 \end{pmatrix}$	$\omega = \omega_{ij} e^i \wedge e^j$ $\in \Lambda^2(\mathrm{T}^*_{q}\mathscr{N})$
Scalar or inner product (from bilinear form g) $g : \mathbb{R}^n \times \mathbb{R}^n \to \mathbb{R}$	$\langle u\|v\rangle = \langle u\|I_n\|v\rangle$ $\langle u^*\|v\rangle = \langle u\|g\|v\rangle$	$\begin{pmatrix} u_1 & ... & u_n \end{pmatrix} g \begin{pmatrix} v^1 \\ ... \\ v^n \end{pmatrix}$	$g(u^*, v) = g_{ij} u^i v^j$ $e^i(e_j) = e_j(e^i) = \delta^i_j$
Exterior[4] product or wedge product	$\|u\rangle \wedge \|v\rangle \in$ $\Lambda^2(\mathrm{T}_{q}\mathscr{N})$	$\vec{u} \times \vec{v} = \begin{vmatrix} \vec{i} & \vec{j} & \vec{k} \\ u^1 & u^2 & u^3 \\ v^1 & v^2 & v^3 \end{vmatrix}$ $\in \mathbb{R}^3 \cong \Lambda^2(\mathrm{T}_{q}\mathbb{R}^3)$ [5]	$e_i \wedge e_j = e_{ij} = -e_{ji}$ $\in \Lambda^2(\mathrm{T}_{q}\mathscr{N})$
Quadratic form or quadratic norm	$\langle v^*\|v\rangle = \langle v\|g\|v\rangle$ $= \|\|v\|\|^2_g$	$\begin{pmatrix} v_1 & ... & v_n \end{pmatrix} g \begin{pmatrix} v^1 \\ ... \\ v^n \end{pmatrix}$	$g(v, v) = g^*(v^*, v^*)$

Definition 0.4. (Isometric transformation) Let $(\mathbb{R}^n, \eta)$ be a smooth manifold with (pseudo-)Euclidean metric η, and let $f : \mathbb{R}^n \to \mathbb{R}^n$ be an endomorphism. We will say that f is an *isometric transformation* if $||x - y||_\eta = ||f(x) - f(y)||_\eta = ||f(x - y)||_\eta$ is satisfied for every pair $x, y \in \mathbb{R}^n$; that is, f is a linear operator that **preserves the distances between points** in $\mathbb{R}^n$.

For a (pseudo-)Riemannian manifold $(\mathscr{N}, g)$, if a tangent hyperplane $\mathrm{T}_x\mathscr{N} \cong (\mathbb{R}^n, \eta)$ at $x \in \mathscr{N}$ has non-degenerate (pseudo-)Euclidean metric η, the isometric transformation $f : \mathrm{T}_x\mathscr{N} \to \mathrm{T}_x\mathscr{N}$ also preserves the length $||v||_\eta = ||f(v)||_\eta$ for every vector $v \in \mathrm{T}_x\mathscr{N}$. Moreover, there exists a matrix representation of $\tilde{v} = f(v)$ given by $|\tilde{v}\rangle = \tilde{v}^j |e_j\rangle = (f^1(v^1, \ldots, v^n), \ldots, f^n(v^1, \ldots, v^n)) = a\,|v\rangle = (|e_j\rangle\, a_i^j\, \langle e^i|)v^i\,|e_i\rangle$, where $a = |e_j\rangle\, a_i^j\, \langle e^i| \in \mathcal{M}_n(\mathbb{R})$ is the matrix representation in the canonical basis of $\mathbb{R}^n$.

Lorentzian manifold

As it is advanced in the title, this Thesis is focused on Lorentzian manifolds, which are fundamental in mathematical physics. For instance, the most elementary case is the four-dimensional Minkowskian spacetime $\mathbb{R}^{1,3}_\eta \equiv (\mathbb{R}^{1,3}, \eta)$ with $\eta = \mathrm{diag}(1, -1, -1, -1)$ or similar, used in special relativity (it corresponds to a signature (1,3) in Def. 0.3). The following notes define concepts such as *Lorentzian metric*, *time coordinate*, *spacetime event*, *timelike direction*, *spacelike direction* and *spacelike hypersurface*.

Definition 0.5 (**Lorentzian metric**)**.** A Lorentzian metric is a particular case of pseudo-Riemmannian metric, of dimension n and signature (γ, ν), in which $\gamma = 1 < n$ or $\nu = 1 < n$. For instance, the four-dimensional Minkowskian space used in special relativity is $\mathbb{R}^{1,3}_\eta \equiv (\mathbb{R}^{1,3}, \eta)$ with $\eta = \mathrm{diag}(1, -1, -1, -1)$, or $\mathbb{R}^{3,1}_\eta \equiv (\mathbb{R}^{3,1}, \eta)$ with $\eta = \mathrm{diag}(-1, 1, 1, 1)$. This Thesis only uses the signature $(1, 3)$ in four dimensions and $(1, 4)$ in five dimensions.

Let (U_q, x) be a local coordinate chart for a Lorentzian manifold $\mathscr{N} \ni q$ with parameterization $x : \mathbb{R}^n \to U_q \in \mathscr{N}$. Usually, local coordinates in $U_q \in \mathscr{N}$ are indexed between 0 and $n-1$, that is $x = (x^0, x^1, \ldots, x^{n-1})$, where the 0-coordinate is the one that has different sign with respect the rest of coordinates. This feature is commonly used to define a *time coordinate*, *timelike directions*, and by orthogonality, *spacelike directions*.

Remark 0.3 (**Time coordinate**)**.** We will say "time coordinate" or simply *time* (represented by t) to the coordinate that has different signature in the Lorentzian metric with respect the other coordinates, which will be regarded as "spatial coordinates". As usual, we will consider the *time* as the first coordinate (denoted by the label or index "0").

Definition 0.6 (**Spacetime event**)**.** Let $(\mathscr{N}, g)$ be a Lorentzian manifold (spacetime), any point $p \in \mathscr{N}$ is also known as position, location or **spacetime event**.

By convention, it is important to distinguish between *spacetime coordinates* and purely *spatial coordinates*, as well as between vectors and dual elements. Specifically, **Greek**

letters $(\alpha, \beta, \dots, \mu, \nu, \dots)$ are commonly used to denote spacetime (subscript or superscript), which range between 0 and 3. **Subscript** on the basis and **superscript** on the coordinates are used to denote (contravariant) vectorial elements, while superscript on the basis and subscript on the coordinates denote (covariant) dual elements. The **summation convention** is applied by default when a subscript or superscript appears on the right side of an equation but do not on the left side. For instance, dual elements u_μ can be directly obtained by contraction of the vector u^ν superscript with the 2-covariant metric components $g_{\mu\nu}$, that is $u_\mu = g_{\mu\nu}u^\nu$ to refer to $u_\mu = \sum_{\nu=0}^{3} g_{\mu\nu}u^\nu$. On the other hand, **Latin letters** can refer to purely spatial components $(i, j, k, l, m, \dots)$ like in the ADM formalism (Sec. 1.3.5.2), or anholonomic components $(a, b, c, d, e, \dots)$ used in tetrad formalism (Sec. 1.2.3).

Definition 0.7 (**Light cone**)**.** We will say that $\ell_p \subset \mathrm{T}_p\mathscr{N}$ is a **light cone** if it consists of all the null vectors $n \in \mathrm{T}_p\mathscr{N}$, that is $\ell_p := \{n \in \mathrm{T}_p\mathscr{N} \ : \quad \eta(n, n) = n_\mu n^\mu = 0\}$.

The light cone is a boundary to distinguish between *timelike* and *spacelike directions*, which is employed in physics to define *causality* between two spacetime events when both are within the same light cone (see for instance Galloway 2000).

Definition 0.8 (**Timelike direction**)**.** A non-null vector $v = (v^\mu)_{\mu=0}^3 \in \mathrm{T}_p\mathscr{N}$ is a **timelike direction** if $\eta(v, v) > 0$ if signature of η is $(1, 3)$, or $\eta(v, v) < 0$ if signature of η is $(3, 1)$. Geometrically, the collection of all timelike vectors v lie in the open subset of $\mathrm{T}_p\mathscr{N}$ formed by the interior of the light cone, which has two halves represented by two semi-axis: the *positive time direction* $(+1, 0, 0, 0) \in \mathrm{T}_p\mathscr{N}$ and the *negative time direction* $(-1, 0, 0, 0) \in \mathrm{T}_p\mathscr{N}$.

Definition 0.9 (**Spacelike direction**)**.** A no-null vector $v = (v^\mu)_{\mu=0}^3 \in \mathrm{T}_p\mathscr{N}$ is a **spacelike direction** if $\eta(v, v) < 0$ if signature of η is $(1, 3)$ and vice versa. Moreover, we will say that two points connected by v are **casually disconnected** since they are placed in the exterior of any light cone.

Definition 0.10 (**Spacelike hypersurface**)**.** A three-dimensional hypersurface $\Sigma_p \subset \mathscr{N}$ is **spacelike** if its normal vector is time-like. Under the viewpoint of dynamical systems, Σ_p is a set of events which are all pairwise causally disconnected (spacelike). Each event $x \in \Sigma_p$ of a spacelike hypersurface $\Sigma_p \subset \mathscr{N}$ is outside the light cone of any other $y \in \Sigma_q$, $q \neq p$.

Dynamical systems in Lorentzian manifolds

The signature of the Lorentzian metric allows us to define a *time domain* as well as a *foliation* (partitioning in leaves) and a *slicing* (partitioning in slices) of a Lorentzian manifold, which are very useful to characterize evolution of subsets over time. This is formally studied in *dynamical systems* theory. The following notes define these concepts in addition to *flow*, *trajectory*, *observation* and *embedding*,

Definition 0.11 (**Dynamical system**)**.** Let X be a non-empty set; for example, let us consider $X \subset \mathscr{N}$ be a subset of a Lorentzian manifold $\mathscr{N}$. A dynamical system is a triplet (T, X, φ), where T is a monoid (for instance the non-negative integers $\mathbb{N} \cup \{0\}$, or the semi-real numbers $\mathbb{R}_{\geq 0}$, with neutral element 0) and φ is a evolution function such that $\varphi : U \subset T \times X \to X$ and

$$\begin{aligned} \varphi(0, x) &= x \\ \varphi(t_2, \varphi(t_1, x)) &= \varphi(t_2 + t_1, x), \end{aligned}$$

for t_1, $t_2 + t_1 \in I(x) \subset T$ and $t_2 \in I(\varphi(t_1, x)) \subset T$, where $I(x) := \{t \in T : (t, x) \in U\}$ for any $x \in X$.

Remark 0.4 (**Time domain**)**.** The monoid T is also called "time domain" because it is the parameter domain of the evolution function φ.

Definition 0.12 (**Flow and trajectory**)**.** Let (T, X, φ) be a dynamical system. The function $\varphi_x : I(x) \subset T \to X$ with $\varphi_x(t) = \varphi(t, x) \in X$ is called the "**flow** through x" and its image (graph) $\gamma_x := \{\varphi(t, x) \ : \ t \in I(x) \subset T\}$ is called the orbit or "**trajectory** through x".

Some of the structures that may be of greatest interest in Lorentzian manifolds is the *foliation*, since it allows to design isomorphisms by using the definition of dynamical systems.

Definition 0.13 (**Foliation**)**.** Let $\mathscr{N}$ be a differentiable manifold of dimension n, for instance a Lorentzian manifold, a foliation is a relation of equivalence classes[6], formed by submanifolds injectively immersed in $\mathscr{N}$, connected and of dimension $p < n$ (the same for all) [Moerdijk and Mrčun 2003]. Moreover, let $\mathscr{F} := \{(U_i, \phi_i)\}_i$ be an atlas (chart collection, covering or partitioning) of $\mathscr{N}$ into differentiable submanifolds $\{U_i\}_i$ equipped with a family of homeomorphisms $\phi_i : \mathbb{R}^n \to U_i$. Then we will say that $\mathscr{F}$ is a **foliated atlas** if in the overlaps $U_i \cap U_j$ the change of coordinates $\phi_i^j := \phi_j^{-1} \circ \phi_i : \mathbb{R}^n \to \mathbb{R}^n$ is of the form

$$\phi_i^j(x) = \phi_i^j(x_{||}, x_\perp) = \Big(\phi_{i\,||}^{j}(x_{||}, x_\perp), \phi_{i\,\perp}^{j}(x_\perp), \Big)$$

where $x = (x_k)_{k=1}^n = (x_\parallel, x_\perp) \in \mathbb{R}^q$ with $x_{||} = (x_k)_{k=1}^p \in \mathbb{R}^p$ and $x_\perp = (x_k)_{k=p+1}^n \in \mathbb{R}^q$ with $q := n - p$. That is, the transformation of **the transverse part ($\perp$) only depends on itself** and vice versa. Therefore, given the "manifold product" $\mathbb{R}^n = \mathbb{R}^{p+q} = \mathbb{R}^p \times \mathbb{R}^q$,

[6]Let S be a nonempty set that splits up into non-overlapping nonempty subsets so-called *partitioning* of S. Moreover, let $\sim$ be an equivalence relation, that is a property that satisfy: (1) $x \sim x$ for all $x \in S$ (reflexive property); (2) if $x \sim y$, then $y \sim x$ (symmetric property); (3) if $x \sim y$ and $y \sim z$, then $x \sim z$ (transitive property); and (4) either $x \sim y$ or $x \nsim y$ is true. An **equivalence class** $[x]$ on $S \ni x$ is the subset of all elements of S that are equivalent to x, that is $[x] = \{y \in S : y \sim x\}$ [Maddox 2005].

whose structure is inherited in the open neighbors $U = U_{||} \times U_{\perp}$, we have:

$$\begin{aligned} \phi^j_{i\,||} : \mathbb{R}^p &\to \mathbb{R}^p \\ x &\mapsto x'_{||} \\ \phi^j_{i\,\perp} : \mathbb{R}^q &\to \mathbb{R}^q \\ x_{\perp} &\mapsto x'_{\perp} \end{aligned}$$

Definition 0.14 (**Spacelike embedding**)**.** Let Σ be a compact (oriented, connected) boundaryless n-manifold. The space of all spacelike smooth embeddings of Σ into a $(n+1)$-dimensional spacetime $\mathscr{M}$ with Lorentzian metric, denoted by $\mathrm{Emb}(\Sigma, \mathscr{M})$, will be called *spacelike embedding space*[7].

Let $\Sigma_{\mathfrak{t}} := \mathfrak{t}(\Sigma)$ be a Cauchy hypersurface for $\mathfrak{t} \in \mathrm{Emb}(\Sigma, \mathscr{M})$, and we will say that Σ is a *reference Cauchy hypersurface* [Gotay *et al.* 2004]. Moreover, the foliation of $\mathscr{M}$ in spacelike Cauchy hypersurfaces allows to define its *slicing*.

Definition 0.15 (**Infinitesimal slicing**)**.** An infinitesimal slicing of a spacetime $\mathscr{M}$ consists of a Cauchy surface $\Sigma_{\mathfrak{t}}$, $\mathfrak{t} \in \mathrm{Emb}(\Sigma, \mathscr{N})$, together with a spacetime vector field $\zeta\mathscr{M}$ along $\Sigma_{\mathfrak{t}}$ everywhere transverse to $\Sigma_{\mathfrak{t}}$, which defines a time direction.

For instance, let $\Sigma_{\mathfrak{t}} \subset \mathscr{M}$ be a fixed spacelike hypersurface and let $e_{\perp}$ denote the future-pointing timelike unit normal vector field on $\Sigma_{\mathfrak{t}}$. Then $(\Sigma_{\mathfrak{t}}, e_{\perp})$ is an infinitesimal slicing of $\mathscr{M}$. In coordinates $\{x^i\}_{i=0}^n$ referred to $\Sigma_{\mathfrak{t}}$, we can expand the time derivative as follows

$$\partial_0 := \frac{\partial}{\partial x^0} \;=\; l\, e_{\perp} + s^i \frac{\partial}{\partial x^i} \tag{0.1}$$

where l is a function on $\Sigma_{\mathfrak{t}}$ (the lapse) and $\mathfrak{s} = s^i \frac{\partial}{\partial x^i}$ is a vector field tangent to $\Sigma_{\mathfrak{t}}$ (the shift). In ADM formalism [Arnowitt *et al.* 2008,Deruelle *et al.* 2010], these lapse and shift functions play a key role. Due to this decomposition, the direction of the time derivative ∂_0 is usually taken as a representative of the infinitesimal slicing $(\Sigma_{\mathfrak{t}}, e_{\perp})$ under the ADM formalism.

Definition 0.16 (**Slicing**)**.** A slicing of an $(n+1)$-dimensional spacetime $\mathscr{M}$ consists of an n-dimensional manifold Σ, so-called reference Cauchy surface, and a diffeomorphism

$$\begin{aligned} \mathfrak{T}_{\mathscr{M}} : \Sigma \times \mathbb{R} &\to \mathscr{M} \\ (x, \lambda) &\mapsto \mathfrak{T}_{\mathscr{M}}(x, \lambda) = \mathfrak{t}_{\lambda}(x) \\ \Sigma \times \{\lambda\} &\mapsto \mathfrak{T}_{\mathscr{M}}(\Sigma \times \{\lambda\}) = \Sigma_{\lambda} \end{aligned}$$

where $\mathfrak{t}_{\lambda} : \Sigma \to \Sigma_{\lambda} \subset \mathscr{M}$ is an embedding defined by $\mathfrak{t}_{\lambda}(x) := \mathfrak{T}_{\mathscr{M}}(x, \lambda)$.

[7] That is, Σ has not any metric initially defined, but any embedding $\mathfrak{t} \in \mathrm{Emb}(\Sigma, \mathscr{N})$ defines a metric on Σ via the pullback.

The slicing parameter λ gives rise to a global notion of "time" on $\mathscr{M}$ which need not coincide with locally defined coordinate time, nor with proper time along the curves $\lambda \to \mathfrak{t}_{\mathscr{M}}(x,\lambda)$ [Gotay *et al.* 2004].

Definition 0.17 (**Global time**)**.** Let $(\Sigma, \mathfrak{T}_{\mathscr{M}})$ be a slicing of $\mathscr{M}$ with reference Cauchy hypersurface Σ and diffeomorphism $\mathfrak{T}_{\mathscr{M}}$ as defined above. We will define the global time time($\mathscr{M}$) of $\mathscr{M}$ as follows:

$$\text{time}(\mathscr{M}) := \{\lambda \in \mathbb{R} \ : \ \mathfrak{t}_\lambda \in \text{Diff}(\Sigma,\ \Sigma_\lambda \subset \mathscr{M})\} \cong \mathbb{R} \tag{0.2}$$

where $\Sigma_\lambda := \mathfrak{T}_{\mathscr{M}}(\Sigma \times \{\lambda\})$ with $\mathfrak{T}_{\mathscr{M}}(x,\lambda) = \mathfrak{t}_\lambda(x) \in \Sigma_\lambda$ for all $x \in \Sigma$.

In this Thesis, we consider that our Lorentzian manifold $\mathscr{N}$ and its ambient manifold $\mathscr{M}$ are foliated into families of Cauchy spacelike hypersurfaces $\{U_{||}\}$ and $\{V_{||}\}$, that is $\mathscr{N} = \cup U_{||}$ and $\mathscr{M} = \cup V_{||}$, which can be labeled by (traverse) timelike charts $\{U_\perp\}$ and $\{V_\perp\}$ respectively. Moreover, if $f : \mathscr{N} \to \mathscr{M}$ is an embedding, the foliation ensures that $f : \{U_{||}\} \to \{V_{||}\}$ and $f : \{U_\perp\} \to \{V_\perp\}$ are also embedding. In general, time($\mathscr{N}$) $\neq$ time($\mathscr{M}$), but it is possible to choose the same global time for some specific embeddings.

Example 0.1 (**Embedded time**)**.** Let $\mathscr{M} = \mathbb{R}^{1,n}_\eta$ be a $(n+1)$–dimensional Minkowskian spacetime that is, of course, a foliated ambient manifold for some n–dimensional Lorentzian manifold $\mathscr{N}$. Therefore, $1 = \dim(V_\perp) = \dim(U_\perp)$, and the traverse sets are equivalent by the homeomorphism f, that is $\{U_\perp\} \cong f(\{U_\perp\}) \cong \{V_\perp\}$. Then, we will say that time($\mathscr{N}$) $:= \{U_\perp\} = f^{-1}(\{V_\perp\})$ is the **embedded time** of $\mathscr{N}$ in $\mathscr{M}$, and the quotient defined by space($\mathscr{N}$) $:= \mathscr{N}/\text{time}(\mathscr{N}) = \Sigma$ is the *reference Cauchy surface* or **spatial representative** of $\mathscr{N}$.

The above example is not equivalent for all embeddings. For instance, it is not immediat for $\mathbb{R}^{2,n}_\eta$, because one can found that $2 = \dim(V_\perp) > \dim(U_\perp) = 1$.

Remark 0.5 (**Redundant time**)**.** Let $(T, \mathscr{N}, \varphi)$ be a dynamical system. If we consider the case with $T = \text{time}(\mathscr{N})$, a redundancy is found since time appears twice in (time($\mathscr{N}$), $\mathscr{N}$, φ). Therefore, our dynamical system can be simplified by $(\mathscr{N}, \varphi)$ with $\varphi : U \subset \mathscr{N} \to \mathscr{N}$.

Definition 0.18 (**Observation**)**.** Let γ_A and γ_B two different timelike trajectories[8] of a dynamical system. We will say that a spacetime event $A \in \gamma_A$ is observed in another event $B \in \gamma_B$ if there exists a light cone that intersects both events. Moreover, we will say that γ_A is an **object trajectory**, and γ_B is an "observer trajectory" or simply **observer**.

Using all the above geometrical concepts, one can define an approach to the concept of **universe**, under the framework of the *general relativity*.

Definition 0.19 (**Universe manifold**)**.** Let $\mathscr{N} \subset \mathscr{M}$ be a submanifold embedded in some pseudo-Riemann manifold. We will say that a $\mathscr{N}$ is a **universe manifold** if it is homeomorphic to a four-dimensional Lorentzian manifold.

[8] We will say that a trajectory or curve is timelike if all its derivarives are timelike directions.

Reference frames

From trihedrons to tetrads

Another key concept in this Thesis is the *reference frame* in four-Lorentizan manifolds $\mathscr{N}$, which moves along the flow φ_p of an observer whose trajectory γ_p passes through $p \in \mathscr{N}$. Reference frames are well-known in Euclidean spaces, in which they are so-called Frenet-Serret trihedrons.

Trihedrons in Euclidean spaces

Let $\gamma : I \subset \mathbb{R} \to \mathbb{R}^3$ be a parameterized ($t \mapsto \gamma(t)$) biregular curve in the ordinary Euclidean space $\mathbb{R}^3$ with domain in the open set $I \subset \mathbb{R}$, and let $s(t) = \int d\gamma = \int_0^t \dot{\gamma}(\xi) d\xi$ be its arc length, also known as proper distance. Since $1 = \langle \gamma'(s) | \gamma'(s) \rangle = ||\gamma'(s)||^2 = |\frac{d}{ds}\gamma(s)|^2$ and $0 = \frac{d}{ds}||\gamma'(s)||^2 = 2\langle \gamma''(s) | \gamma'(s) \rangle$, velocity[9] and acceleration generate a natural orthonormal frame of γ. This frame is given by the unitary velocity $e_1 := \gamma'(s)$, the normal acceleration $e_2 := e_1'(s)/||e_1'(s)||$ and the binormal vector $e_3 := (e_1 \times e_2)/||e_1 \times e_2||$. That Frenet-Serret trihedron $e(s) = (e_1(s), e_2(s), e_3(s))$ evolves in time s forming a **moving reference system** along the curve, according to the Frenet-Serret theorem.

Theorem 0.1. ***(Frenet-Serret theorem)***. *Let a parameterized curve γ with arc length s have non-zero curvature ($\kappa(s) \neq 0$), then the vectors of the trihedron satisfy the following system of equations*

$$e_1' = \kappa e_2, \qquad e_2' = -\kappa e_1 + \tau e_3, \qquad e_3' = -\tau e_2 \tag{0.3}$$

also known as ***Frenet equations*** *with torsion $\tau := -\langle e_2 | e_3' \rangle$.*

Note that each one of the three equations properties of Eq. 0.3 is actually a set of three equations given by the components of the vectors. The theorem is beautifully represented in a matrix form

$$e'(s) = \mathcal{K}(s) e(s) \qquad \Longrightarrow \qquad \begin{pmatrix} e_1' \\ e_2' \\ e_3' \end{pmatrix} = \underbrace{\begin{pmatrix} 0 & \kappa & 0 \\ -\kappa & 0 & \tau \\ 0 & -\tau & 0 \end{pmatrix}}_{\mathcal{K}} \begin{pmatrix} e_1 \\ e_2 \\ e_3 \end{pmatrix} \tag{0.4}$$

with $\mathcal{K} = -\mathcal{K}^T$. Despite the appearance of linearity, in general the system of equations is non-linear (representing any curve in $\mathbb{R}^3$), which depends on the functions of $\kappa(s)$ and $\tau(s)$.

Proof: The first property ($e_1' = \kappa e_2$) and the third property ($e_3' = -\tau e_2$) are immediate by the definition of the vector **normal** and the **torsion**, respectively. Therefore, we only have to prove the second property.

[9] It is a rate of change with respect a time parameter (usually represented by s or t). The term "velocity" is commonly used for vectors and "speed" for scalars. Sometimes, we use the notation dot ($\dot{}$) to abbreviate the expression for the time derivative, for instance $\dot{a} := \partial_t a = \partial a / \partial t$.

Since $1 = ||e_2(s)||^2$, we know that $0 = \langle e_2'(s)|e_2(s)\rangle$, so both $e_2'(s)$ must be a linear combination of e_1 and e_3, both orthogonal to e_2:

$$e_2'(s) = ae_1(s) + be_3(s)$$

The coefficients a and b are obtained by projecting $e_2'(s)$ in each case:

$$a = \langle e_1(s)|e_2'(s)\rangle\,, \qquad b = \langle e_3(s)|e_2'(s)\rangle$$

To see what values a and b take we need to use that

$$0 = \frac{d}{ds}\langle e_1|e_2\rangle = \underbrace{\langle e_1'|e_2\rangle}_{\langle \kappa e_2|e_2\rangle = \kappa} + \langle e_1|e_2'\rangle \quad \Longrightarrow \quad \langle e_1|e_2'\rangle = -\kappa \tag{0.5}$$

$$0 = \frac{d}{ds}\langle e_2|e_3\rangle = \langle e_2'|e_3\rangle + \underbrace{\langle e_2|e_3'\rangle}_{-\tau} \quad \Longrightarrow \quad \langle e_2'|e_3\rangle = \tau \tag{0.6}$$

Frames $e = (e_1, e_2, e_3)$ represent observers moving along a path under the perspective of external maps of coordinates; thus, a field of observers needs to be defined with more of one parameter. Specifically, all the possible observers living on a n-dimensional surface are represented by n parameters.

Remark 0.6. For a (parameterized) two-dimensional surface embedded into the ordinary three-dimensional ambient space, fame fields are easily defined by using the two parameters of the surface. For instance, let φ be a map from two arc-length coordinates $p = (s_1, s_2) \in \mathbb{R}^2$ to a sphere $S_1^2 \subset \mathbb{R}^3$ of unitary radius,

$$\begin{array}{rccl} \varphi: & \mathbb{R}^2 & \to & S_1^2 \subset \mathbb{R}^3 \\ & (s_1, s_2) & \mapsto & \varphi(s_1, s_2) = (\sin s_1 \sin s_2,\, \sin s_2 \cos s_2,\, \cos s_1)\,. \end{array} \tag{0.7}$$

The reference frame in any tangent space $\mathrm{T}_p S_1^2$ is given by $e = (e_1, e_2)$ with $e_\mu := \partial\varphi/\partial s_\mu =: \partial_\mu\varphi$, or simply $e_\mu \equiv \partial_\mu$ interpreted as a set of orthogonal directions, tangent to the manifold S_1^2 described by φ. Finally, its first fundamental form $\mathbf{g}(p)$ is:

$$\mathbf{g}(p) \;=\; (g_{\mu\nu}(p))_{\mu,\nu} \;=\; (e_\mu \cdot e_\nu)_{\mu,\nu} \;=\; \begin{pmatrix} \sin^2 s_1 & 0 \\ 0 & 1 \end{pmatrix}$$

where $\mu, \nu \in \{1, 2\}$.

Inertial frames in Lorentzian manifolds

Definition 0.20 (**Inertial frame**)**.** Let $\xi = (\xi^a)_{a=0}^3 = (\xi^0, \xi^1, \xi^2, \xi^3)$ be an arc-length parameterized curve $\xi : \mathbb{R} \to \mathrm{T}_p\mathscr{N} \cong \mathbb{R}_\eta^{1,3}$ with Minkowskian metric $\eta = (\eta_{ab})_{a,b=0}^3 := \mathrm{diag}(1, -1, -1, -1)$. Then, we will say that $\{d\xi^a\}_{a=0}^3$ induces an **inertial frame** if ξ is non-rotating, that is, $\ddot{\xi}(\lambda) := d^2\xi/d\tau^2(\lambda) = 0$ with arc length τ of ξ (e.g., $\xi(\tau) = (\tau, 0, 0, 0)$).

Let $\xi = (\xi^a)_{a=0}^3$ be an (observer) inertial frame over its own tangent spacetimes $\mathrm{T}_{\gamma_p}\mathscr{N}$ along $\gamma_p \subset \mathscr{N}$. Thus, the four velocity $\dot{\xi}$ is unitary because it is parameterized by *arc length*, also known as **proper time** τ. Of course, it is given by the squared line element $d\tau^2 = \eta_{ab}d\xi^a d\xi^b$ and, since ξ is **inertial**, the τ-based acceleration is zero:

$$0 = \frac{d^2\xi^a}{d\tau^2} = \frac{d}{d\tau}\left(\frac{d\xi^a}{d\tau}\right) = \frac{d}{d\tau}\left(\frac{\partial\xi^a}{\partial x^\mu}\frac{dx^\mu}{d\tau}\right) = \frac{\partial\xi^a}{\partial x^\mu}\frac{d^2x^\mu}{d\tau^2} + \frac{\partial^2\xi^a}{\partial x^\mu\partial x^\nu}\frac{dx^\mu}{d\tau}\frac{dx^\nu}{d\tau} \tag{0.8}$$

where x^μ are arbitrary coordinates (e.g. curvilinear, rotating or accelerated or whatever choosen) for the same object, referred with respect to another observer. Logically, the arc length[10] is independent of the coordinates selected, thus

$$d\tau^2 = \eta_{ab}d\xi^a d\xi^b = \eta_{ab}\frac{\partial\xi^a}{\partial x^\mu}\frac{\partial\xi^b}{\partial x^\nu}dx^\mu dx^\nu = g_{\mu\nu}dx^\mu dx^\nu \tag{0.9}$$

where $g_{\mu\nu}$ are the metric components in the new coordinates,

$$g_{\mu\nu} = g(\partial_\mu, \partial_\nu) = \eta_{ab}\frac{\partial\xi^a}{\partial x^\mu}\frac{\partial\xi^b}{\partial x^\nu} = \eta(e_\mu, e_\nu) =: e_\mu \cdot e_\nu \tag{0.10}$$

and $\partial_\mu := \partial/\partial x^\mu$ is the direction defined by the coordinate x^μ, and can be represented by $\partial_\mu = e_\mu = e_\mu{}^a\partial_a = \partial_\mu\xi^a\partial_a$ with components $e_\mu{}^a := \partial_\mu\xi^a = \partial\xi^a/\partial x^\mu$ in directions of $\partial_a := \partial/\partial\xi^a$. Now, multiplying Eq. 0.8 by $\partial x^\lambda/\partial\xi^a$ and using that $(\partial x^\lambda/\partial\xi^a)(\partial\xi^a/\partial x^\mu) = \delta^\lambda_\mu$, where δ^λ_μ is the Kronecker delta, the Eq. 0.8 is simplified as follows:

$$0 = \frac{d^2x^\mu}{d\tau^2} + \frac{\partial x^\lambda}{\partial\xi^a}\frac{\partial^2\xi^a}{\partial x^\mu\partial x^\nu}\frac{dx^\mu}{d\tau}\frac{dx^\nu}{d\tau} \tag{0.11}$$

Definition 0.21 (**Christoffel symbols**)**.** The set of the derivatives

$$\Gamma^\lambda_{\mu\nu} := \frac{\partial x^\lambda}{\partial\xi^a}\frac{\partial^2\xi^a}{\partial x^\mu\partial x^\nu} = \frac{\partial x^\lambda}{\partial\xi^a}\frac{\partial}{\partial x^\mu}\frac{\partial\xi^a}{\partial x^\nu} = e^\lambda{}_a\partial_\mu e_\nu{}^a\,, \tag{0.12}$$

is known as Christoffel symbols, where $e^\lambda{}_a := \partial x^\lambda/\partial\xi^a$ [Jost 2011].

Using the above definition, Eq. 0.11 is rewritten as follows:

$$0 = \frac{d^2x^\mu}{d\tau^2} + \Gamma^\lambda_{\mu\nu}\frac{dx^\mu}{d\tau}\frac{dx^\nu}{d\tau}\,, \tag{0.13}$$

which is commonly known as **geodesic equation**. Moreover, to found a relation between the inertial frames ξ^a and the coordinates of such object, it is enough to multiply $\Gamma^\lambda_{\mu\nu}$ of Eq. 0.12 by $\partial\xi^a/\partial x^\lambda$ and then

$$\Gamma^\lambda_{\mu\nu}\frac{\partial\xi^a}{\partial x^\lambda} = \frac{\partial^2\xi^a}{\partial x^\mu\partial x^\nu} \quad\Longrightarrow\quad \frac{\partial^2\xi^a}{\partial x^\mu\partial x^\nu} - \Gamma^\lambda_{\mu\nu}\frac{\partial\xi^a}{\partial x^\lambda} = 0 \tag{0.14}$$

[10]The squared arch length $d\tau^2 := g_{\mu\nu}dx^\mu dx^\nu$, typically used in physics, is equivalent to the metric $g = g_{\mu\nu}dx^\mu\otimes dx^\nu$ with symmetrized basis $dx^\mu dx^\nu := \frac{1}{2}(dx^\mu\otimes dx^\nu + dx^\nu\otimes dx^\mu)$ and $dx^\mu\otimes dx^\nu = dx^\nu\otimes dx^\mu$.

Tetrads in Lorentzian spacetimes

Let $(\mathscr{N}, \mathbf{g})$ be a four-dimensional Lorentzian manifold. **Greek index labels** are used to denote a (general) reference frame, i.e., a coordinate system on $\mathscr{N}$: $\{x^\mu\}_{\mu\in\{0,1,2,3\}}$. The associated partial derivatives, which form a basis of local sections of $\mathrm{T}\mathscr{N}$, are denoted by $\{\partial_\mu\}_\mu$, and the corresponding dual basis of the cotangent bundle is denoted by $\{dx^\mu\}_\mu$.

Every observer has a tetrad frame attached, that is, a (local) orthonormal parallelization of $\mathscr{N}$: $\{e_a\}_{a\in\{0,1,2,3\}} = \{e_0, e_1, e_2, e_3\}$. Note that we use **Latin index labels** for the tetrad frame. The tetrad components define a vierbein matrix, $(e^\mu{}_a)_{a,\mu\in\{0,1,2,3\}}$, where $e_a = e^\mu{}_a\partial_\mu$ for $a \in \{0,1,2,3\}$. Analogously, the dual basis is known as the cotetrad frame, $\{e^a = e_\mu{}^a dx^\mu\}_a$, with the dual relationship given by $e^a(e_b) = e_\mu{}^a e^\mu{}_b = \delta^a_b$. The Lorentzian and the Minkowski metrics are denoted by $\mathbf{g} = g_{\mu\nu}dx^\mu dx^\nu$ and $\eta = \eta_{\mu\nu}dx^\mu dx^\nu \equiv diag(1,-1,-1,-1)$, respectively. Hence, the changes of indexes are given by $e_\mu{}^a = g_{\mu\nu}\eta^{ab}e^\nu{}_b$ for $a, \mu \in \{0,1,2,3\}$, since $\eta_{ab} = \mathbf{g}(e_a, e_b) = e_a \cdot e_b$ by definition.

The commutation relations of the derivatives in arbitrary coordinates are zero, $[\partial_\mu, \partial_\nu] = 0$, but tetrads $e_a := e^\mu{}_a\partial_\mu$ may present non-zero commutation relations:

$$[e_a, e_b] = e^\mu{}_a e^\nu{}_b(\partial_\mu e_\nu{}^c - \partial_\nu e_\mu{}^c)e_c := \mathfrak{f}^c{}_{ab}e_c, \tag{0.15}$$

where the $\mathfrak{f}^c{}_{ab}$ are known as the anholonomic coefficients [Koiller *et al.* 2001, Ehlers *et al.* 2005].

The coordinate interval, which does not depend on references, is given by $\mathbf{d}\boldsymbol{\tau} := \partial_\mu dx^\mu = e_a e^a \in \mathrm{T}\mathscr{N} \otimes \mathrm{T}^*\mathscr{N}$. Similarly, the *distance* or *proper time* $d\tau$ is, therefore,

$$\begin{aligned} d\tau^2 := \mathbf{d}\boldsymbol{\tau} \cdot \mathbf{d}\boldsymbol{\tau} &:= (\partial_\mu \cdot \partial_\nu)dx^\mu dx^\nu = g_{\mu\nu}dx^\mu dx^\nu = g_{\mu\nu}e^\mu{}_a e^\nu{}_b\, e^a e^b \\ &= (e_a \cdot e_b)e^a e^b = \eta_{ab}e^a e^b = \eta_{ab}e_\mu{}^a e_\nu{}^b dx^\mu dx^\nu. \end{aligned}$$

Observe that, in the previous expression, the metric is only applied to the first factor of the tensor product.

Chapter 1

Introduction

1.1 From the motive to the motion

1.1.1 Geometrization of dynamics

1.1.1.1 The need for natural mathematical physics

Physics and mathematics have always lived in close contact[1] but, in a deeper way, physics could be interpreted as a particular case of geometry. To better understand this idea, let us take a brief look at history. During a talk, Carl Friedrich Gauss (1777–1855) influenced on Bernhard Riemann (1826–1866) in his well-known extension to n-dimensional manifolds of the Gauss's most notable finding that the curvature of a surface is an intrinsic property, laying therefore the first seeds in the foundations of the Einstein's general relativity.

Under the idea of **geometrodynamics**, William Kingdon Clifford (1845–1879) was strikingly prophetic when he conjectured that "forces and matter might be local irregularities in the curvature of space", even before his work on *Space-Theory of Matter* [Clifford 1876, Lanczos 1970]. However, Riemann and Clifford used only three spatial dimensions, so they could not lead to anything definitive without an adequate extension of the n-dimensional geometry to include the *time dimension*. This happened in the special relativity (SR) theory of Einstein 1905, later geometrized by Minkowski in 1907[2]. The solution for gravity, consistent with SR, raised a decade later, in 1915. According to the Einstein's general relativity (GR), any theory of *spaces curved by stress-energy* needs to be performed in a framework where space and time form a single four-dimensional entity [Einstein and Grossmann 1913]. Hermann Minkowski reformulated Einstein's relativity by employing his program of **geometrization of physics**: "whether gravitational

[1] For instance, the *Euclidean space* was the (ancient Greek) abstraction of our *physical space* by using Euclid's Elements; while *geometry* means "measurement of the world", referring to our physical space.

[2] Remember that, for every classical object, SR generalizes the application of the *Lorentz invariance*, which was only fundamental to transform the *Maxwell equations* of the electromagnetism, in contrast to the Galilean transformations of the *motion of bodies*. Nevertheless, the formal geometrical definition of the *spacetime entity* was performed by Minkowski in 1907, but published postmortem in 1915 [Minkowski 1915].

phenomena can be fully accounted for by non-Euclidean geometry of spacetime without the need to assume that gravitation is a physical interaction." Then, Eddington 1921 mentioned this possibility more explicitly: "gravitation as a separate agency becomes unnecessary."

The geometrization of classical physics or **classical geometrodynamics** was also a central axis of Misner and Wheeler 1957,Wheeler 1961, and Wheeler 1966, who stated that "classical physics can be described in terms of curved empty space, and nothing more". Wheeler introduced the notion of *geons*, gravitational wave packets confined to a compact region of spacetime and held together by the gravitational attraction of the (gravitational) field energy of the wave itself [Blum and Furlan 2022]. Wheeler was intrigued by the possibility that *geons* could affect test particles much like a massive object. This idea aimed to point the way to unify electrodynamics and general relativity. Aligned with this, it was deliberate the title of the Einstein's work "On the electrodynamics of moving bodies", and his later attempt to unify gravity and electromagmetism, also referred as *absolute (tele)parallelism* or *teleparallel gravity* [Einstein 1928,Sauer 2005]. Since he stated that 'the gravitational field can be found only through the discovery of a logically simple mathematical condition," Einstein tirelessly attempted the formulation of a unified field theory, for more than 30 years, by employing the same methods [van Dongen 2010].[3]

The formalism used in quantum electrodynamics is a more recent example of mathematical physics, as well as it was the case of the *weak* and *strong* nuclear interactions. Specifically, the so-called *gauge field theory* is based on unitary $\mathrm{U}(n)$ or special unitary $\mathrm{SU}(n)$ groups, or more generally in any compact and reductive Lie algebra (e.g. Yang-Mills theory). Under this framework, some behaviors of elementary particles can be described including their electroweak dynamics ($\mathrm{U}(1) \times \mathrm{SU}(2)$) and their quantum chromodynamics or strong force ($\mathrm{SU}(3)$) [Zinn-Justin 2019]. More generally, perhaps, all the dynamics of the nature might be expressed in terms of geometry and algebra. In fact, a remarkable segment of the theoretical physics community believes that all these dynamics are really just manifestations of a single basic unified gauge field (or *Ehresmann connection*) and can be manifest themselves in a quantum domain. A key notion may be the *connection*.

1.1.1.2 Connection/gauge theory in Lorentzian manifolds

A *connection* is a purely mathematical term (see Sec. 1.2) commonly used in both differential geometry and gauge theory to describe a reference transformation or *parallel transport* on a fiber bundle, that is a concept to identify, to contrast (gauge) or to connect fibers over nearby points. For instance, for tangent vector bundles defined on a given (pseudo-)Riemannian manifold, the (affine) Levi-Civita connection provides a standard manner to differentiate vector fields and, thus, it is also known as covariant derivative. This intrinsic geometrical perspective was fundamental in GR, as a generalization of the special relativity of Albert Einstein, who stated that Lorentz transformations (natural in

[3]Einstein believed he could find a unified theory of all the existing nature's forces by repeating his thought experiments. Historiography offers examples of both successful and unsuccessful non-empirical science [van Dongen 2021].

electromagnetism) should be valid for the whole nature.

As it is well known, GR produces *gravitomagnetic* effects and Maxwell's equations similar to the classical electromagnetism [Capozziello *et al.* 2009, Bakopoulos and Kanti 2014, Chatterjee *et al.* 2017, Adamek *et al.* 2020]. The awesome similitude between the firstly-discovered natural force (Newtonian gravity) and the later Coulomb electrostatics guided several physicists for centuries to explore an early unification. Quantizing gravity in a satisfactorily way (as required for all the unifications) is still missing, in spite of the remarkable contributions and links of (special and general) relativity to quantum electrodynamics, such as the reference-frame (Lorentz) transformations, the Dirac spinor[4] and the *teleparallel gravities* [Sahin2016, Schwartz 2023]. The Kaluza–Klein theory has been proposed in 1921-1926 as a candidate for a purely classical extension of GR to $(\mathbb{R}^{1,4}, \widetilde{g})$, with a metric $\widetilde{g}$, generalizing $(\mathbb{R}^{1,3}, g)$ as follows [Williams 2020]:

$$\widetilde{g}_{\mu\nu} \equiv g_{\mu\nu} + \phi^2 A_\mu A_\nu, \qquad \widetilde{g}_{5\nu} \equiv \widetilde{g}_{\nu 5} \equiv \phi^2 A_\nu, \qquad \widetilde{g}_{55} \equiv \phi^2, \tag{1.1.1}$$

where $A_\mu := g_{\mu\nu} A^\nu$ is the dual (covector) of the electromagnetic vector field A^μ, ϕ is a scalar field such that $\Box\phi = \frac{1}{4}\phi^3 F^{\alpha\beta} F_{\alpha\beta}$, $F_{\alpha\beta} := \partial_\alpha A_\beta - \partial_\beta A_\alpha$ and $\Box$ is the d'Alembert operator. The main achievement of the theory was to deduce, in a natural way, the free-field Maxwell equations and the electromagnetic stress-energy tensor to curve the spacetime. However, the gradient of ϕ leads to a dominating fifth component of the velocity, in contradiction to experience.

If the particle quotient q/m between charge q and mass m is incorporated into the Kaluza–Klein metric, it can explain some quantum effects, such as the Aharanov–Bohm effect and the London equation (see for instance Ferrari *et al.* 1989). This effect consists on the modification of matter wave, $\exp(\mathrm{i} k_\mu dx^\mu)$, of a charged particle according to the Lagrangian $\exp(\mathrm{i} q A_\mu dx^\mu)$, where k_μ is the wave number and A_μ is the external electric potential.

The extra dimension of the Kaluza–Klein theory was assimilated to the Lie group U(1) used in the gauge formalism of electromagnetism [Krasnov and Percacci 2018]. A more general SU(n) gauge theory was proposed by Yang–Mills (1954), and successfully implemented in the case of SU(2) for *electroweak dynamics* and SU(3) for *quantum chromodynamics*. Currently, it is widely used in *coupled gravity* theories [Anderson *et al.* 2006, Guo *et al.* 2020] and integrated within the *double-copy* or the *squared* gauge theories [Bern *et al.* 2010a, Bern *et al.* 2010b, Borsten and Duff 2015, Anastasiou *et al.* 2017, Borsten 2020, Monteiro *et al.* 2021]. These *supergravities* are based on the original idea of Kaluza–Klein, that is, $g \propto A \otimes A$ where A is the vector field of a *gauge potential* (geometrically, of a *connection* on a principal bundle [Husemoller 1994]; see Sec. 1.2), linked to a colour-kinematic duality. For instance, the *Kerr–Schild–Kunndt metrics* contain classic double copy of a Yang–Mills gauge field, which leads to a Einstein–Yang–Mills system [Bern *et al.* 2010a, Gurses *et al.* 2018].

In this context, *string theories* raised soon, and the so-called M-Theory was for a certain time the most promising theory [Becker *et al.* 2007], but its extra-dimensions (not

[4]Spinors are naturally describen in an extension of general relativity based on the Cartan connection (see for instance Def. 1.2.4).

yet observed) and the few proposed experiments make it difficult to test.[5] Nevertheless, it uses an interesting property of the spacetime Lagrangian density for D-branes, firstly proposed by Born–Infeld for electrodynamics,

$$\mathscr{L} \propto \alpha^{-2}\left(\sqrt{-\det\left(g_{\mu\nu}+\alpha F_{\mu\nu}\right)}-\sqrt{-\det(g_{\mu\nu})}\right) \propto \frac{1}{4}F_{\mu\nu}F^{\mu\nu}, \tag{1.1.2}$$

where $F_{\mu\nu}$ is the Faraday tensor or another field-strength curvature 2-form, while α is related to the tension of a string, D-brane or another quantity such as a *dilaton coupling factor* [Tseytlin 2000, Kogan *et al.* 2003]. Moreover, this idea was used in cosmology within the known as Eddington-inspired Born–Infeld gravity, which uses the symmetric part of the Ricci tensor, $R_{\mu\nu}$, instead of the field-strength, $F_{\mu\nu}$ [Tamang *et al.* 2015].

In contrast to the *string theories*, LQG uses only four-dimensional manifolds $\mathscr{N}$, but taking into account the Wick-rotated (i.e., complex) spacetime. The field states of LQG are invariant under the kinematical symmetry group $SU(2) \times \mathrm{Diff}(\mathscr{N})$ of the connection dynamics, that is, the semi-direct product of the local $SU(2)$ gauge transformations and the diffeomorphisms of $\mathscr{N}$ [Ashtekar *et al.* 2014].

As a guiding principle of most theories, the coupled Einstein–Maxwell equations are based on the assumption that the electromagnetic energy modifies the spacetime in accordance with the *equivalence principle* or following the geometrization of the interactions [Aldrovandi *et al.* 2006, Füzfa 2015].

To study the role of geometry in the spacetime, moving frames were analyzed for three scales: i) the whole Lorentzian manifold (universe), ii) some intermediate objects (galaxies) and iii) smaller spacetime perturbations (spinors). Moreover, another motivation was to explore possible solutions to current problems in physics and especially in cosmology.

1.1.2 Geometrical problems in our spacetime

1.1.2.1 Origin: Inflation or bloating?

Since pseudo-Riemannian geometry was key in the Cartan theory and Einstein's general relativity, modern cosmology was reinforced to study the dynamics and evolution of our manifold, so-called 'universe'. These fundamentals were successful soon: Most of observations supported the standard theory, including SNe type Ia first, and CMB later. However, it required some *ad hoc* assumptions to explain the following (well-known) geometrical issues: (1) "horizon problem" on the homogeneity of regions that were (hypothetically) causally disconnected from themselves, (2) "flatness problem" on the why of the (matter) Lagrangian density is "exactly" equal to the critical density that separates open and close manifolds, and (3) why the universe began to expand. *Inflation theory* attempts to complete the cosmology theory using a hypothetical exponential expansion in the early stages of the universe ($< 10^{-32}$ seconds) due to a kind of *dark energy* (DE), which could favour the high homogeneity and isotropy of the universe today. However, this theory

[5] String theories were an attempt to merge quantum mechanics and the work of Einstein in absence of empirical support. [van Dongen 2021]

presents some additional problems. According to Penrose 2004, Steinhardt 2011, an inflationary universe is much less probable than a non-inflationary universe, and Mosterín 1999, Hollands and Wald 2002 argue that no observations support the validity of this theory.

The standard ΛCDM theory of modern cosmology is based on the classical theory of GR, assumed valid for the universe as a whole. Furthermore, all the versions of the standard model use the same Friedmann equations with the same family of FLRW metrics. Thus, cosmology is constructed on pseudo-Riemannian manifolds $\mathscr{M}$ with a Lorentzian metric g, usually noted as $(\mathscr{M}, g)$. For instance, let $\mathscr{M}$ be an $(n+1)$-dimensional Lorentzian manifold with n spatial dimensions and one temporal. As mentioned before, this dissertation uses the $(1, n)$ signature referring to one positive and n negative eigenvalues of the metric, and notes $\mathbb{R}^{1,n}_{\eta} := (\mathbb{R}^{n+1}, \eta_{1,n})$ for the Minkowskian manifold (typically $n = 3$) with this signature, i.e. with a flat diagonal metric $\eta_{1,n} := \text{diag}(1, -1, ..., -1)$.

A key parameter of the theory, fitted to CMB observations, is the cosmological constant, which represents to a DE [Spergel *et al.* 2007]. Therefore, probably, the most important problem of the ΛCDM theory is the no-direct detection of its related DE, outside the framework of the theory, and what is its natural origin.

A clue to understand the above open issues is starting at the beginning: Eddington 1933 used the analogy of a balloon to explain Hubble's law. According to this heuristic model, if we draw galaxies on a balloon surface that is **bloating**, the galaxies are separating from each other in a similar way as our universe is expanding. Therefore, parallelism is carried out between the balloon 2-surface (2D) and the 3-surface (3D) of our universe, with the radius expanding as a natural function of time. The balloon expansion implies a time dimension, and its curved 3-surface implies that it is contained in a larger dimensional space. The balloon model of Eddington corresponds to a 3-spherical universe embedded in a 4+1 spacetime manifold. This bloating framework based on a support manifold is a starting point to explore alternatives to the inflation in a more natural manner, and therefore this is the first key in the present Thesis.

1.1.2.2 Dynamics: Acceleration or modified inertia?

Hypothesis of homogeneity and isotropy are the basis to choose possible metrics for the universe manifold [Spergel *et al.* 2007]. Modified gravities attempt to generalize the cosmological framework by assuming that its local limit approaches to the GR [Brax 2013, Herfray *et al.* 2016, Cai *et al.* 2016, Kršśák *et al.* 2019, Saridakis *et al.* 2021]. This is the case, for instance, of new geometries like in teleparallel models (e.g. TEGR or STEGR) [Bahamonde *et al.* 2023], adding new terms like in non-local gravity [Zhoolideh-Haghighi and Rahvar 2017] or in tensor-vector-scalar theories (e.g. TeVeS or STVG) [Clifton et al. 2012] and quantized gravities (Fig. 1.1.1).

On the other hand, if the homogeneity hypothesis is not imposed, the accelerated universe's expansion can be explained without the requirement of DE, but by using alternatives such as the *timescape cosmology* of Wiltshire and others, or models based on back-reaction effects of cosmic inhomogeneities [Wiltshire 2007, Preston and Morris

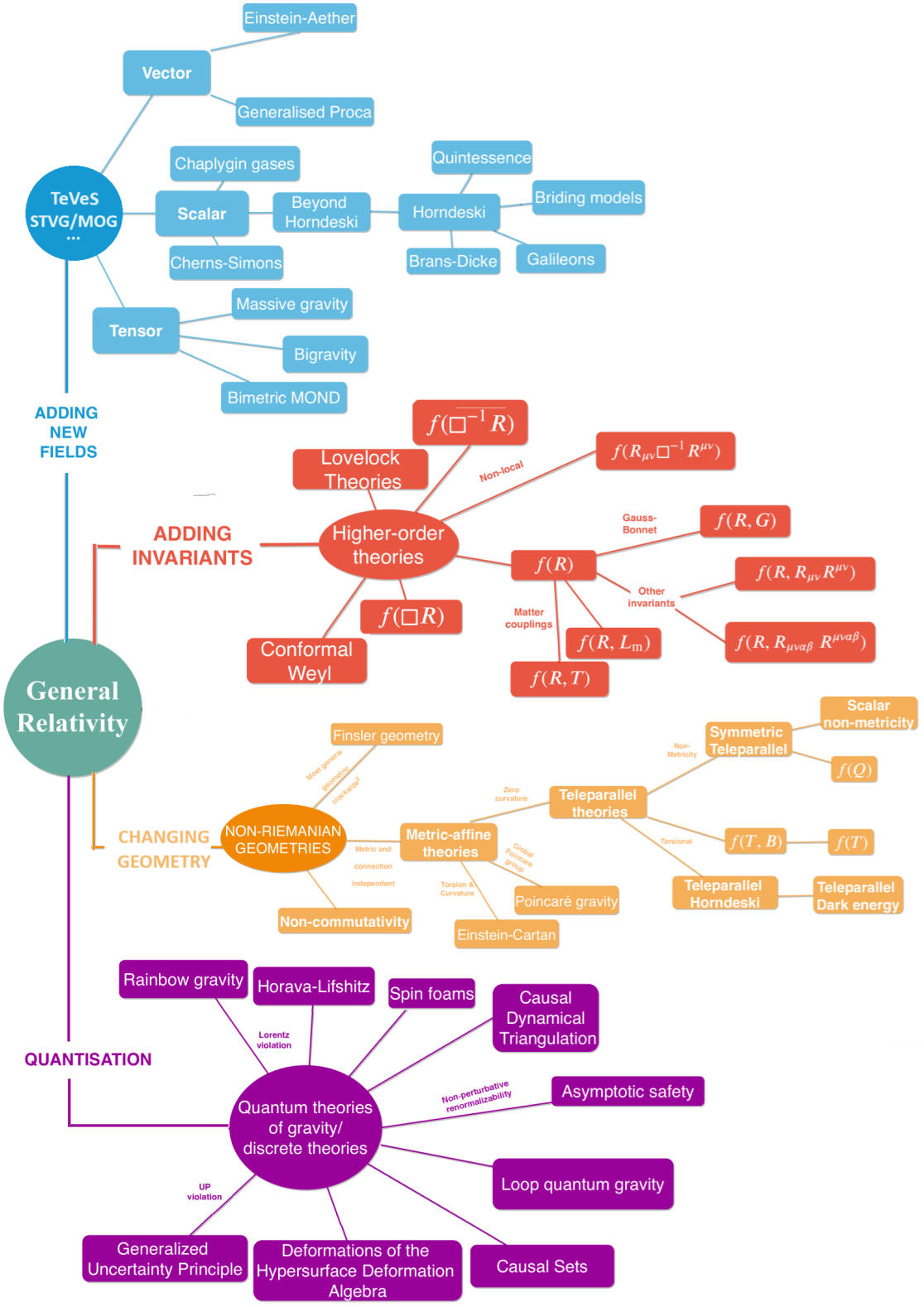

Figure 1.1.1: Approach to different families of modified gravities according to Saridakis *et al.* 2021. The most popular theories apply **geometrical changes** in Lagrangian as a function of torsion or non-metricity like teleparallel models, the **addition of new terms** such as tensor-vector-scalar (TeVeS) theories [Clifton et al. 2012] linked to the Milgrom's Modified Newtonian Dynamics (MOND) [Milgrom 1983,Bekenstein 2004,Chae *et al.* 2020] or the Moffat's scalar–tensor–vector gravity / modified gravity (STVG/MOG) [Moffat et al. 2014, Moffat and Toth 2018] and **quantization** like the LQG [Ashtekar *et al.* 2014].

2014, Dam *et al.* 2017]. Thus, equivalences between temporal acceleration and spatial inhomogeneities can be found.

As mentioned above, ΛCDM theory uses the FLRW metrics, which consider a constant spatial curvature K and a scale factor $a(t)$, which expands with time t, while the time differential is totally separated from the spatial contributions [Speck 2018]. Statically, one can suppose the spatial section of the universe is a 3-sphere S^3 of curvature $K = 1/R^2$, or a 3-hyperboloid H^3 of curvature $K = -1/R^2$, where R is the radius of curvature (i.e., a general curvature is $K = \pm 1/R^2$). The Euclidean space (flat universe) can be taken as the limit as K approaches zero. With this, the metric[6] in comoving spherical coordinates $(x^\mu)_{\mu=0}^3 = (t, r', \theta, \phi)$ is given by:

$$g = g_{\mu\nu} dx^\mu dx^\nu = dt^2 - a(t)^2 \left(\frac{dr'^2}{1 - Kr'^2} + r'^2 d\Sigma^2 \right) \tag{1.1.3}$$

where $d\Sigma^2 := d\theta^2 + sin^2\theta d\phi^2$, while the scale factor $a(t)$ represents the expansion of the spatial sections of the universe, and hence the Hubble parameter (historically regarded as *Hubble "constant"*) is a variable defined as $H := \dot{a}/a = a^{-1}\partial_t a$.[7]

However, the prescription to build the FLRW metric is not natural from an embedding perspective of Lorentzian manifolds. Let $\vec{\ell}$ be spatial coordinates of the Universe; so they can be rewritten by using comoving coordinates $\vec{\ell'}$ and a scaling factor $a(t)$ varying with time t. For instance, if we choose a universe characterized by $S_R^3 := \left\{ \vec{\ell} \in \mathbb{R}^4 : |\vec{\ell}| = R(t) \right\}$, i.e. an expanding 3-sphere of radius $R(t) \in \mathbb{R}_{\geq 0}$ and centred in the origin (singularity in $t = 0$), the scaling factor is $a(t) = R(t)/R(t_o)$ and total spatial coordinates are $\vec{\ell} = a(t)\vec{\ell'} \in S_R^3$. Therefore, the line element contains both spatial and temporal differentials, i.e., $d\ell = a(t)d\ell' + \ell' da(t)$. If the second term is absorbed by an appropriate coordinate change, a radial inhomogeneity appears in the spatial term. It follows that the FLRW model does not include the simplest expanding 3-sphere according to $R(t) = t$, embedded in $\mathbb{R}^{1,4}$. Taking the corresponding scale factor, the Hubble parameter of this **inertial or linear** expansion is $H = \dot{a}/a = 1/t$, which is compatible with the empirical age t of the universe in the so-called **synchronicity problem** [Lima 2007, Melia and Abdelqader 2009, Avelino and Kirshner 2016, Riess *et al.* 2019, Knox and Millea 2020]. For this reason, many alternative cosmological models were built on that equality $1/H = t$, such as the Dirac-Milne model, the coasting universe, the Melia's $R_h = ct$ and the inhomogeneous hyperconical model [Benoit-Lévy and Chardin 2012, Melia and Shevchuk 2012, Monjo 2017, John 2019].

[6] We assume that the basis of the metric is symmetric $dx^\mu dx^\nu := \frac{1}{2}(dx^\mu \otimes dx^\nu + dx^\nu \otimes dx^\mu)$. For a parameterization $\varphi : U \in \mathbb{R}^4 \to \mathscr{M}$, with $q \in U \mapsto p = \varphi(q) \in \mathscr{M}$, the metric is $g = d\varphi^2$ and the arc length is $ds := ||d\varphi||$. In physics, the metric g of a manifold $\mathscr{M} \ni p$ is usually represented by the *squared arc length* ds^2 or by its equivalent squared "differential line element" $d\varphi^2$, since $d\varphi(q) = \partial_\mu \varphi(q)\, dx^\mu$. Thus, $ds^2 = d\varphi^2 = (\partial_\mu \varphi) \cdot (\partial_\nu \varphi) dx^\mu dx^\nu \equiv g_{\mu\nu} dx^\mu dx^\nu = g$, where the dot $(\cdot)$ is the inner product defined in the cotangent space $\mathrm{T}_p^*\mathscr{M} \cong \mathbb{R}_\eta^{1,3}$ with $\eta = \mathrm{diag}(1, -1, -1, -1)$.

[7] We use the notation dot $(\dot{})$ to abbreviate the expression for the time derivative $\dot{a} := \partial_t a = \partial a/\partial t$.

1.1.2.3 Perspective: Two different dynamics?

'Hubble tension' is a term commonly used in cosmology to refer to the discrepancy between different measurements of the current Hubble parameter value (H_0). For instance, the Cepheid SNe sample leads to $H_0 = (73.3 \pm 1.04)$ km s^{-1}Mpc^{-1} when SH0ES uses "cosmic distance ladder" [Riess et al. *et al.* 2021, Riess et al. *et al.* 2022], while Planck Legacy 2018 (PL18) found it to be $H_0 = (67.4 \pm 0.5)$ km s^{-1}Mpc^{-1} [Aghanim *et al.* 2020b] by analysing data from the CMB. In an extensive review, proposals to resolve the Hubble tension were mainly classified in three categories [Di Valentino *et al.* 2021]: dark energy models, inflationary models and modified gravity, among others. Particularly, modified gravity and cosmological models with (extra) non-gravitational interactions have successfully alleviated the H_0 tension, but they can not be simultaneously adjusted to BAO and SNe Ia data [Di Valentino *et al.* 2021]. Radially inhomogeneous universes can also reduce the Hubble tension [Camarena *et al.* 2022, Monjo and Campoamor-Stursberg 2023]. For example, the inclusion of curvature-mass profiles in the LTB metric (ΛLTB) produces similar effects to the standard ΛCDM, with a tension reduction for $0.023 < z < 0.15$ [Camarena *et al.* 2022]. Spatial inhomogeneities can be angular (like LTB) or only radial (like the Hyperconical model), with a different luminosity-angular distance relation [Monjo 2017]. On the other hand, as an 'inhomogeneity in the time', a new constraint on *early dark energy* was recently proposed to solve the problem [Poulin *et al.* 2018, Poulin *et al.* 2019, Kamionkowski and Riess 2022]. Applying this method to the Planck and BOSS data, $H_0 = 69.52^{+0.95}_{-1.21}$ km s^{-1}Mpc^{-1} is obtained, which only partially alleviates the Hubble tension [Herold *et al.* 2022].

The difference between local and global geometry could play a role in determining the origin of the Hubble tension. An example of this is given in Gurzadyan and Stepanian 2021, which hypothesized that the local Hubble flow is due to the repulsive dark-energy term in the weak-field limit of Einstein's field equations. Within this idea, two different perspectives (globally relativistic and locally non-relativistic cosmologies) provide values for the lower and upper constraints of the Hubble parameter: $\sqrt{\Lambda c^2/3} \approx 56.2$ and $\sqrt{\Lambda c^2} \approx 97.3$ km s^{-1}Mpc^{-1}.

Observational Hubble parameter data (OHD), mainly cosmic chronometers (CC) and radial BAO size-based methods, can aid in the exploration of time evolution and the scale differences of cosmological parameters [Yu *et al.* 2018]. For instance, the CC method proposed by Jimenez and Loeb 2002 uses relative galaxy ages to estimate the Hubble parameter, which has been widely considered to directly measure the expansion of the Universe at different redshift scales [Borghi *et al.* 2022, Tomasetti *et al.* 2023]. Instead, BAO data constraint combines the 'sound horizon scale' and the Hubble parameter. Thus, extra data is required to calibrate the size of the sound horizon (usually CMB anisotropy measurements or Lyα forest) and, with this, constrain the Hubble parameter [Cuceu *et al.* 2019]. Galaxy redshift surveys also provide estimations on cosmological parameters by combining to radial BAO lengths. It allows the extraction of (unbiased) sound horizon scale at the baryon drag epoch in a cosmology-independent way [Yu *et al.* 2018].

1.1.2.4 Curvature: Shape or more lensing?

The spatial curvature is not an intrinsic (geometric) property of the universe, but the Ricci scalar curvature is, since the universe is a Lorentzian manifold. Therefore, definition of spatial section of our universe depends on the hypotheses considered to build the coordinates used in each case. For instance, assuming the FLRW coordinates, Lindley D 1987 a total density of universe close to the critical density implies that it could be marginally open or closed. Aligned with this, the Wilkinson Microwave Anisotropy Probe (WMAP) and Plank missions improved the analysis of CMB power spectra and found the results to be compatible with a flat space [Adam *et al.* 2015]. However, the last PL18 analysis led to an enhanced lensing amplitude in CMB power spectra that could be solved with a positive curvature at more than the 99% confidence [Aghanim *et al.* 2020b, Aghanim *et al.* 2020a, DiValentino *et al.* 2020].

An alternative solution is to consider coordinate transformations, by connecting intrinsic and extrinsic global curvatures, since the spatial section depends on the selected coordinates. Specifically, embedded manifolds with non-flat spaces can locally exhibit behaviours analogous to those of a spatially flat FLRW metric [Monjo 2017]. Moreover, positive curvatures of a linearly expanding universe can be transformed to a radial inhomogeneity in the space, and this is assimilated as an acceleration of a (homogeneous) flat space by using some stereographic projection [Monjo 2018, Monjo and Campoamor-Stursberg 2020]. This solution is locally unique but not globally. However, it is possible to define appropriate families of stereographic projections to mimic a flat FLRW manifold from the hyperconical universe. Under the intrinsic viewpoint of the resulting metric, this model can reproduce an apparent dark energy of $\Omega_\Lambda \approx 0.6937$, which is statistically compatible with the PL18 results ($\Omega_\Lambda = 0.6889 \pm 0.0056$) [Monjo 2018].

1.1.2.5 Parameters: Dark quantities or over-fitting?

The well-known equivalence between acceleration and curvature was firstly used in GR to solve classical physics in a geometrical way. Could the same idea solve cosmological tensions? The basic hypothesis is that accelerated expansion is a manifestation of the curvature of the universe, by changing from extrinsic to intrinsic reference frames, or from other modified gravity metrics. That is, the apparent dark energy could be a purely geometrical effect caused by projecting embedded (inhomogeneous) hypersurfaces to maps of a (homogeneous) flat manifold. This idea leads to a modified gravity that is (at least locally) compatible with the standard model, as shown in Monjo 2018, Monjo and Campoamor-Stursberg 2020, Monjo 2023.

Similarly, at least part of the dark matter could actually be considered another geometrical effect of modified gravities, as is the case of modelling disc-galaxy rotation curves with MOND-TeVeS theories [Bekenstein 2004, Chae *et al.* 2020]. Furthermore, inconsistencies have been identified in different candidates of 'dark energy'. For instance, the Kilo-Degree Survey (KiDS-1000) showed differences with a 3σ tension with respect to the prediction of the CMB Planck Legacy analysis [Asgari *et al.* 2021]. On the other hand, the observed cluster substructures are more efficient lenses than predicted by CMD

simulations, by more than an order of magnitude [Meneghetti *et al.* 2020]. To solve some of the above inconsistencies, an'early dark energy' was recently proposed [Poulin *et al.* 2018,Poulin *et al.* 2019,Kamionkowski and Riess 2022]. However, the large number of cosmological parameters might be insufficient for guaranteeing statistical robustness [Liddle 2004]. Perhaps, cosmology is undergoing the classical problem of epicycles.

1.1.3 Hypotheses and objectives

1.1.3.1 Hypotheses of the Thesis

All the considered hypotheses are synthesized here in a global hypothesis: "nature is a particular case of geometry". Henceforth, 'nature' is (at least partially) defined by **geometrical effects of moving frames** in a Lorentzian manifold $(\mathbb{R}^{1,3}, g)$, with a certain metric tensor g, whose tangent spaces are copies of the (flat) Minkowskian spacetime. From this starting point, three specific hypotheses constitute a basis for the developments and claims of this Thesis:

1. **(On inertia).** *Spacetime manifold is inertial.* As a generalization of the first Newton's law (applied to objects) and of the strong equivalence principle (applied to gravity), the first hypothesis states that nature **spacetime manifold presents inertial (linear) dynamics in the absence of external fields**, as it is inherited from an ambient Minkowskian manifold. That is, the 5-dimensional Minkowski spacetime is the basis of the default dynamics in our 4-dimensional Lorentzian manifold (universe) since it inherits a linear expansion by embedding. **We claim** that spacetime dynamics are more natural from this hypothesis than the ad-hoc FLRW metric and the probably overfitted ΛCDM model.

2. **(On natural dynamics).** *Spacetime manifold is responsible for its dynamics.* In a more general way, geometrical definition of a Lorentzian manifold determines the dynamics of observers (moving frames) that live inside, regardless of the matter content. Therefore, Hamiltonian/Lagrangian equations can be derived in a natural manner, and moving frames provides symmetries under the corresponding transformations related to spacetime, object and particle dynamics. Under this framework, **we claim** that *changing from extrinsic (static) to intrinsic (comoving) perspectives* produces fictitious accelerations represented by projections of comoving coordinates.

3. **(On metric-based nature).** *The dynamics of nature are metrically determined.* This hypothesis is a generalization of the previous one, as it states that all the natural dynamics can be expressed in terms of a spacetime-particle field, as a "metric" generalized by integrating the (connection) gauge-based interactions[8] and their

[8]This aims to explore a way to include the electroweak and chromodynamics interactions.

symmetry generators in some *unified field* that plays the role of "metric"[9]. This hypothesis is only partially addressed in this dissertation, but some interesting results about squared $\mathrm{SU}(1,3)$ in teleparallel gravity are displayed. Therefore, **we claim** that our Thesis contributes to a grand unification, as it was also aimed by most of *geometrodynamics* theories. Specifically, we state that moving frames are perturbed by $\mathfrak{su}(1,3)$-symmetry generators to define Lorentzian metrics that could reproduce nature's forces.

1.1.3.2 Specific objectives of the Thesis

This dissertation is designed on the basis of the above three hypotheses in order to address four specific objectives, on i) deriving our Lorentzian manifold, ii) obtaining its dynamics, iii) finding its main symmetries and iv) generalizing for other symmetries. Details of these objectives are defined as follows:

Objective I: Deriving our Lorentzian manifold

According to the hypothesis that *nature is a particular case of geometry*, this dissertation aims to use pure geometrical techniques to built a Lorentzian manifold that represents our spacetime. The model is based on the same idea of the inertial dynamics (linear expansion) as it is the case of Benoit-Lévy and Chardin 2012, Melia and Shevchuk 2012, but analyzes the curvature tensor according to the point of view of a moving frame, that is a hypothetical observer located in the hypersurface of an expanding universe (hypercone section), which a priori may have positive or negative curvature. This contrasts with the Milne and Melia universes, which assume a zero or negative curvature [Benoit-Lévy and Chardin 2012, Melia 2023].

Objective II: Obtaining natural dynamics from our manifold

Taking into account that Lorentzian manifolds are dynamical systems by definition, the second objective is to formulate a natural manner of obtaining dynamics in our manifold. Here, 'natural' means minimal under differential geometry, or without the need of adding *dark quantities* in the Lagrangian density under symplectic geometry. This minimal formulation should also include the derivation of the movement of objects that live inside the manifold considered.

Objective III: Finding main symmetries of our manifold

The third objective is to analyze the symmetry properties of the manifold developed according to the Killing vectors of the metric, the Lagrangian formalism and the ADM equations [Arnowitt *et al.* 1959, Deruelle *et al.* 2010, McFeron and Székelyhidi 2012]. It includes the exploration of conserved quantities and contrast them with physical observables.

[9] In a similar way that energy (from time-translation symmetry) perturbs the metric, we hypothesize that other symmetry-related conserved quantities (e.g. charges from $\mathfrak{su}(1,3)$ generators) perturb the metric too. For instance, *photon* involves symmetries linked to energy and electromagnetic fields as a unique physical entity.

Objective IV: Geometrization of other natural symmetries
The last objective is to explore a proper way to geometrize other nature's interactions and their symmetries by using the idea of moving frames in Lorentzian manifolds. Of course, this ambitious objective is only partially addressed here. The underlying idea is to built local perturbations of the metric like $\eta \to \eta + U \otimes U$, where U represents the (escape) velocity of the expansion, of the galaxies or vector fields related to symmetry generators of particles[10].

1.1.4 Structure of the Thesis

The present Thesis is structured in seven chapters. After the preliminaries of the first chapter (Introduction), the second one develops a **new technique** to derive our (1,3)-Lorentzian manifold according to properties of moving frames from extrinsic to intrinsic perspectives[11]. The following Chapters (3, 4 and 5) are focused on detailing results about dynamics at three embedded scales: I) manifold, II) objects representing large-scale perturbations, and III) particle fields to represent the smallest perturbations. Chapter 6 consists of theoretical and practical applicability of the results, including a minimal embedding theorem and observations at embedded scales. Finally, the last chapter summarizes the main conclusions of the work, specially regarding the proof of the initial hypotheses and the application to the embedded dynamics at the three scales. That is:

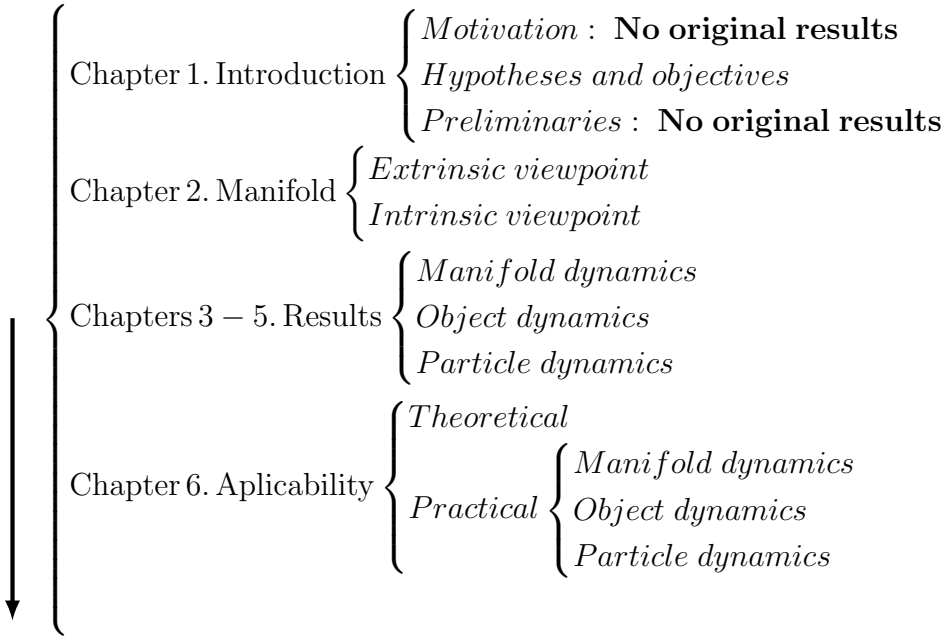

[10]Of course, the proposed metric should be a *spacetime-particle* field, since it depends on the particle characteristics and it does not satisfy an equivalence principle between a "gravitational charge" (or mass) and an "inertial charge" (i.e., the mass, for all the cases) [Friedman 1983]

[11]That is, the inverse way of *embedding*, which is defined from the intrinsic to the extrinsic viewpoint.

1.2 Preliminary I: Connection to the movement

1.2.1 Connections from principal G-bundles

A brief reminder of generalities on *connection* and *field theory* is required to fix the notations used in this Thesis, especially for modern relativity, and *teleparallel gravities* [Pereira 2012, Izaurieta *et al.* 2019, Krššák *et al.* 2019].

Formally, there are different ways to define a *connection*. Probably, the most common definition of *connection* is as a linear map for some fiber bundle E over a n–dimensional manifold $\mathscr{N}$, which describes how to realize *parallel transport* in the tangent bundle $E_p \in E$ over the manifold $\mathscr{N} \ni p$. The fact of "how to carry out *parallel transport* of an object between two fibers" is equivalent to indicating "how much it does (minimally) change when it is transported in parallel" and therefore allows defining a *covariant derivative*. To go into detail, let's introduce some definitions.

Definition 1.2.1 (Principal **G-bundle structure**)**.** [Husemoller 1994, Sharpe 1997] Let $E = \bigcup_p E_p$ be a fiber bundle over a n–dimensional manifold $\mathscr{N}$, which is characterized by a projection map $\pi : E \to M$ and a local basis $b = \{b_k\}_{k=1}^n$ of sections $s : U_i \subset \mathscr{N} \to E$ defined for some neighborhood $U_i \subset \mathscr{N}$ of $p \in M$, which satisfies that $\pi(s(p)) = p$. Moreover, let G be a closed subgroup of the general linear group $\mathrm{GL}(n)$ of degree n. With these ingredients, a G**-bundle structure** for E is a collection of local gauges F_i for E,

$$\begin{aligned} F_i : U_i \times \mathbb{R}^n \quad &\to \quad E|U_i \cong \pi^{-1}(U_i) \\ (p, v) \quad &\mapsto \quad v^1 b_1(p) + v^2 b_2(p) + \cdots + v^n b_n(p) =: s(p) \ \in \ E_p \,, \end{aligned}$$

such that the set $\{U_i\}_i$ covers $\mathscr{N}$ and, for all i, j, the gauge transition function $f_{ij} : U_i \cap U_j \to \mathrm{GL}(n)$ from F_j to F_i has its image in G, that is $f_{ij}(p) = (F_j^{-1} \circ F_i)|_p \in \mathrm{G} \subset \mathrm{GL}(n)$.

An example of G-bundle structure is given by the Poincaré group $\mathrm{IO} = \mathbb{R}^{1,3} \times O(1,3)$ for the vector bundle or tangent space $E = \mathrm{T}\mathscr{N} = \bigcup_p \mathrm{T}_p\mathscr{N}$ of the Minkowski manifold $\mathscr{N} = \mathbb{R}^{1,3} \ni p$. In this case, sections $s : U_i \subset \mathscr{N} \to \mathrm{T}\mathscr{N}$ are vector fields and the IO-bundle structure is the collection of local gauges (i.e., affine maps) from a neighborhood of $p \in \mathscr{N}$ to the tangent space $\mathrm{T}\mathscr{N}$. Other examples can be constructed with bundles E of quantum features (numbers), which are sets of fibers E_p identified with spaces of internal attributes of particles (e.g. spin, isospin. colour, flavour)

Given a G-structure for E, if S is some structure defined for the vector space $\mathbb{R}^n$ that is invariant (symmetric) under the group G, one can define the same structure S on each $E_p = E|\{p\}$ by carrying S over any isomorphism $F_i|_p : \mathbb{R}^n \cong E_p$ with $p \in U_i$. Thus, a G-symmetric structure S defined on $E_p \cong \mathbb{R}^n$ provides a G-structure for $E = \bigcup_p E_p$.

Definition 1.2.2 (***Linear* or *affine* connection**)**.** Let $E \to \mathscr{N}$ be a vector bundle and consider the family of its smooth sections $\Gamma(E)$. A linear (or affine) connection $\mathcal{D}$ on $E \to \mathscr{N}$ is a linear map $\mathcal{D} : \Gamma(E) \ \to \ \Gamma(\mathrm{T}^*\mathscr{N} \otimes E) \cong \Omega^1(\mathscr{N}, E)$ such that

a) $\mathcal{D}(f\sigma) = df \otimes \sigma + f\mathcal{D}\sigma$ (Leibniz rule),

b) $\mathcal{D}\sigma(fu + v) = f\mathcal{D}\sigma(u) + \mathcal{D}\sigma(v)$ (tensorial over $\mathscr{N}$),

for all $\sigma \in \Gamma(E)$, $f \in C^\infty(\mathscr{N})$ and $u, v \in \mathfrak{X}(\mathscr{N})$, where $df(v)$ is the usual directional derivative, and $\Omega^1(\mathscr{N}, E)$ denotes the family of E-valued 1-forms on $\mathscr{N}$. The affine connection is a particular case of the (principal) **Ehresmann connection** on principal fiber bundles[12], equivariant under a Lie group G action.[13]

Remark 1.2.1 (**Equivalent definition of affine connection**)**.** The above definition is equivalent to the bilineal map $\mathcal{D} : \mathfrak{X}(\mathscr{N}) \times \Gamma(E) \to \Gamma(E)$ that is usually denoted as $\mathcal{D}_u\sigma \equiv \mathcal{D}(u, \sigma)$, equivalent to $\mathcal{D}\sigma(u)$ of Def. 1.2.2, for all $u \in \mathfrak{X}(\mathscr{N})$ and $\sigma \in \Gamma(E)$, where $\mathfrak{X}(\mathscr{N})$ is the family of vector fields on $\mathscr{N}$ and $\Gamma(E)$ is the family of sections of $V \to \mathscr{N}$. This is so because the image of $\mathcal{D} : \Gamma(E) \to \Gamma(\mathrm{T}^*\mathscr{N} \otimes E)$ (Def. 1.2.2) requires a vector field $v \in \mathfrak{X}(\mathscr{N})$ to obtain an element of $\Gamma(E)$. Therefore, the connection also satisfy that:

a) $\mathcal{D}_u(f\sigma) = u(f)\,\sigma + f\mathcal{D}_u\sigma$ (Leibniz rule),

b) $\mathcal{D}_{fu+v}\sigma = f\mathcal{D}_u\sigma + \mathcal{D}_v\sigma$ (tensorial over $\mathscr{N}$),

for all $f \in \mathcal{C}^\infty(\mathscr{N})$, $u, v \in \mathfrak{X}(\mathscr{N})$ and $\sigma, \tau \in \Gamma(E)$. Moreover, given a linear connection $\mathcal{D}$ on $E \to \mathscr{N}$, the **covariant derivative** in the direction $u \in \mathfrak{X}(\mathscr{B})$ is given by $\mathcal{D}_u : \Gamma(E) \to \Gamma(E)$, thus the equivalence $\mathcal{D}_u\sigma \equiv \mathcal{D}\sigma(u)$ is clear.

Remark 1.2.2 (**Affine connection in tangent bundles**)**.** Let $\mathscr{N}$ be a smooth manifold with tensor metric g and let $\Gamma(\mathrm{T}\mathscr{N})$ be the space of vector fields on $\mathscr{N}$, that is, the space of smooth sections of the tangent bundle $\mathrm{T}M$. Then, a *connection* on $\mathscr{N}$ can be directly given by the *covariant derivative* $\mathcal{D}$ on $\mathscr{N}$, which is a bilinear map

$$\begin{aligned} \mathcal{D} : \Gamma(\mathrm{T}\mathscr{N}) \times \Gamma(\mathrm{T}M) &\to \Gamma(\mathrm{T}\mathscr{N}) \\ (e_\alpha, e_\beta) &\mapsto \mathcal{D}_{e_\alpha} e_\beta \end{aligned}$$

When the basis vector fields $\{\partial_\alpha\}_{\alpha=0}^3$ are chosen, the covariant derivative is locally given by the Christoffel symbols $\Gamma^\gamma{}_{\alpha\beta}$ as follows

$$\mathcal{D}_{\partial_\alpha}\partial_\beta =: \mathcal{D}_\alpha\partial_\beta = \underbrace{\partial_\alpha\partial_\gamma}_{=0} + \Gamma^\gamma{}_{\alpha\beta}\partial_\gamma$$

Finally, we say that the connection of $\mathcal{D}$ is metrically affine (also referred as 'metric connection') iff it is compatible with the metric, $\mathcal{D}g = 0$, that is

$$\begin{aligned} 0 = \mathcal{D}_\alpha g_{\mu\nu} &= \mathcal{D}_\alpha\, g(\partial_\mu, \partial_\nu) = \partial_\alpha\, g(\partial_\mu, \partial_\nu) - g(\mathcal{D}_\alpha\partial_\mu, \partial_\nu) - g(\partial_\mu, \mathcal{D}_\alpha\partial_\nu) \\ 0 &= \partial_\alpha g_{\mu\nu} - g(\Gamma^\gamma{}_{\alpha\mu}\partial_\gamma, \partial_\nu) - g(\partial_\mu, \Gamma^\gamma{}_{\alpha\nu}\partial_\gamma) \\ 0 &= \partial_\alpha g_{\mu\nu} - \Gamma^\gamma{}_{\alpha\mu} g_{\gamma\nu} - \Gamma^\gamma{}_{\alpha\nu} g_{\mu\gamma} \end{aligned}$$

and, in terms of the metric, the Christoffel symbols are $\Gamma^\gamma{}_{\alpha\beta} = \frac{1}{2} g^{\gamma\mu}\left(\partial_\beta g_{\mu\alpha} + \partial_\alpha g_{\mu\beta} - \partial_\mu g_{\alpha\beta}\right)$ where $g^{\gamma\mu}$ are the components of the dual metric tensor. On the other hand, we will say that a connection has **non-metricity** if $Q_{\alpha\mu\nu} := \mathcal{D}_\alpha g_{\mu\nu} \neq 0$.

[12] In other words, the connection describes how to realize a parallel transport of sections in the fiber bundle $E \to \mathscr{N}$.

[13] It is possible to define a covariance by introducing a Lie group acting on the fibers of the fiber bundle.

Additionally to the non-metricity Q, the connection $\mathcal{D}$ has two main (generally nonzero) geometrical features, the curvature Ω and torsion T, which are two-forms:

$$\begin{aligned} \Omega : \Gamma(\mathrm{T}\mathscr{N}) \times \Gamma(\mathrm{T}\mathscr{N}) &\to \mathrm{Diff}(E, E) \\ (u, v) &\to \Omega(u, v) := [\mathcal{D}_u, \mathcal{D}_v] - \mathcal{D}_{[u,v]} \end{aligned}$$

$$\begin{aligned} T : \Gamma(\mathrm{T}\mathscr{N}) \times \Gamma(\mathrm{T}\mathscr{N}) &\to \Gamma(\mathrm{T}\mathscr{N}) \\ (u, v) &\to T(u, v) := \mathcal{D}_{[u}, v] - [u, v] \end{aligned}$$

where $[u, v] := uv - vu$ is the commutator of u and v, while the notation $\mathcal{D}_{[u}, v] := \mathcal{D}_u v - \mathcal{D}_v u$ is chosen for convenience.

1.2.2 Connections from absolute parallelism

Let $C : \mathbb{R} \to \mathscr{N}$ a parametric curve on the manifold $\mathscr{N}$. Transportation of local geometric objects (e.g., tangent vectors or tensors) along C can be consistently defined by keeping the parallels of the objects. More precisely, there exists a way to connect the properties of the object before and after its transport carried out between an initial and a final tangent space of $\mathscr{N}$. For instance, the *affine connection in tangent bundles* (Def. 1.2.2) describes the parallel transport of tangent vectors from one point to another, providing information on the deviation of a vector field from being parallel transported in a given direction. Therefore, the connection defines a directional derivative but covariant to (or adapting on) the manifold as it changes from a tangent space to another.

A generalization of that is the **Cartan connection**, which is focused on transporting orthogonal frames (moving frames or *repère mobile*) instead of simple vector fields. Therefore, Cartan connection provides more information than the usual affine connection since a reference frame includes several vector directions. In fact, Cartan reformulated (pseudo) Riemannian differential geometry (which is focused on metric manifolds) as a more complete alternative to the general relativity of Einstein, but he further generalized the theory for any arbitrary differentiable manifold, including those given by Lie groups [Sharpe 1997]. Furthermore, it can also be analyzed in terms of base bundles and therefore allows generalizations like for spinor bundles [Husemoller 1994, Friedrich 2000].

Definition 1.2.3 (**Absolute parallelism**)**.** Let $\mathfrak{h}$ be a finite dimensional Lie algebra. Let $\mathscr{N}$ be a smooth manifold with $\dim \mathscr{N} = \dim \mathfrak{h}$. Thus, we define $\mathfrak{h}$-valued absolute parallelism on $\mathscr{N}$ by a 1-form $\omega \in \Omega^1(\mathscr{N}, \mathfrak{h})$ with values in $\mathfrak{h}$ which is non-degenerate in the sense that $\omega_x : T_x\mathscr{N} \to \mathfrak{h}$ is invertible for all $x \in \mathscr{N}$. Thus its inverse induces a linear mapping $\xi : \mathfrak{h} \to \mathfrak{X}(M)$ which is given by $\xi_x(X) := \omega_x^{-1}(X)$, for each $X \in \mathfrak{h}$.

Definition 1.2.4 (**Cartan connection** ω)**.** Let $\mathfrak{h}$ be a finite dimensional Lie algebra and let $\mathfrak{z} \subset \mathfrak{h}$ be a subalgebra of $\mathfrak{h}$. A Cartan connection on the manifold $\mathscr{N}$ is an $\mathfrak{h}$-valued absolute parallelism $\omega : \mathrm{T}\mathscr{N} \to \mathfrak{h}$ such that $[\xi_X, \xi_Y] = \xi_{[X,Y]}$ for $X \in \mathfrak{h}$ and $Y \in \mathfrak{z}$. The restriction of ξ to $\mathfrak{z}$ is a Lie algebra homomorphism and, in this case, $\mathscr{N}$ is a free $\mathfrak{z}$-manifold [Sharpe 1997].

1.2.3 Connections from tetrad frames

In four-dimensional Lorentzian manifolds $\mathscr{N}$, a (global) orthonormal parallelization[14] of the tangent bundle $\mathrm{T}\mathscr{N}$ is a 4-tuple of orthonormal vector fields $\{e_a\}_{a\in\{0,1,2,3\}} = \{e_0, e_1, e_2, e_3\}$, so-called *tetrads*, *tetrad frame* or *frame fields*, that generalizes any observer frame with four directions (pointed with **Latin index labels**). The tetrad components define the *vierbein*[15] matrix, $(e^\mu{}_a)_{a,\mu\in\{0,1,2,3\}}$, where $e_a = e^\mu{}_a\partial_\mu$ for $a \in \{0,1,2,3\}$. Analogously, the dual basis is known as the co-tetrad frame, $\{e^a = e_\mu{}^a dx^\mu\}_a$, with the dual relationship given by $e^a(e_b) = e_\mu{}^a e^\mu{}_b = \delta^a_b$. The Lorentzian and the Minkowski metrics are denoted by $\mathbf{g} = g_{\mu\nu}dx^\mu dx^\nu$ and $\eta = \eta_{\mu\nu}dx^\mu dx^\nu \equiv \mathrm{diag}(1,-1,-1,-1)$, respectively. Hence, the changes of indexes are given by $e_\mu{}^a = g_{\mu\nu}\eta^{ab}e^\nu{}_b$ for $a,\mu \in \{0,1,2,3\}$, since $\eta_{ab} = \mathbf{g}\,(e_a, e_b) = e_a \cdot e_b$ by definition.

Remark 1.2.3 (**Anholonomic observer frame**)**.** A natural question is whether the tetrad frame can be regarded as the basis of partial derivatives associated to a certain reference frame. That is to say, if there exists a coordinate chart $\{x^a\}_{a\in\{0,1,2,3\}}$ such that $e_a = \partial_a$ for all $a \in \{0,1,2,3\}$ (whenever both vectors are defined). This can only be achieved if the Lorentzian manifold $(\mathscr{N}, \mathbf{g})$ is the (flat) Minkowskian spacetime $(\mathbb{R}^4, \eta)$. In such case, the frame $\{x^a\}_a$ is called an **anholonomic** observer, whereas the general frame $\{x^\mu\}_\mu$ is called a holonomic observer [Ehlers *et al.* 2005], and the vierbein matrix is given by $(e^\mu{}_a = \partial x^\mu/\partial x^a)_{a,\mu\in\{0,1,2,3\}}$.

The commutation relations of the derivatives in arbitrary coordinates are zero, $[\partial_\mu, \partial_\nu] = 0$, but tetrads $e_a := e^\mu{}_a\partial_\mu$ may present non-zero commutation relations:

$$[e_a, e_b] = e^\mu{}_a e^\nu{}_b(\partial_\mu e_\nu{}^c - \partial_\nu e_\mu{}^c)e_c := \mathfrak{f}^c{}_{ab}e_c, \tag{1.2.1}$$

where the $\mathfrak{f}^c{}_{ab}$ are known as the anholonomic coefficients [Koiller *et al.* 2001, Ehlers *et al.* 2005].

The coordinate interval, which does not depend on the reference chosen, is given by $\mathbf{d\tau} := \partial_\mu dx^\mu = e_a e^a \in \mathrm{T}\mathscr{N} \otimes \mathrm{T}^*\mathscr{N}$. Similarly, the invariant distance, that is, the arc length of *proper time*, $d\tau$, is found according to

$$\begin{aligned} d\tau^2 := \mathbf{d\tau}\cdot\mathbf{d\tau} &= (\partial_\mu\cdot\partial_\nu)dx^\mu dx^\nu = g_{\mu\nu}dx^\mu dx^\nu = g_{\mu\nu}e^\mu{}_a e^\nu{}_b\, e^a e^b \\ &= (e_a\cdot e_b)e^a e^b = \eta_{ab}e^a e^b = \eta_{ab}e_\mu{}^a e_\nu{}^b dx^\mu dx^\nu. \end{aligned}$$

Definition 1.2.5 (**Cartan connection**)**.** Additionally to the Def. 1.2.4, a Cartan connection can also be defined by a principal connection on the frame bundle of $\mathscr{N}$, noted as $\mathrm{F}\mathscr{N} \to \mathscr{N}$, which is determined by an affine connection on the tangent bundle, $\mathrm{T}\mathscr{N} \to \mathscr{N}$. In a reference frame, this affine connection can be written as $\mathcal{D} = d + \Gamma$, where d is exterior derivative and $\Gamma \in \Omega^1(\mathscr{N}, \mathrm{End}(T\mathscr{N}))$ is a matrix of 1-forms[16], where

[14] The global orthonormal paralellism is intrisically linked to the notion of *absolute paralelism* used in Cartan formalism (Def. 1.2.3).

[15] The German word "vierbein", also "vielbein" (meaning *four-legged* or *quadruped*) is commonly used to refer the matrix of the tetrad components, even also for the tetrads themselves.

[16] That is, $\Gamma : \mathscr{N} \to \mathrm{T}^*\mathscr{N} \otimes End(\mathrm{T}\mathscr{N})$.

$End(\mathrm{T}\mathscr{N})$ denotes the family of endomorphisms of $\mathrm{T}\mathscr{N}$. If we write $\Gamma = \Gamma^{\rho}{}_{\mu\nu}\, dx^{\mu} dx^{\nu} \partial_{\rho}$, where $\Gamma^{\rho}{}_{\mu\nu}$ are the Christoffel symbols of the connection on $\mathrm{T}\mathscr{N} \to \mathscr{N}$, it can be decomposed as

$$\Gamma^{\rho}{}_{\mu\nu} = \overset{\circ}{\Gamma}{}^{\rho}{}_{\mu\nu} + C^{\rho}{}_{\mu\nu}, \tag{1.2.2}$$

where $\overset{\circ}{\Gamma}{}^{\rho}{}_{\mu\nu}$ are the Christoffel symbols of the (torsion-free) Levi-Civita connection [Jost 2011] and $C^{\rho}{}_{\mu\nu}$ are the components of the so-called *contorsion tensor*, which are given by

$$C^{\rho}{}_{\mu\nu} = \frac{1}{2}\left(g^{\beta\rho} g_{\lambda\mu} T^{\lambda}{}_{\beta\nu} + g^{\beta\rho} g_{\lambda\nu} T^{\lambda}{}_{\beta\mu} - T^{\rho}{}_{\mu\nu}\right). \tag{1.2.3}$$

In the expression above, $T^{\rho}{}_{\mu\nu}$ are the components of the torsion tensor, which are given by $T^{\rho}{}_{\mu\nu} := \Gamma^{\rho}{}_{\mu\nu} - \Gamma^{\rho}{}_{\nu\mu}$.

Since the frame bundle is a principal GL(4)-bundle (Def. 1.2.1), a Cartan connection is (locally) determined by a 1-form $\omega \in \Omega^1(\mathscr{N}, \mathfrak{gl}(4))$. If we restrict $\mathfrak{gl}(4)$ to $\mathfrak{so}(1,3)$, the Lie algebra of the Lorentz group, $\mathrm{SO}(1,3)$, the corresponding principal connection is known as the **Lorentz connection**. Geometrically, we are considering a reduction of the principal GL(4)-bundle, $\mathrm{F}\mathscr{N} \to \mathscr{N}$, to a principal $\mathrm{SO}(1,3)$-bundle or **principal spinor bundle**, $P \to \mathscr{N}$, which exists whenever $\mathscr{N}$ is orientable [Husemoller 1994].

The Lorentz connection (sometimes regarded as *spin connection*) satisfies the metricity condition (or metric compatibility) for the Riemann-Cartan geometry, and it can particularized to the (torsionless) *Ricci coefficient of rotation* to obtain GR.

Let $\{S_{ab}\}_{a,b\in\{0,1,2,3\}}$ be the generators of a spin representation of $\mathfrak{so}(1,3)$ onto $\mathbb{C}^4$. In this case, we can write the Lorentz connection, $\omega = \omega_{\mu} dx^{\mu}$, with $\omega_{\mu} = \frac{1}{2}\omega_{\mu}{}^{ab} S_{ab}$ for some functions $\omega_{\mu}{}^{ab}$ that are skew-symmetric in the algebraic indices. The spin connection components are obtained from the affine connection on the tangent bundle. Specifically, they are given by

$$\omega_{\mu}{}^{ab} = \eta^{bc} e_{\nu}{}^{a} (\partial_{\mu} e^{\nu}{}_{c} + \Gamma^{\nu}{}_{\rho\mu} e^{\rho}{}_{c}). \tag{1.2.4}$$

This connection defines the **Fock–Ivanenko** covariant derivative on the associated adjoint (vector) bundle[17] $(P \times \mathfrak{so}(1,3))/\mathrm{SO}(1,3) \to \mathscr{N}$,

$$\mathcal{D}_{\mu} = \partial_{\mu} - \tfrac{i}{2}\omega_{\mu}{}^{ab} S_{ab}. \tag{1.2.5}$$

For a scalar field, the generators are given by $S_{ab} = 0$. Likewise, for a Dirac spinor field [Friedrich 2000], we have $S_{ab} = \frac{i}{4}[\gamma_a, \gamma_b]$, where $\{\gamma_a\}_a$ are generators of the Clifford algebra $Cl_{1,3}(\mathbb{R}, \mathbf{h})$. Finally, for a vector field, they are given by $(S_{ab})^{c}{}_{d} := i(\eta_{bd}\delta^{c}_{a} - \eta_{ad}\delta^{c}_{b})$. In particular, the Fock-Ivanenko covariant derivative of a vector field (w^a) reads

$$\mathcal{D}_{\mu} w^{a} = \partial_{\mu} w^{a} + \eta_{bc} \omega_{\mu}{}^{ab} w^{c}. \tag{1.2.6}$$

[17] The structure group $\mathrm{SO}(1,3)$ acts (vertically, freely and properly) on P. In turn, a Lie group acts on its Lie algebra through the adjoint representation, $ad_g : \mathfrak{so}(1,3) \to \mathfrak{so}(1,3)$, for each $g \in SO(1,3)$. Then, the group $\mathrm{SO}(1,3)$ acts on the product $P \times \mathfrak{so}(1,3)$ and the quotient of this variety can be considered by the action of the group, $(P \times \mathfrak{so}(1,3))/\mathrm{SO}(1,3)$. Since the action is free and proper, such quotient is a differentiable variety; even more, it is a bundle of Lie algebras over $\mathscr{N}$ [Kobayashi 2009].

In any case, the curvature of the Fock-Ivanenko covariant derivative is given by

$$R^{ab}{}_{\mu\nu} := [\mathcal{D}_\mu, \mathcal{D}_\nu]^{a,b} = \partial_\mu \omega_\nu{}^{ab} - \partial_\nu \omega_\mu{}^{ab} + [\omega_\mu, \omega_\nu]^{ab} \equiv (d\omega + \omega \wedge \omega)^{ab}_{\mu\nu}, \tag{1.2.7}$$

where $[\omega_\mu, \omega_\nu]^{ab} = \omega_\mu{}^a{}_c \omega_\nu{}^{cb} - \omega_\nu{}^a{}_c \omega_\mu{}^{cb}$, and the torsion tensor is $T^\rho{}_{\mu\nu} = \Gamma^\rho{}_{\mu\nu} - \Gamma^\rho{}_{\nu\mu}$. The Ricci scalar curvature is given by $R = R^{ab}{}_{\mu\nu} e^\mu{}_a e^\nu{}_b$. The components of the curvature and torsion 2-forms are given by $R_{\mu\nu} = \frac{1}{2} R^{ab}{}_{\mu\nu} S_{ab}$ and $T_{\mu\nu} = T^a{}_{\mu\nu} e_a$, respectively. For the latter, observe that the generators of the Lie algebra of the *translation group* are $\{e_a\}_a$, but they are not contained into the Lorentz group SO(1,3).

1.3 Preliminary II: Spacetime dynamics

1.3.1 Teleparallel gauge-like formalism and equivalence in GR

The following paragraphs are devoted to set additional notations used in this Thesis, especially referred to teleparallel gravity, spacetime algebra and some fundamental concepts of gauge formalism and the Yang–Mills theory, since they are deeply linked. Unless otherwise stated, we use natural units ($c \equiv 1 \equiv \hbar$).

Teleparallel gravities are generalizations of the *teleparallel equivalent to general relativity* (TEGR), which assumes that gravity is modelled by torsion instead of curvature Fig. 1.3.1. That is to say that Riemann curvature and non-metricity are zero. TEGR Euler-Lagrange equations can be obtained from its action, which is dynamically equivalent to the Einstein-Hilbert since they only differ by a boundary term [de Andrade *et al.* 2000, Krššák *et al.* 2019].

Imitating gauge theories, some authors use translational invariance properties to formulate the TEGR theory. However, its "translation-gauge formalism" does not gather the commonly accepted requirements for a complete gauge theory [Fontanini *et al.* 2019]. Independently of the mathematical interpretation, we employ this *gauge-like* formalism due to its very interesting similarities with the classical gauge theories of particle physics.

Definition 1.3.1 (**Minkowski bundle**)**.** As in the previous sections, let $(\mathscr{N}, \mathbf{g})$ be a Lorentzian manifold and assume that, for each point $p \in \mathscr{N}$ with coordinates $\{x^\mu\}_\mu$, there is a *vector bundle* M with Minkowskian metric (i.e., a copy of the Minkowski space for each $p \in \mathscr{N}$, to represent an observer). The *anholonomic coordinates* of this vector bundle are denoted by $\{x^a\}_a$, and the result is known as the **Minkowski bundle** M with coordinates $\{x^\mu, x^a\}_{\mu,a}$[18].

The translation group acts locally on the Minkowski bundle, $x^a \mapsto \hat{x}^a = x^a + \epsilon^a(x^\mu)$. The Lie algebra of the translation group is generated by the partial derivatives of the anholonomic coordinates, $\{\partial_a\}_a$. The fields of the teleparallel gravity are the 1-forms on $\mathscr{N}$ with values on the Lie algebra of the translation group, which are referred as *translational gauge-like potentials*, denoted by $\phi = \phi_\mu dx^\mu$ with $\phi_\mu = \phi_\mu{}^a \partial_a$. An infinitesimal

[18] We need to distinguish between the usual field of coordinates $\{x^\mu\}_\mu$ of the tangent bundle T$\mathscr{N}$ and the "frame fields" own by each observer, so-called *anholonomic coordinates*.

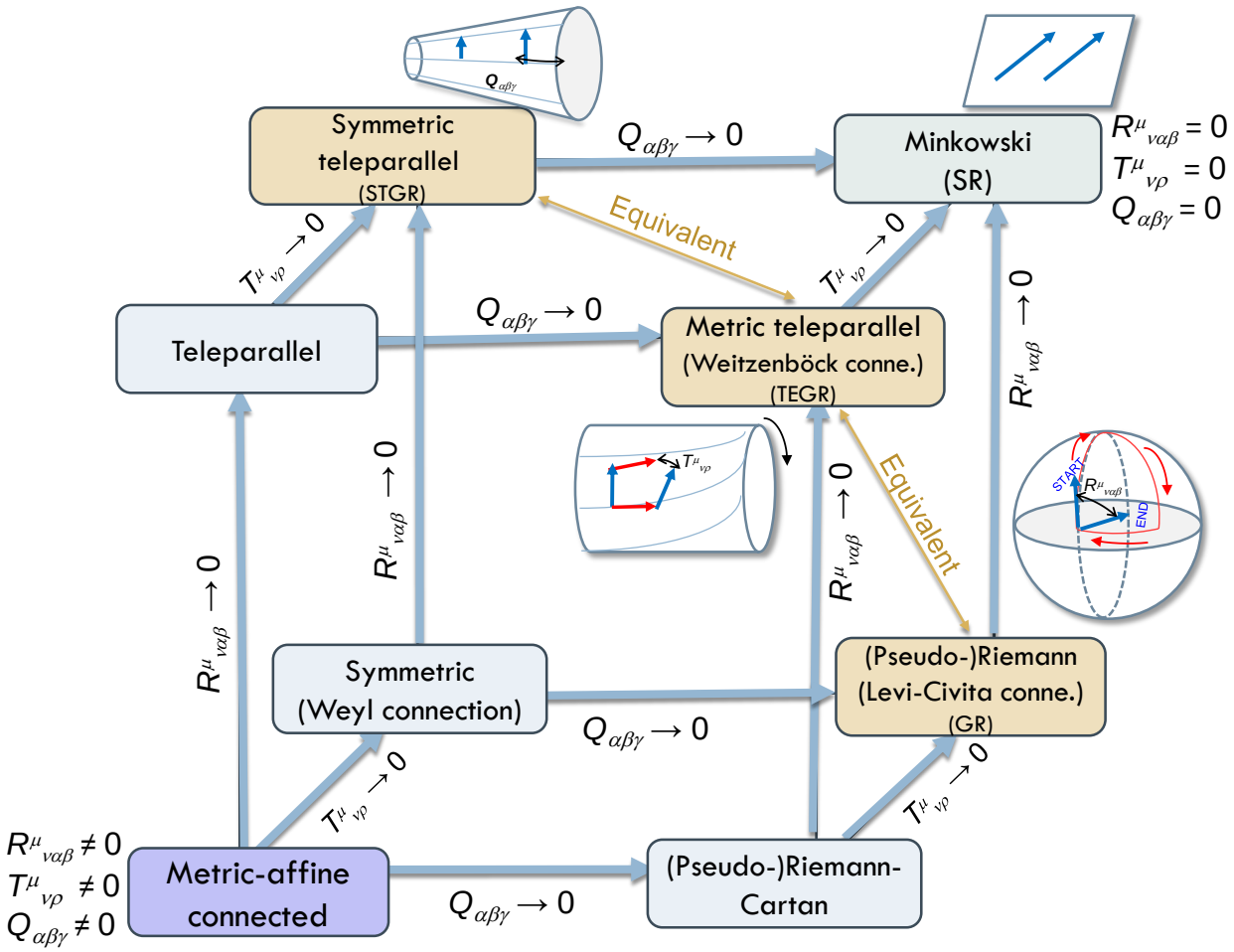

Figure 1.3.1: Relation between different spacetime geometries in the context of gravity theories: Special cases of metric-affine geometries are obtained by switching on/off the curvature $R^{\mu}{}_{\nu\alpha\beta}$ and/or the torsion $T^{\mu}{}_{\nu\rho}$ and/or the non-metricity $Q_{\alpha\beta\gamma}$. The geometric trinity of gravity (yellow labels) is represented by the three shortest ways to the special relativity SR: the STEGR, which uses non-metricity; the TEGR that uses torsion; and the GR that employs curvature. Figure based on Saridakis *et al.* 2021, Capozziello *et al.* 2022.

translation, $\Delta x^a = \epsilon^a(x^\mu)$, yields a transformation of the gauge-like potential such that $\hat{\phi}_\mu{}^a = \phi_\mu{}^a - \partial_\mu \epsilon^a$. That is to say, the action of the translation group is extended to the family of gauge-like potentials. In addition, the gauge-like potential $\phi_\mu = \phi_\mu{}^a \partial_a$ induces a transformation of the vierbein matrix as follows (see e.g. Aldrovandi *et al.* 2006):

$$e_\mu{}^a = \partial_\mu x^a \qquad \mapsto \qquad \hat{e}_\mu{}^a = e_\mu{}^a + \phi_\mu{}^a \quad = \quad \partial_\mu x^a + \phi_\mu{}^a. \tag{1.3.1}$$

This enables us to define the gauge-like derivative in TEGR as $D_\mu = \hat{e}_\mu{}^a \partial_a = \partial_\mu + \phi_\mu$. The corresponding strength field is given by $F_{\mu\nu} = F^a{}_{\mu\nu} \partial_a$, where $F^a{}_{\mu\nu} = \partial_\mu \phi^a{}_\nu - \partial_\nu \phi^a{}_\mu$.

On the other hand, the **Weitzenböck connection** is the affine connection on $\mathrm{T}\mathscr{N} \to \mathscr{N}$ defined from the new tetrad as $\Gamma^\rho{}_{\mu\nu} = \hat{e}^\rho{}_a \partial_\nu \hat{e}_\mu{}^a$. The curvature of this connection vanishes, whereas its torsion is given by $T^\rho{}_{\mu\nu} := \Gamma^\rho{}_{\nu\mu} - \Gamma^\rho{}_{\mu\nu}$. It turns out that the torsion of the Weitzenböck connection is the field strength of the translational gauge-like potential seen from the anholonomic frame:

$$F^a{}_{\mu\nu} = \hat{e}_\rho{}^a T^\rho{}_{\mu\nu} = (e_\rho{}^a + \phi_\rho{}^a) T^\rho{}_{\mu\nu} \tag{1.3.2}$$

TEGR assumes that the inertial effects are represented by the Weitzenböck connection, while the gravity force is given by the contorsion tensor. In fact, equation (1.2.2) yields a decomposition of the geodesic equation in general relativity:

$$0 = \frac{du_\mu}{d\tau} - \mathring{\Gamma}^\rho{}_{\mu\nu} u_\rho u^\nu = \frac{du_\mu}{d\tau} - \Gamma^\rho{}_{\mu\nu} u_\rho u^\nu + C^\rho{}_{\mu\nu} u_\rho u^\nu, \tag{1.3.3}$$

where $u^\mu = dx^\mu / d\tau$ are the components of the 4-velocity. As we see, the Levi-Civita connection contains both inertial effects and gravity forces under the GR framework. Likewise, the dynamical equations for a spinless particle of mass m in a gravitational field $\phi_\mu{}^a$ are [de Andrade and Pereira 1997]

$$\hat{e}_\mu{}^a \frac{du_a}{d\tau} \;=\; \frac{du_\mu}{d\tau} - \Gamma^\rho{}_{\mu\nu} u_\rho u^\nu = -C^\rho{}_{\mu\nu} u_\rho u^\nu \;=\; T^\rho{}_{\mu\nu} u^\rho u^\nu \;=\; F^a{}_{\mu\nu} u_a u^\nu, \tag{1.3.4}$$

where $u^a = \hat{e}_\mu{}^a u^\mu$ are the anholonomic components of the 4-velocity of the particle. Finally, the TEGR Lagrangian density is given by [Krššák *et al.* 2019, de Andrade and Pereira 1997],

$$\mathscr{L} = \frac{\hat{e}}{2\kappa} \left(\frac{1}{4} T^\rho{}_{\mu\nu} T_\rho{}^{\mu\nu} + \frac{1}{2} T^\rho{}_{\mu\nu} T^{\nu\mu}{}_\rho - T^\rho{}_{\mu\rho} T^{\nu\mu}{}_\nu \right) = \frac{\hat{e}}{2\kappa} \left(\frac{1}{4} F^a{}_{\mu\nu} F_a{}^{\mu\nu} \right), \tag{1.3.5}$$

where $\kappa = 8\pi \mathrm{G}$ and $\hat{e} := \det \hat{e}_\mu{}^a = \sqrt{-g}$. This Lagrangian density provides the same dynamics as the Einstein–Hilbert Lagrangian with Ricci scalar R, that is $\mathscr{L}_{GR} = \frac{1}{\kappa} \hat{e} R$, since it only differs in a divergence, $\mathscr{L} - \mathscr{L}_{GR} = -\frac{1}{\kappa} \partial_\mu (\hat{e}\, T^{\nu\mu}{}_\nu)$.

Observe that the TEGR Lagrangian density (Eq. 1.3.5) is very close to the Lagrangian density of a Yang–Mills theory (see Sec. 1.3.4) with group structure U(1). Notice that, from the equations above, it is easy to choose some gauge potential ϕ_μ to imitate the electrodynamic gauge A_μ as, for instance, $\phi_\mu{}^a \propto A_\mu u^a$ with an additional factor $\frac{q}{m}$ to connect the energy m and the coupling factor q. This fact will be central in Chapter 5.

1.3.2 Spacetime algebra

To travel to the quantum world, first we need to introduce some concepts such as the spacetime algebra used in *spinor fields* (i.e. representatives of particles), but we briefly summarize its main features (see Gu 2018a, Gu 2018b for details). Let $(\mathscr{N}, \mathbf{g})$ be a four-dimensional Lorentzian manifold and $M \to \mathrm{T}\mathscr{N}$ be the Minkowski bundle with frames $\{x^\mu, x^a\}_{\mu,a}$, as in the previous section. Recall that the spacetime algebra, also known as the Lorentz algebra, is the Clifford algebra $Cl_{1,3}(\mathbb{R}, \mathbf{h})$, with $\mathbf{h} = \eta$ or $\mathbf{g}$. Let $\{v_\mu\}_\mu$ and $\{\gamma_a\}_a$ be the generators of a representation of the spacetime algebra in the Lorentzian and the Minkowski metrics, respectively. Hence, they satisfy the following relations

$$v_\mu \bullet v_\nu := \frac{1}{2}(v_\mu v_\nu + v_\nu v_\mu) = g_{\mu\nu}\mathbf{1}_4 \tag{1.3.6}$$

$$\gamma_a \bullet \gamma_b := \frac{1}{2}(\gamma_a\gamma_b + \gamma_b\gamma_a) = \eta_{ab}\mathbf{1}_4 \tag{1.3.7}$$

where $\bullet$ is known as the outer product and $\mathbf{1}_4$ denotes the (sometimes omitted) identity matrix. Besides, the exterior product is defined as

$$v_\mu \wedge v_\nu := \frac{1}{2}(v_\mu v_\nu - v_\nu v_\mu) = \frac{1}{2}[v_\mu, v_\nu] \tag{1.3.8}$$

$$\gamma_a \wedge \gamma_b := \frac{1}{2}(\gamma_a\gamma_b - \gamma_b\gamma_a) = \frac{1}{2}[\gamma_a, \gamma_b] \tag{1.3.9}$$

Therefore, the decomposition into the symmetric and skew-symmetric parts is given by $v_\mu v_\nu = v_\mu \bullet v_\nu + v_\mu \wedge v_\nu$, and analogous for $\gamma_a\gamma_b$. The relationship between tetrad components and spacetime generators is given by $v^\mu = e^\mu{}_a \gamma^a$ and $\gamma^a = e_\mu{}^a v^\mu$. They are also related to the Lorentz or spin connection. If one defines $\gamma^a := \gamma_a^{-1}$, the orthogonality property is satisfied, i.e., $\gamma_a \bullet \gamma^b = \delta_a^b \mathbf{1}_4$, and the same holds for v_μ. In particular, $v_\mu \bullet v^\mu = \gamma_a \bullet \gamma^a = \mathbf{1}_4$.

The symbol v_μ for the generators of the representation of $Cl_{1,3}(\mathbb{R}, \mathbf{g})$ is purposely chosen due to its link to the four-velocity covector $u_\mu := dx_\mu/d\tau$ with line element $d\tau := \sqrt{g_{\nu\mu}dx^\nu dx^\mu} = \sqrt{dx_\mu dx^\mu}$, whereas the symbol γ_a is used in honour to the representation by the Dirac gamma matrices. Indeed, distances defined by the generators of the spacetime algebra are analog to the ones defined by the co-vector $u = (u_\mu)_{\mu\in\{0,1,2,3\}}$, that is, $d\tau = u_\mu dx^\mu \in \Omega^1(M)$. Namely, the element of spacetime is now defined as $\mathbf{d\tau} := v_\mu dx^\mu = \gamma_a dx^a$. This enables us to see the spacetime metric as the inner product of the coordinate tangent co-vector fields, where the inner product is defined from the outer product of the algebra generators. More specifically,

$$\begin{aligned}\mathbf{1}_4\, d\tau^2 = \mathbf{d\tau} \bullet \mathbf{d\tau} &= (v_\mu \bullet v_\nu) dx^\mu dx^\nu = \mathbf{1}_4\, g_{\mu\nu} dx^\mu dx^\nu \\ &= (\gamma_a \bullet \gamma_b) dx^a dx^b = \mathbf{1}_4\, \eta_{ab} dx^a dx^b\end{aligned}$$

For each vector field (w^a), the total time derivative is given by

$$\mathbf{D}_\tau w^a := (v^\mu \mathcal{D}_\mu) w^a = \mathbf{d}_\tau w^a + \eta_{bc}\omega_\mu{}^{ab} w^c v^\mu \tag{1.3.10}$$

where $\mathcal{D}_\mu$ is the Fock-Ivanenko covariant derivative, and $\mathbf{d}_\tau = v^\mu \partial_\mu = \gamma^a \partial_a$. Observe that the classical definition is obtained in straightforward manner by replacing $v^\mu \mapsto u^\mu$ and the outer product by the standard product.

1.3.3 Classical-to-quantum bridge

To bridge the classical and quantum viewpoints of coordinates, we set a hypothesis on the spatial density of a particle located at the point $x \in \mathscr{N}$ with 4-velocity $\mathbf{u} = \gamma_\mu u^\mu$.[19] The volumetric density of a particle is a delta-type distribution,

$$\wp(y) = \frac{1}{\sqrt{|g(y)|}}\delta^4(y-x), \qquad y \in \mathscr{N}\,, \tag{1.3.11}$$

which contrasts to the quantum density operator $\hat{\wp} := |\psi\rangle\langle\bar{\psi}|$ for Dirac spinors $|\psi\rangle$. For each subset $U \subset M$, the probability of finding the particle in U is given by

$$\varrho(y) = \int_U \wp(y)\mathrm{d}\tau_x := \frac{1}{\sqrt{|g(y)|}}\int_U \delta^4(y-x)\mathrm{d}\tau_x = \begin{cases} 1 & \text{if } y \in U \\ 0 & \text{if } y \notin U \end{cases}\,,$$

where locally $d\tau_x = \sqrt{|g(x)|}d^4x \in \Omega^4(\mathscr{N})$. Therefore, the classical (point) density of probability current is simply $\wp\mathbf{u}$.

On the other hand, quantum field theory considers the current density from spinors (fields instead of point particles) [Friedrich 2000]. Let ψ be a Dirac spinor representing particles and P be any operator. The **expectation value** is given by the L^2 inner product over P,

$$\langle P\rangle_\psi := \mathfrak{Re}\,\langle\bar{\psi}|\,P\,|\psi\rangle\,, \tag{1.3.12}$$

where $\bar{\psi} := \psi^\dagger\gamma_0$ is the Dirac adjoint in this Hilbert space. Quantum mechanics defines density current as $u^\mu := \mathfrak{Re}\,\langle\bar{\psi}|\,\hat{U}^\mu\,|\psi\rangle$ with the momentum operator $\hat{U}^\mu = \frac{\mathrm{i}}{m}\partial^\mu$ evaluated for some mass $m \in \mathbb{R}_{>0}$. Now, the components of the spacetime current $\mathbf{j} = \gamma_\mu j^\mu$ are $j^\mu := \langle\bar{\psi}|\,\gamma^\mu\,|\psi\rangle$. Therefore, our hypothesis is that $\mathbf{j}$ should be equivalent to the classical current $\varrho\mathbf{u}$, so

$$\mathbf{j} = \gamma_\mu\bar{\psi}\gamma^\mu\psi \;\simeq\; \wp\,\gamma_\mu u^\mu \implies \langle\gamma^\mu\rangle_\psi = \varrho|_x\,u^\mu = u^\mu. \tag{1.3.13}$$

where x is the measured position of the "classical particle" and thus $\langle\hat{\wp}\rangle_\psi = \langle\mathbf{1}_4\rangle_\psi = \varrho|_x = 1$. Moreover, for a 4-momentym $\mathbf{m} := \gamma_\mu m^\mu = \gamma^\mu m_\mu$, Eqs. 1.3.12 and 1.3.13 lead to

$$\langle\mathbf{m}\rangle_\psi = m\,\langle\mathbf{u}\rangle_\psi = mu_\mu\,\langle\gamma^\mu\rangle_\psi = mu_\mu u^\mu = m = \langle\rho\rangle_\psi\,, \tag{1.3.14}$$

where $\rho := \varrho m$ is the classical point energy density and $\mathbf{u} = \gamma^\mu u_\mu = \gamma_\mu u^\mu$. From now onwards, we use the symbol "$\simeq$" to refer to the classical-to-quantum bridge:

$$a \simeq b \quad\Longleftrightarrow\quad \langle a\rangle_\psi = \langle b\rangle_\psi\,, \tag{1.3.15}$$

which has the property that $C\,a \simeq C\,b$ for any $C \in \mathbb{R}$. Therefore, one recovers the (quantum) momentum operator $\mathrm{i}\partial_\mu \simeq m_\mu$ and the Dirac equation for $\psi = \psi_0\exp(-\mathrm{i}\,m\gamma_\nu dx^\nu)$,

$$\mathrm{i}\gamma^\mu\partial_\mu \simeq m\,, \tag{1.3.16}$$

or, similarly, $\mathrm{i}\gamma^\mu\partial_\mu - m \simeq 0$.

[19] Notice that our particle-related vectors are expressed in of the generators of the spacetime algebra, $\{\gamma_\mu\}_{\mu=0}^3$, as a basis.

1.3.4 Yang–Mills theory

In quantum field theories, spinor fields are the main (dynamical) objects of study, which are sections of a spinor bundle over the Lorentzian manifold $\mathscr{N}$. The measurement or *gauge* of these objects transforms under special unitary groups, $\mathrm{SU}(n)$, producing *gauge symmetries* that lead to the Yang–Mills theories [Anderson *et al.* 2006]. A parallel can be drawn between chromodynamics, which uses SU(3) as a structure group, and the present work, that uses SU(1,3) as a structure group. For this reason, *colour* will be used for gauge fields on SU(1,3). The Yang–Mills developments are based on a *gauge potential field* $A \in \Omega^1(P, \mathfrak{su}(1, n-1))$ that, geometrically, corresponds to a connection 1-form on a given *principal* $\mathrm{SU}(n)$*-bundle*, $P \to \mathscr{N}$, with $(\mathscr{N}, \mathbf{g})$ being a Lorentzian manifold. Equivalently, gauge theories can be formulated on vector bundles. Let $\{\lambda_I\}_{I=1}^{n^2-1}$ be the *(hyper)colour* generators, i.e., the generators of a representation of $\mathfrak{su}(1, n-1)$. The structure constants, f_{IJ}^K, encode the Lie algebra structure of $\mathfrak{su}(1, n-1)$: $[\lambda_I, \lambda_J] = i f_{IJ}^K \lambda_K$. Moreover, the colour generators satisfy the orthogonality condition $\mathrm{Tr}(\lambda_I \lambda_J) = \frac{1}{2}\delta_{IJ}$.

Gauge transformations are defined by introducing a phase $\varphi(x) = \lambda_I \varphi^I(x)$, at each point $x \in \mathscr{N}$ of the manifold $\mathscr{N}$, to any physical wave $\Psi(x)$, that is,

$$\Psi(x) \mapsto \hat{\Psi}(x) = \exp(i\varphi(x))\Psi(x). \tag{1.3.17}$$

The invariance of physical measures of $\Psi(x)$ leads to a (gauge) covariant derivative, ∇_μ, that satisfies the gauge transformation $\nabla_\mu \Psi(x) \mapsto \widehat{(\nabla_\mu \Psi)}(x) = \exp(i\varphi(x))\nabla_\mu \Psi(x)$. Assuming that $(\mathscr{N}, \eta)$ is the (flat) Minkowski spacetime and writing locally $A(x) = A_\mu(x)dx^\mu$, $x \in \mathscr{N}$, the gauge covariant derivative is given by the following matrix operator,

$$\nabla_\mu = \mathbf{1}\partial_\mu - iq\lambda_I A_\mu^I = \mathbf{1}\partial_\mu - iqA_\mu, \tag{1.3.18}$$

where $A_\mu = \lambda_I A_\mu^I$, $\mathbf{1}$ is the identity matrix (matching the size of the algebra generators) and q is a coupling constant. The gauge potential, under a gauge transformation $U : \mathscr{N} \to \mathrm{SU}(1, n-1)$, is given by

$$A_\mu(x) \mapsto \hat{A}_\mu(x) = U(x)A_\mu(x)U(x)^\dagger - iq^{-1}(\partial_\mu U(x))U(x)^\dagger, \tag{1.3.19}$$

where $U(x) = \exp(i\lambda_I \varphi^I(x))$ and the subscript $\dagger$ denotes the Hermitian adjoint. Up to first order, the previous expression reads

$$A_\mu(x) \mapsto \hat{A}_\mu(x) = A_\mu(x) - i[\lambda_J, \lambda_K]A_\mu^J(x)\varphi^K(x) + q^{-1}\lambda_I \partial_\mu \varphi^I(x). \tag{1.3.20}$$

The strength of the field is, geometrically, the curvature of the gauge field, i.e., the 2-form $\mathscr{F} = dA + A \wedge A \in \Omega^2(P, \mathfrak{su}(1, n-1))$. This curvature is a basic form of the adjoint type, which enables us to regard it as a form on the base spacetime, $\mathscr{N}$, with values on the adjoint bundle, $\tilde{\mathfrak{su}}(1, n-1) = (P \times \mathfrak{su}(1, n-1))/\mathrm{SU}(1, n-1)$. It is given locally by the commutation of the covariant derivative:

$$\mathscr{F}_{\mu\nu} := \mathrm{i}q^{-1}[\nabla_\mu, \nabla_\nu] := \lambda_I \mathscr{F}_{\mu\nu}^I = \lambda_I \left(\partial_\mu A_\nu^I - \partial_\nu A_\mu^I - q f_{JK}^I A_\mu^J A_\nu^K\right). \tag{1.3.21}$$

As the relation $[\nabla_\alpha, \mathscr{F}^I_{\nu\rho}] = \nabla_\alpha \mathscr{F}^I_{\nu\rho}$ holds, the Bianchi identity (Eq. 1.3.22) and the Jacobi identity (Eq. 1.3.23) are equivalent.

$$(\nabla_\mu \mathscr{F}_{\nu\rho})^I + (\nabla_\rho \mathscr{F}_{\mu\nu})^I + (\nabla_\nu \mathscr{F}_{\rho\mu})^I = 0, \tag{1.3.22}$$

$$[\nabla_\mu, [\nabla_\nu, \nabla_\rho]] + [\nabla_\rho, [\nabla_\mu, \nabla_\nu]] + [\nabla_\nu, [\nabla_\rho, \nabla_\mu]] = 0. \tag{1.3.23}$$

By defining the dual strength as $\tilde{\mathscr{F}}^{\mu\nu} = \frac{1}{2}\varepsilon^{\mu\nu\rho\sigma}\mathscr{F}_{\rho\sigma}$, where $\varepsilon^{\mu\nu\rho\sigma}$ is the Levi-Civita tensor, the Bianchi identity reads $\nabla_\rho \tilde{\mathscr{F}}^{\mu\nu} = 0$.

The gauge potential field has the property of being self-interacting and the equations of motion are semi-linear. This means that one can handle this theory only by perturbation with small nonlinearities.

In a four-dimensional manifold, by denoting $g = \det(\mathbf{g})$, the Lagrangian density without sources reads

$$\mathscr{L}_{\mathscr{F}} = -\frac{1}{2}\sqrt{-g}\, Tr(\mathscr{F}^2) = -\frac{1}{4}\sqrt{-g}\, \tilde{\mathscr{F}}^{\mu\nu}\mathscr{F}_{\mu\nu}. \tag{1.3.24}$$

Similarly, if we consider N spinor sources $\Psi = \{\Psi_k\}_{k=1}^N$ of energy $\{m_k\}_{k=1}^N$, it incorporates an additional term and no null equations of motion

$$\mathscr{L}_{\mathscr{F}+\Psi} = \sqrt{-g}\left(-\frac{1}{4}\tilde{\mathscr{F}}^{\mu\nu}\mathscr{F}_{\mu\nu} + \bar{\Psi}^k\left(i\gamma^\mu\nabla_\mu - m_k\right)\Psi_k\right) \tag{1.3.25}$$

where $\bar{\Psi}^k := \gamma^0 {\Psi_k}^\dagger$ and $\{\gamma^\mu\}_\mu$ are the generators[20] of the Clifford algebra $\mathrm{Cl}_{1,3}(\mathbb{R})$. The corresponding field equations are

$$\nabla_\mu \tilde{\mathscr{F}}^{\mu\nu} = J^\nu, \tag{1.3.26}$$

where $J^\nu := \lambda_I J^\nu_I$ are the currents, with $J^\nu_I = q\bar{\Psi}^k\gamma^\nu\lambda_I\Psi_n$, which is equivariant under gauge transformations and satisfies the continuity equation $\nabla_\mu J^\mu_I = 0$.

1.3.5 Dynamic field theory

1.3.5.1 Noether current and symmetry

Since the dynamics of *moving frames* is essential in this Thesis, the preliminaries also include a brief reminder of the dynamical field theory. Let $\mathscr{N}$ be a spacetime manifold with the target space $\mathscr{C}$ determined by the values of the fields at arbitrary points. Taking m real-valued scalar fields, $\{\phi_1, \ldots, \phi_m\} =: \phi$, the target manifold is $\mathscr{C} \subset \mathcal{C}^\infty(\mathbb{R}^m)$. We assume $\mathscr{S}[\phi]$ is the integral over $\mathscr{N}$ of a function called Lagrangian density $\mathscr{L}$, which depends on ϕ, its derivative and the position, $\mathscr{L}(\phi, \partial_\mu\phi, x^\mu)$. Note that the classical Lagrangian L is the volume integral of the Lagrangian density $\mathscr{L}$, i.e. $L = \int \mathrm{d}^n x\, \mathscr{L}$. The action functional $\mathscr{S} : \mathscr{C} \to \mathbb{R}$, is given by:

$$\mathscr{S}[\phi] \;=\; \int_{\mathscr{N}} \mathrm{d}^n x\; \mathscr{L}[\phi(x), \partial_\mu\phi(x), x] \tag{1.3.27}$$

[20] In physics, the matrix representation of the spacetime algebra $\mathrm{Cl}_{1,3}(\mathbb{R})$ is called *gamma matrices* or *Dirac matrices*.

In addition to this, some boundary conditions are required. The Euler-Lagrange equations for extremals of $\mathscr{S}$ are thus:

$$\partial_\mu \left(\frac{\partial \mathscr{L}}{\partial(\partial_\mu \phi)} \right) - \frac{\partial \mathscr{L}}{\partial \phi} = 0 \,, \tag{1.3.28}$$

Definition 1.3.2 (**Functional derivative**)**.** The functional derivative of a functional $\mathscr{S} : \mathcal{C}^\infty(\mathscr{N}) \to \mathbb{R}$ is the map $D\mathscr{S} : \mathcal{C}^\infty(\mathscr{N}) \to \mathcal{C}^\infty(\mathscr{N})^*$, where $\mathcal{C}^\infty(\mathscr{N})^*$ is the dual space of $\mathcal{C}^\infty(\mathscr{N})$, defined as

$$D\mathscr{S}[\phi](h) := \left. \frac{d}{d\epsilon} \right|_{\epsilon=0} \mathscr{S}[\phi + \epsilon\, h], \qquad \forall \phi, h \in \mathcal{C}^\infty(\mathscr{N}). \tag{1.3.29}$$

The functional derivative is also denoted by $D\mathscr{S}[\phi] = \delta\mathscr{S}/\delta\phi$, thus the notation $\delta\mathscr{S} = D\mathscr{S}\,\delta\phi$ resembles a 1-form [Courant and Hilbert 1989].

Remark 1.3.1. The previous definition is valid for a boundaryless spacetime manifold $\mathscr{N}$. In the case of a manifold with boundary we only consider test functions such that $h \in \mathcal{C}^\infty(\mathscr{N})$ such that $h|_{\partial\mathscr{N}} = 0$ and $\partial_\mu h|_{\partial\mathscr{N}} = 0$ for $1 \leq \mu \leq m$.

Definition 1.3.3 (**On-shell solution**)**.** A solution (subspace of $\mathscr{C}$) is called an *on-shell* solution if it consists of functions ϕ such that all functional derivatives D of the action functional $\mathscr{S}$ at ϕ are zero, that is:

$$D\mathscr{S}[\phi](h) = 0 \in \mathbb{R} \;\text{ for all } h \in \mathcal{C}^\infty(\mathscr{N}) \implies D\mathscr{S}[\phi] = 0 \in \mathcal{C}^\infty(\mathscr{N})^* \,, \tag{1.3.30}$$

where ϕ satisfies the given boundary conditions. In contrast, a solution is *off shell* if Eq. 1.3.30 is not satisfied for some functional derivative of the action functional.

If a functional derivative D allows some off-shell solution, we will say that D generates an off-shell symmetry. If this only holds on shell, we will say that D generates an on-shell symmetry. Then, we say D is a generator of an one-parameter symmetry Lie group [Peskin and Schroeder 2018].

Theorem 1.3.1 (**Noether current**)**.** *Given an infinitesimal transformation on $\mathscr{C}$, generated by a functional derivation D such that*

$$D\left[\int_{\mathscr{N}} \mathrm{d}^n x\, \mathscr{L} \right] = \int_{\partial\mathscr{N}} \mathrm{d}s_\mu\, F^\mu[\phi(x), \partial\phi, \partial\partial\phi, \ldots] \tag{1.3.31}$$

for all compact manifolds $\mathscr{N}$, i.e. $D[\mathscr{L}(x)] = \partial_\mu F^\mu(x)$ for all x, where we set $\mathscr{L}(x) = \mathscr{L}[\phi(x), \partial_\mu\phi(x), x]$. Then the following quantity:

$$J^\mu := \frac{\partial \mathscr{L}}{\partial(\partial_\mu \phi)} D[\phi] - F^\mu \tag{1.3.32}$$

satisfies the continuity equation $\partial_\mu J^\mu = 0$.

Therefore, J^μ is the Noether current associated with the symmetry. If we consider noncompact manifolds $\mathscr{N}$ with currents that decay sufficiently fast at infinity, the current can be integrated over a space-like slice $\mathscr{X}$. In this case, the continuity equation implies that we get a conserved quantity $\mathscr{Q}$ called the Noether charge:

$$\mathscr{Q} := \int_{\mathscr{X}} d^3x\, J^0 \tag{1.3.33}$$

1.3.5.2 Hamiltonian of Lorentzian manifolds

Let $(\mathscr{N}, g)$ be a four-dimensional Lorentzian manifold with metric g of signature $(1,3)$. Then, let g evolve in a dynamical system linked to a characteristic Lagrangian density $\mathscr{L}_m = \rho$ so-called **mass** density. General relativity and some modified gravities can be represented by a functional action $\mathscr{S}[g]$ that depends on a real scalar function $f \in \mathcal{C}^\infty(\mathbb{R}^N, \mathbb{R})$ of a set of N scalars built using the Riemann curvature tensor $R^\rho_{\alpha\beta\gamma}$ or the Ricci tensor $R_{\beta\gamma} := R^\beta_{\alpha\beta\gamma}$ among others, for example the Ricci scalar curvature $R := g^{\alpha\gamma}R_{\beta\gamma}$, or using scalars from torsion T like in parallel gravities [Achour *et al.* 2016, Krššák *et al.* 2019]. That is

$$\mathscr{S}[g] = \int d^4x\sqrt{-g}\,(f(R,\dots) + \mathscr{L}_m) \tag{1.3.34}$$

where the gravitational constant is normalized to $16\pi\mathrm{G} \equiv 1$. For instance, the standard Einstein-Hilbert action is simply given by $f(R,\dots) = R - \Lambda$, where Λ is a (*cosmological*) constant. In this case, Lagrangian equations are the equations of motion for the metric field, well-known as the Einstein field equations

$$G_{\alpha\beta} - \Lambda g_{\alpha\beta} = 8\pi\mathrm{G}P_{\alpha\beta}\,, \tag{1.3.35}$$

where $G_{\alpha\beta} := R_{\alpha\beta} - g_{\alpha\beta}R/2$ is the Einstein tensor and $P_{\alpha\beta} := -2\delta\mathscr{L}_m/\delta g^{\alpha\beta} + g_{\alpha\beta}\mathscr{L}_m$ is the stress-energy tensor.

If the manifold is foliated into a family of spacelike hypersurfaces (Def. 0.10), we can introduce a Hamiltonian formulation according to the ADM formalism [Arnowitt *et al.* 1959, Arnowitt *et al.* 2008, Deruelle *et al.* 2010]. This is useful because, from the Hamiltonian $\mathcal{H} := p\dot{q} - \mathscr{L}$, a set of *equations of motion* can be obtained for the generalized coordinates q and momenta p as $\dot{q} = \partial\mathcal{H}/\partial p$ and $\dot{p} = -\partial\mathcal{H}/\partial q$. Still according to the ADM formalism, the spatial submanifold can be interpreted as an embedding into the global spacetime and thus the metric elements can be separated in a temporal part g_{00} and another spatial part g_{ij} with $i,j \in \{1,2,3\}$. Moreover, ADM takes $\mathscr{L}_m = 0 = \Lambda$ and then the Lagrangian density can be rewitten as:

$$\mathscr{L} = -g_{ij}\partial_t\pi^{ij} + lh + 2l_i\pi^{ij}{}_{;j} - 2\partial_i s^i \tag{1.3.36}$$

where $l := (g^{00})^{-1/2}$ is the lapse, $l_i := g_{0i}$ is the shift, π^{ij} are conjugate momenta, h is the

Hamiltonian constraint and s^i are auxiliary momenta given by:

$$\pi^{ij} = \sqrt{-g}\left(\Gamma^0_{pq} - g_{pq}\Gamma^0_{rs}g^{rs}\right)g^{ip}g^{jq} \tag{1.3.37}$$

$$h = -\sqrt{g_s}R^k_k - \frac{1}{\sqrt{g_s}}\left(\frac{1}{2}\pi^2 - \pi^{ij}\pi_{ij}\right) \tag{1.3.38}$$

$$s^i = l_{0j}\pi^{ij} - \frac{1}{2}l^{0i}\pi + \nabla^i\sqrt{-g} \tag{1.3.39}$$

where $l^i := g^{0i}/g^{00}$, $\pi_{ij} := g_{ik}g_{jl}\pi^{kl}$, $\pi = g_{ij}\pi^{ij}$, $g := \det g_{\mu\nu}$ is the determinant of the metric and $g_s := \det g_{ij}$ is the determinant of the spatial metric. The ADM equations for the metric evolution are:

$$\partial_t g_{ij} = 2\frac{1}{\sqrt{-g_s g^{00}}}\left(\pi_{ij} - \frac{1}{2}\pi g_{ij}\right) + \nabla_i g_{0j} + \nabla_j g_{0i} \tag{1.3.40}$$

In this context, it is of special interest to study the evolution of the metrics with nonzero *lapse* ($g_{00} \neq 1$) and *shift* ($g_{0r} \neq 0$). This is the case of the manifold considered[21] in this Thesis.

1.3.6 Dynamics in the standard cosmology

1.3.6.1 Friedmann-Lemaître-Robertson-Walker metric

The universe is assumed to be a dynamical system characterized by maximum spatial symmetry, which included homogeneity and isotropy in the spatial sections of the metric. All these features are represented by the well-known Friedmann-Lemaître-Robertson-Walker (FLRW) metric $g = \mathrm{diag}(g_{tt}, g_{r'r'}, g_{\phi\phi}, g_{\theta\theta})$ that, expressed in spherical coordinates (t, r', ϕ, θ), are

$$g = g_{tt}dt^2 + g_{r'r'}dr'^2 + g_{\phi\phi}d\phi^2 + g_{\theta\theta}d\phi^2 \;=\; dt^2 + a(t)\left(\frac{dr'^2}{1 - Kr'^2} + r'^2 d\Sigma^2\right) \tag{1.3.41}$$

where $a : \mathbb{R}_{>0} \to \mathbb{R}_{>0}$ is a scale factor, $d\Sigma := \sin^2\phi d\theta^2 + d\phi^2$ and K is the spatial curvature. Notice that FLRW-based standard model set the lapse function as a constant $g_{tt} = 1$ or, alternatively, it uses another coordinate t' such that $dt' := \sqrt{g_{tt}}dt$ and therefore $g_{t't'} \equiv 1$ again. However, it may be not adequate in general for all the expanding manifolds, because time dilation is expected in an accelerated expansion of the spatial coordinates [Melia 2022, Melia 2023]. In fact, the condition $g_{tt} = 1$ implies the strong equivalence principle (SEP) applied to a free-fall observer (e.g. satellite-based measurements), thus it is useful to obtain light-derived quantities such as the *luminosity distance* or the *angular diameter distance* (defined in Appendix A).

[21] That is, an apparent inhomogeneous universe built from an appropriate transformation of the hyperconical metric

Then, the Ricci tensor components are $R_{tt} = -3\ddot{a}/a$, for the temporal coordinate, and $R_{ii} = -g_{ii}(a\ddot{a} + 2\dot{a}^2 + 2K)/a^2$ for the spatial coordinates, while the Ricci scalar curvature is

$$R_{FLRW} = -\frac{6}{a^2}(\ddot{a}a + \dot{a}^2 + K) \tag{1.3.42}$$

where K is assumed to be constant, for simplicity.

1.3.6.2 Friedmann equations

The dynamics of the universe is given by the Friedmann equations, which are derived from the Einstein field equations (Eq. 1.3.35. If one assumes that the universe is a homogeneous perfect fluid at rest (of density ρ and pressure p), with constant spatial curvature K, the following Friedmann equations are derived [Křížek and Somer 2023]:

$$\left(\frac{\dot{a}}{a}\right)^2 = \frac{8\pi\mathrm{G}\rho}{3} + \frac{\Lambda}{3} - \frac{K}{a^2} \tag{1.3.43}$$

$$\left(\frac{\ddot{a}}{a}\right) = -\frac{4\pi\mathrm{G}}{3}(\rho + 3p) + \frac{\Lambda}{3} \tag{1.3.44}$$

Defining the Hubble parameter as $H := \dot{a}/a$ and identifying the critical density defined by $\rho_{crit} := 3{H_0}^2/8\pi G$, where H_0 is the current value for the Hubble parameter, Eq. 1.3.43 is usually rewritten as:

$$\frac{H^2}{{H_0}^2} = \frac{\rho}{\rho_{crit}} + \frac{\rho_\Lambda}{\rho_{crit}} - \frac{K}{{H_0}^2 a^2}\,, \tag{1.3.45}$$

where ρ_Λ is the dark energy density, defined as $\rho_\Lambda := \Lambda/8\pi\mathrm{G}$. Assuming that matter density ρ is cold (non ultra-relativistic), its equation of state $w := p/\rho$ is approximately $w \approx 0$, and it varies by the expansion as a^{-3}. If the universe is dominated by radiation or ultra-relativistic particles, $w \approx 1/3$ and ρ varies as a^{-4}. Therefore, Eq. 1.3.45 can be rewritten as follows:

$$\frac{H^2}{{H_0}^2} = \Omega_r \left(\frac{a_o}{a}\right)^4 + \Omega_m \left(\frac{a_o}{a}\right)^3 + \Omega_K \left(\frac{a_o}{a}\right)^2 + \Omega_\Lambda\,, \tag{1.3.46}$$

where $\Omega_i := \rho_i/\rho_{crit}$ are the ΛCDM parameters for radiation (ρ_r), matter (ρ_m), dark energy (ρ_Λ) and curvature ($\Omega_K := -K/H_0^2 a_o^2$). Since the redshift z depends on the scale factor as $1 + z = a_o/a$, trivially, the parameter Hubble $H = \dot{a}/a$ depends on the redshift z too [Liddle 2003]. International projects assuming the ΛCDM model, such as the Wilkinson Microwave Anisotropy Probe (WMAP) and the Planck Mission, have estimated that $\Omega_r \approx 8.4 \cdot 10^{-5}$, $\Omega_m = 0.3089 \pm 0.0062$, $\Omega_\Lambda = 0.6911 \pm 0.0062$ and $\Omega_K \approx 0$. Finally, the deceleration parameter is defined by

$$q = -\frac{\ddot{a}a}{\dot{a}^2} = -1 - \frac{\dot{H}}{H^2}\,, \tag{1.3.47}$$

which is $q \approx \frac{1}{2}\Omega_m - \Omega_\Lambda \approx -0.54$ for $\Omega_r \approx 0 \approx \Omega_K$. Then, the Ricci scalar curvature (Eq. 1.3.42) is rewritten as

$$R_{FLRW} = -\frac{6\dot{a}^2}{a^2}\left(\frac{\ddot{a}a}{\dot{a}^2} + 1\right) = -6H^2\,(1-q)\ . \tag{1.3.48}$$

Under a geometrical viewpoint, this result is probably the most important of the standard cosmology since the scalar curvature is a geometrical invariant, while spatial curvature is not.[22]

Moreover, since GR assumes that the scalar curvature R of our manifold depends on the total density, and taking into account that it varies with time, the spatial curvature K could also be a function of time instead of the constant value considered in the $FLRW$ metric and in the Friedmann equations (Eq. 1.3.43–1.3.44).

1.3.6.3 Embedding of FLRW metrics

As mentioned in Sec. 1.1.2.2 (e.g., see Eq. 1.1.3), the FLRW metric is derived from the hypothesis of that our manifold $\mathscr{N}$ is spatially homogeneous and isotropic, and then a scale factor $a(t)$ is added ad-hoc to the spatial sections as a function that depends on a global time $t \in \mathbb{R}$. Therefore, this corresponds to a static embedding of spatial three-manifolds (hypersphere, plane or hyperboloid) into a four-Euclidean space (i.e., a minimal embedding or *class one*), plus a temporal dimension.

However, the resulting metric can also be embedded into pseudo-Euclidean spacetimes $\mathscr{M}$. According to Akbar 2017, the $K = 1$ FLRW manifold $\mathscr{N}$ is embedded in a class one (i.e. five-dimensional ambient Minkowskian spacetime). However, the $K = 0$ and $K = -1$ FLRW geometries are of *embedding class two*, and their corresponding pseudo-Euclidean spaces have strictly one negative ($\mathscr{M} = \mathbb{R}^{1,5}_\eta$ or $\mathscr{M} = \mathbb{R}^{5,1}_\eta$) and two negative eigenvalues ($\mathscr{M} = \mathbb{R}^{2,4}_\eta$ or $\mathscr{M} = \mathbb{R}^{4,2}_\eta$), respectively[23].

The $K = 1$ case is easily embedded by considering spherical coordinates $(t, \gamma, \phi, \theta) \in \mathbb{R}^4$ from the following (equivalent to Eq. 1.3.41):

$$g_{\mathscr{N}} \ = \ dt^2 - a(t)\left(d\gamma^2 + d\phi^2 + \sin^2\phi\, d\theta^2\right)\ , \tag{1.3.49}$$

where we identify that $r' := \sin\gamma$ is the comoving distance[24], and the five-dimensional Minkowski metric with coordinates $(\tau, \rho, \gamma, \phi, \theta) \in \mathbb{R}^5$ is:

$$g_{\mathscr{M}} \ = \ d\tau^2 - d\rho^2 + \rho^2\left(d\gamma^2 + d\phi^2 + \sin^2\phi\, d\theta^2\right)\ . \tag{1.3.50}$$

[22] In other words, the spatial curvature depends on the selection of coordinates.

[23] Recall the notation of pseudo-Riemannian manifolds, $\mathbb{R}^{n,m}_\eta := (\mathbb{R}^{n+m}, \eta)$, where with use η for flat metrics, which are also named pseudo-Euclidean space in general, or Minkowskian space when $n = 1$ or $m = 1$. Therefore, the metric is explicitly $\eta = (\underbrace{+1, \ldots, +1}_{n}, \underbrace{-1, \ldots, -1}_{m})$.

[24] Notice that $\gamma = \arcsin r'$, so $d\gamma^2 = dr'^2/(1 - r'^2)$.

Let $\varphi:\ U\subset\mathbb{R}^4\ \to\ \mathscr{N}\subset\mathscr{M}:=(\mathbb{R}^5,\eta_{1,4})$ be a parameterization of the $K=1$ FLRW hypersurface $\mathscr{N}\subset\mathscr{M}$ such that

$$\begin{array}{rcl}\varphi:\ U\subset\mathbb{R}^4 & \to & \mathscr{N}\subset(\mathbb{R}^5,\eta_{1,4})\\ p & \mapsto & \varphi(p)=(\tau,x,y,z,u)=:(\tau,\vec{\rho})\ \ \in\mathbb{R}\times S^3_\rho\subset\mathbb{R}\times\mathbb{R}^4\\ \| & & \|\\ (t,\gamma,\phi,\theta) & \mapsto & (b(t),a(t)\sin\gamma\sin\phi\sin\theta,\ a(t)\sin\gamma\sin\phi\cos\theta,\ a(t)\sin\gamma\cos\phi,\ a(t)\cos\gamma)\end{array}\tag{1.3.51}$$

where $\vec{\rho}:=(x,y,z,u):=(\rho\sin\gamma\sin\phi\sin\theta,\ \rho\sin\gamma\sin\phi\cos\theta,\ \rho\sin\gamma\cos\phi,\ \rho\cos\gamma)$ is a four-dimensional spatial vector expressed in spherical coordinates with $\rho:=||\vec{\rho}||=a(t)$, and $u:=a(t)\cos\gamma$, used to represent the hypersphere $S^3_\rho\subset\mathbb{R}^4$. Therefore, the partial derivatives of the parameterization are:

$$\begin{array}{rcl}\partial_t\varphi & = & (\dot{b}(t),0,0,0,0)+\dot{a}(t)(0,\sin\gamma\sin\phi\sin\theta,\ \sin\gamma\sin\phi\cos\theta,\ \sin\gamma\cos\phi,\ \cos\gamma)\\ \partial_\gamma\varphi & = & a(t)\cos\gamma(0,\sin\phi\sin\theta,\ \sin\phi\cos\theta,\ \cos\phi,\ 0)-a(t)\sin\gamma(0,0,0,0,1)\\ \partial_\phi\varphi & = & a(t)\sin\gamma\cos\phi(0,\sin\theta,\ \cos\theta,\ 0,\ 0)-a(t)\sin\gamma\sin\phi(0,0,0,1,0)\\ \partial_\theta\varphi & = & a(t)\sin\gamma\sin\phi(0,\cos\theta,\ -\sin\theta,\ 0,\ 0)\end{array}$$

and the metric of $\mathscr{N}$ is

$$g_{\mathscr{N}}\ =\ (\dot{b}(t)^2-\dot{a}(t))dt^2-a(t)^2\left(d\gamma^2+d\phi^2+\sin^2\phi\,d\theta^2\right)\ ,\tag{1.3.52}$$

where $a(t)$ and $b(t)$ must satisfy that

$$\dot{b}(t)^2-\dot{a}(t)^2=1\ \ \Rightarrow\ \ \dot{b}(t)^2=1+\dot{a}(t)^2\,.\tag{1.3.53}$$

For whatever the value of $\dot{a}(t)^2>0$ is, the coordinate $\tau=b(t)$ has a speed $|\dot{\tau}|>1$ faster than one.[25] On the other hand, if we repeat the same calculations but for the $K=-1$ case (e.g. into a $\mathbb{R}^{2,3}$ pseudo-Euclidean manifold), the resulting embedded hyperboloid requires the condition of

$$\dot{b}(t)^2+\dot{a}(t)^2=1\ \ \Rightarrow\ \ \dot{b}(t)^2=1-\dot{a}(t)^2\,.\tag{1.3.54}$$

and thus the general case (including $\dot{a}(t)\geq 1$) needs to be embedded into a six-dimensional manifold[26]. Finally, the $K=0$ case also require a six-dimensional ambient space, in general [Akbar 2017].

[25]The construction of this coordinate seems artificial under the viewpoint of Lorentz invariance of the nature. Only the static universe with $\dot{a}=0$ produces a natural time coordinate $\tau\propto t$.

[26]Notice that the basic (linear) expansion $\dot{a}(t)=1$ is automatically excluded for the five-dimensional embedding of $K=-1$ FLRW metric.

Chapter 2

Background Lorentzian manifold $\mathcal{H}^4$

2.1 A very brief introduction ...

2.1.1 ... to our universe: a Lorentzian manifold

This Chapter corresponds to the **first original contribution** of the Thesis [Monjo 2018, Monjo and Campoamor-Stursberg 2020], which is the definition (Sec. 2.2 and 2.3) and development (Sec. 2.4 and 2.5) of a family of minimally[1] embedded Lorentzian manifolds. As a novelty of this work, hyperconical metrics are naturally derived from an extrinsic perspective, by using moving reference frames (i.e., under dynamical considerations).

Let $\mathscr{M}$ be an ambient (or support) manifold, homeomorphic to some flat m-dimensional pseudo-Riemannian space. Thus, the first idea is to employ ambient spaces with minimum dimension to build our four-dimensional *universe manifold* $\mathscr{N}$ of signature $(1,3)$. Specifically, we explore the possibility of deriving *natural*[2] hypersurfaces living in a five-dimensional manifold $\mathscr{M} \cong \mathbb{R}^{1,4}$ or $\mathscr{M} \cong \mathbb{R}^{2,3}$. The second intuitive idea is that a simple way to build four-dimensional manifolds $\mathscr{N} \subset \mathscr{M}$ with homogeneous *Cauchy surfaces*[3] is to consider symmetric parameterizations with positive, zero or negative spatial curvature. These ideas are also motivated from the alleged existence of an absolute reference frame in our universe, sliced[4] in space-like Cauchy surfaces Σ, and with a global time t; which are: a) the CMB rest frame for the spatial sections (Σ), since a CMB dipole is produced by the velocity of the solar system (627 km/s) with respect to this rest frame [Kamionkowski and Knox 2003]; and b) the *age of the universe* (t), measured from independent techniques $(13.6 \pm 0.02$ Gyr$)$[5].

[1] An embedding $f : \mathscr{N} \to \mathscr{M}$ of $\mathscr{N}$ in $\mathscr{M}$ is minimal when $\dim(\mathscr{M})$ is the minimum possible dimension to realize the embedding. In our case, we suppose that the ambient spacetime $\mathscr{M}$ is homeomorphic to the five-dimensional Minkowskian spacetime $\mathbb{R}^{1,4}_\eta$, while our embedded Lorentzian manifold $\mathscr{N}$ is a family of hypercones $\mathscr{N} = \mathcal{H}^4$ such that $\mathrm{T}_p\mathscr{N} \cong \mathbb{R}^{1,3}_\eta$, where $p \in \mathscr{N}$.

[2] Here, *natural* means that all the speeds are lesser or equal to one, in contrast to Eq. 1.3.53.

[3] See Def. 0.15 for deeper details.

[4] See Def. 0.16 and the following ones to find the appropriate definitions.

[5] See for example Adam *et al.* 2015, OMalley *et al.* 2017, Schlaufman *et al.* 2018, Schlaufman *et al.* 2018, Jimenez *et al.* 2019, Aghanim *et al.* 2020a, Aghanim *et al.* 2020b.

2.1.2 . . . to the motion: dynamical embeddings

Despite the possibility of pseudo-Euclidean embeddings (Sec. 1.3.6.3), standard metrics of the universe (i.e. FLRW metrics) are classically derived in two steps: The first step is to obtain spatial sections from a static embedding into a flat four-dimensional Euclidean space, and the second step is to introduce a time-dependent scale factor $a(t)$ and the temporal coordinate t. However, this "composite" or "superposition" procedure is not adequate for (dynamical) Lorentzian manifolds, since time and space are mixed in the same continuous spacetime.

Let $\vec{\ell}$ be spatial coordinates of an expanding manifold; so they can be rewritten by using comoving coordinates $\vec{\ell'}$ and a scaling factor $a(t)$ varying with time t. For instance, let $S^3_R := \left\{\vec{\ell} \in \mathbb{R}^4 : |\vec{\ell}| = R(t)\right\}$ be an expanding 3-sphere of radius $R(t) \in \mathbb{R}_{\geq 0}$ and centred in the origin, but the reasoning is equivalent for the symmetric 3-hyperboloid space. Then, the scaling factor is $a(t) = R(t)/R(t_0)$ and total spatial coordinates are $\vec{\ell} = a(t)\vec{\ell'} \in S^3_R$. Therefore, the differential arc length contains both spatial and temporal contributions, i.e., $d\ell = a(t)d\ell' + \ell' da(t)$. Notice that the second term can be assimilated in the spatial term as a radial inhomogeneity. To solve this problem we need to introduce the *dynamical embedding*.

Our notion of *dynamical embedding* assumes a (flat) ambient spacetime where our curved Lorentzian manifold lives and evolves according to a *global time* (Def. 0.17). Then, we hypothesize that local observers measure distances according to their *comoving path* and isometric transformations are explored. Therefore, this concept is different to the *local dynamical embedding* defined by Capistrano *et al.* 2022, which is locally evolving in a five-dimensional bulk with Nash deformations.

It is also different of the *dynamic embedding* defined by [Noskov 2013], so-called Model of Embedded Spaces (MES), which is based on the hypothesis that any matter particle (an element of distributed matter) has its own space, and the real spacetime of the universe is the resultant *dynamic embedding* of eigenspaces of matter. This last idea is very close to the *geons* of Wheeler and to the *gravity source* proposed in this Thesis (see Def. 5.3.1).

2.2 Extrinsic Lorentzian hypercone

2.2.1 What is it?

This Section is an early definition of the family of hyperconical metrics, used throughout the Thesis, except for *particle field dynamic* (Chapter 5 and Sec. 6.3) since it only requires *small* Minkowskian neighborhoods (i.e., with spatial sections of diameter $\ll 1$). In order to better understand the main motivations of the work, we prefer to first introduce an intuitive construction of the metrics here (Sec. 2.2 and Sec. 2.3), and then, a (more formal) mathematical derivation is displayed in Sec. 2.4.

2.2.2 The universe manifold ($\mathcal{H}^4$)

Although there exists infinity ways to define Lorentzian manifolds, our first attempt (linear expansion) produced good results (Chapters 3 and 4). Thus, we assume that the distance between any two paths $X, O \in \mathcal{C}(\mathbb{R}_{>0}, \mathscr{M})$, in a 5-dimensional flat manifold $\mathscr{M}$, expands as a function of a *global time*[6] coordinate $t \in \mathbb{R}_{>0}$, that is $X(t), O(t) \in \mathscr{M}$, so we fix for instance the point of $O(t)$ as a reference:

$$\mathcal{H}^4 := \{X(t) \in \mathscr{M} \ : \ ||X(t) - O(t)|| = \beta_0 t\} . \tag{2.2.1}$$

Here, $\beta_0^2 \in \mathbb{R}$ is assumed to be constant with respect to the time $t \in \mathbb{R}_{>0}$. Notice that for the homogeneous equation (with $\beta_0 = 0$), the manifold $\mathcal{H}^4$ is a light hypercone (with positive spatial curvature and linear expansion). That is, since the extra dimension is used to built spatial sections (with positive, zero or negative curvature), the resulting dynamics of $\mathcal{H}^4$ is a linear or **inertial expansion**, inherited[7] from the metric of the ambient space.

First let $\mathscr{M}$ be homoemorphic to $\mathbb{R}^{1,4}$; for instance, a 5-Minkowskian spacetime-like manifold defined by $(\mathbb{R}_{\geq 0} \times \mathbb{R}^4, \eta_{1,4})$[8], with inner product $(\cdot)$ given by the usual Minkowskian metric η of signature (1, 4).[9]

Then, let $C := (\mathrm{T}_O\mathscr{M}, I_d)$ be a coordinate chart so that the coordinates of the points $X(t), O(t) \in \mathscr{M}$ are respectively $X(t) = (x^0, ..., x^4)$ and $O(t) = \mathbf{0} := (0, ..., 0)$, with the identity map I_d. We rewrite the coordinates of $X(t)$ as $(t_X, \vec{r}, u)$ for convenience, where $\vec{r} := (x^1, x^2, x^3) \in \mathbb{R}^3$ is the ordinary 3-vector, $u := x^4 \in \mathbb{R}$ is the additional (fourth) spatial dimension, and $t_X := x^0 \in \mathbb{R}_{\geq 0}$ is the time dimension. Choosing $t_X = t$, the equation of the hypersurface $\mathcal{H}^4$ is now $\nu^2 t^2 - \vec{r}^2 - u^2 = 0$ with "**speed**" ν such that $\nu^2 := 1 - \beta_0^2$ and $\beta_0 \neq 1$. Note that the hypercone with $\nu > 0$ is an asymptotic limit of

[6] See Def. 0.17.

[7] For $\beta_0 = 0$ in 2.2.1, the inseparable relationship between space and time induces a linear expansion of embedded objects.

[8] It is evident that $\mathscr{M}$ is not differentiable in the point $O(t) = \mathbf{0}$, so one could build a differentiable manifold as $\mathscr{M} := (\mathbb{R}_{>0} \times \mathbb{R}^4, \eta_{1,4})$. However, let us to extend the manifold to include the "singular" point $O(t)$ for its interest as an origin of coordinates.

[9] All the five dimensions of our *ambient spacetime* are *macroscopic* in contrast to the extra dimension of Kaluza-Klein that was supposed to be curled up and microscopically compactificated as a thin cylinder that resembles a line.

hyperboloid manifolds. In fact, if the constraint is taken as $t^2-\vec{r}^2-u^2=\alpha$ with constant $\alpha\neq 0$, the spaces are known as *de Sitter universes* [Wise 2015, Gryb 2015]. Moreover, $\mathcal{H}^4$ is not a Dirac-Milne universe [Benoit-Lévy and Chardin 2012] because $\mathcal{H}^4$ admits positive spatial curvature for $\beta_0<1$, being a (speed-light-expanding) unitary 3-sphere for $\beta_0=0$.

The above coordinates and considering the two minimum ambient manifolds (i.e. $\mathbb{R}^{1,4}$ or $\mathbb{R}^{2,3}$) can be compactly noted as $\mathscr{M}\cong\mathbb{R}^5_{\eta\pm}:=(\mathbb{R}^5\setminus\{\mathbf{0}\},\eta_\pm)$[10] with metric $\eta_\pm:=(+1,-1,-1,-1,\pm1)$, where we can identify $\mathbb{R}^5_{\eta+}\equiv\mathbb{R}^{2,3}$ and $\mathbb{R}^5_{\eta-}\equiv\mathbb{R}^{1,4}$. Thus, using this notation, the **family of hypercones** is defined as follows:

Definition 2.2.1 (**Hypercone**)**.** We will say that $\mathcal{H}^4_{\beta\pm}\subset\mathbb{R}^5_{\eta\pm}:=(\mathbb{R}^5\setminus\{\mathbf{0}\},\eta_\pm)$ is an embedded hypercone if satisfies that

$$\mathcal{H}^4_{\beta\pm}:=\{(t,\vec{r},u)\in\mathbb{R}^5_{\eta\pm}:t^2-\vec{r}^2\pm u^2=\beta^2_\pm t^2\}\tag{2.2.2}$$

with constant $\beta_\pm\in\{\beta^2\in\mathbb{R}:\pm(\beta^2-1)>0\}$ and $\vec{r}\in\mathbb{R}^3$. That is, $\beta^2_+>1$ and $\beta^2_-<1$. Alternatively, it can be considered a Wick rotation for the coordinate u with η_-.

Remark 2.2.1 (**The manifold $(\mathcal{H}^4_{\beta\pm},\,\eta_\pm)$ is spatially homogeneous**)**.** The homogeneity of $\mathcal{H}^4_{\beta\pm}$ is verifiable because it can be foliated by spatial hypersurfaces Σ_t such that, for all $p,q\in\Sigma_t$ and for all t, there exists a transformation (diffeomorphism) carrying the point p to point q and leaving the metric invariant. In other words, a spherical[11] submanifold $S^3_{t\pm}$ can be defined for each time t as the intersection between the hypercone $\mathcal{H}^4_{\beta\pm}$ and the isochronous hyperplane at this time t:

$$S^3_{t\pm}:=\left\{(t,\vec{r},u)\in\mathbb{R}^5:\vec{r}^2\mp u^2=\nu^2t^2\right\}\subset\mathcal{H}^4_{\beta\pm}\tag{2.2.3}$$

That is, the (global) time coordinate t is considered as the age of the universe (radius) and the t-isochronous 3-sphere or 3-hyperboloid $S^3_{t\pm}$ could be homeomorphic to its expanding spatial section (Eddington idea), locally conformally flat. Consequently, the universe manifold is globally hyperbolic, i.e, each $S^3_{t\pm}$ is also a *Cauchy surface*[12] [Eardley 1986]. For instance, let (t,θ,ϕ,γ) be spherical coordinates of $\mathcal{H}^4_{\beta\pm}$ such that $u=\nu t\cos\gamma$ and $|\vec{r}|=\nu t\sin\gamma$. Then, a natural foliation of $\mathcal{H}^4_{\beta\pm}$ is given by the Cauchy surfaces $\{S^3_{t\pm}\}_t$ and their transversal timelike curves $\left\{x|_\gamma:\mathbb{R}_{>0}\to\mathcal{H}^4_{\beta\pm}\right\}$ with constant angle; for example, $\gamma\in[0,\pi/2)$ for $\mathcal{H}^4_{\beta-}$ with $\beta_-=0$, and thus $t\mapsto x|_\gamma(t)=(t,\ \nu t\sin\gamma\,\vec{e}_r,\ \nu t\cos\gamma)\in\mathcal{H}^4_{\beta-}$, where $\vec{e}_r:=\vec{r}/|\vec{r}|$ is a constant direction in $\mathbb{R}^3$.

Remark 2.2.2 (**The manifold $(\mathcal{H}^4_{\beta\pm},\,\eta_\pm)$ is spatially isotropic**)**.** Note that $\mathcal{H}^4_{\beta\pm}$ can be covered by a set of timelike curves $\{x|_\gamma\}\subset\mathcal{H}^4_{\beta\pm}$ and for all $p\in x|_\gamma$ and for all $v,w\in\mathrm{T}_pS^3_{t\pm}$ orthogonal to $x|_\gamma$ there exists a transformation (diffeomorphism) leaving fixed p and carrying v to w, and leaving the metric invariant. These curves $\{x|_\gamma\}$ are called comoving observers.

[10] The point $\mathbf{0}$, origin of coordinates, is now removed to avoid division problems in the Eq. 2.3.2

[11] Of course, it is a 3-sphere for $\nu^2>0$ and a 3-hyperboloid for $\nu^2<0$. For the last case, we need to apply a Wick rotation to transform imaginary to real coordinates.

[12] Remember that a *Cauchy surface* is any subset of spacetime that is intersected by every causal (timelike) curve exactly once.

Since the universe manifold $\mathcal{H}^4_{\beta\pm}$ is sliced in spatial Cauchy hypersurfaces with a global time t, its expansion is an **absolute movement** with respect to the origin of coordinates, $O = (0, \vec{0}, 0)_C \in \mathscr{M}$, which is fixed (with respect to chart $C = (\mathrm{T}_O\mathscr{M}, I_d)$). Therefore, the minimum movement of spacelike trajectories corresponds to the comoving observers with coordinates $(t, \vec{0}, \nu t)_C \subset \mathcal{H}^4_{\beta\pm}$. These trajectories are interpreted as paths at rest with respect to the expanding universe $S^3_{t\pm}$.

Definition 2.2.2 (**Dynamical embedding**)**.** Let $\mathbb{R}^{1,3}_g := (\mathbb{R}_{>0} \times \mathbb{R}^3,\ g)$ be a Lorentzian manifold with Lorentzian metric g and global notion of time[13] in $\mathbb{R}_{>0}$. We will say that $f^{-1} : \mathbb{R}^{1,3}_g \to \mathcal{H}^4_{\beta\pm} \subset \mathbb{R}^5_{\eta\pm}$ is a **dynamical embedding** of $\mathbb{R}^{1,3}_g$ in $\mathbb{R}^5_{\eta\pm}$, that is an intrinsic perspective of comoving observers, if there exists some diffeomorphism so-called **inverse comoving chart**,

$$f : (\mathcal{H}^4_{\beta\pm} \subset \mathbb{R}^5_{\eta\pm},\ \eta_\pm) \to \mathbb{R}^{1,3}_g\ , \tag{2.2.4}$$

such that the metric g generates the (local) distances in every open neighborhood $U \subset \mathcal{H}^4_{\beta\pm}$ and produces the same proper time as in the Minkowski spacetime.

Remark 2.2.3 (**Dinamical embedding is distorting**)**.** The above diffeomorphism f is not the usual "inverse chart" [14] because the origin of measurements is static in $\mathbb{R}^5_{\eta\pm} \supset \mathcal{H}^4_{\beta\pm}$ and comoving in $\mathcal{H}^4_{\beta\pm} \cong \mathbb{R}^{1,3}_g$, which is generally a distorting transformation f between both perspectives of the same manifold $\mathcal{H}^4_{\beta\pm}$ for spatial large distances but nor for small neighborhoods ($|\vec{r}| \ll 1$), since the transformation should be locally conformal.

[13] According to Def. 0.17.

[14] For embedded hypersurfaces (Riemannian manifolds) into static Euclidean spaces, charts are also static (non-dynamical systems), and therefore the induced metric g is directly given by the arc length over the hypersurface.

2.3 From moving frames to dynamical embedding

2.3.1 Problem of measuring arc length (proper time)

According to the Eq. 2.2.3 of the Remark 2.2.1, a representative Cauchy hypersurface of our manifold is given by $S^3_{t\pm} = \{(t, \vec{r}, u) \in \mathbb{R}^5 : \vec{r}^2 \mp u^2 = \nu^2 t^2\}$ for $\nu^2 = 1 - \beta^2_\pm \in \mathbb{R}$. However, the value of ν^2 is actually not free at all. As one can find in Proposition 2.4.1 and in Lemma 3.2.1, it is requited to be $\nu^2 = 1$ (i.e., $\beta_\pm = \beta_0 = 0$). Despite this constraint, we employ $\beta_\pm$ as a presumed free parameter of the model in order to analyse its role in dynamical effects $\mathcal{H}^4_{\beta\pm} \subset \mathbb{R}^5_{\eta\pm}$ with $\eta_\pm = \mathrm{diag}(+1, -1, -1, -1, \pm 1)$.

In $\mathcal{H}^4_{\beta\pm}$, inertial observers are comoving with the linear expansion, thus the definition of *observed length* is not immediate[15]. To preserve the proper time, the initial[16] reference instant $t_0 \in \mathbb{R}_{\geq 0}$ is fixed by the observer although its actual position $X(t) := (t, s(t)) := (t, \vec{r}(t), u(t)) \in \mathcal{H}^4_{\beta\pm} \subset \mathbb{R}^5_{\eta\pm}$ is moving as $X : I \subset \mathbb{R}_{>0} \to \mathcal{H}^4_{\beta\pm}$, a function of the time t due to the expansion. That is, an expanding deformation needs to be applied to the spatial coordinates $s := (\vec{r}, u) : I \subset \mathbb{R}_{>0} \to \mathbb{R}^4$ of the observer.

According to the embedding geometry, an observer that lives in the path X will measure local distances in $\mathrm{T}_{x(t)}\mathcal{H}^4_{\beta\pm}$ as in the Minkowskian space $\mathbb{R}^{1,3}_\eta := (\mathbb{R}^4, \eta_{1,3})$, that is $x : I \subset \mathbb{R}_{>0} \to \mathbb{R}^{1,3}_\eta$. Therefore, the proper time must be the same. For instance, let $x_0, x_t \in \mathbb{R}^{1,3}_\eta$ be two spacetime events of an observer with coordinates $x_0 := x(t_0) = (t_0, \vec{0})$ and $x_t := x(t) = (t, \vec{0})$ with $0 < t_0 < t$. Their extended points in $\mathcal{H}^4_{\beta\pm}$ are ${x_0}' = X(t_0) = (t_0, \vec{0}, \nu t_0)$ and ${x_t}' = X(t) = (t, \vec{0}, \nu t)$, as we can take (not tangent) spaces $\mathbb{R}^{1,3}_\eta$ that intersect to $\mathcal{H}^4_{\beta\pm}$ at points x_0 and x_t. From Eq. 2.2.4, we need to find the inverse of a *moving chart* (Def. 2.2.2), that is, a smooth map $f : (\mathcal{H}^4_{\beta\pm} \subset \mathbb{R}^5_{\eta\pm}, \eta_\pm) \to (\mathbb{R}_{>0} \times \mathbb{R}^3, g) \cong \mathbb{R}^{1,3}_g \cong \mathrm{T}_{x(t)}\mathcal{H}^4_{\beta\pm}$ such that the metric g inherits the spatial section of $\mathcal{H}^4_{\beta\pm}$, but produces the same local ($\vec{r} = \vec{0}$) spacetime distance at rest in $\mathbb{R}^{1,3}_g$ as it does for $\mathbb{R}^{1,3}_\eta$. As x_t and x_0 are at rest by definition in $\mathbb{R}^{1,3}_\eta$, the distance turns out to be the proper time of the observer:

$$t - t_0 = ||x_t - x_0||_{\eta_{1,3}} = ||f({x_t}') - f({x_0}')||_g \tag{2.3.1}$$

where $||\ ||_{\eta_{1,3}}$ is the usual Minkowski vector norm, while $||\ ||_g$ is the Lorentzian norm generated by the metric g.

[15] In static embeddings of a manifold $\mathscr{E}$, the metric elements $g_{ab} = e_a \cdot e_b$ are directly obtained from the basis elements $\{e_a\}_a$ (generators of the tangent bundle) given by the derivatives $e_a = \partial\varphi/\partial x^a$ of the manifold parameterization $\varphi : U \subset \mathbb{R}^\nu \to \mathscr{E} \subset \mathscr{M}$, which provides an embedding into its ambient space $\mathscr{M}$ with scalar product $(\,\cdot\,)$. However, a dynamical Lorentzian manifold (expanding at the speed of light) cannot be directly transformed from the static reference of the ambient spacetime to the moving frames of a comoving observer.

[16] Here, the initial instant is a specific value of the time coordinate to make measurements with respect the time.

2.3.2 Observer path solution

Let $y' : t \mapsto y'(t) = (t, \vec{r}, \nu t)$ and $x' : t \mapsto x'(t) = (t, \vec{0}, \nu t) \in (\mathcal{H}^4_{\beta\pm}, \eta_\pm)$ be two comoving paths for $t \in I \subset \mathbb{R}_{>0}$, considering the second one as an observer; that is, taking $y'_0 := y'(t_0)$ and $x'_0 := x'(t_0)$ as a point of the past. If the observer performs measurements in t_0 and t, there exists a deformed path $y''(t) := \mathscr{T}_t y'(t)$ intersecting $\mathcal{H}^4_{\beta\pm}$ during these measurements, with changes in $0 < t_0 < t$ due to a *deformation operator*, $\mathscr{T}_t$, such as

$$\begin{aligned} \mathscr{T}_t : (\mathcal{H}^4_{\beta\pm} \subset \mathbb{R}^5_{\eta\pm},\ \eta_\pm) &\rightarrow \mathbb{R}^5_{\eta\pm} \\ {y_0}' = (t_0, s(t_0)) &\mapsto {y_0}''(t) := \left(t_0, \frac{t}{t_0} s(t_0)\right) \end{aligned} \tag{2.3.2}$$

where $t_0 \in \mathbb{R}_{>0}$ and $s : t \in \mathbb{R}_{>0} \mapsto s(t) := (\vec{r}(t), \nu t) \in \mathbb{R}^4$ are respectively the temporal and spatial components of the path $y : t \in \mathbb{R}_{>0} \mapsto y(t) = (t, s(t)) = (t, \vec{r}, \nu t) \in \mathcal{H}^4_{\beta\pm}$.

With this, $x'' = x'$ and ${x_0}'' = (t_0, \vec{0}, \nu t) \in \mathbb{R}^5_{\eta\pm}$. Now, the u-component of the difference $x' - {x_0}''$ is zero, and the proper time is the same that Eq. 2.3.1. Therefore a metric g for $\mathrm{T}_{{x_0}''}\mathcal{H}^4_{\beta\pm}$ should be induced by the quadratic form of variations of $X := x' - {x_0}''$ in $\mathbb{R}^5_{\eta\pm}$:

$$||d\,(x - x_0))||^2_g = ||d\,(f(x') - f({x_0}'))||^2_g = ||d\,(x' - {x_0}'')||^2_{\eta_\pm} = ||dX||^2_{\eta_\pm}\ . \tag{2.3.3}$$

where $dx(t) \equiv d\tilde{x}(q)$ for some parameterization $\tilde{x} : \mathbb{R}^4 \mapsto \mathcal{H}^4_{\beta\pm}$ of each path $x : \mathbb{R} \to \mathcal{H}^4_{\beta\pm}$.

Therefore, Eq. 2.3.3 is equivalent to saying that the observers fix the time coordinate for measurements using a initial time t_0, but they are moving with respect to $O := (0, \vec{0}, 0)$. Thus, their reference line is $\widehat{O} : t \mapsto \widehat{O}(t) := \mathscr{T}_t x'(t_0) = (t_0, \vec{0}, \nu t) = x''_0 \in \mathbb{R}^5_{\eta\pm}$ with $t \in I \in \mathbb{R}_{>0}$ (note that $\widehat{O}(I) \not\subset \mathcal{H}^4_{\beta\pm}$ and only intersects at $t = t_0$). This reference line allows us to define the notion of *moving charts*.

2.3.3 Extrinsic hyperconical metric tensor

Let $t \in \mathbb{R}_{>0} \mapsto \vec{r}(t) \in \mathbb{R}^3$ be a three-dimensional Euclidean curve and $t \in \mathbb{R}_{>0} \mapsto u(t) \in \mathbb{R}$ be a map to represent the extra spatial dimension mentioned above. Thus, let $\widehat{O} : t \mapsto \widehat{O}(t) := \mathscr{T}_t(t_0, \vec{0}, \nu t_0) = (t_0, \vec{0}, \nu t) \in \mathbb{R}^5_{\eta\pm}$ be a reference line, and let

$$\begin{aligned} X : \mathbb{R}_{>0} &\rightarrow \hat{\mathcal{H}}^4_{\beta\pm} := \{x - \widehat{O}\ :\ x \in \mathcal{H}^4_{\beta\pm}\} \subset \mathbb{R}^5_{\eta\pm} \\ t &\mapsto X(t) := (t - t_0,\ \vec{r}(t),\ u(t) - \nu t) \end{aligned} \tag{2.3.4}$$

be the parameterization of any $\widehat{O}$-referred curve on the *deformed* hypersurface $\hat{\mathcal{H}}^4_{\beta\pm} \cong \mathcal{H}^4_{\beta\pm}$ (but $\hat{\mathcal{H}}^4_{\beta\pm} \neq \mathcal{H}^4_{\beta\pm}$) generated by $\widehat{O}$, that is, measured by an observer of $\mathcal{H}^4_{\beta\pm}$ with reference path $\widehat{O}$ in $\mathbb{R}^5_{\eta\pm}$, as in Sec. 2.3.2. Then, let

$$\begin{aligned} \tilde{X} : U \subset \mathbb{R}^4 &\rightarrow \hat{\mathcal{H}}^4_{\beta\pm} \\ y := (t, \theta, \phi, \gamma) &\mapsto \tilde{X}(y) = (t - t_0,\ \nu t \sin\gamma\, \vec{e}_r(\theta, \phi),\ \nu t \cos\gamma - \nu t) \\ &\qquad\quad \| \\ &\qquad X(t) = (t - t_0,\ \ \vec{r}(t),\ \ u(t) - \nu t) \end{aligned}$$

be a parameterization of $\hat{\mathcal{H}}^4_{\beta\pm}$ where $\vec{e}_r(\theta,\phi) := (\sin\theta\cos\phi,\ \sin\theta\sin\phi,\ \cos\theta) \in \mathbb{R}^3$ are spatial components[17].

Therefore, the metric $d\tilde{X}^2 \equiv g = g_{\mu\nu}dy^\mu dy^\nu = (\eta_\pm)_{\alpha\beta}dX^\alpha dX^\beta \equiv dX^2$ with the coordinates $(y^\mu)^3_{\mu=0} = (t,\theta,\phi,\gamma)$ is given by the *differential element*[18] $dX = (dX^\alpha)^4_{i=0}$, which is equivalent to the one defined in Eq. 2.3.3. This is easily obtained knowing that $d\vec{r}'$ can be decomposed in the spherical coordinates as $d\vec{r}' = dr'\vec{e_r} + r'd\vec{e}_r(\theta,\phi)$, where $d\vec{e}_r(\theta,\phi) = d\theta\vec{e_\theta} + \sin\theta d\phi\vec{e_\phi}$ is orthogonal to the radial direction $\vec{e_r} := \vec{r}/|\vec{r}|$. Since $dt_0 = 0$, the non-zero elements of the **hyperconical metric** g for the reference $\widehat{O}$ are:

$$\begin{array}{rcl} g_{tt} &=& 2k^{-1}(b-1)+1 \\ g_{rr} &=& -a^2/b^2 \\ g_{\theta\theta} &=& -a^2r'^2 \\ g_{\phi\phi} &=& -a^2r'^2\sin^2\theta \\ g_{tr} &=& -a\frac{r'}{t_0}b^{-1} \end{array} \tag{2.3.5}$$

where $b := \sqrt{1-kr'^2/t_0^2}$, with $k^{-1} := \nu^2 = 1-\beta_0^2$, and $a = t/t_0$ is the scale factor.

Remark 2.3.1. Note that if $\mathscr{T}_{t_0}$ is used instead of $\mathscr{T}_t$, a static metric equivalent to the FLRW universes but without expansion is obtained. That is, the line defined by $X' : (t,\vec{r},u) \mapsto X'(t) = (t-t_0,\vec{r}',u-\nu t_0) := (t-t_0,(t_0/t)\vec{r},u-\nu t_0)$ leads to static FLRW metrics of curvature $k = 1/\nu^2$ for $t_0 \equiv 1$.

To explicitly show some example of the hyperconical metric g at a local scale ($r' \ll t_0$), the squared arc length [19] $ds^2 := ||d\tilde{X}||^2 = g_{ij}dx^idx^j$ of Eq. 2.3.5 for $k=1$ is approximately

$$ds^2 \approx dt^2\left(1-\frac{r'^2}{t_0^2}\right) - \frac{t^2}{t_0^2}\left(\frac{dr'^2}{1-\frac{r'^2}{t_0^2}} + r'^2d\Sigma^2\right) - \frac{2r't}{t_0^2}\frac{dr'dt}{\sqrt{1-\frac{r'^2}{t_0^2}}} \tag{2.3.6}$$

where $r' := (t_0/t)r \ll t_0$ is the **comoving distance**.

Symmetrical spatial elements g_{ii} obtained from Eq. (2.3.5) are compatible with some FLRW metrics, but elements $g_{tt} \neq 1$ and $g_{tr} \neq 0$, respectively, imply *lapse* and *shift* terms, as in the ADM formulation of gravity [Deruelle *et al.* 2010]. To compare g with the FLRW metrics, a diagonal version of the metric is given by the coordinate change

[17] For instance, one can choose $\vec{e}_r(\theta,\phi) := (\sin\theta\cos\phi,\ \sin\theta\sin\phi,\ \cos\theta)$, and therefore, the derivatives are $d\vec{e}_r(\phi,\theta) := -(\cos\theta\cos\phi\,d\theta - \sin\theta\sin\phi\,d\phi,\ \cos\theta\sin\phi\,d\theta + \sin\theta\cos\phi\,d\phi,\ -\sin\theta\,d\theta) = (\cos\theta\cos\phi,\ \cos\theta\sin\phi,\ -\sin\theta)d\theta + (-\sin\phi,\ \cos\phi,\ 0)\sin\theta d\phi = d\theta'\vec{e_\theta} + \sin\theta' d\phi\vec{e_\phi}$, where $\vec{e_\phi} := (-\sin\phi,\cos\phi,0)$ and $\vec{e_\theta} = (\cos\theta\cos\phi,\cos\theta\sin\phi,-\sin\theta)$ are orthonormal directions in $\mathbb{R}^3$.

[18] The notion of *differential element* or *differential line element*, $dX = \partial_\alpha X\,dx^\alpha$, is commonly used in physics to represent the derivatives of the parameterization X of the manifold (or of any curve on the manifold), so its quadratic form dX^2 is identically equal to the metric of the manifold.

[19] Recall that the squared arc length $ds^2 := ||d\tilde{X}||^2 = g_{ij}dx^idx^j$ is also equivalent to the metric $g = g_{ij}dx^i\otimes dx^j$ with symmetrized basis $dx^idx^j := \frac{1}{2}(dx^i\otimes dx^j + dx^j\otimes dx^i)$ and $dx^i\otimes dx^j = dx^j\otimes dx^i$.

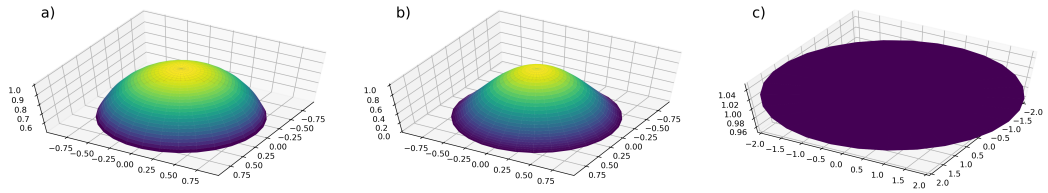

Figure 2.3.1: Isochronous hypersurfaces normalized to universe age scale ($t_0 \equiv 1$) for: a) linearly expanding homogeneous space (t-isochronous), obtained by considering coordinates such that $g_{tr} \neq 0$ and $g_{tt} \neq 1$; b) linearly expanding inhomogeneous space (t'-isochronous), obtained by considering coordinates such that $g'_{tr} = 0$ and $g'_{tt} = 1$; c) apparently-accelerated flat (homogeneous) space according to locally conformal map (distorted azimuthal projection).

$t \rightarrow t' := t\sqrt{2k^{-1}(b-1)+1}$, which is equivalent to selecting $g'_{tt} = 1$, $g'_{tr} = 0$ and:

$$g'_{rr} = g_{rr} - \frac{g_{0r}^2}{g_{00}} = -a(t',r')^2 \frac{1-k^{-1}(b-1)^2}{b^2(2k^{-1}(b-1)+1)} \tag{2.3.7}$$

$$g'_{\phi\phi} = -a(t',r')^2 r'^2 sin^2\theta \tag{2.3.8}$$

$$g'_{\theta\theta} = -a(t',r')^2 r'^2 \tag{2.3.9}$$

where $a(t',r') = t'/(t_0\sqrt{2k^{-1}(b-1)+1})$. Despite this, important differences remain in the FLRW metric.[20]

The result is an (apparent)[21] inhomogeneous hypersurface similar to the Lemaître-Tolman-Bondi (LTB) type [Yan *et al.* 2015, Yoo and Watanabe 2012], but with the same scale factor a for the radial and angular components of the metric (in contrast with the LTB universes, that distinguish between angular and radial expansion). Differences are also found comparing with the McVittie metric, which is an asymptotically spatially flat FLRW metric for the largest distances [Pérez *et al.* 2019]. To compare with similar FLRW metrics, we can see that the t'-isochronous hypersurface is similar to a paraboloid, in contrast to the homogeneous hypersphere given by the t-isochronous (Fig. 2.3.1).

The metric tensor constructed from $\widehat{O}$ describes a universe with linear expansion, directly proportional to its age or time, t. With this, the expansion rate or Hubble parameter[22] is $H(t,0) = 1/t$. The most current value of the Hubble parameter is $H(t_0,0) = 1/t_0$ and, taking the age of the universe as $t_0 = (1.380 \pm 0.004) \cdot 10^{10}$ years [Adam *et al.* 2015, Aghanim *et al.* 2020b], a value $H_o = 70.9 \pm 0.2$ km $\cdot$ s^{-1} $\cdot$ Mpc^{-1} compatible with the

[20] As a curiosity about this result, I must confess that my initial goal in Monjo 2017 was to reproduce a metric of the FLRW family, by deriving it from a natural way of embedding, thus avoiding "artificial gluing" of the scale factor $a(t)$ multiplied by the static spatial section. However, I accidentally found Eq. 2.3.5, 2.3.6 and 2.3.7.

[21] It is only "apparent" because the scalar curvature (Eq. 2.3.12 is the same when it is evaluated at every point ($r' \equiv 0$).

[22] Recall that, for a scale factor a that depends on the position, $(t,\vec{r}) \in \mathbb{R}^{1,3}_g \mapsto a(t,\vec{r}) \in \mathbb{R}_{>0}$, the Hubble parameter H is defined by the map $(t,\vec{r}) \in \mathbb{R}^{1,3}_g \mapsto H(t,\vec{r}) := \dot{a}(t,\vec{r})/a(t,\vec{r})$.

local observations is obtained [Monjo 2017, Lin *et al.* 2019, Riess *et al.* 2019, Knox and Millea 2020].

On the other hand, the local limit of Eq. 2.3.6, with $r' \ll t_0$ and $a(t) \approx 1$ with $t \approx t_0$, approaches the radial component of the metric to be

$$g_{rr} \approx -a(t)^2 \frac{1}{1-\frac{r'^2}{t_0^2}} \approx -\left(1+\frac{r'^2}{t_0^2}\right) \simeq -1 - u_r \cdot u_r \tag{2.3.10}$$

where $u_r = r/t = r'/t_0$ is the escape velocity associated with the Hubble expansion. This term contributes as a local perturbation of the metric, which is $g \approx \eta - u \otimes u$ with radial velocity $u = (u_t, u_r, 0, 0)$, except of the shift term of the metric. The implications of this metric are analyzed in Chapter 3. Furthermore, a generalization of this type of perturbations is analyzed in Chapter 4, based on escape velocity in galaxies, and in Chapter 5, for particle field dynamics.

2.3.4 Some features

Scalar curvature, expansion rate and comoving distance can be easily obtained from the hyperconical metric (Eq. 2.3.5).

Curvature. Let $R_{\alpha\beta}$ be local coordinates of the Ricci curvature tensor defined for signature (1,3),

$$R_{\alpha\beta} := R^{\mu}_{\alpha\mu\beta} = \partial_\mu \Gamma^{\mu}_{\alpha\beta} - \partial_\beta \Gamma^{\mu}_{\mu\alpha} + \Gamma^{\mu}_{\rho\mu}\Gamma^{\rho}_{\alpha\beta} - \Gamma^{\mu}_{\rho\beta}\Gamma^{\rho}_{\alpha\mu} \tag{2.3.11}$$

where $\Gamma^{\mu}_{\alpha\beta}$ are the Christoffel symbols. It is found that the manifold is only maximally symmetric in the spatial components ($R_{ij} = 1/3 \cdot R g_{ij}$) at a local scale ($r' = 0$, i.e. $b = 1$) (see Appendix C). In this case, the spatial part of the Ricci tensor R_{ij} approximates $R_{ij} \approx -2k(\dot{a}/a)^2 g_{ij}$. This contrasts with the non-accelerated case for the FLRW metric, i.e. $R^{FLRW}_{ij} = -2\left(\dot{a}/a\right)^2 g^{FLRW}_{ij} - 2K/a^2 g^{FLRW}_{ij}$, where K is the spatial curvature of the FLRW metric. Taking the scalar curvature

$$R := R^{\alpha}_{\alpha} = -\frac{6k^2}{t^2}\frac{2b - \frac{1}{3}(2b^2+1) + k - 1}{(2b - b^2 + k - 1)^2}\,, \tag{2.3.12}$$

is simplified to

$$R = -\frac{6k}{t^2} = -\frac{6}{\nu^2 t^2}$$

for every point ($r' = 0$), as a 3-sphere (of radius νt) embedded into $\mathbb{R}^{1,4}$, and like in the Anti-de Sitter spaces. For $k = 1$ (i.e. $\beta_0 = 0$), the Ricci scalar corresponds to the case of FLRW metric with linear scale factor $a = t/t_0$ and curvature $K = 0$, i.e., this is a space apparently flat under the FLRW view.

Expansion rate. Let (U, φ) be a coordinate sustem and $a : I \subset \mathbb{R}_{\geq 0} \to \mathbb{R}_{\geq 0}$ be a scale factor of the metric. Then, the expansion rate or *Hubble parameter* H is defined by the relative derivative $H := a^{-1}\partial a/\partial t'$ with respect the time coordinate t. For the

hyperconical model, the scale factor a is initially defined as linear by hypothesis. The **expansion rate** or *Hubble parameter* is derived using the diagonal coordinates as $H_{hyp} := a^{-1}\partial a/\partial t'$, i.e.

$$H_{hyp} = \frac{1}{t'} = \frac{1}{t_0}\frac{a(t_0)}{a(t)} =: \frac{1+z}{t_0} \tag{2.3.13}$$

where the redshift $1+z$ is defined according to the relative scale factor $a(t_0)/a(t)$.

Comoving distance. Let $r' := (t/t_0)r$ be the comoving distance, that is the distance $r' := |\vec{r}'|$ of the spatial coordinate used in the above subsection. Then, two comoving measures can be distinguished from the hyperconical metric: the radial coordinate ${r'}_{hyp}$ of the null geodesic (see Def. A.2.2 of Appendix A.2) under the extrinsic view and the physical (proper) radial distance $\hat{r}'_{hyp}$ obtained by projection to the intrinsic view of the hyperconical universe. That is:

$${r'}_{hyp}(z) = \frac{1}{H_o}\xi_k^{-1}(\ln(1+z)) \tag{2.3.14}$$

$$\hat{r}'_{hyp}(z) := f^{\alpha}_{\hat{r}}(t_0, {r'}_{hyp}) \tag{2.3.15}$$

where $f^{\alpha}_{\hat{r}}$ is a projection map (detailed in Secs. 3.4-3.4.2) and the function ξ_k, obtained from the null geodesic curve under the diagonal hyperconical metric, is given by

$$\xi_k\left(\frac{r'}{t_0}\right) := \int_0^{r'} \frac{\sqrt{1-k^{-1}(1-b)^2}}{b(2k^{-1}(b-1)+1)}\frac{dr'}{t_0} \tag{2.3.16}$$

where $b = b(r') := \sqrt{1-kr'^2/t_0^2}$. Notice that the domain of ξ_k is not defined for a certain region of the comoving coordinate r', which is given by the deformation $\mathscr{T}_t$.

2.4 Minimal dynamical embedding

2.4.1 What is it?

This section develops a formal proof that the minimal dynamical embedding of $(1,3)$-dimensional Lorentzian (homogeneous and spatially isotropic) manifolds is given by the hyperconical metric, that is a linearly expanding universe with an apparent radial inhomogeneity. Therefore, the specific objective of this section is to derive the hyperconical metric in a natural way.

2.4.2 Minimal singular manifold

In the 5-Minkowskian spacetime, $\mathbb{R}^5_{\eta\pm} := (\mathbb{R}^5, \eta_\pm)$ with $\eta_\pm = \text{diag}(+1,-1,-1,-1,\pm 1)$, the maximum homogeneous and isotropic Lorentzian manifolds can be spatially flat, hyperboloid or hyperspheric. However, the unique homogeneous manifold without boundary that has finite volume is the hypersphere.

Proposition 2.4.1 (**Regular dynamical manifolds are closed**). *If $\mathscr{N} \subset \mathbb{R}^5_{\eta\pm}$ is a minimal singular (or maximal regular) four-dimensional object with finite parameter time, it also has finite spatial volume, so it is closed.*

Proof. As a regular (smooth) hypersurface, $\mathscr{N}$ can be parameterized by a coordinate system. Moreover, as a dynamical system, its evolution depends on a timelike coordinate. Because $\mathscr{N}$ is maximal regular, it is globally hyperbolic, foliated by Cauchy hypersurfaces, and there exists a causality parameterization by "proper time" t, like an arc length, for which the evolution speed c of the Cauchy hypersurfaces is unity, $c = 1$. Because the timeline of $\mathscr{N}$ is finite by hypothesis, there exist two times $t_-, t_+ \in \mathbb{R}$ (finite) for which $\mathscr{N}(t)$ is not defined (does not exist) at t_- but is at t_+, and there also exists a time $t_0 \in (t_-, t_+)$ for which the Volume$(\mathscr{N}(t)) < \epsilon$ approaches 0 by minimal singularity hypothesis (excluding 0). Therefore, the finite c and the finite t lead to a finite volume, $0 < \text{Volume}(\mathscr{N}(t)) < \infty$. ■

Therefore, only the expanding hyperspheres $S^3_t \subset \mathbb{R}^5_{\eta-} \equiv \mathbb{R}^{1,4}_\eta$ are maximal regular objects embedded in Lorentzian (dynamical) manifolds. Moreover, taking t as a temporal parameter and the unitary velocity ($c \equiv 1$) by regular parameterization, the foliation of these hyperspheres is built by a hypercone

$$\mathcal{H}^4 \;:=\; S^3_{\mathbb{R}_{>0}} \;:=\; \left\{ X \;\in\; \mathbb{R}_{>0} \times \mathbb{R}^4 \subset \mathbb{R}^{1,4}_\eta \;:\; ||X||_{\eta_{1,4}} = 0 \right\}, \tag{2.4.1}$$

and, therefore, we obtain that $\beta_0 = \beta_\pm = 0$ for Eq. 2.2.2. In Minkowskian coordinates, $(t,x,y,z,u) =: (t,\vec{r},u)$, the equation of the hypercone is $0 = ||X||_{\eta_{1,4}} = t^2 - x^2 - y^2 - z^2 - u^2 = t^2 - \vec{r}^2 - u^2$, or simply $\vec{r}^2 + u^2 = t^2 = c^2t^2$, since $c \equiv 1$.

Finally, *moving charts* are required to represent comoving observers as well as to obtain the metric tensor g and the corresponding intrinsic viewpoint of the hypercone.

2.4.3 Embedding from moving frames

An observer living in $\mathcal{H}^4$ will measure local (differential) distances as in its tangent Minkowskian spacetime $\mathbb{R}^{1,3}_{\eta} := (\mathbb{R}^4, \eta_{1,3})$. To check this, one takes an infinitesimal difference between three paths $X, X_0, X_0' : \mathbb{R} \to \mathcal{H}^4$ and intersects on the hypersurface $S^3_t \subset \mathcal{H}^4$ in $X(t)$, $X_0(t)$ and $X_0'(t)$, respectively. For instance, X_0 represents a comoving observer with coordinates $X_0(t) = (t, \vec{0}, t)$ and $X(t) = (t, \vec{r}, u)$ is the image of any arbitrary path on the hypercone $\mathcal{H}^4$, while $X_0'(t) := (t_0, \vec{0}, t)$ is defined as the image of an observer **reference path** at time $t_0 \in \mathbb{R}_{>0}$. Notice that the observer and its reference path image are not the same, $X_0 \neq X_0'$, but they coincide for each measurement at the time $t = t_0$, if it is set as a particular constant value. Therefore, similarly to the length of curves on the hypersurface $\hat{\mathcal{H}}^4_{\beta\pm}$ (Def. 2.3.4), the X_0- and X_0'-referred *arc lengths*[23] of X are

$$ds^2 := d(X - X_0)^2(t) = (0, d\vec{r}, d(u-t))^2 \tag{2.4.2}$$

$$ds'^2 := d(X - X_0')^2(t) = (dt, d\vec{r}, d(u-t))^2 . \tag{2.4.3}$$

that only differ in the temporal coordinate. The last term contributes to the following:

$$d(u-t) = d(t\cos\gamma - t) = -t\sin\gamma d\gamma + (\cos\gamma - 1)dt \tag{2.4.4}$$

where $\gamma = \arcsin\frac{r}{t}$, then,

$$d(u-t)^2 = t^2\sin^2\gamma d\gamma^2 + (\cos\gamma - 1)^2 dt^2 - 2t\sin\gamma(\cos\gamma - 1)dtd\gamma \tag{2.4.5}$$

where $\sin\gamma = r'/t_0 = r/t$ with comoving coordinate r' of r at the measuring time t_0. Notice that $d(\sin\gamma) = dr'/t_0 = dr/t - rdt/t^2$, so $dr = (t/t_0)dr' + r'/t_0 dt$ and $d\vec{r} = d(r\vec{e_r}) = dr\vec{e_r} + rd\Sigma\vec{e_\Sigma}$. Thus,

$$d\vec{r}^2 = \left(\frac{t}{t_0}\right)^2 (dr'^2 + r'^2 d\Sigma^2) + \frac{r'^2}{t_0^2}dt^2 + 2\frac{t}{t_0}\frac{r'}{t_0}dr'dt \tag{2.4.6}$$

Now, adding both the spatial term (Eq. 2.4.6) and the u-dimension contribution (Eq. 2.4.5) to Eqs. 2.4.2 and 2.4.3, they display

$$ds^2 := (2\cos\gamma - \mathbf{2})\,dt^2 - \frac{t^2}{t_0^2}\left(\frac{dr'^2}{1 - \frac{r'^2}{t_0^2}} + r'^2 d\Sigma^2\right) - 2\frac{t}{t_0}\frac{r'}{t_0}\frac{dr'dt}{\cos\gamma} \tag{2.4.7}$$

$$ds'^2 := (2\cos\gamma - \mathbf{1})\,dt^2 - \frac{t^2}{t_0^2}\left(\frac{dr'^2}{1 - \frac{r'^2}{t_0^2}} + r'^2 d\Sigma^2\right) - 2\frac{t}{t_0}\frac{r'}{t_0}\frac{dr'dt}{\cos\gamma} \tag{2.4.8}$$

[23]Recall that, for a parameterization $s := X - X_0$ of any manifold $\mathscr{H}^4$ such as $s : U \subset \mathbb{R}^4 \to \mathscr{H}^4 \subset \mathscr{M}$, the metric $g = g_{\alpha\beta}\,dx^\alpha dx^\beta$ is given by the $\mathscr{M}$-scalar product $(\,\cdot\,)$ of derivatives $ds = \partial_\alpha s\,dx^\alpha$, that is $ds^2 = ds \cdot ds = \partial_\alpha s \cdot \partial_\beta s\,dx^\alpha dx^\beta = g$.

where boldface numbers highlight the difference in the temporal contribution. Finally, one can check the local limit for $r' \ll t_0$ is only Minkowskian for the second equation,

$$ds^2\big|_{r'\ll t_0} = -\frac{t^2}{t_0^2}\left(dr'^2 + r'^2 d\Sigma^2\right) \tag{2.4.9}$$

$$ds'^2\big|_{r'\ll t_0} = dt^2 - \frac{t^2}{t_0^2}\left(dr'^2 + r'^2 d\Sigma^2\right) . \tag{2.4.10}$$

Proposition 2.4.2 (**Minimal dynamical embedding**). *The hyperconical metric (Eq. 2.4.8) is the minimal dynamical embedding of the hypercone $\mathcal{H}^4 \subset \mathbb{R}^{1,4}_\eta$ with metric $\eta =$ diag$(+1,-1,-1,-1,-1)$.*

Proof. To obtain a four-dimensional metric that inherits dynamics of $\mathcal{H}^4$, moving charts defined with respect to $X'_0(t) = (t_0, \vec{0}, t)$ adequately represent observers to measure at any time t_0. To probe that it is a unique solution, we suppose that another reference is $Y'_0(t) = (\tau(t), \vec{\rho}(t), \nu(t))$. If $Y_0(t_0) \in \mathcal{H}^4$, it means that $\tau(t_0)^2 = \vec{\rho}(t_0)^2 + \nu(t_0)^2$ for each $t = t_0$. Moreover, there exists a coordinate change $Y'_0 \to Y''_0$ in which $\vec{\rho} \to 0$ by simple displacement $\Delta Y = (0, \vec{\rho}, 0)$, so the hypercone's equation $\tau_0^2 := \tau(t_0)^2 = \nu(t_0)^2$ leads to

- $Y''_0(\tau(t)) = (\tau_0, \vec{0}, \tau)$ or
- $Y''_0(\tau(t)) = (\tau, \vec{0}, \tau_0)$ or
- $Y''_0(\tau(t)) = (\tau, \vec{0}, \tau)$ or
- $Y''_0(\tau(t)) = (\tau_0, \vec{0}, \tau_0)$

but the last three cases are rejected because they do not reproduce the local Minkowskian distance. Therefore, only the first solution $Y''_0(\tau) = (\tau_0, \vec{0}, \tau)$, with $(t \to \tau)$-transformation, is valid; which corresponds to the reference of moving charts for the hyperconical metric of Eq. 2.4.8. ■

2.5 Intrinsic Lorentzian hypercone

2.5.1 What is it?

This section develops the final step of the *dynamical embedding*, that is the intrinsic perspective of the hyperconical manifolds by using coordinate changes according to locally conformal stereographic projections to find the *inverse comoving chart* (2.2.2).

2.5.2 Need of projections

Radial inhomogeneity obtained from the comoving frames can be assimilated as a **fictitious acceleration** that should be intrinsically equivalent to the one provided by the ΛCDM dynamics (i.e. acceleration linked to the well-known *dark energy*). To show the equivalence, this section develops a family of transformations that lead to a family of solutions. However, they need to be reduced to a unique solution at a local scale (i.e., evaluated at each point), as it is shown in Prop. 6.1.1 of Chapter 6.

Let $f : \mathcal{H}^4_{\beta\pm} \subset \mathbb{R}^5_{\eta\pm} \to \mathbb{R}^{1,3}_g$ be the inverse of a comoving chart (Def. 2.2.2) between $\mathbb{R}^{1,3}_g$ and $\mathcal{H}^4_{\beta\pm}$. According to the Eq. 2.3.2 and 2.3.4, the deformation $\mathscr{T}_t : \mathcal{H}^4_{\beta\pm} \to \mathbb{R}^5_{\eta\pm}$ leads to an output that still has the unobserved spatial u-coordinate. Thus, there exists some projection map $f^\alpha : \mathbb{R}^5_{\eta\pm} \to \mathbb{R}^{1,3}_g$ to remove u, satisfyig that $f = f^\alpha \circ \mathscr{T}_t$, that is

$$\begin{array}{ccc} \mathcal{H}^4_{\beta\pm} & \xrightarrow{\mathscr{T}_t} & \mathbb{R}^5_{\eta\pm} \\ f \big\downarrow & \swarrow f^\alpha & \\ \mathbb{R}^{1,3}_g & & \end{array}$$

Definition 2.5.1 (**Intrinsic comoving distance**)**.** Let $f : \mathcal{H}^4_{\beta\pm} \subset \mathbb{R}^5_{\eta\pm} \to \mathbb{R}^{1,3}_g$ be the inverse of a comoving chart. If r' is a comoving distance for $\mathcal{H}^4_{\beta\pm}$, we will say that $\hat{r}' := f(r')$ is the corresponding **intrinsic comoving distance**.

Finally, let $(t, \vec{r}', u)$ be new coordinates such that $\vec{r}' := (t_0/t)\vec{r}$ is the so-called **comoving spatial position**. Then, each map is applied to these comoving coordinates as follows:

$$f^\alpha(t, \vec{r}', u) = (f^\alpha_{\hat{t}}(t, \vec{r}'), f^\alpha_{\hat{r}}(t, \vec{r}')) =: (\hat{t}, \vec{\hat{r}}') \in \mathbb{R}^{1,3}_g \,. \tag{2.5.1}$$

For instance, the morphisms $f, f^\alpha : (t, \vec{r}', u) \mapsto (\hat{t}, \vec{\hat{r}}') \in \mathbb{R}^{1,3}_g$ can be **trivially** chosen such that $\hat{t}(\vec{r}', t) = t$, $\vec{\hat{r}}'(\vec{r}', t) = \vec{r}'$, for all $\vec{r}'^2 < \nu^2 t^2$ satisfying the constraint condition of $\mathcal{H}^4_{\beta\pm}$. However, it is possible to use other projections f^α that modify spatial distances $|\vec{r}'| \neq |\vec{\hat{r}}'|$ at **large scales** (i.e., f approaches to a trasformation for large distances).[24]

[24]Recall that, for spatial vectors $\vec{r} = (x, y, z) \in \mathbb{R}^3$, we are denoting the usual (Euclidean) norm by $|\vec{r}|^2 := x^2 + y^2 + z^2$, in contrast to a Lorenztian norm $||X||^2_g$ induced by the metric g, as in Eq. 2.4.1.

Remark 2.5.1. The deformation $\mathscr{T}_t : \mathcal{H}^4_{\beta\pm} \to \mathbb{R}^5_{\eta\pm}$ produces a radial inhomogeneity that can be assimilated as an acceleration (as a function of the time) by a redefinition of the coordinates. In fact, projections f^α can be used to recover the homogeneously flat FLRW metric with acceleration (see Sec. 2.5 and Sec. 3.4).

To obtain an *intrinsic comoving distance* $\vec{\hat{r}}'$ (with coordinates $(\hat{t}, \vec{\hat{r}}') \in \mathbb{R}^{1,3}_g$), several families of projection maps $\{f^\alpha\}_\alpha$ can be considered to transform the original comoving coordinates $(t, \vec{r}', u) \in \mathbb{R}^5_{\eta\pm}$, but they should satisfy several requirements:

(1) *Projection type.* To preserve local measurement of proper distances, it must be an azimuthal and locally conformal projection; that is, $f^\alpha_{\hat{t}}(t, \vec{0}) \equiv t$, $f^\alpha_{\hat{r}}(t, \vec{0}) \equiv 0$ and $f^\alpha_{\hat{r}}(t, \vec{\epsilon}) \approx \vec{\epsilon}$ for $|\vec{\epsilon}| \ll t$. Therefore, it is spatially isotropic $f^\alpha_{\hat{r}}(t, \vec{r}') = f^\alpha_{\hat{r}}(t, r')\vec{r}'/r'$ for all $\vec{r}'$ such as $r' := |\vec{r}'| > 0$.

(2) *False boundary.* As $\mathscr{T}_t$ is a local projection (performed by an observer), it produces an apparent boundary at a certain distance[25]. Particularly, the function $\xi_k(r'/t_0)$ of Eq. 2.3.16 is only real in $r' \in [0, r'_k)$ where

$$r'_k := \frac{t_0}{2}\sqrt{4-k} \tag{2.5.2}$$

is the boundary of $\mathscr{T}_t(\mathcal{H}^4_{\beta\pm}) \ni r'$, where ξ_k diverges (Eq. 2.3.16). The existence of this limit leads to a divergence in the first derivative of the projection, i.e. $df^\alpha_{\hat{r}}(t, r')/dr|_{r'=r'_k} = \infty$.

(3) *Corrected boundary.* To find the correction of the map f^α, it must be taken into account that the intrinsic measurement of $|\vec{\hat{r}}'|$ in $\mathbb{R}^{1,3}_g$ is limited by the maximum arc length in $\mathcal{H}^4_{\beta\pm}$, that is $\pi\nu t_0 = \max(\gamma\nu t_0) = \max(|\vec{\hat{r}}'|) = f^\alpha_{\hat{r}}(t_0, r'_k)$.

Remark 2.5.2 (**non-global uniqueness**)**.** A global projection map $f^\alpha_{\hat{r}}$ that satisfies conditions (1) and (2) is not unique. For instance, a distorted stereographic projection **on the angles are**

$${}_a f^\alpha_{\hat{r}}(t_0, r'(\gamma)) = \nu t_0 \gamma \Delta^\alpha(\gamma/\gamma_0) \tag{2.5.3}$$

$$\Delta^\alpha(x) := \frac{1}{(1-x)^\alpha}\,, \tag{2.5.4}$$

where $\gamma := \gamma(r') = \sin^{-1}(r'/\nu t_0)$, $\gamma_0 := \gamma(r'_k)$ and $\Delta^\alpha : [0,1) \to [0,\infty)$ is a stereographic projector characterized by a radially-distorting parameter $\alpha \in \mathbb{R}_{\geq 0}$, which is applied to a normalized height $x \in [0,1)$. For an observer, the intrinsic measurement of the distances (including the height) is locally given by the arc length $(\nu t_0 \gamma)$ in $\mathcal{H}^4_{\beta\pm}$.

Adding the condition (3), Eq. 2.5.3 is only valid for a small region ($\gamma \ll 1$) because it diverges when $\gamma \to \gamma_0$, and then it requires eliminating this divergence. For example, one can select the inverse stereographic projection

$${}_b f^\alpha_{\hat{r}}(t_0, r'(\gamma)) = 2\nu t_0 \tan^{-1}\frac{\gamma\Delta^\alpha(\gamma/\gamma_0)}{2}\,. \tag{2.5.5}$$

[25] That is, image of the function ξ_k (Eq. 2.3.16) approaches to infinity for some finite region of its domain.

That is, the projection $f^{\alpha}_{\hat{r}}$ remains one-parametric (α). For the temporal projection, it is supposed that $\hat{t} = f^{\alpha}_{\hat{t}}(t, \vec{r}) = t$.

2.5.3 Derivation of projections

2.5.3.1 Projective comoving path

The above developments are performed by considering a distorting stereographic projection on the angles, that is a resulting comoving distance of $\hat{r}' = \nu t_0 \gamma/(1-\gamma/\gamma_0)^{\alpha}$. However, it is convenient to define a stereographic projection by using the 5-Minkowskian coordinates $(t, \vec{r}, u) \to (\hat{t}, \hat{u})$, that is $\hat{r}' = r'/(1-\gamma/\gamma_0)^{\alpha}$.

Let $Q_\gamma : (0, t_0] \subset \mathbb{R} \to \mathbb{R}^4$ be a comoving path with angular coordinate $\gamma \in [0, \pi/2)$ with respect the u-axis, and let $Q_\gamma(t) = (t, \vec{r}'(t), u(t)) \in \mathbb{R}^4$ be the position of any object at $t \in \mathbb{R}_{>0}$ with $\vec{r} = r\vec{e}_r$ such as $r^2 := \vec{r}\cdot\vec{r}$ and $\vec{e}_r := \vec{r}/r$. Moreover, let $(\vec{r}', u') := (t_0/t)(\vec{r}, u)$ be the comoving spatial coordinates. Then, the position of any object can be expressed in spherical coordinates as follows:

$$Q_\gamma(t) = \begin{pmatrix} t \\ \vec{r} \\ u \end{pmatrix} = \frac{t}{t_0}\begin{pmatrix} t_0 \\ \vec{r}' \\ u' \end{pmatrix} = \frac{t}{t_0}\begin{pmatrix} t_0 \\ t_0 \sin\gamma\ \vec{e}_r \\ t_0 \cos\gamma \end{pmatrix} . \tag{2.5.6}$$

Then, each point $Q_\gamma(t)$ is projected to the "past value", $Q_\gamma(t_0)$, by a line that passes through the point $\widehat{O}(t_0) := (0, \vec{0}, 0)$.

2.5.3.2 Distorted stereographic projection

Let $\alpha \in (0, 1]$ be a free 'distortion parameter' of a **projection** $f^{\alpha} : (t, r') \mapsto (\hat{t}, \hat{r}')$, and $\lambda \subset \mathbb{R}$ be a 'scale factor' that linearly transforms time $t \mapsto \hat{t} := t\lambda$ and distorts the comoving length $\hat{r}'$ as $r' \mapsto \hat{r}' := r'\lambda^{\alpha}$ for some set value of α. Moreover, we define an α-distorted line as follows:

Definition 2.5.2 (α**-distorted line**)**.** Let $P = (t_P, \vec{r}_P, u_P)$ and $Q = (t_Q, \vec{r}_Q, u_Q)$ be to points of $\mathbb{R}^5_{\eta\pm}$, and let $\alpha \in (0, 1]$ be the distortion parameter. We will say that $F : \mathbb{R} \to \mathbb{R}^5_{\eta\pm}$ is an α-distorted line from P to Q when

$$F(\lambda) = \begin{pmatrix} \hat{t} \\ \vec{\hat{r}} \\ \hat{u} \end{pmatrix} = \begin{pmatrix} t_P + (t_Q - t_P)\lambda \\ \vec{r}_P + (\vec{r}_Q - \vec{r}_P)\lambda^{\alpha} \\ u_P + (u_Q - u_P)\lambda \end{pmatrix} ,$$

thus $X(0) = P$ and $X(1) = Q$, univocally. In fact, X is a straight line for $\alpha = 1$, with null distortion.

Now, let $Q : t \mapsto Q(t) \in \mathbb{R}^5_{\eta\pm}$ be any path, that is $Q \in \mathcal{C}(\mathbb{R}_{>0}, \mathbb{R}^5_{\eta\pm})$, and let $F_Q : \mathbb{R} \to \mathcal{C}(\mathbb{R}_{>0}, \mathbb{R}^5_{\eta\pm})$ be a family of α-distorted lines. Thus, $F_{Q(t)} : \lambda \mapsto F_{Q(t)}(\lambda) \in \mathbb{R}^5_{\eta\pm}$ is drown from $P := (0, \vec{0}, u_0)$ to $Q(t) = (t, \vec{r}, u)$, parameterized such as $F_{Q(t)}(0) = P$ is the

origin of projection with $u_0 := -t_0$ (i.e. the "south pole" of $\mathcal{H}^4$) and $F_{Q(t)}(1) = Q(t)$ is the targeted point to be projected onto the hyperplane $\hat{u} = t_0$ (i.e. the tangent spacetime at "north pole" of $\mathcal{H}^4$, where observer lives). Therefore, there is an α-distorted line for each targeted point $Q(t)$.

The α-distortion of $\vec{r}' = r'\vec{e}_r \;=\; t_0 \sin\gamma\, \vec{e}_r \;\mapsto\; \hat{r}'\vec{e}_r := t_0 \sin\hat{\gamma}\, \vec{e}_r$, is actually performed for the angles $\gamma \mapsto \hat{\gamma}$, preserving the direction $\vec{e}_r$. Therefore, the following equivalent families are parameterizations of the distorted projection:

$$F^{(a)}_{Q(t)}(\lambda) = \begin{cases} \hat{t} = t\lambda \\ \hat{r}' = r'\lambda^{\alpha} \\ \hat{u} = u_0 + (u - u_0)\lambda \end{cases} \qquad \rightleftarrows \qquad F^{(b)}_{Q(t)}(\lambda) = \begin{cases} \hat{t} = t\lambda^{1/\alpha} \\ \hat{r}' = r'\lambda \\ \hat{u} = u_0 + (u - u_0)\lambda^{1/\alpha}\,, \end{cases}$$

We assume that observers, located at $Q(t) = (t_0, 0, 0, 0, t_0) \in \mathbb{R}^5_{\eta\pm}$ for every $t_0 \in \mathbb{R}_{>0}$, measure proper times in its tangential Minkowskian hyperplane. When the points are projected onto the Minkowskian hyperplane $\hat{u} = t_0$, a solution for the distorted stereographic projection (f^{α}) is given by some $\lambda = \lambda_s(t, \gamma)$,

$$t_0 = -t_0 + (t\cos\gamma + t_0)\,\lambda_s \;\;\Rightarrow\;\; \lambda_s(t,\gamma) = \frac{2}{(1 + \frac{t}{t_0}\cos\gamma)}\,. \tag{2.5.7}$$

Therefore, the transformation $r' \mapsto \hat{r}' := r'\lambda^{\alpha}$ is reduced to find the value of α and the geometrical relation between the time t and the comoving coordinate r' or γ.

2.5.4 Time relationship

2.5.4.1 Local approach uniqueness

Each hypersphere of radius t is locally projected (expanded) to the hyperesphere of radius $t_0 > t$ by distorting the spatial coordinates $\vec{r}'$. Extra-dimension u' should disappear taking some adequate reference chart (e.g. by using polar coordinates or using a flattening projection).

Moreover, according to Monjo 2017, there exists a linear relationship between the redshift z and the spatial coordinate $r'/t_0 = \sin\gamma$, so the map $\gamma \mapsto z(\gamma)$ can be defined. Taking into account that the inhomogeneous scale factor $\dot{a}/a = t/t_0$ is related to redshift z as $z \mapsto t(z)/t_0 = 1/(1+z)$, there exists a map $\gamma \mapsto t(\gamma)$. Specifically, it is

$$z \;\mapsto\; \frac{t(z)}{t_0} = \frac{1}{1+z} \;=\; \sum_{n=0}^{\infty} b_n \left(\frac{r'}{t_0}\right)^n = 1 - b_1\frac{r'}{t_0} + O\left(\frac{r'^2}{t_0^2}\right) \;\;\Longrightarrow\;\; \frac{t(\gamma)}{t_0} = 1 - \sin\gamma + O(\gamma^2)\,, \tag{2.5.8}$$

with $b_1 = 1$ at a local neighbourhood. Therefore, the projection parameter of Eq. 2.5.7 is now:

$$t_0 = -t_0 + (t\cos\gamma + t_0)\,\lambda_s \;\;\Rightarrow\;\; \lambda_s(t(\gamma),\gamma) \approx \frac{2}{(1 + \left(1 - \sin\gamma + b_\ell \sin^2\gamma\right)\cos\gamma)} \tag{2.5.9}$$

where b_ℓ is a fitting parameter that depends of the spatial scale considered. For very local scales ($\gamma \ll 1$), the approximated Eq. 2.5.9 is **uniquely determined** by

$$\lambda_s(t(\gamma), \gamma) \approx \frac{1}{1 - \frac{\gamma}{2}} \tag{2.5.10}$$

And one can check that the transformation is locally ($\gamma = 0$) isometric.

2.5.4.2 Global approach

Applying $\gamma \to 0$ to the $t(\gamma)$ relationship before the projection, the extra-dimension u logically satisfies the condition of that $(t_0/t)u = \lambda_s u = \hat{u}$ because $t(0) = t_0$. However, in general $\lambda_s \neq t_0/t$, and non-zero differences $D := ((t_0/t)u - \hat{u})/\hat{t} \neq 0$ are found for $\gamma > 0$. A global approach for the $t(\gamma)$ relationship can be derived by assuming that there exists an apparent maximum angle $\gamma_0 \in \mathbb{R}_+$ such as $D = 1$. Linearly with γ, the $t(\gamma)$ relationship can be estimated as follows (Appendix F):'

$$(t_0\lambda^{-1} - t)\cos\gamma \approx t_0\gamma/\gamma_0 \tag{2.5.11}$$

With this, Eq. 2.5.7 is:

$$t_0 \approx -t_0 + \left(t_0\left(\frac{1}{\lambda} - \frac{\gamma}{\gamma_0\cos\gamma}\right)\cos\gamma + t_0\right)\lambda_u \quad \Rightarrow \quad \lambda_u \approx \frac{2 - \cos\gamma}{1 - \frac{\gamma}{\gamma_0}} \approx \frac{1}{1 - \frac{\gamma}{\gamma_0}} \tag{2.5.12}$$

On the other hand, the relative difference $(t_0\lambda_s^{-1} - t)/t_0 \in (0, 1)$ should be at the maximum when the domain limit $\gamma \to \pi/3$ is reached (see, for instance, Monjo 2018); therefore $\gamma_0 = (\pi/3)/\cos(\pi/3) = 2\pi/3 \approx 2.09$. In contrast, by equaling the hyperconical-based Hubble parameter to the ΛCDM-dependent one 3.4.3, it is analytically found that

$$\alpha = \frac{5}{18}\gamma_0(1 + \epsilon) \quad \to \quad \gamma_0 = \frac{18}{5(1 + \epsilon)}\alpha \tag{2.5.13}$$

for some $|\epsilon| < 1/2$. For example, one finds $\epsilon = 0$ when the hyperconical-based Hubble parameter is compared to the ΛCDM-dependent Hubble parameter up to third order 3.4.3, and $\epsilon = -\frac{1}{10}$ for the local approach ($\gamma_0 = 2$ from Eq. 2.5.10 and therefore $\gamma_0 = 4\alpha$, with $\alpha = 0.5$).

2.5.5 Dynamical compatibility of the projections

The value of the distorting parameter α can be constrained by symplectic symmetries.

Lemma 2.5.1 (**Distortion is locally** $\alpha = \frac{1}{2}$)**.** *The value of the distorting parameter is determined by symplectomorphism as* $\alpha = \frac{1}{2}$.

Proof. To find the values of α that produce consistent dynamics, it is enough to apply any projection map $f^\alpha(\gamma) = (f^\alpha_{\hat{t}}(\gamma), f^\alpha_{\hat{r}}(\gamma))$ and assume symplectomorphism:

- Let $\{(q,p) \in \mathcal{C}^1(\mathbb{R}_{>0},\mathbb{R}^3) \times \mathcal{C}^1(\mathbb{R}_{>0},\mathbb{R}^3) \mid \gamma \in [0,\pi)\}$ be a dynamical system represented by symplectic coordinates (q,p), where $q := \vec{r}' = r'\vec{e}_r$ represents the position and $p := c_0\,\Delta\vec{r}'/\Delta t = c_0\,(\vec{e}_r\Delta r'/\Delta t + r'\Delta\vec{e}_r/\Delta t)$ is the conjugate momentum with some constant $c_0 \in \mathbb{R}_{>0}$. Assuming $\lambda \in \mathbb{R}$ as an independent parameter, spacetime transformation is locally $(\Delta t, \Delta r') \mapsto (\Delta\hat{t}, \Delta\hat{r}') = (\Delta t\,\lambda, \Delta r'\lambda^\alpha)$, so symplectic coordinates locally change as $(q,p) \mapsto (\hat{q},\hat{p}) = (q\lambda^\alpha, p\lambda^{\alpha-1})$, and the symplectic form

$$\omega = dq \wedge dp = d\hat{q} \wedge d\hat{p} = dq \wedge dp\,\lambda^{2\alpha-1} \tag{2.5.14}$$

should be locally conserved. For the simple comoving case ($dp = 0$), it is found that $\omega = 0$ for every $\alpha \in \mathbb{R}$. Otherwise, it is necessary to set $\alpha = \alpha_s \equiv 0.5$ for dynamical systems with $p \neq 0$ and $\lambda \neq 1$. ■

2.5.6 Dynamically-embedded hyperconical manifold

After applying the comoving expansion $\mathscr{T}_t : \mathcal{H}^4 \to \mathbb{R}^5_{eta\pm}$ and the distorting stereographic projection $f^\alpha : (t, r', u) \to (\hat{t}, \hat{r}', \hat{u})$, the dynamically embedded hypercone $\mathbb{R}^{1,3}_g = f(\mathcal{H}^4) = f^\alpha \circ \mathscr{T}_t(\mathcal{H}^4)$ presents new (transformed) metric, $g \to \hat{g}$, and becomes (apparently) spatially flat[26] by assimilating the radial inhomogeneity by some scale factor $\hat{a} : t \in \mathbb{R} \mapsto \hat{a}(t) \in \mathbb{R}$ with **fictitious acceleration**, and with time lapse $\hat{g}_{00} \equiv 1$ for an adequate redefined time coordinate $\hat{t}$. Thus, the square differential line is the flat FLRW metric,

$$ds^2 = d\hat{t}^2 - \hat{a}(\hat{t})^2\left(dr'^2 + r'^2 d\Sigma^2\right). \tag{2.5.15}$$

Now, the new scale factor provides an expansion rate of $\tilde{h} := \hat{a}^{-1}d\hat{a}/d\hat{t}$ linked to the same comoving distance $\hat{r}'$ after the projection. This is given by the null geodesic with no angular variations ($d\Sigma = 0$) in the considered metric (see Appendix A.2). This distance can be written using a variable so-called redshift (z) and the Hubble parameter ($\tilde{h}$) with the scale factor expressed as $\hat{a}/\hat{a}_0 = 1/(1+z)$ where $\hat{a}_0 \equiv 1$ is the current value of $\hat{a}$. For example, using spherical coordinates in a diagonal metric, the comoving distance is given by:

$$\int_0^{\hat{r}'} \frac{\sqrt{\hat{g}_{\hat{r}'\hat{r}'}}d\hat{r}'}{\hat{a}(\hat{t})} = -\int_{\hat{t}_0}^{\hat{t}} \frac{d\hat{t}}{\hat{a}(\hat{t})} = \int_0^z \frac{dz}{\tilde{h}(z)} \tag{2.5.16}$$

And taking that the metric is spatially flat, $\hat{g}_{\hat{r}'\hat{r}'} = \hat{a}(\hat{t})^2$,

$$r'\lambda^\alpha = \hat{r}' = \int_0^z \frac{dz}{\tilde{h}(z)}\,. \tag{2.5.17}$$

Remark 2.5.3. For non-flat $k\Lambda$CDM metrics, it is necessary to replace $\hat{r}' \to \frac{1}{\sqrt{k}}\sin^{-1}(\sqrt{k}\hat{r}')$ for $k > 0$ and $\hat{r}' \to \frac{1}{\sqrt{k}}\sinh^{-1}(\sqrt{k}\hat{r}')$ for $k < 0$.

[26] Of course, the hypercone $\mathcal{H}^4$ is not spatially flat, but every observer will see it as if it were flat.

Therefore, the problem is "reduced" to find the expression of λ^α in order to know the transformation[27] between the extrinsic distances r' and the intrinsic distances $\hat{r}'$.

[27]Of course, every coordinate transformation is isometric for the spacetime manifold, but it can be non-isometric for the resulting spatial submanifold (i.e. the spatial section).

Chapter 3

Results I. Manifold dynamics

3.1 Introduction to basic results

This Chapter aims to show **original content** on additional implications of our developments presented in the previous Chapter, as an alternative to the standard ΛCDM model, but *intrinsically equivalent*[1] to this one, at a *local scale*[2] [Monjo 2018, Monjo and Campoamor-Stursberg 2023]. ΛCDM-dependent observations suggest that the universe is spatially flat, accelerating and composed of predominately dark energy and dark matter. However, despite of the great agreement of the standard cosmology with this, the nature also of dark energy still remains an open issue. In fact, it is not measured from model-independent observations. Moreover, observations of the universe's flatness are also based on the validity assumption of the current model. Changing the frame theory, the same observations can be explained using another geometry, even with positive curvature [Jimenez *et al.* 2009].

Recently, geometrical interpretations for the dark energy have been explored [Mannheim 2006, Mannheim 2007, Maia et al. 2005]. For instance, conformal gravity can be used to obtain effects similar to both dark energy and matter [Mannheim 2006]. The hypothesis of the conformal cosmology is based on the invariance of the geometry under any local conformal transformation [Mannheim 2007]. Alternatively, Maia et al. 2005 obtained dark energy as warp in the universe given by the extrinsic curvature within a FLRW universe embedded into a five-dimensional constant curvature bulk.

According to the Chapter 2, we claim that our spacetime manifold is characterized by some metric with linear expansion, isotropy and a (fictitious) radial inhomogeneity, obtained by transformations that preserves the proper time. These metrics are compatible with observations of luminosity distance of 580 SNe Ia from the Supernova Cosmology Project [Monjo 2017]. This Chapter demonstrates that there exists a family of locally con-

[1] Throughout the Thesis, we distinguish between *intrinsic* and *extrinsic* perspective of the manifold, referring to the measurements made within the manifold itself and those made in the ambient space, which are linked by a coordinate transformation due to the moving reference frames used for measurements.

[2] Here, "*local scale*" means that all the functions are evaluated for every point (e.g. with spatial coordinate $r = 0$).

formal transformations that lead the (linearly expanding and curved) metrics to become the spatially flat FLRW metric, assimilating the spatial inhomogeneity as an acceleration in time. That predicted a dark energy density about $\Omega_\Lambda \approx 0.69$ (presented in Monjo 2018), compatible with the standard-model-dependent observation ($\Omega_\Lambda = 0.690(6)$[3]) [Adam *et al.* 2015, Aghanim *et al.* 2020b]. The relation between radial inhomogeneity, Lagrangian curvature terms and effective dark energy is also found in other modified gravities, but without a prediction of its value [Buchert *et al.* 2006, Nojiri and Odintsov 2007, Ellis 2011, Olmo 2011, Preston and Morris 2014, Buchert *et al.* 2020].

3.2 Result I-1: Analysis of symmetries

3.2.1 Euler-Lagrange equations

Since we are considering a manifold with linear expansion, this section aims to obtain the symmetries under the perspective of dynamical systems.

Let $\mathscr{S}$ be the *action* functional for describing the hyperconical manifold $\mathcal{H}^4$ embedded in $\mathscr{M} = \mathbb{R}^{1,4}_\eta$. It corresponds to a constant $m \neq 0$ multiplied by the distance $\tau := ||X-O||_\eta$ of the relative path of $X - O \in \mathscr{M}$ under the metric η, and the Lagrangian L coincides with the constant product $m\beta_0$. That is,

$$\mathscr{S}[\tau(t)] = \int_{\mathcal{H}^4} m d\tau = \int_0^t m\beta_0 dt \tag{3.2.1}$$

This retrieves the constraint $||X-O||_\eta = \beta_0 t$, viewed under the extrinsic viewpoint of the manifold. However, if a path $x = x(t) \subset \mathbb{R}^{1,3}_g$ is analyzed with respect to the comoving observers, the new action is given by $\tau(t) = ||x(t)||_g$:

$$\mathscr{S}[X(t)] = \int_0^t m\sqrt{g_{\alpha\beta}\frac{dx^\alpha}{d\tau}\frac{dx^\beta}{d\tau}}d\tau \cong \int_0^t \frac{m}{2} g_{\alpha\beta}\overset{\bullet}{x}^\alpha \overset{\bullet}{x}^\beta d\tau \tag{3.2.2}$$

where the derivative $\overset{\bullet}{x}^\mu := dx^\mu/d\tau$, with respect the proper time τ, is indicated by the $\bullet$ symbol to distinguish it from the usual derivative $\dot{x}^\mu := dx^\mu/dt$, with respect to a time coordinate t; moreover, it is used the homomorphism between the extremal $\delta\sqrt{\Box} = 0$ and $\frac{1}{2}\delta\Box = 0$ (see Def. 1.3.2). Therefore, the Lagrangian functional for $\mathbb{R}^{1,3}_g$ can be taken as $L = \frac{1}{2} g_{\alpha\beta}\overset{\bullet}{x}^\alpha \overset{\bullet}{x}^\beta$. Euler-Lagrange equations provided by the above action are the corresponding geodesic equations $\overset{\bullet\bullet}{x}^\rho = -\Gamma^\rho_{\alpha\beta}\overset{\bullet}{x}^\alpha \overset{\bullet}{x}^\beta$, being $\Gamma^\rho_{\alpha\beta}$ the Christoffel symbols of

[3] The value in parenthesis is the interval error of last significant figure.

second kind, the non-vanishing ones being:

$$\Gamma^i_{j0} = \frac{\dot{a}}{a}\delta^i_j \tag{3.2.3}$$

$$\Gamma^0_{ij} = -g_{ij}\frac{\dot{a}}{a}\frac{k(1-b)}{2b-b^2+k-1} \tag{3.2.4}$$

$$\Gamma^r_{rr} = \frac{1}{b^2}\frac{kr'}{t_0^2}\frac{b+k-1}{2b-b^2+k-1} \tag{3.2.5}$$

$$\Gamma^r_{\phi\phi} = -r'\sin^2\theta\frac{b+(k-2)b^2+b^3}{2b-b^2+k-1} \tag{3.2.6}$$

$$\Gamma^r_{\theta\theta} = -r'\frac{b+(k-2)b^2+b^3}{2b-b^2+k-1} \tag{3.2.7}$$

$$\Gamma^\theta_{\theta r} = \Gamma^\phi_{\phi r} = \frac{1}{r'} \tag{3.2.8}$$

$$\Gamma^\theta_{\phi\phi} = -\sin\theta\cos\theta \tag{3.2.9}$$

$$\Gamma^\phi_{\phi\theta} = \cot\theta \tag{3.2.10}$$

where $\delta^i_i = 0$ for $i \neq j$ and $\delta^i_i = 1$ for $i = j$, while $a = t/t_0$ and $b = \sqrt{1-kr'^2/t_0^2}$.

Angular velocities $\overset{\bullet}{\theta}$ and $\overset{\bullet}{\phi}$ remain spherical symmetry as in the flat Minkowski universe. However, time and radial coordinates present a flux:

$$\overset{\bullet\bullet}{t} = -\frac{k(1-b)}{2b-b^2+k-1}\frac{t}{t_0^2}\left(\frac{\overset{\bullet}{r}{}'^2}{b^2} + r'^2\overset{\bullet}{\Sigma}{}^2\right) \tag{3.2.11}$$

$$\overset{\bullet\bullet}{r}{}' = -2\frac{\overset{\bullet}{r}{}'\overset{\bullet}{t}}{t} - \frac{\frac{kr'}{b^2t_0^2}(b+k-1)}{2b-b^2+k-1}\overset{\bullet}{r}{}'^2 + \frac{b+(k-2)b^2+b^3}{2b-b^2+k-1}r'\overset{\bullet}{\Sigma}{}^2 \tag{3.2.12}$$

where $\overset{\bullet}{\Sigma} = d\Sigma/d\tau$, with $d\Sigma^2 := d\theta^2 + \sin^2\theta\, d\varphi^2$ representing the angular coordinates, $\overset{\bullet}{r}{}'^2 := -g_{ii}\overset{\bullet}{x}{}^i\overset{\bullet}{x}{}^i$ is the square of the spatial velocity, and it is taken $H := \dot{a}/a = 1/t$. The local limit ($r'/t_0 \ll 1$) without rotation ($\overset{\bullet}{\Sigma} = 0$) for Eq. (3.2.11) is only non-zero at the third order, and Eq. (3.2.12) is non-zero for the first order:

$$\overset{\bullet\bullet}{t} \approx -\frac{kr'^2t}{2t_0^4}\overset{\bullet}{r}{}'^2 \tag{3.2.13}$$

$$\overset{\bullet\bullet}{r}{}' \approx -\frac{2}{t}\overset{\bullet}{r}{}'\overset{\bullet}{t} - \frac{kr'}{t_0^2}\overset{\bullet}{r}{}'^2 \tag{3.2.14}$$

where $\overset{\bullet}{t} = dt/d\tau := \varsigma$, and therefore $\overset{\bullet\bullet}{t} = \varsigma\dot{\varsigma}$, while $\overset{\bullet}{r}{}' = \varsigma\dot{r}'$ and $\overset{\bullet\bullet}{r}{}' = \varsigma^2(\ddot{r}' + \dot{\varsigma}\dot{r}')$. Considering $\overset{\bullet\bullet}{r}{}' \approx \varsigma^2\ddot{r}'$, and taking the comoving relation $r' := (t_0/t)r$, Eq. (3.2.13) and (3.2.14) are approximately:

$$\dot{\varsigma} \approx -\varsigma\frac{kr^2}{2t^3}\left(\dot{r} - \frac{r}{t}\right)^2 \tag{3.2.15}$$

$$\ddot{r} \approx -\frac{kr}{t^2}\left(\dot{r} - \frac{r}{t}\right)^2 \tag{3.2.16}$$

As might be expected, the comoving case ($\dot{r} = r/t$) is a solution of the Eq. (3.2.16), for which the linear expansion is stationary ($\ddot{r} = 0 = \dot{\varsigma}$).

3.2.2 ADM-Hamiltonian equations

To obtain Hamiltonian equations of an expanding Lorentzian manifold, it is necessary to apply the Einstein field equations to the studied metric. Thus, it is obtained that **vacuum energy** density of the manifold is locally equal to $R_u \approx -6k/t^2$ in appropriate units (see 3.3.1). According to this, the total Lagrangian density of the dynamical manifold is given by the following action:

$$\mathscr{S} = \int d^4x \mathscr{L} = \int d^4x \sqrt{-g}\,(R - R_u + \mathscr{L}_m) \tag{3.2.17}$$

where $\mathscr{L}_m$ is the term of mass.

As spacetime is foliated into a family of spacelike surfaces Σ_t, the spatial submanifold can be interpreted as an embedding into the spacetime (in our case $\mathcal{H}^4$). And therefore, the ADM formalism can be used to obtain a set of *equations of motion* for the generalized coordinates, which corresponds to the spatial elements $\{g_{ij}\}_{i,j}$ of the metric with $i, j \in \{1, 2, 3\}$ (see Sec. 1.3.5.2). We consider the local limit

$$R_u \approx -\frac{6k}{t^2} = -\frac{k}{2}\left(g^{ij}\partial_t g_{ij}\right)^2 \tag{3.2.18}$$

and then Lagrangian density can be rewitten according to ADM formalism (Eq. (1.3.36)), but with an additional term from the curvature R_u:

$$\mathscr{L} = -g_{ij}\partial_t \pi^{ij} + lh + 2l_i \pi^{ij}{}_{;j} - 2\partial_i s^i + \sqrt{-g}R_u \tag{3.2.19}$$

where $l := (g^{00})^{-1/2}$ is the lapse, $l_i := g_{0i}$ is the shift, h is the Hamiltonian constraint (Eq. (1.3.38)), s^i is an auxiliary momenta (Eq. (1.3.39)), but π^{ij} is now the modified conjugate momenta (which slightly different to Eq. (1.3.37)):

$$\pi^{ij} \;=\; \sqrt{-g}\left[\left(\Gamma^0_{pq} - g_{pq}\Gamma^0_{rs}g^{rs}\right) g^{ip}g^{jq} - \frac{\partial R_u}{\partial(\partial_t g_{ij})}\right] \tag{3.2.20}$$

where $g := \det g_{\mu\nu}$ is the determinant of the metric, in contrast with $g_s := \det g_{ij}$, that is the determinant of the spatial metric.

Lemma 3.2.1 (**Positive spatial curvature**). *Hyperconical universes with* ***vacuum energy*** *density have positive curvature* $k = 1$.

Proof. Since the definition of the origin for r' is arbitrary (because it represents each observer), the curvature obtained in the limit of $r' = 0$ is the same for all the observers. Therefore, we use that the local limit represents every point of the manifold. Then,

taking into account the hyperconical metrics, Eq. 3.2.4 is locally ($r' \ll t_0$) equivalent to $\Gamma^0_{ij} = -g_{ij}(kr'^2)/(2t_0^2 t)$ and therefore Eq. (3.2.20) is simplified as follows:

$$\begin{aligned}\pi^{ii} &= \sqrt{-g}\left[\left(-g_{ii}\frac{kr'^2}{2t_0^2 t} + g_{ii}\delta^m_m\frac{kr'^2}{2t_0^2 t}\right)(g^{ii})^2 + k(g^{ii})^2\partial_t g_{ii}\right] = \\ &\approx \sqrt{-g}\frac{kg^{ii}}{t}\left(\frac{kr'^2}{t_0^2}+2\right) = 2\sqrt{-g}\frac{kg^{ii}}{t} = \sqrt{-g}k(g^{ii})^2\partial_t g_{ii} \qquad (3.2.21)\end{aligned}$$

where the metric determinant is locally $g = g_s = -a(t)^6 r'^4 \sin^2\theta$, since $g^{00} = 1$. The ADM equations for the metric evolution are given by the Eq. (1.3.40), and using that $\pi_{ij} = g_{ia}g_{jb}\pi^{ab}$ and $g_{ij} = 0$ for $j \neq i > 0$, we find that $\pi_{ii} = \pi g_{ii} = \pi^{ii}{g_{ii}}^2$. That is:

$$\begin{aligned}\partial_t g_{ii} &= \frac{1}{\sqrt{-g_s g^{00}}}\pi^{ii}{g_{ii}}^2 + 2\nabla_i g_{0i} = \\ &= \frac{\sqrt{-g}}{\sqrt{-g_s g^{00}}}\cancel{(g^{ii})^2 g_{ii}^2}\, k\,\partial_t g_{ii} + \cancel{2\nabla_i g_{0i}} \approx 0 \underset{locally}{=} k\,\partial_t g_{ii} \implies k = 1 \qquad (3.2.22)\end{aligned}$$

Therefore, as it was found in **Prop.** 2.4.1, now we trivially find that $k = 1$, where it is used that the covariant derivative of the shift g_{0r} is locally zero:

$$\nabla_r g_{0r} = \partial_r g_{0r} - \Gamma^r_{0r}g_{rr} - \Gamma^r_{rr}g_{0r} = -\frac{a}{t_0} + \frac{a^2}{t} = 0 \qquad (3.2.23)$$

with $a = t/t_0$. Therefore, the dynamics of the used metric is compatible with the ADM formalism applied to the modified Lagrangian density $\mathscr{L}$. ■

3.2.3 Killing Vectors

As is well known, the Killing vectors K^μ correspond to the infinitesimal generators of the isometries of the metric tensor [Chen *et al.* 2015, Paliathanasis 2016], hence, in terms of the Levi-Civita connection, we have the identity $g(\nabla_X K, Y) = g(X, \nabla_Y K)$. In local coordinates the Killing equation is given by

$$\nabla_\mu K_\nu + \nabla_\nu K_\mu = 0. \qquad (3.2.24)$$

An important property of the Killing vectors is the conservation of a quantity Q respect to the *affine parameter* λ (i.e. proportional to the arc length); that is, $dQ/d\lambda = 0$, where:

$$Q := K_\mu \frac{dx^\mu}{d\lambda} \qquad (3.2.25)$$

Note that this quantity corresponds to the Noether charge conserved by the coordinate transformation

$$x^\mu \longrightarrow x^\mu + d\varphi^\mu(\lambda) = x^\mu + K^\mu d\lambda \qquad (3.2.26)$$

and one can identify $Q = K^\mu \pi_\mu$ where $\pi_\mu := \partial L/\partial \dot{x}^\mu$ is the generalized momentum and L is the Lagrangian functional in $\mathbb{R}^{1,3}_g$.

For our case, the first Killing vector is determined by the independence of the metric Eq. (2.3.5) with respect to the coordinate ϕ, hence $K_{(1)} = \delta^\mu_\phi \partial_\mu = (0,0,0,1)$. The other two Killing vectors, resulting from the angular symmetry, can be obtained from Eq. (3.2.24) as $K_{(2)} = (0, 0, -\cos\phi, \cot\theta \sin\phi)$ and $K_{(3)} = (0, 0, \sin\phi, \cot\theta\cos\phi)$, respectively. These vector fields are easily seen to generate a copy of $\mathfrak{so}(3)$ the angular momenta $\ell_{(i)} = g_{\mu\nu} K^\mu_{(i)} dx^\nu/d\lambda$ are preserved, according to Eq. (3.2.25). For simplicity, we choose the coordinates with $\theta = \pi/2$, so that the direction of angular momentum is on the z-axis (i.e. $\theta = 0$) and thus the motion is in the xy-plane:

$$\ell_{(1)} = a(t)^2 r'^2 \frac{d\phi}{d\lambda} = r^2 \frac{d\phi}{d\lambda} \tag{3.2.27}$$

where for computational convenience we use that $r = a(t)r'$ and $\lambda = \tau$.
Concerning the translation symmetries, we have to distinguish between local and global symmetries. Spatial translations are clearly not global for the analyzed metric, but a temporal translation is found for the static conformal metric g' given by $d\lambda^2 := a(t)^{-2} dX^2$, i.e. changing the time coordinate as $d\eta := a(t)^{-1} dt$. The time-like conformal Killing vector is thus $K_{(\eta)} = \partial_\eta$. This implies the conservation of the *energy*

$$E(r') = g'_{\mu\nu} K^\nu_{(\eta)} \frac{dx^\mu}{d\lambda} = \left(2k^{-1}\left(b(r') - 1\right) + 1\right) \frac{d\eta}{d\lambda} \tag{3.2.28}$$

in a static universe. Note that, locally,

$$E(r') \approx (1 + 2\Phi(r'))\, \gamma, \tag{3.2.29}$$

where $2\Phi(r') := -r'^2/t_0^2$ and $\gamma = dt/d\tau = d\eta/d\lambda$. If we take into account the relation between r'^2/t_0^2 and the density of the Universe (see Eq. (3.3.3)), then Eq. (3.2.29) can be interpreted as an analogue to the potential gravitational energy. Spatial translations close to $r' \approx 0$ are local symmetries for the three orthogonal spatial directions $x^{i'}$, with $i = 1, 2, 3$, where $x^{1'} := r' \sin\theta\cos\phi$, $x^{2'} := r' \sin\theta \sin\phi$, $x^{3'} := r'\cos\theta$. As the metric is locally flat for these coordinates, the space-like Killing vectors are trivially $K_{(i')} = \partial_{i'}$, and the linear momentum conserved is $P^i = a(t) dx^{i'}/d\tau$. Finally, the three *Lorentz boosts* $B_{(i)} = x^i \partial_0 - t\partial_i$ are symmetries for the ordinary coordinates $x^i = a(t) x^{i'}$. Summarising, there are $10 = 3 + 1 + 3 + 3$ Killing vectors of either global/local type, corresponding to the three global angular rotations $K_{(i)}$, the temporal translation $K_{(\eta)}$ for the conformal static universe, as well as three local spatial translations $K_{(i')}$ and three local boosts $B_{(i)}$ as it is locally found in GR [Chen *et al.* 2015].

3.3 Result I-2: Analysis of dynamics

3.3.1 Friedmann equations

According to the new theoretical frame (Chapter 2), a modified Lagrangian density can be obtained from the local **Friedmann equations**, assuming GR valid for that scale. While most of studies find the universe's metric as a solution of these equations, the work of Monjo 2017 found new Friedmann equations and the value of the *energy parameters* as a solution of the proposed inhomogeneous "empty" metric. Locally, equations with positive curvature ($k = 1$) are equivalent to the spatially flat FLRW case (assuming linear expansion). Additionally, taking $\rho_{crit}(t) = \rho_o + \rho_\Lambda$, where $\rho_{crit}(t) := 3kH^2/8\pi G$ and $\rho_\Lambda := \Lambda/8\pi G$, the hyperconical model leads to:

$$4\pi \mathrm{G}\rho_o(1+w) = \frac{k}{t^2} \tag{3.3.1}$$

$$\Lambda t^2 = k\frac{1+3w}{1+w} \tag{3.3.2}$$

where w is the parameter so-called **equation of state** of the manifold.

Definition 3.3.1 (**Zero active mass**)**.** Let w be a equation of state corresponding to the dynamical evolution of a manifold. We will say that the manifold has "zero active (gravitational) mass" if $w = -1/3$.

Lemma 3.3.1 (**Linear expansion implies zero active mass**)**.** *If GR is valid at least for local scales, all manifolds with linear expansion have zero active mass, for both FLRW and hyperconical metrics.*

Proof. The proof is trivial for FLRW metrics by using their corresponding second Friedmann equation (Eq. A.1.4). Because the total mass density required to active acceleration is $\rho + 3p = (1 + 3w)\rho$, the result is that only $w = -1/3$ implies 'zero active mass', that is linear expansion. Moreover, for the hyperconical metrics (Eq. 3.3.1 and 3.3.2), assuming that Λ is finite and constant in GR, one of the following two possibilities should be satisfied:

1. In the limit as t approaches 0, w approaches $-1/3$.
2. If $\Lambda \neq 0$, it is expected that $\Lambda t^2 = 3$ for a certain t, causing that $w \to \infty$.

As the second point is not possible for any fluid, one has that $\Lambda = 0$, G is constant, and $w = -1/3$ for any time t. Therefore, the hyperconical manifold also has 'zero active mass'. ■

In addition, if mass is homogeneously and isotropically distributed throughout the universe, we can define a mass function $m(r) := 4\pi\rho_o r^3/3$, and Eq. 3.3.1 can be formulated as:

$$\frac{k}{t^2} = \frac{8\pi \mathrm{G}\rho_o}{3} = \frac{2\mathrm{G}m(r)}{r^3} \tag{3.3.3}$$

Note that for $k = 1$, we get $\dot{r} = r/t = \sqrt{2\mathrm{G}m(r)/r}$, i.e. Hubble's law is an escape velocity. If this approach is considered for the spatial components of the hyperconical metric, $g_{rr} = -a(t)^2/(1 - r^2/t^2)$, it locally approaches to the Schwarzschild components, $g_{rr} = -a(t)^2/(1 - 2\mathrm{G}m(r)/r)$, as expected for inhomogeneous metrics (e.g. LTB and McVittie metrics [Yan *et al.* 2015, Pérez *et al.* 2019]). Summarising, inhomogeneous metric with a locally valid GR leads to $\Omega_\Lambda = \rho_\Lambda/\rho_{crit} = 0$, but if that metric is projected on a spatially flat FLRW metric (forcing GR to be generally valid), the inhomogeneity is assimilated as an acceleration [Monjo 2018, Monjo and Campoamor-Stursberg 2023].

3.3.2 Modified Lagrangian density

From the Lemma 3.3.1 and the assumption that GR is valid at local scales, it follows that the expansion of the universe is compatible with the equation of state $w = -1/3$ for the energy density, i.e., $\rho_0 = \rho_{crit}$ and $p_0 = -\rho_{crit}/3$. This simplifies the Einstein field equations to:

$$G_{\alpha\beta} := R_{\alpha\beta} - \frac{1}{2}Rg_{\alpha\beta} = 8\pi\mathrm{G}P_{\alpha\beta} = 8\pi\mathrm{G}\left(P^0_{\alpha\beta} + P^m_{\alpha\beta}\right), \tag{3.3.4}$$

where $P^m_{\alpha\beta}$ is the stress-energy tensor of the ordinary matter-energy and $P^0_{\alpha\beta} = (\rho_0 + p_0)u_\alpha u_\beta - p_0 g_{\alpha\beta}$ is the stress-energy tensor of the background spacetime, which is assimilable to a *dark* energy with $w = -1/3$ and density equal to $\rho_{crit} = 3k/8\pi\mathrm{G}t^2$. We deduce that total Lagrangian density is locally equal to:

$$\mathscr{L} = \frac{1}{16\pi\mathrm{G}}\left(R + \frac{6k}{t^2}\right) + \mathscr{L}_{\mathscr{M}}, \tag{3.3.5}$$

where $\mathscr{L}_{\mathscr{M}} = \Delta\rho$ is the Lagrangian term of the ordinary mass-energy density $\Delta\rho$. Note that the scalar curvature term $R + 6k/t^2$ corresponds to the local difference between the total Ricci scalar R and the local limit of the Ricci scalar estimated for the empty hyperconical universe, $R_u \approx -6k/t^2$. The modified Einstein-Hilbert action is now

$$S = \int d^4x\mathscr{L} = \int d^4x\sqrt{-g}\left[\frac{1}{16\pi\mathrm{G}}\left(R - R_u\right) + \mathscr{L}_m\right] \tag{3.3.6}$$

Therefore, a *modified gravity* is required for the general case. The simplest modification for the Lagrangian density is given by the general difference $\Delta R := R - R_u$, that is

$$\mathscr{L} = \frac{\Delta R}{16\pi\mathrm{G}} + \mathscr{L}_{\mathscr{M}} \;=\; \frac{R}{16\pi\mathrm{G}} + \underbrace{\rho_0 + \Delta\rho}_{:=\rho}, \tag{3.3.7}$$

which corresponds to a simple type of modified gravity Lagrangian density, which leads to equations similar than those obtained using a spatially flat FLRW universe. Moreover, the new Einstein field equations (Eq. 3.3.4) for the total contribution R are given by the

ones of the $\Delta R = g^{\mu\nu}\Delta R_{\mu\nu} = R - R_u$ as follows:

$$R_{00} - \frac{1}{2}R\,g_{00} - \frac{3}{t^2}g_{00} = \Delta R_{00} - \frac{1}{2}\Delta R\,g_{00} = 8\pi \mathrm{G} P^m_{00} \tag{3.3.8}$$

$$R_{ij} - \frac{1}{2}R\,g_{ij} - \frac{1}{t^2}g_{ij} = \Delta R_{ij} - \frac{1}{2}\Delta R\,g_{ij} = 8\pi \mathrm{G} P^m_{ij}\,, \tag{3.3.9}$$

where $P^m_{\mu\nu}$ is the ordinary stress-energy tensor. The extra blue term is equivalent to consider a "cosmological (almost) constant", or dark energy with equation of state $w = -1/3$, as mentioned above. In other words, the modification of the Lagrangian can be interpreted as a redefinition of the energy density baseline or *spacetime vacuum energy*,

$$\rho_0 = -\frac{1}{16\pi \mathrm{G}}R_u = \frac{3k}{8\pi \mathrm{G} t_0^2} = \rho_{crit}\,, \tag{3.3.10}$$

given by the global curvature $R_u = -6k/t_0^2$ and, therefore, it is the critical energy density with $k = 1$, as it is obtained by self-consistency of spacetime dynamics (Lemma 3.2.1 of Sec. 3.2). Defining an apparent energy $M_u := \frac{4}{3}\pi t_0^3 \rho_0$ of the spacetime, it is found that the age or cosmic horizon t_0 is

$$M_u = \frac{4}{3}\pi t_0^3 \frac{3}{8\pi \mathrm{G} t_0^2} = \frac{t_0}{2\mathrm{G}} \implies t_0 = 2\mathrm{G}M_u\,, \tag{3.3.11}$$

like the Schwarzschild radius of a gravitational system.

3.4 Result I-3: Intrinsic equivalence of dynamics

3.4.1 Equivalence in *proper* and in *angular diameter* distances

The ΛCDM and hyperconical models can be respectively interpreted as the intrinsic and extrinsic views of a same local universe, i.e. when distance approaches to zero. This local compatibility between the spatially flat FRW metric and the hiperspherical extrinsic metric (hyperconical universe) leads to an equivalence of the proper or comoving distance obtained according both models when only the intrinsic view is used. Specifically, the equivalence in (proper[4]) *intrinsic comoving distance* $\hat{r}'_{hyp}(z)$ of the hyperconical model (Def. 2.5.1) is compared to the one of the standard model ($\hat{r}'_\Lambda(z)$), which allow us to define an (intrinsic) apparent Hubble parameter $\hat{H}(z)$ for the hyperconical model, that also should coincide with the one of the standard model. That is,

$$\int_0^{z'} \frac{dz}{H_\Lambda(z)} =: \hat{r}'_\Lambda(z') \equiv \hat{r}'_{hyp}(z') =: \int_0^{z'} \frac{dz}{\hat{H}(z)} \tag{3.4.1}$$

[4]More exactly, the "proper distance" is usually defined by the product of the scale factor a and the comoving distance $\hat{r}'$, that is $\hat{r} := a\,\hat{r}'$. However, we can assume that the scale factor $a = 1/(1+z)$ is simplified here, because they should coincide too.

for $z \ll 1$, with the corresponding curvatures ($K = 0$ for the FLRW metric used in ΛCDM, and $k \equiv 1$ for the hyperconical model). In other words, the goal is to find the projection map $f^{\alpha}_{\hat{r}}$ that satisfies a second order (regional) equivalence between an apparent flat Hubble parameter $\hat{H}(z)$ (derived from the projected hyperconical universe) and the measured flat Hubble parameter (according to the ΛCDM model). To analyze the theoretical regional compatibility between both theories, the function $\hat{H}(z)$ is obtained and compared with H_Λ. From the right side of the Eq. 3.4.1 and considering Eqs. 2.3.14 and 2.3.15, it is easy to find that

$$\hat{H}(z) = \left[\frac{d}{dz'}\left(f^{\alpha}_{\hat{r}} \circ \xi_k^{-1} \circ \int_0^{z'} dz \frac{1}{H_{hyp}(z)}\right)\right]^{-1}(z) \tag{3.4.2}$$

where it is taken as $t_0 \equiv 1$ and thereby $H_{hyp}(z) = 1 + z$. The function ξ_k is that provided by Eq. 2.3.16 and the projection map $f^{\alpha}_{\hat{r}}$ is supposed equal to either ${}_a f^{\alpha}_{\hat{r}}$ (Eq. 2.5.3) or ${}_b f^{\alpha}_{\hat{r}}$ (Eq. 2.5.5). To distinguish both cases, the related Hubble parameters are denoted as ${}_a\hat{H}(z)$ and ${}_b\hat{H}(z)$.

Moreover, the angular diameter[5] distance (r_A) defined in Def. A.2.3 should also coincide, at least for small neighborhoods ($z \ll 1$). Again, for the flat ΛCDM model, it is

$$(r_A)_\Lambda := \frac{\hat{r}'_\Lambda(z)}{1+z} \equiv \frac{\hat{r}'_{hyp}}{1+z} =: (r_A)_{hyp}\,. \tag{3.4.3}$$

According to the selected projections, the similitude between both models is remarkable at local scale; but globally, our tested approaches ("toy models") are not equivalent to the standard model (Fig. 3.4.1). However, there must exist a unique exact solution for that equivalence, although it has not analytic formula. Let us see some approximate solutions for small neighbors ($z \ll 1$).

3.4.2 Second-order solutions

3.4.2.1 Compatibility analysis

Because the standard ΛCDM model has shown good results even for high redshifts, the theoretical compatibility of a hypothetical projection map (eg. Eq. 2.5.3 or Eq. 2.5.5) can be considered with their two free parameters: $\alpha \in (0, 1]$ and $\gamma_0 \in \mathbb{R}_{>\nvDash}$. Expanding the theoretical expression of H_Λ (Eq. A.1.6) in terms of Taylor-Maclaurin series up to second order, $H^{(2)}_\Lambda$, it is found that

$$\begin{aligned} H^{(2)}_\Lambda &= \sqrt{\Omega_r + \Omega_m + \Omega_\Lambda} + \frac{4\Omega_r + 3\Omega_m}{\sqrt{\Omega_r + \Omega_m + \Omega_\Lambda}}\frac{z}{2} \\ &+ \frac{8\Omega_r^2 + (24\Omega_\Lambda + 12\Omega_m)\Omega_r + 12\Omega_m\Omega_\Lambda + 3\Omega_m^2}{(\Omega_r + \Omega_m + \Omega_\Lambda)^{3/2}}\frac{z^2}{8} \end{aligned} \tag{3.4.4}$$

[5]For flat metrics, the "angular distance" coincides with the "proper distance".

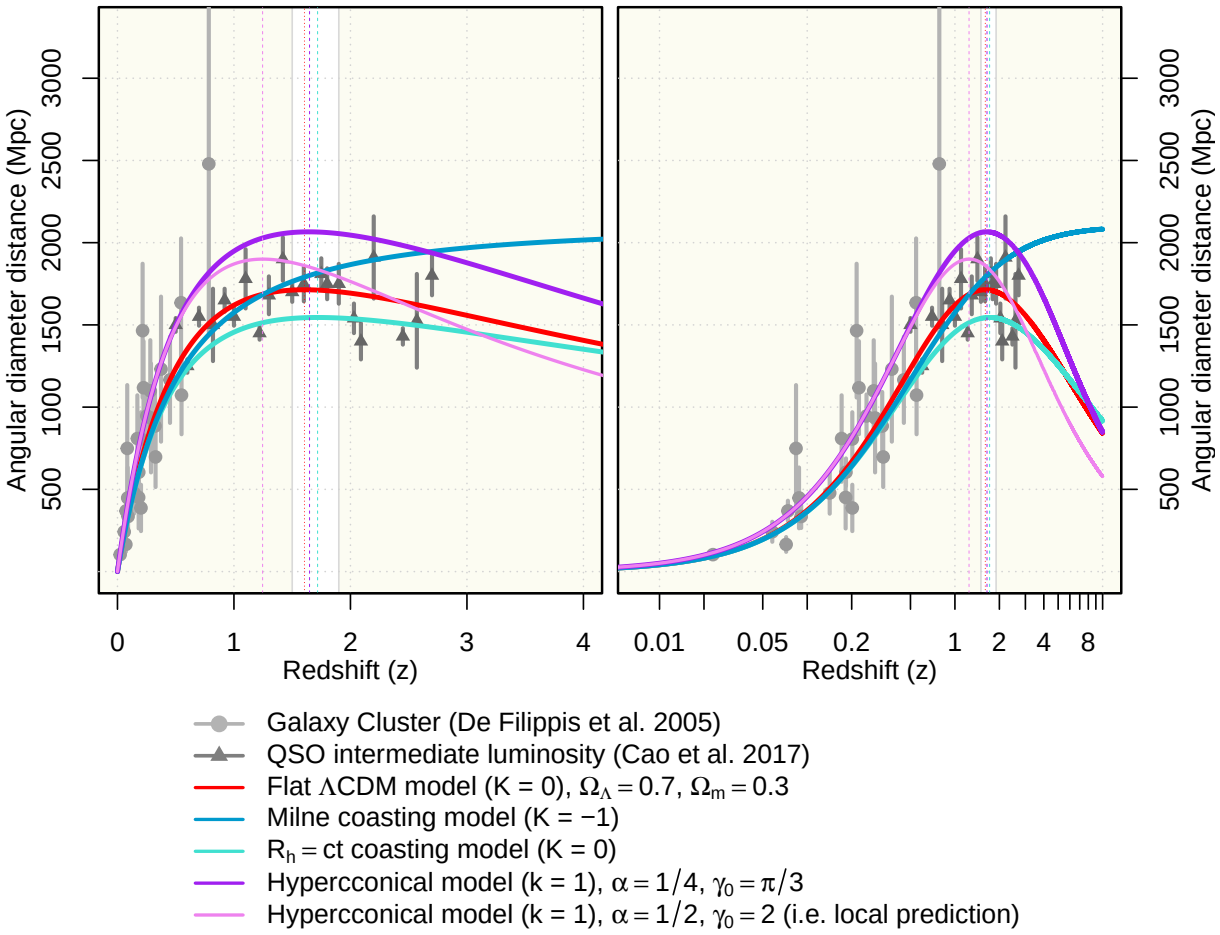

Figure 3.4.1: Theoretical predictions of angular diameter distances $r_A(z)$ according to Monjo 2024 for different cosmological models and comparison with model-independent observations collected from 25 galaxy clusters and 21 samples gathered from 107 quasar intermediate luminosity. The white vertical windows corresponds to the $1.5 \leq z \leq 1.9$ preferred range for 140 compact quasar cores. Dotted vertical lines represent the location of the maximum angular diameter distance for each model.

The Hubble parameter derived from the projected hyperconical universe (Eq. 3.4.2), expanded up to second order provides:

$$\hat{H}^{(2)} = 1 + \frac{\gamma_0 - 2\alpha\sqrt{k}}{\gamma_0} z + \\ + \frac{5\alpha^2 k - 2\alpha\sqrt{k}\gamma_0 - 3\alpha k + m\gamma_0^2}{2\gamma_0^2} z^2 \tag{3.4.5}$$

where either $m = 2$ (for $f_{\hat{r}}^{\alpha} = {}_a f_{\hat{r}}^{\alpha}$, Eq. 2.5.3) or $m = 5/2$ (for $f_{\hat{r}}^{\alpha} = {}_b f_{\hat{r}}^{\alpha}$, Eq. 2.5.5), with α assumed as approximately constant at second order.

Therefore, the equivalence expressed in the Eq. 3.4.1 leads to three equations corresponding to the zero, first and second orders of $H_{\Lambda}^{(2)}$ and $\hat{H}^{(2)}$. The zeroth order corresponds to the trivial flat FLRW universe $\Omega_r + \Omega_m + \Omega_\Lambda = 1$. The first order is dependent on the family shape parameter α. Even taking the normalization $k \equiv 1$ and assuming that $0 \approx \Omega_r \ll 1$, there are still three unknowns $(\Omega_m, \Omega_\Lambda, \alpha)$, with two equations. Thus, the second order equality is required to solve the system $H_{\Lambda}^{(2)} = \hat{H}^{(2)}$.

An important point is that, using the stereographic projection of the angle $\gamma \to \gamma/(1 - \gamma/\gamma_0)^{\alpha}$, the corresponding system up to third order ($H_{\Lambda}^{(3)} = \hat{H}^{(3)}$) is incompatible with a constant α and $\Omega_r \approx 0$. Thereby, the Eq. 2.5.3 and Eq. 2.5.5 should be considered just as a second order approximation with constant α. Nevertheless, to obtain a third-order approach, projections on the comoving distance $r' \to r'/(1 - \gamma/\gamma_0)^{\alpha}$ are adequate (see Sec. 3.4.3).

3.4.2.2 Existence of solutions

The second-order solutions for the system $H_{\Lambda}^{(2)} = \hat{H}^{(2)}$, given by Eqs. 3.4.4 and 3.4.5, are:

$$\Omega_\Lambda = \frac{3\alpha^2 k + 2\alpha\sqrt{k}\gamma_0 - \alpha k}{2\gamma_0^2} + \omega_\Lambda \tag{3.4.6}$$

$$\Omega_m = \frac{2\alpha k(1 - 3\alpha)}{\gamma_0^2} + \omega_m \tag{3.4.7}$$

$$\Omega_r = \frac{9\alpha^2 k - 2\alpha\sqrt{k}\gamma_0 - 3\alpha k}{2\gamma_0^2} + \omega_r \tag{3.4.8}$$

where $\omega_\Lambda = 1/2$ or $(6 + k)/12$, $\omega_m = 0$ or $-k/3$, $\omega_r = 1/2$ or $(2 + k)/4$ depending on whether ${}_a\hat{H}$ or ${}_b\hat{H}$ is used, as well $\Omega_\Lambda + \Omega_m + \Omega_r = 1$.

Let α be a free parameter now (i.e. $\alpha \neq 0.5$). Considering $k \equiv 1$ and $\Omega_r \approx 0$ ($\Omega_r = 9.0 \pm 0.5 \cdot 10^{-5}$), the numerical solutions correspond to two complex conjugate sets:

$$\begin{aligned} \alpha &= 0.2830219501(1) \pm c_\alpha i \\ \Omega_\Lambda &= 0.6937181(2) \pm c_\omega i \\ \Omega_m &= 0.306192(6) \mp c_\omega i \end{aligned} \tag{3.4.9}$$

where $c_\alpha = 0.204263(4)$ or $0.320386(2)$, $c_\omega = 0.260076(4)$ or $0.407928(3)$ depending on whether ${}_a\hat{H}$ or ${}_b\hat{H}$ is used, and the value in parenthesis is the interval error of last significant figure. Note that the real part of Ω_Λ and Ω_m are compatible with the observations updated by the Planck Mission ($\Omega_\Lambda = 0.6911 \pm 0.0062$ and $\Omega_m = 0.3089 \pm 0.0062$, [Adam *et al.* 2015]). If other positive values of k are considered ($0 < k < 1$), the real values predicted for the parameters remain about $\Omega_\Lambda = 0.699 \pm 0.005$, $\Omega_m = 0.3001 \pm 0.005$ and $\alpha = 0.280 \pm 0.003$.

Lemma 3.4.1 (**Existence of a real solution**). *Let ${}_af_{\hat{r}}^{\alpha}, {}_bf_{\hat{r}}^{\alpha} \in \mathcal{C}^\infty([0,\gamma_0),\mathbb{R}_{>0})$ be two projection maps (Eq. 2.5.3 and 2.5.5 with $t = t_0$) that are used in Eq.3.4.2 to find equivalences described in Eq. 3.4.1. If both equivalences produce the same real part of Ω_Λ and Ω_m, there exist a homotopy $\mathcal{F} : [0,\gamma_0) \times [0,1] \to \mathbb{R}_{>0}$ that transforms from $\mathcal{F}(\gamma,0) = {}_af_{\hat{r}}^{\alpha}(\gamma)$ to $\mathcal{F}(\gamma,1) = {}_bf_{\hat{r}}^{\alpha}(\gamma)$ in such a way that there exists a value of $\lambda \in (0,1)$ for which $\mathcal{F}(\gamma,\lambda)$ produces exactly real cosmological parameters, i.e. the imaginary part is zero, $c_\omega = 0$.*

Poof. To prove the existence of this configuration of $\mathcal{F}$, it is enough to define two more general projection maps ${}_af_{\hat{r}}^{{}_a\alpha}, {}_bf_{\hat{r}}^{{}_b\alpha} \in \mathcal{C}^\infty([0,\gamma_0),\mathbb{R}_{>0})$,

$$ {}_af_{\hat{r}}^{{}_a\alpha}(\gamma) = \nu t_0 \frac{\gamma}{\left(1-\frac{\gamma}{\gamma_0}\right)^{{}_a\alpha(\gamma)}} \tag{3.4.10} $$

$$ {}_bf_{\hat{r}}^{{}_b\alpha}(\gamma) = 2\nu t_0 \tan^{-1} \frac{\gamma}{2\left(1-\frac{\gamma}{\gamma_0}\right)^{{}_b\alpha(\gamma)}} \tag{3.4.11} $$

where the curves ${}_a\alpha(\gamma)$ and ${}_b\alpha(\gamma)$ solve $c_\omega = 0$ for ${}_a\hat{H}(z)$ and ${}_b\hat{H}(z)$, respectively (Fig. 3.4.2).

Considering the real part of Eq. 3.4.9 for H_Λ and the solution curves ${}_a\alpha(\gamma)$ and ${}_b\alpha(\gamma)$, we find that ${}_a\hat{H}(z) = {}_b\hat{H}(z) = H_\Lambda(z)$ (Fig. 3.4.2); that is, ${}_af_{\hat{r}}^{{}_a\alpha}(\gamma) = {}_bf_{\hat{r}}^{{}_b\alpha}(\gamma)$ for all $\gamma \in [0,\gamma_0)$. Trivially, there exist homotopies $\mathcal{F}_a(\gamma,\lambda) \in [{}_af_{\hat{r}}^{\alpha}(\gamma),\ {}_af_{\hat{r}}^{{}_a\alpha}(\gamma)]$ and $\mathcal{F}_b(\gamma,\mu) \in [{}_bf_{\hat{r}}^{{}_b\alpha}(\gamma),\ {}_bf_{\hat{r}}^{\alpha}(\gamma)]$ for $\lambda,\mu \in [0,1]$. Therefore, one of the possible transformations is $\mathcal{F}(\gamma,\lambda) := \lambda\,\mathcal{F}_b(\gamma,\lambda) + (1-\lambda)\,\mathcal{F}_a(\gamma,\lambda) \in [{}_af_{\hat{r}}^{\alpha}(\gamma),\ {}_bf_{\hat{r}}^{\alpha}(\gamma)]$ for $\lambda \in [0,1]$ that solves $c_\omega = 0$ is $\mathcal{F}(\gamma,1/2)$. ■

3.4.3 Third-order solutions

The second-order expansions were performed by using a distorting stereographic projection on the angles, that is a resulting comoving distance of $\hat{r}' = \nu t_0 \gamma/(1-\gamma/\gamma_0)^\alpha$. However, the definition of stereographic projection can be directly applied to the Minkowskian coordinates $(t,\vec{r},u) \to (\hat{t},\hat{u})$ according to the Sec. 2.5.3.2, that is $\hat{r}' = r'/(1-\gamma/\gamma_0)^\alpha$. Under this last perspective, theoretical compatibility between the standard and hyperconical models is up to third order to equalise the intrinsic Hubble parameter.

By applying the Taylor-Maclaurin expansion to both ΛCDM and hyperconical Hubble parameters (around the point at $\gamma = 0$), system of equations are obtained up to the

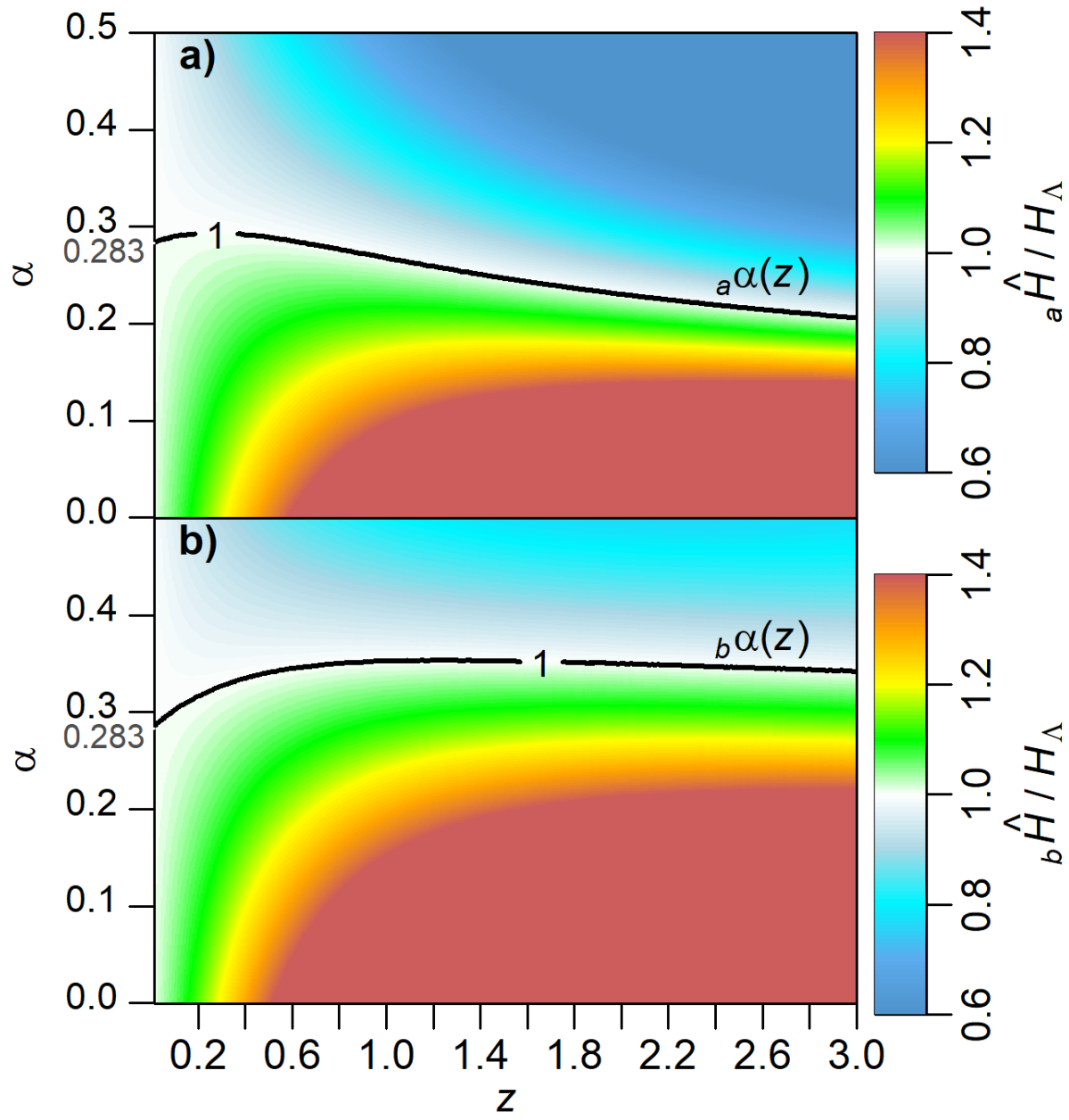

Figure 3.4.2: Theoretical compatibility between the Standard Model and the projected hyperconical universe: *a*) Solution curve $_a\alpha(z)$ found for $_a\hat{H} = H_\Lambda$, *b*) Solution curve $_b\alpha(z)$ found for $_b\hat{H} = H_\Lambda$

second order depending on the (global or local) approach considered. Applying Eq. 2.5.10 to the ($\alpha = 0.5$)-distorted projection and comparing to a simple ΛCDM model with $\Omega_r = 0 = \Omega_K$, it is locally found

$$\Omega_\lambda = \frac{2}{3}, \;\; \Omega_m = \frac{1}{3}, \;\; b_\ell = -\frac{5}{8} \tag{3.4.12}$$

A third-order global approach can be applied for $\Omega_K \neq 0$. Under this approach, $\lambda = \lambda_u$ (Eq. 2.5.12) and the angle $\gamma_0 = 2(1+\delta)$ is rewritten for some $|\delta| < 0.05$ to allow γ_0 ranging close to 2 and 2.09 (e.g. from local to global approaches), while the distortion parameter α is expressed as $\alpha = \frac{5}{18}\gamma_0(1+\epsilon)$. If $\epsilon = 0$ is considered (Appendix G), we get

$$\begin{aligned}
\Omega_\Lambda &= \frac{1}{1+\delta}\left(\frac{13}{18} + \frac{11}{36}\delta - \frac{5}{9}\delta^2\right) - \frac{1}{3}\Omega_r \\
\Omega_m &= \frac{1}{1+\delta}\left(\frac{1}{3} - \frac{1}{2}\delta - \frac{10}{9}\delta^2\right) - \frac{8}{3}\Omega_r \\
\Omega_K &= \frac{1}{1+\delta}\left(-\frac{1}{18} + \frac{43}{36}\delta + \frac{5}{3}\delta^2\right) + 2\Omega_r,
\end{aligned} \tag{3.4.13}$$

where $\delta = \pi/3 - 1$ can be taken if $\gamma_0 = 2\pi/3$. In particular, for $\Omega_r = 0 = \Omega_k$, two solutions of δ are found ($\delta \approx -0.76$ and $\delta \approx 0.044$ corresponding to $\gamma_0 \approx 0.49$ and $\gamma_0 \approx 2.09 \approx \frac{2}{3}\pi$) with both displaying the same matter $\Omega_m \approx 0.30$ and dark energy $\Omega_\Lambda \approx 0.70$. However, $|\delta| < 0.05$ is rejected by hypothesis. Similar results regarding dark energy/matter are found if $0 < \epsilon \leq \delta$ is restricted with a unique solution. For instance, with $\epsilon = \delta$ and $\Omega_r = 0$,

$$\begin{aligned}
\Omega_\Lambda &= \frac{13}{18} - \frac{25}{54}\delta + O(\delta^2) \\
\Omega_m &= \frac{1}{3} - \frac{55}{27}\delta + O(\delta^2) \\
\Omega_K &= -\frac{1}{18} + \frac{5}{2}\delta + O(\delta^2)\,.
\end{aligned} \tag{3.4.14}$$

The third-order contact point with $\Omega_r = 9.0(5)\cdot 10^{-5}$ and free Ω_K leads to similar dark energy values ($\Omega_\Lambda = 0.7032646(20)$), but a ΛCDM-closed universe ($\Omega_K = -0.01507(1)$) with more apparent dark matter ($\Omega_m = 0.311715(20)$). The emerging curvature coincides with the low distorting factor $\alpha = 0.573$ compared to $\alpha \approx 0.5765(1)$ obtained for an almost spatially flat universe ($\Omega_K = -0.008240(16)$). Similar results are found for the second-order global approach: The minimum distorting factor $\alpha = 5/9$ leads to a higher positive curvature ($\Omega_k = -1/18$) compared to $\alpha = 0.579857642(1)$, which is obtained by setting $\Omega_k = 0$. These findings are in concordance with the observation that a closed universe can provide a physical explanation for avoiding the so-enhanced lensing factor [DiValentino *et al.* 2020].

The curvature value is separated with respect to the best fit of PL18 temperature power spectra ($\Omega_K = -0.045(15)$), but is within the confidence level when lensing data

are added ($\Omega_K = -0.012(6)$) and also within the limits from the combination of Planck CMB temperature, polarization, and lensing power spectra ($\Omega_K = -0.0096(61)$). If BAO data are considered, the curvature is close to zero but statistically compatible with positive values ($\Omega_K = 0.0007 \pm 0.0019$). In conclusion, the constraints from the PL18 CMB spectra on curvature, parameterized through the energy density parameter lead to $0.007 > \Omega_K > -0.095$ at the 99%. The best PL18 fitting ($\Omega_K = -0.045(15)$) is only compatible with the modelled values under second-order contact point ($\Omega_K = -1/18 \approx -0.055$) (Table 3.1). The predicted value of $\Omega_K = -1/18$ is also aligned to the estimations of $\Omega_K = -0.07^{+0.12}_{-0.15}$ and $\Omega_K = -0.076 \pm 0.012$ found by combining cosmic chronometers and BAO data [Favale *et al.* 2023, Benisty and Staicova 2021].

Table 3.1: Intrinsic-viewpoint prediction: apparent cosmological parameters by equivalence between ΛCDM and (projected) hyperconical models for second- and third-order contact point, and considering local (L) and global (G) approaches. The fixed parameters are indicated with "(*set*)". The last significant figure error is shown in parentheses. The Hubble parameter (H_0/kms^{-1}Mpc^{-1}) is directly obtained from the *time factor* (F_t) assuming an age of $13.80(3) \cdot 10^9$ years.

Parameter	2^{nd}order(L), $\Omega_K = 0$	2^{nd}order(G), $\Omega_K \neq 0$	2^{nd}order(G), $\Omega_K = 0$	3^{rd}order(G), $\lvert\epsilon\rvert < \lvert\delta\rvert$	3^{rd}order(G), $\lvert\epsilon\rvert > \lvert\delta\rvert$	3^{rd}order(G), $\epsilon = \delta$
ϵ	0.081776(1)	$\mathbf{0}$ (*set*)	−0.00344(1)	−0.01482(1)	0.034462(4)	0.018718(2)
δ	−	$\mathbf{0}$ (*set*)	$\frac{\pi}{\mathbf{3}} - \mathbf{1}$ (*set*)	$\frac{\pi}{\mathbf{3}} - \mathbf{1}$ (*set*)	$\mathbf{0}$ (*set*)	0.018718(2)
α	$\mathbf{0.5}$ (*set*)	$\frac{5}{9} \approx 0.555$	0.579857642(1)	0.5731(1)	0.57466(4)	0.5765(1)
Ω_K	$\mathbf{0}$ (*set*)	$\frac{-1}{18} \approx -0.055$	$\mathbf{0}$ (*set*)	−0.015070(17)	−0.011819(15)	−0.008240(16)
Ω_r	$\mathbf{0}$ (*set*)	$\mathbf{0}$ (*set*)	$\mathbf{9.0}(5) \cdot 10^{-5}_{(set)}$	$\mathbf{9.0}(5) \cdot 10^{-5}_{(set)}$	$\mathbf{9.0}(5) \cdot 10^{-5}_{(set)}$	$\mathbf{9.0}(5) \cdot 10^{-5}_{(set)}$
Ω_m	$\frac{1}{3} \approx 0.333$	$\frac{1}{3} \approx 0.333$	0.297517827(1)	0.311715(20)	0.304056(17)	0.294737(18)
Ω_Λ	$\frac{2}{3} \approx 0.667$	$\frac{13}{18} \approx 0.722$	0.702482173(1)	0.7032646(20)	0.707674(4)	0.713413(3)
F_t	0.935881(1)	0.951745(1)	0.9663756(1)	0.9579073(17)	0.963691(4)	0.971050(3)
H_0	66.38(10)	67.50(10)	68.54(11)	67.94(11)	68.35(12)	68.87(13)

Chapter 4

Results II. Object dynamics

4.1 Introduction to moving objects

4.1.1 Limits of general relativity?

The second **original result** of this Thesis is the formulation of a new **modified gravity** (modified GR) [Monjo 2023], based on the direct geometrical implications of large-scale perturbations of our proposed Lorentzian metric (the hyperconical universe).

In Lorentzian manifolds, all free-falling objects are moving according to GR, which has been validated at least for local scales, such as the solar system, among others [Ciufolini *et al.* 2019, Touboul *et al.* 2022]. To reach this, parameterized post-Newtonian (PPN) techniques and the weak equivalence principle (WEP, equalising the inertial and gravitational masses) are usually considered [Dittus and Lämmerzahl 2007, Liu *et al.* 2022]. For instance, by employing the Pantheon sample of Type Ia supernova data, Liu *et al.* 2022 showed that GR is better fitted to the observations than the PPN model.

Results of similar works are also collected by Will 2014, who reviewed the validation of GR in other experiments such as: WEP in the Eötvös experiment, local Lorentz invariance, clock experiments, light deflection, the Shapiro time delay, the perihelion advance of Mercury, the Nordtvedt effect in lunar motion, and frame-dragging among others. Similar successes are achieved by the GR-based standard cosmological model (ΛCDM) fitted to CMB data, for instance, when it models the first peak location of baryon acoustic oscillations [Aghanim *et al.* 2020b]. Concerning tests on gravitational waves produced by black hole mergers, when we consider noise effects and inaccurate approximations, all the findings up to date are compatible with general relativity [Will 2014].

Nevertheless, the strong equivalence principle (SEP) is recognized as the most appropriate to distinguish GR from other viable theories of gravity [Chae *et al.* 2020]. The SEP affirms that internal dynamics of a self-gravitating system under free fall (into an external gravitational field) should not depend on the external field strength. In other words, every observer falling in a gravitational field can choose a locally inertial coordinate system for a sufficiently small region such that the laws of nature take the same form as in an unaccelerated Minkowskian frame in absence of gravitation [Chae *et al.* 2020, Goto *et al.*

2010]. However, according to the results of Chae et al. [Chae *et al.* 2020], external field effects (EFE) are statistically detected at more than four standard deviations (4σ) from 153 rotating galaxies of the Spitzer Photometry and Accurate Rotation Curves (SPARC) database. This outcome points to a breakdown of the SEP, supporting modified gravity theories beyond GR, since tidal effects from neighboring galaxies in the standard ΛCDM framework are not enough to explain it [Banik and Zhao 2022].

Applying the standard gravity model, excess rotation appears in most galaxies, highlighting a discrepancy between the visible matter and the required mass to support the observed velocities. To solve this problem, galaxy rotation curves are usually modeled by the hypothetical presence of CMD in the halos [Bhattacharya *et al.* 2013, Beck and Sarkis 2023]. However, these hypothetical halos predict a systematically deviating relation from the observations, while all aspects of rotation curves appear to be more naturally explained by modified gravities [McGaugh *et al.* 2007, Chae 2022]. Furthermore, the empirically derived densities of the dark matter halos for low-mass galaxies are half of what is predicted by CMD simulations [deBlok *et al.* 2008].

Alternatively, modified gravities could explain the empirical mass-discrepancy acceleration relation since it is found as a function of the visible matter M_b [Trippe 2014, Merritt 2017, Goddy *et al.* 2023]. In other words, the local ratio between observed and expected velocities is strictly predictable given only the observed distribution of visible matter in the galaxy, without the need of additional (e.g., dark-matter based) variables. The empirical law is known as mass-luminosity relation or baryonic Tully-Fisher relation (BTFR),

$$M_b = A\, v^{\epsilon} \tag{4.1.1}$$

for a 'flat' velocity curve v observed in a galaxy disk, with $\epsilon \approx 4$ (see for instance Goddy *et al.* 2023). Or similarly, it can be expressed as a mass-discrepancy acceleration relation (MDAR) [McGaugh 2004, Di Cintio and Lelli 2016],

$$\frac{M_b + M_{CDM}}{M_b} = \frac{v^2}{v_K^2} = C|a_N|^{-\beta} = C\left(\frac{r}{v_K^2}\right)^{\beta} \implies v^4 = C^2 r^{2\beta}\, v_K^{4(1-\beta)} \approx C^2 \mathrm{G} M_b \tag{4.1.2}$$

where $\beta \approx 0.5$, $M_b + M_{CDM}$ is the total mass including CMD and $C^2\mathrm{G} \approx: A^{-1}$ is approximately inverse of the same constant as used in Eq. 4.1.1, while Newtonian acceleration $|a_N| = \mathrm{G}M_b/r = v_K^2/r$ is expressed as a function of the Kepler speed v_K and the distance r to the galactic center. To solve the problem, some authors suggested that dark matter presents a stronger coupling to the baryon matter and, therefore, both matter contents are linked by an effective law [Blanchet 2007, Katz 2016, Barkana 2018]. However, the excess rotation only occurs where the acceleration induced by the visible matter is lower than a typical scale (almost constant value) of gravitation, pointing to a more general problem involving spatial scales than a problem involving matter types, as the relic galaxies seem to point [Comeron *et al.* 2023]. Therefore, most of observations suggest the need to modify the standard gravity models [Trippe 2014, Merritt 2017].

4.1.2 Limits of Newtonian dynamics?

Milgrom 1983 proposed modified Newtonian dynamics (MOND) as a possible alternative to the cold dark mass hypothesis. Milgrom's law is expressed in terms of the external force F and the acceleration a experienced by the objects,

$$F = m\ a\ \cdot \mu\left(\frac{a}{a_0}\right)\ , \tag{4.1.3}$$

where a_0 was proposed to be a new universal constant, with values around $a_0 \approx 1.2 \cdot 10^{-10}$ m/s^2. That is the second Newton's law but multiplied by an *unknown*[1] scalar function $\mu : \mathbb{R}_{\geq 0} \to \mathbb{R}_{\geq 0}$ of interpolation, such that $\mu\left(\frac{a}{a_0}\right) \approx 1$ for $a \gg a_0$, recovering Newton's $F = ma$, but it presents a 'deep MOND behaviour' for $a \ll a_0$,

$$F = m\frac{a^2}{a_0}\,, \tag{4.1.4}$$

or an equivalent in a Newtonian gravity system of mass $M = M_b$,

$$\frac{\mathrm{G}Mm}{r^2} = m\frac{\left(\frac{v^2}{r}\right)^2}{a_0} \implies v^4 = \mathrm{G}Ma_0\ , \tag{4.1.5}$$

which corresponds to the typical 'flat velocity' of most of galaxy rotation curves. Other versions of MOND are commonly used, such as the *quasi-linear MOND* or QUMOND, and the *aquadratic Lagrangian* (AQUAL) formulation of MOND [Banik and Zhao 2022]. A remarkable finding on the value of a_0 is its possible relation with the age t of the universe, since $a_0 \approx \frac{1}{6}c/t$. Therefore, this Chapter explores a connection to the cosmological models.

MOND and other similar approaches can (at least partially) explain the excess rotation of galaxies or the equivalent mass-discrepancy acceleration without the requirement of dark matter halos [Gentile 2008, Asencio *et al.* 2022]. According to the results of Asencio *et al.* 2022, gravitational distortion of dwarf galaxies support solutions based on modified gravity theories rather than the existence of dark matter. Particularly, the lack of low surface brightness in dwarfs towards its centre is incompatible with ΛCDM expectations but consistent with MOND. Chae 2024 found robust evidences of MOND in the low acceleration orbits of widely separated binary stars. Banik and Zhao 2022 published an extensive review of most observed evidences and concluded that MOND-type gravities are "favoured by a wealth of data across a huge range of astrophysical scales, ranging from the kpc scales of galactic bars to the Gpc scale of the local supervoid and the Hubble tension, which is alleviated in MOND through enhanced cosmic variance."

However, the Milgrom's MOND theory presents important limitations to explain some observed dynamics, such as these found in the QSO Lyα forest and the Bullet Cluster [Aguirre *et al.* 2001, Clowe *et al.* 2006, Angus *et al.* 2006]. This issue could be solved by a more general theory with variable a_0 and/or with a relativistic formulation with MOND behaviour at the $a \ll a_0$ limit.

[1] There are several (empirical) proposals of interpolation function $\mu\left(\frac{a}{a_0}\right)$, but with serious limitations for galaxy clusters [Banik and Zhao 2022].

4.1.3 Relativistic formulation of MOND?

Relativistic formulations of gravity with MOND behaviour were initially proposed by Bekenstein and Milgrom 1984 but presented problems of superluminical solutions that were solved later by modifying the 'physical metric' to $\tilde{g}_{\alpha\beta} = e^{-2\phi} g_{\alpha\beta} + u_\alpha u_\beta \left(e^{-2\phi} - e^{2\phi}\right)$ with vector field u_α determined by the Lagrangian

$$\mathscr{L}_v = -\frac{1}{16\pi \mathrm{G}} \left[\left(\frac{K}{2} F^{\alpha\mu} F_{\alpha\mu} \right) + 4\lambda \left(g^{\mu\nu} u_\mu u_\nu - 1 \right) \right] \sqrt{-g} \tag{4.1.6}$$

where G is the Newtonian constant, K is another constant, $F_{\alpha\beta} = \partial_\alpha u_\beta - \partial_\beta u_\alpha$ and λ is a Lagrange multiplier field included to enforce the normalization of the vector field, while the scalar function ϕ depends on the dynamics of the tensor $\mathrm{h}_{\alpha\beta} := g_{\alpha\beta} + u_\alpha u_\beta$. With these ingredients, Bekenstein 2004 defined the Tensor–vector–scalar gravity (TeVeS) model. However, TeVeS shows some problems in simulating stars, highly unstable on the scale of approximately two weeks [Seifert 2007]. Therefore, the construction of TeVeS requires an undetermined number of terms to solve all the raised problems [Mavromatos *et al.* 2009]. Furthermore, any covariant MOND theory should also be valid at cosmological scales [Famaey and McGaugh 2012], since GR and the Friedmann–Lemaître–Robertson–Walker (FLRW) metric are the basis of the Friedmann equations (used in the standard ΛCDM model).

Under this perspective, Skordis and Złośnik proposed an alternative relativistic MOND (RMOND) with additional terms analog to the FLRW action [Skordis and Złośnik 2021]. This new proposal showed that its action expanded to the second order is free of ghost instabilities and discussed its possible embedding in a more fundamental theory. Additionally to the galacting and lensing phenomentology, RMOND also is in agreement with the observed CMB and matter power spectra on linear cosmological scales

4.1.4 A natural relativistic formulation

Consistently with the antecedents above, this Chapter shows a new formulation of MOND-like dynamics with the minimum possible number of Lagrangian terms using natural features of the hyperconical universes in agreement with previous work [Monjo 2017, Monjo 2018, Monjo and Campoamor-Stursberg 2020, Monjo and Campoamor-Stursberg 2023]. To address this goal, a hyperconical model was built by concatenating two steps. First, the use of moving frames produces an apparent radial inhomogeneity from the extrinsic viewpoint of the expansion. Second, stereographic projections assimilate the radial inhomogeneity as a fictitious acceleration under the intrinsic perspective.

Specifically, let homogeneous universes have positive ($k > 0$), null ($k \approx 0$) or negative ($k < 0$) curvature. Thus, according to Chapter 2, moving frames in linearly expanding homogeneous universes lead to an apparent radial inhomogeneity in the isotropic spacetime, whose metric is

$$ds^2 \approx dt^2 \left(1 - kr'^2\right) - \frac{t^2}{t_0^2} \left(\frac{dr'^2}{1 - kr'^2} + r'^2 d\Sigma^2 \right) - \frac{2r't}{t_0^2} \frac{dr'dt}{\sqrt{1 - kr'^2}} \tag{4.1.7}$$

where $r' \ll t_0$ is the comoving distance, Σ represents the angular coordinates and $t_0 \equiv 1$ is the current value for the age t of the universe. Both the Ricci curvature scalar and Friedmann equations derived from this universe for $k = 1 = 1/t_0^2$ are locally equivalent to those obtained for a flat ΛCDM model with linear expansion.

Observational compatibility of both extrinsic and intrinsic viewpoints was checked with Type Ia supernovae data [Monjo 2017], ascertaining that the intrinsic measurement fits better (with $k > 0$) when the luminosity distance is employed to analyze redshifts. Theoretical compatibility between the expansion of the hyperconical model and the standard ΛCDM model is checked in Sec. 3.4. Particularly, compatibility demonstrates that there exists a projection that assimilates the radial inhomogeneity as a fictitious acceleration in the expansion, like the ΛCDM model. Particular solutions are detailed in Sec. 3.4.2 and 3.4.3.

Assuming that GR is valid at least at a local scale and applying ADM formalism to analyze the consistency of the hypercone-based dynamics, three remarkable results are displayed in Chapter 3: (1) the total energy density of the universe is inactive since the equation of state is $w = -\frac{1}{3}$; (2) the spatial curvature of the hyperconical manifold needs to be $k = 1$; and (3) the Lagrangian density $\mathscr{L}$ requires a slight modification to

$$\mathscr{L} = \frac{1}{16\pi \mathrm{G}} \Delta R + \mathscr{L}_m \tag{4.1.8}$$

where $\mathscr{L}_m$ is the matter Lagrangian density and $\Delta R = R - R_u$ is the difference between the scalar curvature R of the gravitational system and the scalar curvature R_u of the background metric (hyperconical universe). Locally[2], if $k = 1$, it is $R_u = -1/t_0^2$, with age t_0 of the universe.

Moreover, according to the previous chapters, the result of the Lemma 3.2.1 for $k = 1$ predicts: (1) a third-order ΛCDM-compatible (apparent) acceleration when the hyperconical universe is projected to an intrinsic viewpoint; (2) consequently, an apparent dark energy of about $\Omega_\Lambda = 0.70$ is found as a constant for any age of the universe; (3) dark matter is another parameter whose value could be totally or partially consequence of the distortion projection; and (4) the Hubble tension observed between direct geometrical methods (e.g., distance ladder) and indirect methods (e.g., CMB) can be explained by the difference between the extrinsic and intrinsic viewpoints of the hyperconical universe.

The present section assumes that GR needs to be adapted to the results of the previous chapters, especially concerning the 'zero active mass' ($w = -\frac{1}{3}$) of Lemma 3.3.1, also proposed by Melia 2017, and the modified Lagrangian density (Eq. 4.1.8).

[2]Here, locally means that the scalar curvature is evaluated at each point ($r' \equiv 0$).

4.2 Result II-1: Perturbed metric by objects

4.2.1 Mass of perturbation

In the case of an (unperturbed) homogeneous universe, linear expansion of $\mathcal{H}^4$ can be expressed in terms of the vacuum energy density, $\rho_0(t) =^3 3/(8\pi \mathrm{G} t^2)$ linked to $\rho_0(t_0) = \rho_{crit}$, where G is the Newtonian gravitational constant. That is, one can define an inactive (vacuum) mass or energy $\mathscr{N}(r) = \rho_0 \frac{4}{3}\pi r^3$ for a distance equal to r with respect to the *reference frame origin*. By using the relation between the original coordinates $(dt, dr, r\, d\Sigma)$ and the comoving ones $(dt, a(t)\, dr', a(t) r' d\Sigma)$, the spatial dependence of the metric (with $\nu = 1$) is now

$$\frac{r'^2}{t_0^2} = \frac{r^2}{t^2} = \frac{2\mathrm{G}\rho_0 \frac{4}{3}\pi r^3}{r} = \frac{2\mathrm{G}\mathscr{N}(r)}{r} \tag{4.2.1}$$

Definition 4.2.1 (**Mass of perturbation**)**.** From the modified Lagrangian density displayed in Eq. 4.1.8, a perturbation (Appendix D) of the vacuum density $\rho_0 \to \rho_M(r) := \rho_0 + \Delta\rho$ leads to a mass $M := \frac{4}{3}\pi r^3 \Delta\rho$, which is likewise obtained by perturbing the spatial curvature term,

$$\frac{r'^2}{t_0^2} \;\to\; \frac{\hat{r}'^2}{\hat{t}_M^2} := \frac{\hat{r}'^2}{\hat{t}_0^2} + \frac{2\mathrm{G}M}{\hat{r}} \tag{4.2.2}$$

with total radius of curvature $\hat{t}_M =^4 \hat{t}_M(\hat{r})$, reference time $\hat{t}_0 = t_0$, and comoving distance $\hat{r}' := \frac{t}{t_0}\hat{r}$ for center-referred coordinate $\hat{r}$ of M.

Notice that $\hat{r}$ and $\hat{r}'$ are coordinates of an object with respect to the position of a central mass M, in contrast to the radial r and comoving distance r' of any object with respect to any observer.

4.2.2 Approach to the Schwarzschild metric

An exact and spherically symmetric solution for the Einstein field equations (Eq. 1.3.35) at vaccum (null Ricci curvature tensor, $R_{\alpha\beta} = 0$) is the Schwarzschild solution, which needs to be embedded in a six-dinensional spacetime (see Appendix E). However, an approximation to the Schwarzschild solution can be obtained into a flat five-dimensional ambient space from the hyperconical metric. For instance, let $(t, \vec{r}, u) := (t, x, y, z, u) \in \mathbb{R}^{1,4}_\eta$ be Cartesian coordinates, including an extra spatial dimension u in the five-dimensional Minkowski plane. As used in hyperconical embedding (Appendix B), $u := t\cos\gamma - t$ is chosen to mix space and time. Now, it includes a gravity field with central mass M observed at a distance $\hat{r}$ such that $\sin^2\gamma := \hat{r}'^2/t_0^2$ is considered according to the Definition 4.2.1.

[3]Recall that, for a more efficient (abusive) language, $\rho_0(t)$ means that a map $\rho_0 : \mathbb{R}_{>0} \to \mathbb{R}_{>0}$ is evaluated for a time $t \mapsto \rho_0(t)$.

[4]Similarly to the above, $\hat{t}_M = \hat{t}_M(\hat{r})$ is an abbreviated way to define the map $\hat{t}_M : \mathbb{R}_{>0} \to \mathbb{R}_{>0},\ \hat{r} \mapsto \hat{t}_M(\hat{r})$ while it is assumed its evaluation for a specific value of the parameter $\hat{r} \in \mathbb{R}_{>0}$.

Then, the background metric of the hyperconical universe (Eq. 4.1.7) can be approximated up to second order ($r'^2/t_0^2 \ll 1$) as follows:

$$ds^2_{hyp} \approx dt^2\left(1-\frac{r'^2}{t_0^2}\right) - \frac{t^2}{t_0^2}\left[\left(1+\frac{r'^2}{t_0^2}\right)dr'^2 + r'^2 d\Sigma^2\right] - \frac{2r't}{t_0^2}dtdr' \quad (4.2.3)$$

where the curvature $1/t_0^2$ contributes to the vacuum energy density $\rho_0(t) = 3/(8\pi \mathrm{G}t^2)$. The conservative condition of curvature for empty hyperconical universes is $k \equiv 1 \equiv \nu$, or $\beta_0 = 0$, as derived from dynamical systems in Lemma 3.2.1. Considering this condition, and adding a perturbation[5] in density such as $\rho_0 \to \rho_0 + \Delta\rho(\hat{r})$, the spatial curvature term (Eq. 4.2.1) is now expressed in coordinates $(\hat{t}, \hat{r})$ projected with respect to the center of perturbation (with curvature $1/\hat{t}_M^2$), that is

$$\frac{r'^2}{t_0^2} \to \frac{\hat{r}'^2}{\hat{t}_M^2} = \frac{2\mathrm{G}(\rho_0 + \Delta\rho(\hat{r}))\frac{4}{3}\pi\hat{r}^3}{\hat{r}} = \frac{\hat{r}'^2}{t_0^2} + \frac{2\mathrm{G}M(\hat{r})}{\hat{r}} \ll 1\,, \quad (4.2.4)$$

where $M(\hat{r}) := \rho_0(\hat{r})\frac{4}{3}\pi\hat{r}^3$ is the energy of the perturbation, like in Def. 4.2.1. Finally, the total metric $g = g_{\mu\nu}dx^\mu dx^\nu$ can be obtained by replacing Eq. 4.2.4 in Eq. 4.2.3,

$$g \approx \left(1 - \frac{\hat{r}'^2}{t_0^2} - \frac{2\mathrm{G}M}{\hat{r}}\right)d\hat{t}^2 - \frac{\hat{t}^2}{t_0^2}\left[\left(1 + \frac{r'^2}{t_0^2} + \frac{2\mathrm{G}M}{\hat{r}}\right)d\hat{r}'^2 + \hat{r}'^2 d\Sigma^2\right] - \frac{2\hat{r}'\hat{t}}{t_0^2}d\hat{t}d\hat{r}' \quad (4.2.5)$$

and considering $\hat{r}'/t_0 \ll 2\mathrm{G}M/\hat{r} \ll 1$, a Schwarzschild-like[6] metric is obtained:

$$g_{Sch} := g\big|_{\hat{r}' \ll t_0} \approx \left(1 - \frac{2\mathrm{G}M}{\hat{r}}\right)d\hat{t}^2 - \frac{\hat{t}^2}{t_0^2}\left[\left(1 + \frac{2\mathrm{G}M}{\hat{r}}\right)d\hat{r}'^2 + \hat{r}'^2 d\Sigma^2\right]. \quad (4.2.6)$$

which is also $g_{Sch} \approx \eta + h$, where the Schwarzschild perturbation is $h := g - g^{back}$ for $g^{back} := g|_{M=0}$ and flat metric η. This result is aligned to the Schwarzschild-like metric obtained by Mitra 2013 for FLRW metrics, specifically for the case of $K = 0$. Finally, using the Kerr-Schild coordinate time, $\hat{t} \mapsto \hat{t}' = \hat{t} + \phi(\hat{r})$, with $\phi'(\hat{r}) := 2\mathrm{G}M/(1 - 2\mathrm{G}M)$, the Kerr-Schild perturbation for $\hat{t} = t_0$ is

$$h_{\mu\nu}\big|_{Schw} = \eta_{\mu\nu} - \frac{2\mathrm{G}M}{\hat{r}}k_\mu k_\nu\,, \quad (4.2.7)$$

where k_μ is a null four-vector, for instance $k_\mu = (1, 1, 0, 0)$ [Gurses *et al.* 2018].

Remark 4.2.1 (**Metric components and speeds relationship**)**.** Notice that the Schwarzschild metric (Eq. 4.2.7) is similar to the $g \approx \eta + u \otimes u$ obtained in Eq. 2.3.10 (except for the shift term), since one can define an escape velocity by $v_E := \sqrt{2\mathrm{G}M/\hat{r}'}$ and thus $g_{rr} = -1 - u_E u_E$; while for the empty spacetime, it is $u_H := \hat{r}'/t_0$ and $g_{rr} = -1 - u_H u_H$. Therefore, in general terms, one can define a total escape velocity by $u^2 := u_H^2 + u_E^2$.

[5]Since the locally-conformal projection of coordinates lead to an apparently flat (i.e. homogeneous) metric (Sec. 2.5.6), we assume that, for some reference frame, the perturbation can be defined only in the diagonal of the metric.

[6]For our gravitational approach, the shift term is neglected in comparison to the g_{tt} component.

In summary, the first-order approach from the 5-dimensional embedded hyperconical metric (Eq. 4.2.6) differs to the Schwarzschild vacuum solution by the scale factor t^2/t_0^2. Therefore, classical Newtonian limit of the GR is also recovered in the hyperconical model, because the largest contribution to the gravity dynamics is given by the temporal component of the metric perturbation h_{tt}. That is, the Schwarzschild geodesics are linearized by

$$\frac{d^2x^\mu}{d\tau^2} \approx \frac{1}{2}\eta^{\mu\nu}\frac{\partial}{\partial x^\nu}h_{tt}\left(\frac{d\hat{t}}{d\tau}\right)^2 \,, \tag{4.2.8}$$

where $h_{tt} \approx -2\mathrm{G}M/\hat{r}$. Nevertheless, the following section (see Sec. 4.3.3) describes a more general case for large structures, which need to consider distorting stereographic projections $r \to \hat{r}$, obtaining that:

$$h_{tt} \;\approx\; -\frac{2\mathrm{G}M}{r} + \frac{2}{\gamma_0}\frac{r}{t}$$

where $\gamma_0 \geq 2$ is a parameter that produces a MOND-like regime, depending on the geometry of the gravitational system considered. For example, for galaxy rotation curves, it is $\gamma_0 \approx 10$ [Monjo 2023].

4.3 Result II-2: Distorted measurements

4.3.1 Projective angles

For closed and homogeneous universes, without density perturbations nor projective transformations, all inertial velocities v are due to the expansion of the universe like in an empty spacetime. For each angle γ, the Hubble law is simply $v_H = Hr = \frac{r}{t} = c\sin\gamma$, with Hubble parameter $H = \frac{1}{t}$ and a domain $\gamma \in [0, \gamma_U)$ for the spatial coordinates (Eq. 2.3.5), satisfying $\sin\gamma_U = \sqrt{3/4}$, which is $\gamma_U = \frac{1}{3}\pi \approx 1$ [Monjo 2017, Monjo 2018]. This is the projective domain for an empty hyperconical universe with positive curvature $k = 1$, specifically $\gamma_U := \sin^{-1}\sqrt{1 - k/4} = \pi/3$ [Monjo 2018]. Then, projecting the (positively-curved) hyperconical universe onto a plane, the resulting projected angle is $\gamma \in [0, \gamma_0)$ with a maximum angle γ_0 that is double γ_U [Monjo and Campoamor-Stursberg 2023]:

$$\gamma_U \;\mapsto\; \gamma_0 \approx \frac{\gamma_U}{\cos\gamma_U} \approx \frac{2}{3} \approx 2\,. \tag{4.3.1}$$

See Appendix 2.5.3.2 for more details. After the projection, our model becomes theoretically compatible with the standard ΛCDM model up to the third order of approximation (providing the same cosmological parameters of $\{\Omega_\Lambda \approx 0.7, \Omega_m \approx 0.3, \Omega_K \approx 0\}$) for every time t_0 [Monjo and Campoamor-Stursberg 2023]. That is, the dark energy and matter are interpreted as apparent quantities for the observers since the observed paths of light are intrinsic in the manifold. Nevertheless, the cosmic timeline is the same as in the extrinsic perspective, with a linear expansion and 'zero active mass' ($w = -\frac{1}{3}$) [Monjo and Campoamor-Stursberg 2020].

The projective angle defined in Eq. 4.3.1 changes when vacuum energy is perturbed. In such a case, the gravitational system (Eq. 4.2.4) results in a characteristic scale of $r_{cs}(M) := \hat{t}_M(\hat{r}) \sin \gamma_M(\hat{r})$ given by a maximum angle $\gamma_M \geq \gamma_U = \frac{\pi}{3}$ that is approximately constant, $\gamma_M \in [\pi/3, \pi/2)$, but it slightly depends on the radial distance $\hat{r}$ and on a function of the mass M. Since the gravitational system perturbs the cosmological geometry with an escape velocity of $v_E^2(\hat{r}) = \frac{2\mathrm{G}M}{\hat{r}}$, the following is expected:

$$\sin^2 \gamma_M(\hat{r}) = \frac{r_{cs}^2(M)}{\hat{t}_M^2(\hat{r})} = \frac{r_{cs}^2(M)}{\hat{t}^2} + \frac{2 r_{cs}^2(M)\, \mathrm{G}M}{\hat{r}^3} = \sin \gamma_U + \beta(\hat{r}) \frac{2\mathrm{G}M}{\hat{r}}\,, \tag{4.3.2}$$

with $\beta(\hat{r}) := r_{cs}^2/\hat{r}^2 \gg 1$, which is $\sin^2 \gamma_M(\hat{r}) \approx \sin^2 \gamma_U + \beta(\hat{r}) v_E^2(\hat{r})$ by approaching $\sin^2 \gamma_U \approx r_{cs}^2/t^2$ when $2\mathrm{G}M \ll r_{cs}(M) \approx \hat{t}$. On the opposite side, $\sin^2 \gamma_M \approx \sin^2 \gamma_{gc} \approx 1$ for regions close to the galaxy center (angle γ_{gc} when $\hat{r} = 2\mathrm{G}M \ll \hat{t}$), but with small cosmological perturbations on the surroundings as

$$1 \approx \sin^2 \gamma_{gc} \approx \frac{r_{cs}^2(M)}{\hat{t}_M^2(\hat{r})} + \frac{r_{cs}^2(M)}{3\,\hat{t}^2} \approx \frac{4}{3} \beta(\hat{r}) \frac{\hat{r}^2}{\hat{t}^2} + \beta(\hat{r}) \frac{2\mathrm{G}M}{\hat{r}}\,. \tag{4.3.3}$$

Since $t_M^2(r) \in (4\mathrm{G}^2M^2, t^2]$ and $r_{cs}^2(M) \in (4\mathrm{G}^2M^2, \frac{3}{4}\hat{t}^2]$, $r_{cs}^2(M)$ is increasing from $r_{cs}^2(M) = \hat{t}_M^2(\hat{r}) = 4\mathrm{G}^2M^2 \ll \hat{t}^2$ up to $r_{cs}^2(M) = \frac{3}{4} t_M^2(\hat{r}) = \frac{3}{4} t^2 = t^2 \sin^2 \gamma_U$, reducing the maximum angle from $\gamma_M = \frac{\pi}{2}$ to $\gamma_M = \frac{\pi}{3}$. At galactic scales, Eq. 4.3.3 can be approached by $\sin^2 \gamma_{gc} \approx \sin^2 \gamma_M(r) + \beta(\hat{r}) v_H^2(\hat{r}) \approx \sin^2 \gamma_U + \beta(\hat{r}) v_E^2(\hat{r}) + \beta(\hat{r}) v_H^2(\hat{r})$ and, applying the quotient to remove the dependency on $\beta(\hat{r})$, it is

$$\frac{\sin^2 \gamma_M(\hat{r}) - \sin^2 \gamma_U}{\sin^2 \gamma_{gc} - \sin^2 \gamma_U} \approx \frac{v_E^2(\hat{r})}{v_H^2(\hat{r}) + v_E^2(\hat{r})} = \frac{\rho}{\rho_0 + \rho}\,, \tag{4.3.4}$$

where $\rho_0 = 3/(8\pi \mathrm{G} \hat{t}^2)$ is the vacuum energy density at the time $\hat{t}$. For galaxies and small gravitational systems, the escape velocity v_E^2 is strongly related to the Kepler orbital speed $v_K^2 \approx 2v_K^2$, and two limiting cases are $\sin \gamma_M \approx 1$ when orbital speed is $v_K(\hat{r}) \sim v_E(\hat{r}) \gg v_H(\hat{r})$ and $\sin \gamma_M \approx \frac{\sqrt{3}}{2}$ when orbital speed is $v_K(\hat{r}) \sim v_E(\hat{r}) \ll v_H(\hat{r})$. In sum, $\gamma_U \cong \pi/3$ and $\gamma_{gc} \cong \pi/2$ are assumed to be constant, while γ_M (or γ_0) depends on the energy density perturbation.

4.3.2 Background metric projection

Henceforth, the speed of light $c \equiv 1$ will be not omitted in the equations to compare with real observations later. Let λ_u be the scaling factor of a stereographic projection (Appendix 2.5.3.2) of the coordinates $(r, u) = (ct \sin \gamma,\ ct \cos \gamma)$,

$$\lambda_u \approx \frac{1}{1 - \frac{\gamma}{\gamma_0}}\,, \tag{4.3.5}$$

where $\gamma_0 = \gamma_U / \cos \gamma_U = \frac{2}{3}\pi$, since empty spacetimes have $\gamma_M = \gamma_U$. For non-empty matter densities, we contend that γ_M depends on the escape velocity of the gravity system

considered, assuming that dependency on distances is weak, thus γ_0 is approximately constant for each case. The spatial distortion is given by an exponent $\alpha > 0$ in the scaling factor λ, such as:

$$\lambda_u^\alpha \approx 1 + \frac{\alpha\gamma}{\gamma_0} \approx 1 + \frac{\alpha r'}{\gamma_0 t_0 c}\,. \tag{4.3.6}$$

Therefore, the coordinates are

$$\hat{r}' = \lambda_u^\alpha t_0 \gamma \approx \lambda_u^\alpha r' \approx \left(1 + \frac{\alpha r'}{\gamma_0 t_0 c}\right) r' \tag{4.3.7}$$

$$\hat{t} = \lambda_u t = \left(1 + \frac{r'}{\gamma_0 t_0 c}\right) t \tag{4.3.8}$$

At a local scale, $\alpha = 1/2$ is required to guarantee consistency in dynamical systems (see Sec. 2.5.5), but the parameter α is not essential here since the contribution of $\lambda_u^\alpha r'$ can be neglected compared to the contribution of $\lambda_u t$ in curvature effects.

Applying this projection to the metric and the corresponding geodesics, it is easy to obtain a first-order approach of the cosmological perturbation that contributes to modify the Newtonian dynamics in the classical limit.

4.3.3 First-order perturbed metric

The perturbed metric components (Eq. 4.2.5, or more specifically Eq. 4.2.6) are written in terms of projected[7] coordinates with respect to the central mass. Assuming that γ_0 is approximately constant, the differential and quadratic form of the time coordinate are

$$\begin{aligned} d\hat{t} &\approx \left(1 + \frac{r'}{\gamma_0 t_0 c}\right) dt + \frac{t}{\gamma_0 \pi t_0 c} dr' \\ d\hat{t}^2 &\approx \left(1 + \frac{r'}{\gamma_0 t_0 c}\right)^2 dt^2 + \left(\frac{t}{\gamma_0 t_0 c}\right)^2 dr'^2 + 2\left(1 + \frac{r'}{\gamma_0 t_0 c}\right)\frac{t}{\gamma_0 t_0 c}\frac{dr'}{dt} dt^2 \approx \\ &\approx \left(1 + \frac{2r'}{\gamma_0 t_0 c} + \frac{2t\dot{r}'}{\gamma_0 t_0 c}\right) dt^2 \quad + \quad \text{upper-order terms}\,. \end{aligned} \tag{4.3.9}$$

By using these prescriptions, the projected coordinates $(\hat{t}, \hat{r}')$ can be expressed in terms of the original ones (t, r'). Finally, the new expression of the Schwarzschild-like metric (Eq. 4.2.6) is simplified up to first-order perturbation terms assuming that radial variations $(d\hat{r}')$ are neglected in regular orbits[8], $d\hat{r}' \ll \hat{r}' d\Sigma \ll d\hat{t}$:

$$g_{Sch} = g_{\mu\nu} dx^\mu dx^\nu \approx \left(1 - \frac{2\mathrm{G}M}{c^2 \hat{r}}\right) c^2 d\hat{t}^2 - \frac{\hat{t}^2}{t_0^2}\hat{r}'^2 d\Sigma^2 \approx \tilde{g}_{tt} c^2 dt^2 + \tilde{g}_{ii} (dx^i)^2\,.$$

[7] Since the perturbation is intrinsically measured by an observer, we assume that projection plays a role in the gravity system as a fictitious acceleration that depends on the "cosmic coordinates" selected.

[8] Here, spatial components of the metric are irrelevant because Schwarzschild geodesics are dominated by the time component.

Here, one identifies a projected perturbation $\tilde{h}_{tt}$ of the time component of the metric, $\tilde{g}_{tt} = \eta_{tt} + \tilde{h}_{tt} = 1 + \tilde{h}_{tt} = 1 + v_H v_H/c^2 + v_E v_E/c^2$ with escape velocities $v_H := \hat{r}/\hat{t}$ and $v_E := \sqrt{2\mathrm{G}M/\hat{r}}$. Thus, if M is the mass of a central gravity source, the first-order perturbation of the temporal component of the metric is

$$\begin{aligned}
\tilde{h}_{tt} &\approx -\frac{2\mathrm{G}M}{rc^2}\left(1 - \frac{\alpha r}{\gamma_0 tc}\right) + \frac{2}{\gamma_0 c}\left(\frac{r}{t} + \frac{t}{t_0}\dot{r}'\right) \\
\frac{\partial}{\partial t}\tilde{h}_{tt} &\approx -\frac{2\mathrm{G}M}{rc^2}\left(\frac{\alpha r}{\gamma_0 t^2 c}\right) + \frac{2}{\gamma_0 c}\left(-\frac{r}{t^2} + \frac{1}{t_0}\dot{r}'\right) \approx \frac{2\alpha\mathrm{G}M}{\gamma_0 t^2 c^3} + \frac{2}{\gamma_0 c}\left(\frac{\dot{r}'}{t_0} - \frac{r}{t^2}\right) \\
\frac{\partial}{\partial r}\tilde{h}_{tt} &\approx -\frac{2\mathrm{G}M}{r^2c^2} + \frac{2}{\gamma_0 tc}
\end{aligned}$$

where the relation between the comoving distance r' and the spatial coordinate r has been used; that is, $r'/t_0 = r/t$.

4.3.4 First-order perturbed geodesics

Under the Newtonian limit of the GR, the largest contribution to the gravity dynamics is given by the temporal component of the metric perturbation $\tilde{h}_{tt}$. That is, the Schwarzschild geodesics,

$$\frac{d^2x^\mu}{d\tau^2} \approx \frac{1}{2}\eta^{\mu\nu}\frac{\partial}{\partial x^\nu}\tilde{h}_{tt}\left(\frac{cdt}{d\tau}\right)^2 , \tag{4.3.10}$$

is perturbed by the distorted steoreographic projection.

On the right side of Eq. 4.3.10, one finds time-like and space-like components from the metric perturbation $\tilde{h}_{tt}$, with a (flat) metric signature $\eta_{\mu\nu} = \eta^{\mu\nu} = \mathrm{diag}(1,-1,-1,-1)$,

$$\frac{d^2\hat{s}}{d\tau^2} \approx \left(\frac{1}{2}\frac{\partial}{\partial x^0}\tilde{h}_{tt}\,e_t \;-\; \frac{1}{2}\frac{\partial}{\partial x^i}\tilde{h}_{tt}\,e_i\right)\left(\frac{cdt}{d\tau}\right)^2 , \tag{4.3.11}$$

where the four-position $\hat{s} := (c\Delta t, x^i) = c\Delta t\,e_t + x^i\,e_i \in \mathbf{R}^{1,3}$ is assumed, with $\Delta t := t - t_0$.

Considering a Schwarzschild metric with cosmological perturbation for a test particle orbiting around a central mass M, its geodesic equation is

$$\begin{aligned}
\frac{d^2\hat{s}}{c^2dt^2} &\approx \frac{1}{2}\frac{\partial\tilde{h}_{tt}}{c\partial t}\,e_t \;-\; \frac{1}{2}\frac{\partial\tilde{h}_{tt}}{\partial x^i}\,e_i = \frac{1}{2}\frac{\partial\tilde{h}_{tt}}{c\partial t}\,e_t \;-\; \frac{1}{2}\frac{\partial\tilde{h}_{tt}}{\partial r}\frac{\partial r}{\partial x^i}\,e_i \\
\frac{d^2\hat{s}}{c^2dt^2} &\approx -\left(\cancel{-\frac{\dot{r}'}{\gamma_0 t_0 c^2}} + \frac{r}{\gamma_0 c^2 t^2} + \frac{\alpha\mathrm{G}M}{\gamma_0 t^2 c^4}\right)e_t \;-\; \left(\frac{\mathrm{G}M}{c^2r^2} + \frac{1}{\gamma_0 ct}\right)\frac{x^i}{r}\,e_i
\end{aligned} \tag{4.3.12}$$

where the first term of the right side is **neglected for orbits**. This is a simple space-like vector, but for $r/t \ll 1$, it is mostly determined by the Newtonian acceleration $a_N := -\frac{\mathrm{G}M}{r^2}\frac{x^i}{r}\,e_i$ within the spatial component. For a free-falling particle with central-mass reference coordinates $\mathbf{x} = x^i e_i = (r,0,0) = \mathbf{r} \in \mathbb{R}^3$, it experiences a spatial acceleration as

$$\mathbf{a} := a^r e_r := \frac{d^2\mathbf{r}}{dt^2} \approx \;-\;\left(\frac{\mathrm{G}M}{r^2} + \frac{c}{\gamma_0 t}\right)\frac{\mathbf{r}}{r} \;=\; a_N - \frac{c}{\gamma_0 t}\frac{\mathbf{r}}{r}\,. \tag{4.3.13}$$

That is, an acceleration anomaly is obtained in the spatial direction, about $|\mathbf{a} - a_N| \approx \gamma_0^{-1} c/t$. However, the total acceleration also has time-like component (i.e., with direction e_t).

The anomaly $\mathbf{a} - a_N$ is similar to the low limit predicted by Moffat MOdified Gravity (MOG), also known as Scalar–Tensor–Vector–Gravity (STVG) theory [Moffat et al. 2014, Moffat and Toth 2018]. Specifically, The MOG acceleration law for a point source in weak gravitational fields and low velocities is [Moffat and Toth 2018, Harikumar *et al.* 2022]:

$$\begin{aligned} a &:= -\frac{\mathrm{G}M}{r^2}\left(1 + \alpha_G - \alpha_G \exp(-\mu r)(1+\mu r)\right) \approx \\ &\approx -\frac{\mathrm{G}M}{r^2}\left(1 + 2\alpha_G \mu^2 r^2\right) \approx -\frac{\mathrm{G}M}{r^2}\left(1 + 2\alpha_G \frac{D^2}{M} r^2\right) \approx a_N - 2\mathrm{G}\alpha_G D^2 \,, \end{aligned} \quad (4.3.14)$$

where $\mu = D/\sqrt{M}$ and $\alpha_G \approx 10\, M/(\sqrt{M} + E)^2$ with MOG universal constants $D = 6.25 \cdot 10^3 M_{sun}^{1/2}$ kpc^{-1} and $E = 2.5 \cdot 10^4 M_{sun}^{1/2}$, and it is assumed that $\mu r \ll 1$ in $\exp(-\mu r) \approx 1 - \mu r$. For $M \gg E$, one obtains $\alpha_G \approx 10$ and the anomaly is $|\mathbf{a} - a_N| \approx 20\, \mathrm{G}D^2 \approx 1.1 \cdot 10^{-10}\mathrm{m/s}^2 \approx \gamma_0^{-1} c/t$ for $\gamma_0 \approx 6$, which is very similar to the prediction of Eq. 4.3.13.

4.4 Result II-3: Object acceleration

4.4.1 Time-like contribution to the centrifugal acceleration

By using the Eq. 4.3.12 plus additional assumptions, it is possible to derive an expression for rotation velocity curves of galaxies and their mass-discrepancy acceleration relationship. The assumptions we are referring to are that: i) extrinsic curvature of our universe contributes to centrifugal acceleration in the time-like direction, and ii) for orbital velocity, the variation of radial distance can be approximated to zero, which is $\dot{r}' = dr'/dt \approx 0$, compared to the other contributions. On the left side of Eq. 4.3.12, centrifugal acceleration has also both time-like and space-like components in the mostly spatial radius direction, $e_s := \hat{s}/||\hat{s}|| = -e_t \sinh\gamma - e_{\vec{r}} \cosh\gamma$, where $\hat{s}$ is the position vector with respect to the central mass M and $e^t e_t = -e^{\vec{r}} e_{\vec{r}} = -e^s e_s = 1$ since the metric signature is $(+,-,-,-)$. Notice that the (new) coordinates in the direction e_s are given by a Lorentz rotation with a relative speed of the Hubble law $v_H := \frac{r}{t} = c \sin\gamma$, that is, $\gamma = \arcsin(\frac{r}{ct}) = \arcsin(\frac{r'}{ct_0})$.

Thus, the time-like contribution to the centrifugal acceleration is nonzero and it is proportional to $1/(ct)$ as the spatial contribution is proportional to $1/r$. Using these ingredients, centrifugal acceleration is rewritten in terms of the spatial velocity v and the acceleration direction e_s, as follows:

$$\hat{a} := \frac{d^2\hat{s}}{c^2 dt^2} = -\omega_t^2 ct\, e_t \sinh\theta - \omega_r^2 r\, e_{\vec{r}} \cosh\theta = \underbrace{-\left(\frac{1}{ct} e_t e^t + \frac{1}{r} e_{\vec{r}} e^{\vec{r}}\right)}_{=:\, S^{-1}} \frac{v^2}{c^2} e_s = S^{-1} \frac{v^2}{c^2} e_s \,, \tag{4.4.1}$$

where $S^{-1} := -\left(\frac{1}{ct} e_t e^t + \frac{1}{r} e_{\vec{r}} e^{\vec{r}}\right)$ is an auxiliary matrix, while $\omega_t := v/t$ and $\omega_r := v/r$ are the angular speeds in the time- and space-like directions, respectively, assuming a tangential speed v.

4.4.2 Acceleration curve

By using this assumption, a mass-discrepancy acceleration relation can be derived. Applying the inverse S of the diagonal matrix S^{-1} to the Eq. 4.4.1, in this way

$$\frac{v^2}{c^2} e_s = -\left(ct e_t e^t + x^i e_i e^i\right) \frac{d^2 s}{c^2 dt^2} \approx\; ct \left(\frac{\alpha \mathrm{G} M}{\gamma_0 t^2 c^4} + \frac{r}{\gamma_0 c^2 t^2}\right) e_t \;+\; \left(\frac{\mathrm{G} M}{c^2 r^2} + \frac{1}{\gamma_0 ct}\right) \frac{x^i x_i}{r}\, e_i \,, \tag{4.4.2}$$

an effective space-like direction ($||e_s||^2 = e_s e^s = -1$) is found, and the absolute value of the velocity is given by

$$\begin{aligned}
\frac{v^4}{c^4} = -\left|\left|\frac{v^2}{c^2}e_s\right|\right|^2 &\approx -\left[\left(\frac{\alpha \mathrm{G}M}{\gamma_0 t c^3} + \frac{r}{\gamma_0 c t}\right)^2 - \left(\frac{\mathrm{G}M}{c^2 r} + \frac{r}{\gamma_0 c t}\right)^2\right] = \\
&\approx \left(\frac{\mathrm{G}M}{c^2 r}\right)^2 + \frac{2\mathrm{G}M}{\gamma_0 t c^3} - \left(\frac{\alpha \mathrm{G}M}{\gamma_0 t c^3}\right)^2 - \frac{2\alpha \mathrm{G}M\, r}{\gamma_0^2 t^2 c^4} \\
&\approx \left(\frac{\mathrm{G}M}{r c^2}\right)^2 \left(1 - \frac{\alpha^2 r^2}{\gamma_0^2 c^2 t^2}\right) + \frac{2\mathrm{G}M}{\gamma_0 t c^3}\left(1 - \frac{\alpha r}{\gamma_0 c t}\right) \\
&\approx \left(\frac{\mathrm{G}M}{r c^2}\right)^2 + \frac{2\mathrm{G}M}{\gamma_0 t c^3}\,, \qquad (4.4.3)
\end{aligned}$$

which satisfies two well-known limits of Newton's dynamics and Milgrom's MOND:

$$v \approx \sqrt{\frac{\mathrm{G}M}{r}} \qquad \text{if } \frac{\mathrm{G}M}{r^2} \gg \frac{2c}{\gamma_0 t} := a_0 \qquad (4.4.4)$$

$$v \approx \sqrt[4]{\frac{2\mathrm{G}Mc}{\gamma_0 t}} \qquad \text{if } \frac{\mathrm{G}M}{r^2} \ll \frac{2c}{\gamma_0 t} = a_0\,, \qquad (4.4.5)$$

where a_0 is the Milgrom's acceleration parameter and $M = M(r)$ is the total mass within the central sphere of radius r. Finally, the velocity curve $v = v(r)$ can be re-expressed in terms of the escape velocity $v_E := \sqrt{2\mathrm{G}M(r)/r}$ or of the Kepler speed $v_K := \sqrt{\mathrm{G}M(r)/r} = \sqrt{|a_N|}$ as follows:

$$v^4 = v_K^4 + v_K^2\, r\frac{2c}{\gamma_0 t} = \frac{1}{4}v_E^4 + v_E^2\, r\frac{c}{\gamma_0 t}\ . \qquad (4.4.6)$$

Therefore, the predicted mass-discrepancy acceleration relation is

$$\frac{v^4}{v_K^4} = 1 + \frac{r}{v_K^2}\frac{2c}{\gamma_0 t} \implies \left(\frac{v}{v_K}\right)^2 = \sqrt{1 + \frac{1}{|a_N|}\frac{2c}{\gamma_0 t}}\ . \qquad (4.4.7)$$

Chapter 5

Results III. Particle dynamics

5.1 Introduction to moving particles

5.1.1 Motivation: metric-based motion

In this Chapter, we present **original developments** [Monjo et al. 2024] to address the hypothesis that *all the natural dynamics can be expressed in terms of a spacetime-particle field*; that is, produced by vector fields U that perturb the metric as $g \approx \eta + U \otimes U$ in a similar way to the moving frames in GR. Therefore, this Chapter aims to lay a foundation for exploring possible *quantum gravity* in comparison to other natural interactions.

The starting point in GR is the statement (principle) on the equivalence between the gravitational mass (energy) and the inertial mass (energy). However, this principle is not applicable to other interactions. Furthermore, gravity has no stress-energy tensor, but locally it is possible to define a work (energy) given by the gravity potential, which is transformed into kinetic energy. Both depend on the reference system and, therefore, are important actors in GR. A key idea is to define an adequate energy origin to perturb the metric. As a consequence, the interaction energy (mass) may be different from the inertial energy (mass) because of the definition of the reference frame and energy origins.

5.1.2 The last hypothesis

More specifically, the principle developed here is the Hypothesis 3 of the Thesis. This is equivalent to search a bridge between the Cartan covariant derivative and the $\mathrm{SU}(1,n-1)$ gauge derivative for some $n \in \mathbb{N}$ to go towards a possible *quantum gravity* (Sec. 5.3). For this purpose, the spacetime generators γ_a are perturbed (Sec. 5.2.2) by an $\mathrm{SU}(1,n-1)$ gauge potential field A_μ involving the gauge phase of the matter-energy fields (Sec. 5.2.1) such that $v^\mu \approx e^\mu{}_a \gamma^a + O(A_\mu)$. In order words, we assume that the set of generators $\{v_\mu\}_\mu$ contains information of some dynamics of the Standard Model. Our goal is to show how the Yang–Mills $\mathrm{SU}(1,n-1)$ dynamics emerges from locally perturbed tetrads, and to check some related features, such as the recovery of electrodynamics (Sec. 6.3).

5.2 Result III-1: Coloured Lorentzian manifold

5.2.1 Perturbed spinor frames

This subsection presents the main developments for a *unified quantum field theory* applied to small perturbations in the metric, which are linked to some *physical particles* or *spinors*[1]. The novelty of this result is that the *unified quantum field theory* encompasses GR and electrodynamics, as well as it explores a general way to produce $\mathfrak{su}(1,3)$-based interactions applied to spinors. The key idea is to perturb angular phases of spinors by using the corresponding transformations to produce effects on the spacetime, which we will call "coloured spacetime algebra" (Sec. 5.2.2).

Let $\Psi = \{\psi_n\}_{n=1}^4 = \{\psi_1, \psi_2, \psi_3, \psi_4\}$ be a set of 4 Dirac spinor fields[2] on a 4-manifold $\mathscr{N}$, that is, a set of 4 column vectors of fermions or pairs of Weyl spinors. Recall that each Dirac spinor has 4 components $\psi_n(\psi_n^\mu)_{\mu=0}^3$; therefore, they can be represented by matrices $|\Psi\rangle \in \mathcal{M}_4(\mathbb{C}) = \mathbb{C} \times Cl_{1,3}(\mathbb{R}, g)$, and the total spin of Ψ is an integer value between -2 and 2. These spinor fields represent *particles* with the same energy, $m \in \mathbb{R}$, ideally expressed by the 4-moment $\mathbf{m}$, i.e., a matrix satisfying $\mathbf{m} \cdot \mathbf{m} = m^2 \mathbf{1}_4$, where $\mathbf{1}_4$ is the identity matrix. The moment can be decomposed in components by means of the generators of the spacetime algebra, $\{m_\mu := \mathbf{m} \cdot \gamma_\mu\}_\mu$, thus yielding the set of angular wavenumbers of Ψ. As a physical assumption, we identify these angular wavenumbers with classical momenta,

$$\mathbf{m} \cdot \gamma_\mu = m_\mu = m u_\mu \mathbf{1}_4 := m \frac{dx_\mu}{d\tau} \mathbf{1}_4. \tag{5.2.1}$$

Therefore, the velocity is $\mathbf{u} := \mathbf{m}/m = \gamma^\mu u_\mu$. In addition, the spacetime element is given by $\mathbf{d\tau} := \gamma_\mu dx^\mu$, whence $\mathbf{m} \cdot \mathbf{d\tau} = m_\mu dx^\mu$. As a result, we may write

$$\Psi := \Psi_0(\mathbf{m}) \exp\left(-i \int \mathbf{m} \cdot \mathbf{d\tau}\right). \tag{5.2.2}$$

From now on, the integration symbol $(\int)$ is omitted

$$\Psi \simeq \Psi_0(\mathbf{m}) \exp\left(-i\, \mathbf{m} \cdot \gamma_\mu\, dx^\mu\right). \tag{5.2.3}$$

Let $\mathbf{A} = A_\mu \gamma^\mu$ be a gauge potential field, expressed by using the spacetime algebra [Dressel *et al.* 2015], while let $A = A_\mu dx^\mu \in \Omega^1(\mathscr{N}, \mathfrak{su}(1,3))$ be a connection on some principal $\mathrm{SU}(1,3)$-bundle over $\mathscr{N}$, whose components $A_\mu = A_\mu^I \lambda_I$ are represented by using a basis $\{\lambda_I\}_{I=1}^{15}$ of $\mathfrak{su}(1,3)$.

Moreover, let $\partial_\mu \mapsto \nabla_\mu := \partial_\mu - \mathrm{i} q A_\mu$ be the transformation of its covariant derivative with a coupling factor $q \in \mathbb{R}_{>0}$. In coordinates, this is equivalent to the introduction of a phase $\varphi(x)$ to the spinor field given by the appearance of the potential

[1] In geometry, the *smallest physical particles* known as *fermions* are mathematically represented by Dirac spinors, or pairs of Weyl spinors, with half-integer *spin*

[2] We use the notion of spinor bundles defined as vector bundles whose fibers carry spinor representations of the Clifford algebras $Cl_{1,3}(\mathbb{R}, g)$ and, then, spinor fields are sections of spinor bundles [Trautman 2008].

field **A**. According to Eq. 1.3.20 with vanishing starting potential, i.e., $\nabla_\mu^{(init)} = \partial_\mu$, the final potential field is $A_\mu(x) = q^{-1}[\nabla_\mu^{(init)}, \varphi(x)] = q^{-1}[\partial_\mu, \varphi(x)] = q^{-1}\partial_\mu\varphi(x)$. Therefore, the phase $\varphi(x) = \lambda_I\varphi^I(x) = qA_\mu^I(x)\lambda_I dx^\mu = qA_\mu(x)dx^\mu$ has 15 'angular' parameters $\{\varphi^I(x)\}_{I=1}^{15}$, and it is added to transform the field by the unitary operator $U(x) := \exp(\mathrm{i}\varphi(x)) = \exp(\mathrm{i}qA_\mu(x)dx^\mu)$. To compensate this phase, the covariant derivative acts like the Hermitian adjoint operator $U^\dagger(x) := \exp(-\mathrm{i}\varphi(x)) = \exp(-\mathrm{i}qA_\mu(x)dx^\mu)$ as follows

$$\Psi \;\mapsto\; \hat{\Psi} = \Psi_0(\mathbf{m}) \exp\left(-i\left(\mathbf{m}\cdot\gamma_\mu + qA_\mu\right)dx^\mu\right). \tag{5.2.4}$$

The operator $U^\dagger(x) = \exp(-\mathrm{i}qA_\mu(x)dx^\mu) \approx \exp(-\mathrm{i}q\int A_\mu(x)dx^\mu)$ is also related to the Wilson loop, a generalization of the Aharanov-Bohm effect [Ferrari *et al.* 1989, Alfonsi *et al.* 2020].

It can be easily verified that the gauge covariant derivative $\nabla_\mu = \partial_\mu - \mathrm{i}qA_\mu$ satisfies the symmetric transformation $\hat{\Psi}^\dagger\hat{\nabla}_\mu\hat{\Psi} = \Psi^\dagger\nabla_\mu\Psi$, with

$$\hat{\nabla}_\mu = U(x)\nabla_\mu U^\dagger(x). \tag{5.2.5}$$

Moreover, the compensatory phase $\varphi(x) = qA_\mu(x)dx^\mu = q(\mathbf{A}(x)\cdot\gamma_\mu)dx^\mu = q\mathbf{A}(x)\cdot\mathbf{d}\boldsymbol{\tau}$ yields the following transformation,

$$(\gamma_\mu\cdot\mathbf{m})dx^\mu \;\mapsto\; \left(\gamma_\mu + qA_\mu\cdot\frac{\mathbf{m}}{m^2}\right)\cdot\mathbf{m}\,dx^\mu, \tag{5.2.6}$$

where we have used that $\mathbf{m}\cdot\mathbf{m} = m^2\mathbf{1}_4$. We denote by $\hat{\gamma}_\mu$ the perturbed spacetime generators,

$$\gamma_\mu \;\mapsto\; \hat{\gamma}_\mu := \gamma_\mu + A_\mu\cdot\frac{q}{\mathbf{m}} = \gamma_\mu + a_\mu^I\lambda_I\cdot\frac{\mathbf{m}}{m}, \tag{5.2.7}$$

where we denote $a_\mu^I := qA_\mu^I/m$ and $1/\mathbf{m} := \mathbf{m}/m^2$ for simplicity. Here, the four-vector A_μ^I has one timelike and three spacelike components, analogous to a four-velocity. On the other hand, it is possible to interpret the compensatory phase of Eq. 5.2.6 as an energy perturbation, $\mathbf{m} \;\mapsto\; \hat{\mathbf{m}} := \mathbf{m} + q\mathbf{A}$. This is equivalent to Eq. 5.2.7, since $\gamma^\mu\cdot\mathbf{m}\cdot\hat{\gamma}_\mu = \mathbf{m} + q\mathbf{A} = \hat{\mathbf{m}}$. Now, one can define $\hat{\mathbf{u}} := \hat{\mathbf{m}}/m = \gamma^\mu\hat{u}_\mu = \mathbf{u} + q\mathbf{A}/m$, where

$$u_\mu \;\mapsto\; \hat{u}_\mu := \mathbf{u}\cdot\hat{\gamma}_\mu = \mathbf{1}_4 u_\mu + A_\mu\frac{q}{m} \;\in \mathbb{R}\oplus\mathfrak{su}(1,n-1), \tag{5.2.8}$$

with $A_\mu = A_\mu^I\lambda_I$ and, therefore, **one needs** that $n = 4$. Here, $\mathbb{R}$ is regarded as a subspace of $\mathfrak{gl}(4,\mathbb{C})$ via the injection $a \mapsto a\mathbf{1}_4$. Note that Eqs. 5.2.7 and 5.2.8 satisfy the relation defined by Eqs. 1.3.13 and 1.3.14. The velocity component $\hat{u}_\mu$ is an element of $\mathbb{R}\oplus\mathfrak{su}(1,3)$ because $\lambda_I \in \mathfrak{su}(1,3)$ and $A_\mu^I, q/m, u_\mu \in \mathbb{R}$. Therefore, the velocity $\hat{\mathbf{u}} = \gamma^\mu\hat{u}_\mu$ implies that the translation $d\hat{\mathbf{x}} = \hat{\mathbf{u}}\,d\tau$ is an element of $\mathbb{R}^{1,3}\oplus\mathfrak{u}(1,3)$, which includes the Poincaré algebra $\mathbb{R}^{1,3}\oplus\mathfrak{o}(1,3)$. Thus, all the above calculations performed with A_μ can be replicated for any element of $\mathbb{R}^{1,3}\oplus\mathfrak{u}(1,3)$.

Moreover, notice that the perturbation of the 4-velocity is a *current* term qA_μ/m, similar to the Ferrari proposal [Ferrari *et al.* 1989] and the *London equation* in electrodynamics [Fröhlich and Werner 2013, Badía-Majós *et al.* 2006], interpreted as the ground state of

the tetrad under the gauge selected, consistent with the Dirac equation. Up to first order, by applying the change of $0 \mapsto A_\mu$ to the co-tetrad transformation $e^a \mapsto \hat{e}^a$ (Eq. 1.3.1), and by assuming local invariance of the spacetime algebra, $\gamma^a := e_\mu{}^a \gamma^\mu \equiv \hat{e}_\mu{}^a \bullet \hat{\gamma}^\mu$, Eq. 5.2.7 yields

$$e_\mu{}^a \gamma^\mu = \hat{e}_\mu{}^a \bullet \hat{\gamma}^\mu \approx \left(e_\mu{}^a + \phi_\mu{}^a\right) \bullet \left(\gamma^\mu - A^\mu \frac{q}{\mathbf{m}}\right) \quad \Longrightarrow \quad \phi_\mu{}^a \bullet \gamma^\mu \approx e_\mu{}^a A^\mu \bullet \frac{q}{\mathbf{m}} = A^a \bullet \frac{q}{\mathbf{m}},$$

where we write $A^a := e_\mu{}^a A^\mu$. The co-tetrad perturbation $\phi_\mu{}^a$ **is now a matrix** that is not unique. We use the following as an ansatz,

$$\phi_\mu{}^a := -\mathrm{i}qA_\mu{}^a := qA^a \frac{m_\mu}{m^2} = \frac{q}{m} A^a u_\mu = A^a \bullet \frac{q}{\mathbf{m}} \bullet \gamma_\mu, \tag{5.2.9}$$

where $A_\mu{}^a := \mathrm{i}A^a m_\mu / m^2$ and $m_\mu = m u_\mu \mathbf{1}_4$, being $u_\mu := dx_\mu / d\tau$ the 4-velocity covector (recall Eq. 5.2.1). The constant $-\mathrm{i}q$ is explicitly stated by convenience. Since $e_a(e^b)\mathbf{1}_4 = \hat{e}_a(\hat{e}^b) = \hat{e}^\mu{}_a \bullet \hat{e}_\mu{}^b = \delta_b^a \mathbf{1}_4$, the tetrad perturbation is $\phi^\mu{}_a = e^\mu{}_b e^\nu{}_a \phi_\nu{}^b \approx -\mathrm{i}qA^\mu{}_a$, with $\hat{e}^\mu{}_b = e^\mu{}_a - \phi^\mu{}_a$. Here, $A_\mu{}^a = e_\mu{}^b e_\nu{}^a A^\nu{}_b$ is implicitly related to the teleparallel gauge potential $\phi_\mu = \phi_\mu{}^a \partial_a$, which implies the following classical-to-quantum bridge (Eq. 1.3.15):

$$A_a \simeq A^\mu{}_a \partial_\mu = A_a \bullet \frac{i}{\mathbf{m}} \bullet \gamma^\mu \partial_\mu \,. \tag{5.2.10}$$

The expression of the gauge potential (Eq. 5.2.10) is fundamental for the proposed translation gauge, $\phi_\mu{}^a = -\mathrm{i}qA_\mu{}^a$. However, the Dirac-like equation (see Eq. 1.3.16),

$$\frac{i}{\mathbf{m}} \bullet \gamma^\mu \partial_\mu \simeq \mathbf{1}_4,$$

is only valid for expectation values of the spinor $\Psi = \Psi_0(\mathbf{m}) \exp(-i\,\mathbf{m} \bullet \mathbf{d}\boldsymbol{\tau})$ selected, i.e.,

$$\frac{i}{m} u^\mu \left\langle \partial_\mu \right\rangle_\Psi = 1.$$

For other cases, it is necessary to consider the replacement $\mathbf{m} \leftrightarrow i\gamma^\mu \partial_\mu \tilde{\Psi}$, as it corresponds to a new field $\tilde{\Psi}$.

5.2.2 Coloured spacetime algebra for spinors

Given the set of spinors $\Psi(x) = \Psi_0(\mathbf{m}) \exp(-i\,\mathbf{m} \bullet \mathbf{d}\boldsymbol{\tau})$, we define an *extended teleparallel gauge* (ETG) translation of the coordinates,

$$\Delta x^a \approx -\left(\,\mathrm{I}_4\, \phi_\nu{}^a{}_{scalar} + \phi_\nu{}^a\,\right) \Delta x^\nu \tag{5.2.11}$$

where $\phi_\nu{}^a{}_{scalar}$ is the usual TEGR perturbation, $\phi_\nu{}^a$ is the perturbation developed in the section above and, therefore, $\Delta x \in \mathbb{R}^{1,3} \oplus \mathfrak{u}(1,3)$. To explore possible limits of the electromagnetism, we neglect the scalar term $\phi_\nu{}^a{}_{scalar} \approx 0$.

Now, $\Delta x^a \approx -\phi_\nu{}^a \Delta x^\nu \simeq \mathrm{i}qA_\nu{}^a \Delta x^\nu$ is linked to the SU(1,3) gauge transformation and the Wilson line, which modifies the trajectories and therefore also the (oscillating) local coordinates $\{x^\mu\}$, which become **matrices**. This ETG relation yields the following transformations:

$$\gamma_\mu \quad \mapsto \quad \hat{\gamma}_\mu := \gamma_\mu + A_\mu \bullet \frac{q}{\mathbf{m}}, \tag{5.2.12}$$

$$dx^\mu \quad \mapsto \quad \hat{dx^\mu} \approx \mathbf{1}_4 dx^\mu - A^\mu \bullet \frac{q}{\mathbf{m}} \bullet \gamma_\nu dx^\nu \;\simeq\; \mathbf{1}_4 dx^\mu + \mathrm{i}qA_\nu{}^\mu dx^\nu, \tag{5.2.13}$$

$$\partial_\mu \quad \mapsto \quad \hat{\partial}_\mu \approx \mathbf{1}_4 \partial_\mu + A_\mu \bullet \frac{q}{\mathbf{m}} \bullet \gamma^\nu \partial_\nu \;\simeq\; \mathbf{1}_4 \partial_\mu - \mathrm{i}qA_\mu. \tag{5.2.14}$$

where $\simeq$ is the classical-to-quantum bridge (Eq. 1.3.15), and

$$A_\mu = A_\mu{}^a \partial_a \simeq A_\mu \bullet \frac{i}{\mathbf{m}} \bullet \gamma^a \partial_a, \qquad \frac{q}{\mathbf{m}} \bullet \gamma_\nu = \frac{q}{m^2} m_\nu = \frac{q}{m} u_\nu \mathbf{1}_4.$$

In particular, the new coordinates satisfy

$$\hat{\gamma}_\mu \bullet \hat{\gamma}_\nu \bullet \hat{dx^\mu} \bullet \hat{dx^\nu} = \boldsymbol{d\tau} \bullet \boldsymbol{d\tau} = \gamma_\mu \bullet \gamma_\nu dx^\mu dx^\nu.$$

Moreover, the following must be satisfied: $\mathbf{1}_4 = \mathbf{1}_4 \partial_\mu dx^\mu = \hat{\partial}_\mu \bullet \hat{dx^\mu}$, from which we deduce that $(A_\mu u^\nu)\partial_\nu dx^\mu = \partial_\mu (A^\mu u_\nu \, dx^\nu) = (A^\mu \partial_\mu dx^\nu) u_\nu$ with $u_\nu \partial_\mu dx^\nu = u_\nu \partial_\mu u^\nu d\tau = 0$ and $\partial_\mu A^\mu = 0$. Applying the derivative $\hat{\partial}_\mu$ to our particular set of spinors, $\Psi(x)$, we obtain $\hat{\partial}_\mu \hat{\Psi} \approx -i(m_\mu + qA_\mu)\Psi \;\; = \nabla_\mu \Psi$. Naturally, the condition $\hat{\partial}_\mu \hat{\Psi} = \partial_\mu \Psi$ is satisfied, which is equivalent to $\hat{\partial}_\mu \bullet \hat{dx^\mu} = \partial_\mu dx^\mu$, where the new coordinates behave like matrices. In other words, the transformed spacetime basis for a particle-field Ψ, $(\hat{dx^\mu},\ \hat{\partial}_\mu)$, is equivalent to the introduction of a (non-abelian) Wilson phase, $-\varphi = -A_\mu dx^\mu$, to the field while keeping the original basis $(dx^\mu,\ \partial_\mu)$.

Observe that the *London equation current* with gauge field A^μ in SU(1,3) transforms the spacetime coordinates as follows:

$$\hat{x}^\mu \;\approx\; \mathbf{1}_4 x^\mu - \int \frac{q}{m} A^\mu u_\nu dx^\nu = \mathbf{1}_4 x^\mu - \int \frac{q}{m} A^\mu d\tau \;\; \in \mathbb{R} \oplus \mathfrak{su}(1,3)\,. \tag{5.2.15}$$

Hence, $\hat{x}^\mu \;\approx\; (\eta^{\mu\nu} - qA^\mu u^\nu/m)\, x_\nu$.

Moreover, the 4-velocity transforms as

$$\hat{u}^\mu \;\approx\; \mathbf{1}_4 u^\mu - \frac{q}{m} A^\mu. \tag{5.2.16}$$

We conclude from Eq. 5.2.8 that it satisfies $\hat{u}^\mu \bullet \hat{u}_\mu = \mathbf{1}_4$.

The matricial structure of the 4-velocity $\hat{u}^\mu$ and spacetime coordinates $\hat{x}^\mu$ can be interpreted, respectively, by the classical-to-quantum bridge to the m-normalized momentum operator $\hat{U}^\mu := \frac{1}{m}\hat{P}^\mu := \frac{i}{m}\left(\mathbf{1}_4 \partial^\mu + qA^\mu\right)$ and the corresponding translation/position operator $\hat{X}^\mu$.

5.3 Result III-2: Towards a quantum gravity

5.3.1 Coloured metric

The perturbed *metric coordinates* evaluated at x for $\Psi(x)$ are given by the perturbed spacetime generators (Eq. 5.2.12). Taking $\hat{e}_\mu := \hat{e}_\mu{}^a\partial_a = e_\mu + \phi_\mu$, the metric components are now matrices themselves:

$$\begin{array}{rcccl} g_{\mu\nu} & := & \hat{\gamma}_\nu \bullet \hat{\gamma}_\nu & = & \hat{e}_\mu \bullet \hat{e}_\nu \\ & \approx & \eta_{\mu\nu}\mathbf{1}_4 + 2\dfrac{q}{m}A_{(\mu}u_{\nu)} & \approx & \eta_{\mu\nu}\mathbf{1}_4 + 2\phi_{\mu\nu}, \end{array} \tag{5.3.1}$$

where $A_{(\mu}u_{\nu)} := (A_\mu u_\nu + A_\nu u_\mu)/2$ and $\phi_{\mu\nu} = \phi_{(\mu} \bullet e_{\nu)}$. The inverse is given by

$$g^{\mu\nu} = (g^{-1})^{\mu\nu} \approx \eta^{\mu\nu}\mathbf{1}_4 - 2\frac{q}{m}A^{(\mu}u^{\nu)} \approx \eta^{\mu\nu}\mathbf{1}_4 - 2\phi^{\mu\nu}.$$

Alternatively, the metric components can be written as $g_{\mu\nu} \approx \eta_{\mu\nu}\mathbf{1}_4 + \hat{u}_\mu \bullet \hat{u}_\nu - u_\mu u_\nu \mathbf{1}_4$ and $g^{\mu\nu} \simeq \eta^{\mu\nu}\mathbf{1}_4 + \hat{u}^\mu \bullet \hat{u}^\nu - u^\mu u^\nu \mathbf{1}_4$. Observe that $\hat{e}_\mu$ and e_μ behave like tetrads of directions or *four-velocities* in the corresponding algebra and frame, while $\phi_{\mu\nu}$ is identified as a linearized perturbation. Now, the coordinates and the metric components are complex matrices, since the perturbation generators $\{A_\mu u_\nu\}_{\mu,\nu}$ are not elements of $Cl_{3,1}(\mathbb{R})$.

Remark 5.3.1 (**Spacetime-particle field**)**.** Geodesics derived from this metric depend on each particle mass-charge (q/m), so they are not features of the spacetime but of the spacetime-particle field, as an indivisible entity.

Definition 5.3.1 (**Simply gravity**)**.** Let $g_{\mu\nu} := \mathbf{1}_4\eta_{\mu\nu} + \sum_r \varsigma_r\, \hat{u}^r_\mu \hat{u}^r_\nu$ be the metric components with perturbation such that $(\hat{u}^r_\mu \hat{u}^r_\nu) : \mathscr{N} \to \mathbf{1}_4\mathbb{R} \oplus \mathfrak{su}(1,3) \oplus (\mathfrak{su}(1,3) \otimes \mathfrak{su}(1,3))$ is multiplied by a scalar field $\varsigma_r : \mathscr{N} \to \mathbb{R}$. The effects of the perturbation will be named "simply gravity" whenever each perturbation component is a purely diagonal matrix $(\hat{u}^r_\mu \hat{u}^r_\nu)(x) \in \mathbf{1}_4\mathbb{R}$, that is, $\varsigma_r\, \hat{u}^r_\mu \hat{u}^r_\nu = \mathbf{1}_4 \varsigma_r\, k_\mu k_\nu$ for some Kerr–Schild unitary vector field $k = (k_\mu)_\mu : \mathscr{N} \to \mathrm{T}\mathscr{N}$. Moreover, if $\eta_{0,0}\,\varsigma_r \leq 0$ the metric represents a usual (simply) **gravity spacetime**, while for $\eta_{0,0}\,\varsigma_r > 0$, it leads to a (simply) **gravity source**, corresponding to "matter sources" instead of "effects on spacetime curvature".

Remark 5.3.2 (**Geons**)**.** The idea of "geons" conceptualized by Wheeler 1961 is very similar to the simply gravity sources defined above.

5.3.2 Double-copy gauge potential

To derive more interesting effects, it is necessary to analyze the second-order terms. In particular, one can pay attention to the definition of the origin of the SU(1,3) gauge potential. The corresponding perturbation of the spacetime algebra is given by

$$\gamma_\mu \;\mapsto\; \hat{\gamma}_\mu := \gamma_\mu + \kappa\, A_\mu \bullet \mathbf{A}(0)\,, \tag{5.3.2}$$

where the origin of the (Coulomb/Cornell-like) potential,

$$\mathbf{A}(0) = \frac{q}{\kappa \mathbf{m}} = \frac{q}{\kappa m^2}\,\mathbf{m} \in \mathscr{M}_4(\mathbb{C}),$$

is a matrix proportional to the momentum $\mathbf{m} = m^\mu \gamma_\mu = m_\mu \gamma^\mu$. If we denote by $\hat{\mathbf{A}} := \mathbf{A} - \mathbf{A}(0)$ the relative gauge with coordinates $\hat{A}_\mu := \hat{\mathbf{A}} \bullet \gamma_\mu$, then the second terms of the metric are found as above, but using with double gauge copy of $\hat{A}$ instead (Recall Eq. 5.3.1):

$$\begin{array}{rcccl} g_{\mu\nu} & = & \hat{\gamma}_\mu \bullet \hat{\gamma}_\nu & = & \eta_{\mu\nu} - \kappa \hat{A}_\mu \bullet \hat{A}_\nu + \kappa A_\mu(0) \bullet A_\nu(0) \\ & & & = & \eta_{\mu\nu} - \kappa A_\mu \bullet A_\nu + 2qA_{(\mu}u_{\nu)}/m, \end{array} \tag{5.3.3}$$

where $A_\mu = \mathbf{A} \bullet \gamma_\mu$ is now a SU(1,3) gauge potential (boson) and the last term represents a **gravity source** at $x = 0 \in \mathbb{R}^4$ (see Def. 5.3.1), while the first perturbation term, $A_\mu \bullet A_\nu$, corresponds to a **gravity spacetime** linked to a pair of entangled bosons (i.e., a candidate for *graviton*).

Since $A_\mu \in \mathfrak{su}(1,3) \subset \mathfrak{u}(1,3)$ and $u \in \mathbb{R}^{1,3}$, perturbations of the complexified metric

$$g \approx \eta + \hat{A} \otimes \hat{A} = \eta + (u \oplus A) \otimes (u \oplus A) \tag{5.3.4}$$

can be identified, via the canonical isomorphisms of tensor products, with elements of the $(\mathbb{R}^{1,3} \oplus \mathfrak{u}(1,3)) \otimes (\mathbb{R}^{1,3} \oplus \mathfrak{u}(1,3))$ space instead of the classical $\mathbb{R}^{1,3} \otimes \mathbb{R}^{1,3}$ tensorial space.

Observe that when the perturbation components are purely diagonal, the metric provides a $Cl_4(\mathbb{C})$ algebra generated by $\{\hat{\gamma}_\mu\}_{\mu=0}^3$ (from Eq. 5.2.12). As a particular case, one can recover the classical double copy used in the Kaluza–Klein and the Kerr–Schild–Kundt metrics, $g \approx \eta + A \otimes A$ (e.g., the black holes of Kerr–Newman and Reissner–Nordström) [Monteiro *et al.* 2021], and can consider higher-order corrections to the Lagrangian (see Sec. 5.3.4) by following analogies with the Born–Infeld / D-Brane actions [Kogan *et al.* 2003]. Similarly, the durst-based linearised metric, $g \approx \eta + u \otimes u$, can be recovered as a limiting case of the torsion-based *coloured gravity*[3] metric.

Schematically, torsion of the developed metric describes a double-helix-like structure consisting of pairs $A \otimes A$ of entangled $\mathfrak{su}(1,3)$ vector fields or *bosons* (e.g. QED-carrier photons or QCD-carrier gluons). Geometrically, these potential fields are interpreted as the connection of a double-copy gauge transformation generated by an extended Poincaré algebra $\mathbb{R}^{1,3} \oplus \mathfrak{u}(1,3)$. And physically, these bosons are virtual particles of "exchange" in each interaction (transformation) of the extended Poincaré symmetry group.

The features of the double-gauge metric are very rich and deserve to be analyzed in detail in some future work. The simplest case is the abelian U(1) electrodynamics, which is developed in **Sec. 6.3**.

From the compatibility hypothesis on both sides of the metric perturbation (A, u), we conclude that the natural algebra is built with $\mathfrak{su}(1,3)$. The idea of the double-copy gauge potential $A \otimes A \in \mathfrak{su}(1,3) \otimes \mathfrak{su}(1,3)$ is linked to some remarkable isomorphisms.

[3]Notice that our definition of *coloured gravity* is not the same that the *colour-decorated gravity* defined by Gwak *et al.* 2016 and completed by Gomis *et al.* 2021, who used three-dimensional Poincaré algebra by including a colour symmetry factor (coloured Poincaré algebra) for *(anti) de Sitter* spacetimes.

For instance, the chiral group for spinors is SU(2) × SU(2). The representatives of the spacetime algebra are isomorphic to 2×2 quaternion matrices, $M_2(\mathbb{H})$, and to the double 2×2 unitary matrices, $U(2)$, that is, $Cl_{1,3}(\mathbb{R}) \simeq \mathfrak{gl}(2,\mathbb{H}) \simeq \mathfrak{u}(2)\oplus\mathfrak{u}(2)$. On the other hand, the quaternion formulation of the GR provides interesting links to electrodynamics [Sachs 1968, Crater *et al.* 2011].

The complexification of the spacetime algebra leads to the Dirac algebra, $Cl_4(\mathbb{C}) \simeq Cl_{1,3}(\mathbb{R}) \otimes \mathbb{C} \simeq \mathfrak{u}(2) \oplus \mathfrak{u}(2) \oplus \mathfrak{u}(1)$, which contains the electroweak interaction algebra, $\mathfrak{su}(2) \oplus \mathfrak{u}(1)$. Moreover, the reoriented elements of $Cl_{1,3}(\mathbb{R})$ representing generators of SU(3) bring the well-known, grade-preserving transformations of the Lorentz group and comprise enough structure for both the colour- and the flavor-SU(3) [Schmeikal 2001, Schmeikal 2004]. Nevertheless, the Dirac-algebra generators can be used to linearly span the whole algebra $\mathfrak{gl}(4,\mathbb{C})$, that is, any 4×4 complex matrix can be expressed by using the sixteen Dirac matrices as a basis [Red'Kov *et al.* 2008, Vaz and Rocha 2016]. The $\mathfrak{su}(1,3)$ algebra allows to model quarks and leptons within the same symmetry [Marsch and Narita 2015, Barbieri and Tesi 2018], while $\mathfrak{u}(1,3)$ is important to describe strong interactions of quarks and gluons in a nonperturbative domain at large interaction distances [Khruschev 2004]. Therefore, perhaps the $\mathfrak{su}(1,3)$ algebra also leads to a similar quark-lepton model as in the $\mathfrak{su}(4)$ case.

Among the important subalgebras of $\mathfrak{su}(1,3)$ we enumerate $\mathfrak{su}(3)$ and $\mathfrak{su}(2) \oplus \mathfrak{u}(1)$, which are redutive of maximal rank. However, $\mathfrak{su}(3) \oplus \mathfrak{su}(2) \oplus \mathfrak{u}(1)$ cannot be embedded into $\mathfrak{su}(1,3)$ [Red'Kov *et al.* 2008, Cembranos and Diez-Valle 2019], although it admits an embedding into the double $\mathfrak{su}(1,3)$. Therefore, the *(1,3)-colour* symmetries can be broken into the *3-colour* and the *hypercharge* symmetries of the Standard Model, thanks to the coupling factors and the partial composition of the Higgs boson [Schmeikal 2004, Cembranos and Diez-Valle 2019, Almeida 2003, Ferreti 2014, Cossu *et al.* 2019, Gertov *et al.* 2019]. The role of this breaking is played by perturbation properties of $Cl_4(\mathbb{C})$. The solution to obtain compatibility of the above mentioned facts is to describe the perturbation of the spacetime algebra using the Lie algebra $\mathfrak{su}(1,3) \oplus \mathfrak{su}(1,3)$.

5.3.3 Covariant derivative

The covariant derivative, $D_\mu := \hat{e}_\mu{}^a\partial_a$, is given by the co-tetrad components. The (non-trivial) co-tetrads and tetrads are given by

$$\hat{e}^a = \hat{e}_\mu{}^a dx^\mu \approx e^a + \phi_\mu{}^a dx^\mu \approx e^a + \phi^a, \tag{5.3.5}$$

$$\hat{e}_a = \hat{e}^\mu{}_a\partial_\mu \approx e_a - \phi^\mu{}_a\partial_\mu \approx e_a - \phi_a, \tag{5.3.6}$$

respectively, where the identities $\phi_a = \phi^\mu{}_a\partial_\mu$ and $\phi^a = \phi_\mu{}^a dx^\mu$ have been used, and the identity matrices have been omitted for brevity. In terms of the potential field, the previous expressions read

$$\hat{e}^a \approx e^a + \phi^a \approx e^a + \frac{q}{m}A^a u_\mu dx^\mu \simeq e^a - \mathrm{i}qA_\mu{}^a dx^\mu, \tag{5.3.7}$$

$$\hat{e}_a \approx e_a - \phi_a \approx e_a - \frac{q}{m}A_a u^\mu\partial_\mu \simeq e_a + \mathrm{i}qA_a. \tag{5.3.8}$$

Therefore, the Cartan covariant derivative, D_μ, coincides with the teleparallel gauge,

$$D_\mu \equiv \hat{\partial}_\mu \equiv \hat{e}_\mu = \hat{e}_\mu{}^a \partial_a \approx e_\mu + \frac{q}{m} A_\mu u^a \partial_a \simeq \partial_\mu - \mathrm{i}qA_\mu = \nabla_\mu. \tag{5.3.9}$$

Finally, the *expectation* equivalence $\nabla_\mu \simeq D_\mu$ between the SU(1,3) gauge derivative and the teleparallel derivative can be set for each *particle-field* involved (expectation value). This equivalence is of major relevance to ensure the consistence of the theory for non-abelian fields $\mathbf{A}$.

5.3.4 Coloured Gravity Lagrangian density

Thanks to the equivalence of the covariant derivatives, the 2-form torsion tensor yields the field strength of the teleparallel translational gauging (Eq. 1.3.2), which behaves like a 2-form curvature. Therefore, by introducing the perturbed co-tetrads (Eq. 5.3.7) in the field strength and by applying expectation values (Eq. 1.3.12), we obtain the SU(1,3) field strength (geometrically, the curvature 2-form):

$$F_{\mu\nu} := F^a{}_{\mu\nu}\partial_a = [D_\mu, D_\nu] = (D_\mu \hat{e}_\nu{}^a - D_\nu \hat{e}_\mu{}^a)\partial_a \approx \frac{q}{m}\mathscr{F}_{\mu\nu}u^a\partial_a \simeq -iq\mathscr{F}_{\mu\nu}, \tag{5.3.10}$$

where $\mathscr{F}_{\mu\nu} := \mathrm{i}q^{-1}[\nabla_\mu, \nabla_\nu]$ is the SU(1,3) curvature 2-form. From now on, we will refer to $\mathbf{A}$ as the *Coloured Gravity Field*. Moreover, the torsion scalar yields the Yang–Mills scalar,

$$F^a{}_{\mu\nu} \simeq \frac{q}{m}\mathscr{F}_{\mu\nu}u^a \quad \mapsto \quad F^a{}_{\mu\nu}F_a{}^{\mu\nu} \simeq \frac{q^2}{m^2}\mathscr{F}_{\mu\nu}\mathscr{F}^{\mu\nu}\,, \tag{5.3.11}$$

which is valid for the spinor Ψ.

By introducing the perturbed co-tetrads in the *torsion scalar* of the TEGR Lagrangian density (Eq. 1.3.5), and by including a source Lagrangian with energy density ρ, i.e., $\mathscr{L}_m = -\hat{e}\,\rho$, we arrive at

$$\mathscr{L} = \frac{\hat{e}}{2\kappa}\left(-\frac{1}{4}F^a{}_{\mu\nu}F_a{}^{\mu\nu}\right) + \mathscr{L}_m \;\simeq\; \frac{\hat{e}}{2\kappa}\left(-\frac{1}{4}\frac{q^2}{m^2}\mathscr{F}_{\mu\nu}\mathscr{F}^{\mu\nu}\right) + \mathscr{L}_m\,. \tag{5.3.12}$$

For a perfect fluid, the *source energy* is $\hat{m} = I_w m$ where $I_w := (1+5w)/(1+w)$, as shown in Eq. H.1.9 of the Appendix H. Therefore, the total energy density is $\hat{\rho} = \bar{\Psi} I_w m \Psi$, while the proper energy density is $\rho = \bar{\Psi} m \Psi = I_w^{-1}\hat{\rho}$. However, in our case the *source energy* is the gauge field $\mathbf{A}$.

Let $\mathbf{A}(0)$ be the gauge field evaluated at the test particle position with four-current $\mathbf{q} = q\gamma_\mu$, of scalar charge q. The total density energy is $\mathbf{q}\cdot\mathbf{A}(0)$, where $\mathbf{A}(0) \approx \mathbf{q}/4\pi r_m$ is the potential in the particle, which is valid for short distances r_m (see, for instance, Şafarík 2003). Since our gauge fields behave as perfect fluids with $w = 1/3$ (cf. Eq. H.1.7 of the Appendix H), the proper energy density has a factor $I_w^{-1} = 1/2$. Moreover, we need to introduce a normalized factor, $f_m = i\gamma^\mu D_\mu/m + \mathscr{O}$, where $\mathscr{O}$ are the other terms related to the Dirac equation or to the Bargmann–Wigner equations, i.e.,

$$\rho \;=\; \Psi^\dagger \hat{m}_q f_m \Psi \;\;=\;\; \bar{\Psi}\,\frac{1}{2}\mathbf{q}\cdot\Delta\mathbf{A}\left(\frac{i}{m}\gamma^\mu D_\mu + \mathscr{O}\right)\Psi\,, \tag{5.3.13}$$

where $\Delta\mathbf{A} := \mathbf{A} - \mathbf{A}(0) \approx -\mathbf{A}(0)$ and $\bar{\Psi} := \Psi^\dagger\gamma^0$ is the Dirac adjoint, with $\Psi^\dagger$ being the Hermitian adjoint. On the macroscopic scale, with a large number of particles, the factor f_m needs to be replaced by $f_m \mapsto \mathbf{1}$. Similarly, by changing $\bar{\Psi}\hat{m}_q\Psi\left(\mathbf{x}\right) \mapsto \hat{m}_q\delta^4(\mathbf{x}-\mathbf{y})$ we obtain a density of the electric energy $\hat{m}_q$ at the point $\mathbf{y}$. In addition, the divergence term of the Ricci scalar, $-\partial_\mu(T^{\nu\mu}{}_\nu\hat{e}/\,\kappa)$, is useful for the Einstein–Hilbert Lagrangian of GR to recover the classical Einstein field equations and the Maxwell's equations by considering the matter Lagrangian, $\mathscr{L}_m = -\hat{e}\rho \approx \frac{1}{2}\hat{e}\,\mathbf{q}\cdot\mathbf{A}(0)$ (see Sec. 6.3.5).

By hypothesis, we assume that the minimum distance corresponds to the particle event horizon $r_m = 2\mathrm{G}m$. This implies that the potential origin is $\mathbf{A}(0) \approx \mathbf{q}/(8\pi\mathrm{G}m) = \mathbf{q}/(\kappa\, m)$, thus yielding

$$\begin{aligned}
\mathscr{L} &= \frac{\hat{e}}{2\kappa}\left(-\frac{1}{4}F^a{}_{\mu\nu}F_a{}^{\mu\nu}\right) - \hat{e}\rho \simeq \\
&\simeq \frac{\hat{e}}{2\kappa}\left(-\frac{1}{4}\frac{q^2}{m^2}\mathscr{F}_{\mu\nu}\mathscr{F}^{\mu\nu}\right) + \frac{q^2\hat{e}}{2\kappa\, m}\,\bar{\Psi}\left(\frac{i}{m}\gamma^\mu D_\mu + \mathscr{O}\right)\Psi \simeq \\
&\simeq \frac{\hat{e}}{2\kappa}\frac{q^2}{m^2}\left(-\frac{1}{4}\mathscr{F}_{\mu\nu}\mathscr{F}^{\mu\nu} + \bar{\Psi}\,\left(i\gamma^\mu\nabla_\mu + m\mathscr{O}\right)\,\Psi\right), \qquad (5.3.14)
\end{aligned}$$

which produces the same Euler–Lagrange equations than the Yang–Mills Lagrangian, $\mathscr{L}_{\mathscr{F}+\Psi}$ (recall Eq. 1.3.25). However, this one has a different coupling factor between fermions and gravity compared to the first-order tetradic Palatini action, whose Lagrangian density is

$$\mathscr{L} = \hat{e}\,\left(\frac{1}{2\kappa}\hat{e}^\mu{}_a\hat{e}^\nu{}_b R_{\mu\nu}{}^{ab} + \bar{\Psi}(\mathrm{i}\gamma^\mu D_\mu - m)\Psi\right), \qquad (5.3.15)$$

where $\hat{e} := \det\hat{e}_\mu{}^a = \sqrt{-g}$, $\kappa = 8\pi\mathrm{G}$ and $R_{\mu\nu}{}^{ab}$ is the curvature of the spin connection. The interpretation of the different coupling factor is that the SU(1, 3) Yang–Mills interactions would be particular cases of the coloured gravity in which the spinor are coupled. In other words, thanks to the spatial gauge choice for the potentials, the gravitational constant, κ, has no affect to first order of the perturbative interactions.

Chapter 6

Applicability and analysis

What is it?

This Chapter presents **original results** on applicability and analysis of all the previous developments. That includes the observation-based confrontation of our predictions on fictitious accelerations: i) at large scales [Monjo 2018, Monjo and Campoamor-Stursberg 2023], ii) for object dynamics (galaxies) [Monjo 2023] and iii) for particle fields [Monjo et al. 2024].

6.1 Theoretical applicability on the cosmic acceleration

6.1.1 Inhomogeneity and fictitious acceleration

This subsection summarises the proof that radial inhomogeneity of the hyperconical metric behaves in a similar way as a fictitious acceleration. That is, it produces the same effect on the redshift measured by an observer, as detailed in Monjo 2018, Monjo and Campoamor-Stursberg 2023.

Specifically, the lapse and shift terms of the hyperconical metric (Eq. 2.4.8) can be assimilated as a radial inhomogeneity according to new coordinates. Applying a coordinate change in time $t \to t'$ to the metric, such as $t' := t\sqrt{2\cos\alpha - 1}$, it is equivalent to selecting $g'_{00} = 1$, $g'_{0r} = 0$, $g'_{\phi\phi} = -a^2 r'^2 sin^2\theta$, $g'_{\theta\theta} = -a^2 r'^2$ and:

$$g'_{r'r'} = g_{r'r'} - \frac{g_{0r}^2}{g_{00}} = -a(t', r')^2 \frac{2 - \cos\gamma(r')}{2\cos^2\gamma(r')} \tag{6.1.1}$$

where it is assumed the positive curvature $k = 1$ as it was found in Monjo and Campoamor-Stursberg 2020, and $a(t', r') = t'/(t_0\sqrt{2\cos\gamma - 1})$ is the same scale factor but expressed in the new coordinates. From the definition of luminosity distance [Monjo 2017], the comoving distance r' is derived as a function of redshift z,

$$\xi_1\left(\frac{r'}{t_0}\right) := \int_0^{r'} \frac{\sqrt{2 - \cos\gamma(r')}}{\cos\gamma(r')} \frac{dr'}{t_0} = \int_0^z \frac{dz'}{1+z} \tag{6.1.2}$$

$$\int_0^{\gamma(r')} \sqrt{2 - \cos\gamma}\, d\gamma = \ln(1+z)$$

$$\gamma(r') + O[\gamma^3] = z + O[z^2] \tag{6.1.3}$$

Isolating the comoving distance r' and applying a locally conformal projection map f_{γ_0} (e.g. 2.5.10) to change this coordinate to the intrinsic distance $\hat{r}'$, it is the same that:

$$r' = t_0 \xi_1^{-1}(\ln(1+z)) \tag{6.1.4}$$

$$\hat{r}' = f_{\gamma_0}(t_0, r') \tag{6.1.5}$$

The hypothesis is that intrinsic (projected) distances of the linear expanding and closed hyperconical model behaviours like the accelerated and flat ΛCDM model. Taking the Maclaurin series on redshift for the Hubble parameter of both models ($H_{\Lambda CDM}$ and $\hat{H}^{intr}_{hyp}$), the first order is

$$H_{\Lambda CDM}(z) = \sqrt{\Omega_r + \Omega_m + \Omega_\Lambda} + \frac{4\Omega_r + 3\Omega_m}{\sqrt{\Omega_r + \Omega_m + \Omega_\Lambda}} \frac{z}{2} + O(z^2)$$

$$\hat{H}^{intr}_{hyp}(\hat{r}'(z)) = 1 + \frac{\gamma_0 - 2\alpha}{\gamma_0} z + O(z^2) \tag{6.1.6}$$

where $\alpha = 0.5$ is the unique distorting parameter compatible under symmetric transformations in dynamical systems (see Sec. 2.5.5).

Proposition 6.1.1 (**Local inhomogeneity-acceleration equivalence**). *Given the redshift measured by comoving observers in the linearly expanding hyperconical metric, there exists* ***a unique local equivalence*** *(stereographic projection) between radial inhomogeneity of that metric and an acceleration of the spatially flat FLRW metric.*

Proof. Let $\lambda \subset \mathbb{R}$ be a scale factor that transforms time $t \mapsto \hat{t} := t\lambda$ and distorts the comoving length $\hat{r}'$ as $r' \mapsto \hat{r}' := r'\lambda^{\alpha}$. Moreover, let $F_Q : \mathbb{R} \to \mathbb{R}^5$ be a pencil with $F_Q(\lambda) \in \mathbb{R}^5$ parameterized such as $F_Q(1) = Q(t) = (t, \vec{r}, u)$ and $F_Q(0) = \hat{Q}(0) := (0, \vec{0}, u_0)$ with $u_0 := -t_0$. A transformation, given by $\vec{r}' = r'\vec{e}_r \;=\; t_0 \sin\gamma\, \vec{e}_r \;\mapsto\; \hat{r}'\vec{e}_r := t_0 \sin\hat{\gamma}\, \vec{e}_r$, is performed for the angles $\gamma \mapsto \hat{\gamma}$, preserving the direction $\vec{e}_r$. Therefore, that pencil is:

$$F_Q \begin{cases} \hat{t} = t\lambda \\ \hat{r}' = r'\lambda^{\alpha} \\ \hat{u} = u_0 + (u - u_0)\lambda \end{cases}$$

where $\alpha = 0.5$ (see Sec. 2.5.5). When the points are projected on the hyperplane $\hat{u} = t_0$, the solution for the distorted stereographic projection is given by some $\lambda = \lambda_s(t, \gamma)$,

$$t_0 = -t_0 + (t\cos\gamma + t_0)\,\lambda_s \quad \Rightarrow \quad \lambda_s(t,\gamma) = \frac{2}{(1 + \frac{t}{t_0}\cos\gamma)} \tag{6.1.7}$$

Taking into account the inhomogeneous scale factor related to redshift z as a function of the comoving distance,

$$\frac{t}{t_0} = \frac{1}{1+z} = 1 - \frac{r'}{t_0} + O\left(\frac{r'^2}{t_0^2}\right) = 1 - \sin\gamma + O\left(\sin^2\gamma\right) = 1 - \gamma + O\left(\gamma^2\right) , \tag{6.1.8}$$

the projection parameter is found:

$$t_0 = -t_0 + (t\cos\gamma + t_0)\,\lambda_s \quad \Rightarrow \quad \lambda_s(t(\gamma),\gamma) \approx \frac{2}{(1 + (1-\gamma)\cos\gamma)} \tag{6.1.9}$$

At local scales ($\gamma \ll 1$), it is useful to approximate Eq. 6.1.9 as

$$\lambda_S(t(\gamma),\gamma) \approx \frac{1}{1 - \frac{\gamma}{2}} \tag{6.1.10}$$

Now, taking the Eq. 6.1.6 for the local value of $\gamma_0 = 2$,

$$\hat{H}^{intr}_{hyp}\left(\hat{r}'(z)\right) \;\approx\; 1 \;+\; \frac{1}{2}z + O(z^2) \tag{6.1.11}$$

and comparing to the Hubble parameter for the spatially flat FLRW metric,

$$\begin{cases} 1 & = \sqrt{\Omega_r + \Omega_m + \Omega_\Lambda} \\ \frac{1}{2}z & = \frac{4\Omega_r + 3\Omega_m}{\sqrt{\Omega_r + \Omega_m + \Omega_\Lambda}}\frac{z}{2} \end{cases} \tag{6.1.12}$$

Therefore, $\{\Omega_m = \frac{1}{3} - \frac{4}{3}\Omega_r,\ \Omega_\Lambda = \frac{2}{3} + \frac{1}{3}\Omega_r\}$ is the **unique local solution** as a function of the radiation density (Ω_r). Simplifying with $\Omega_r \approx 0$, we see that $\Omega_m \approx \frac{1}{3}$ and $\Omega_\Lambda \approx \frac{2}{3}$ under the first-order approach. ■ Second- and third-order approaches are not unique but display similar results [Monjo 2018, Monjo and Campoamor-Stursberg 2023] .

Theorem 6.1.1 (**Fictitious acceleration**). *If $\mathscr{N} \subset \mathbb{R}^{1,4}_{\eta}$ is a minimal singular (or maximal regular) four-dimensional hypersurface with finite parameter time, every comoving on-shell observer will experience a (unique) local fictitious acceleration.*

Proof. By the Prop. 2.4.1, maximal regularity of $\mathscr{N}$ implies that it is closed and, by homogeneity, $\mathscr{N}$ is an expanding hypersphere. Moreover, from the Prop. 2.4.2, embedding of $\mathscr{N}$ is unequivocally described by the linearly expanding hyperconical metric, which presents an apparent radial inhomogeneity. Finally, according to the Prop. 6.1.1, local projection of the inhomogeneity leads to a (unique) local fictitious acceleration, measured by every comoving observer. ■

6.1.2 Zero active mass

As developed in the above sections, the intrinsic viewpoint of the hyperconical universe leads to a fictitious acceleration (usually represented by a kind of dark energy $\Omega_\Lambda \approx 0.7$) that compensates the expected gravity of an estimated matter amount ($\Omega_m \approx 0.3$, mostly dark matter) to obtain a total density equal to the critical density. This implies that the metric should be spatially flat with the same scale factor that a linear expansion, which is equivalent to a total zero active mass (or equation of state $w = -\frac{1}{3}$).

Remark 6.1.1 (**Zero active mass**: The background metric of the universe does not depend on the matter content)**.** Linear expansion is directly inherited from the minimal embedding into a 5-dimensional Minkowskian space. However, the standard model is based on the validity of general relativity for the cosmological scales, which establishes that spacetime curvature is intrinsically determined by the matter content. According to the FLRW family of metrics, the spatial curvature of the universe is positive (closed) if the universe is dominated by matter, negative (open) if the universe is dominated by the expansion mechanism (whatever it is) and flat (or critical) if there exists a perfect equilibrium between the matter-related gravity to be closed and the expansion-based pressure to be open. If the universe behaviours as a flat-space manifold, that means that gravity and expansion pressure are perfectly balanced to avoid that matter content impacts on the metric (notice that it is only flat in the space since Ricci scalar $R = -6\dot{a}^2/a$ is not zero due to the contribution of the expansion scale factor a). In other words, an "apparently flat space" implies a zero active gravitational mass-energy and it also implies a linear expansion.

6.2 Modelling of large-scale dynamics

6.2.1 Observations of manifold dynamics

6.2.1.1 Local-to-global tensions

The main applicability of the geometrical model developed is the falsifiability of cosmological approaches (e.g. Lorentzian metrics) by using real physical observations.

Table 6.1: Extrinsic-viewpoint prediction. The values of the Hubble parameter (H_0 in $\mathrm{km \cdot s^{-1} \cdot Mpc^{-1}}$) according to the linear expansion (unprojected Hyperconical model [Monjo 2017]) by using several ages of the universe (t_0 in 10^9 years) and statistical tensions with respect to the most current local observations: $H_0 = 73.30 \pm 1.04\,\mathrm{km \cdot s^{-1} \cdot Mpc^{-1}}$ (SH0ES, LMC-CS) [R22: Riess et al. *et al.* 2022] and $69.8 \pm 1.7\,\mathrm{km \cdot s^{-1} \cdot Mpc^{-1}}$ (TRGB) [F19: Freedman *et al.* 2019] at 68% C.L. Estimations of the age of the universe (gigayears) were collected from: O17: OMalley *et al.* 2017, Schlaufman *et al.* 2018, S18: Schlaufman *et al.* 2018, J19: Jimenez *et al.* 2019 and A19: Aghanim *et al.* 2020a.

Age estimation technique	t_0 (Gyr)	$H_0 = 1/t_0$	σ/R22	σ/F19
Very-low-metallicity stars [J19]	13.40(45)	73.0 (2.1)	0.1	1.5
Galactic globular clusters [O17, S18]	13.2(4)	74.1 (2.4)	0.3	1.8
ΛCDM-dependent TT [A19]	13.83(37)	70.71(26)	2.5	0.5
ΛCDM-dependent EE [A19]	13.64(15)	71.69(65)	1.5	1.1
ΛCDM-dependent TT,TE,EE [A19]	13.80(24)	70.86(40)	2.3	0.6

For instance, the significant difference or not between local and global values of the expansion rate H_0 is a key feature that distinguishes between homogeneous and inhomogeneous spaces. Specifically, our model suggests that fictitious acceleration emerges when a radially inhomogeneity is projected in a homogeneous chart (as found in Monjo 2018). This phenomenon is similar to that one showed by Kovács *et al.* 2020: by using the inhomogeneous Average Expansion Rate Approximation (avERA) model, Hubble tension can be explained without dark energy.

In fact, the local-to-global ratio $H_0(L)/H_0(G) = 1$ is the well-known $\Omega_\Lambda = 0.72(1)$ solution found by Perlmutter *et al.* 1999, which is very close to our theoretical value of $\Omega_\Lambda = 0.7375(4)$, produced by the equality $F_t := t_0 H_0 \equiv 1$ between the age of universe age (t_0) and the Hubble time ($1/H_0$), globally and without any projection [Monjo 2017].

The hyperconical model assumes a factor $F_t \equiv 1$ (that is $H_0 \equiv 1/t_0 \approx 71.0\,\mathrm{kms^{-1}Mpc^{-1}}$ assuming PL2018+BAO $t_0 \approx 13.8 \cdot 10^9$ years), as a universe expansion driven by the course of time. This natural expansion leads to a distant/local ratio values of Hubble parameter as $\rho_z := H(z)/H_0 = 1 + z$, which is compatible with the observations of [Riess *et al.* 2018a]. For instance, the estimated value of $\rho_{1.5} = H(z = 1.5)/H_0 = 2.69^{+0.86}_{-0.52}$ is in agreement with our predicted value of $\rho_{1.5} \equiv 2.5$.

When the hyperconical universe is forced by flattening to reproduce the ΛCDM model, the estimation of the time factor is reduced ($F_t < 1$) due to an apparent (emerging) acceleration, which reproduces a minimum value of H_0 at a local scale (second-order contact point) with values very close to the Planck observations.

The corresponding local observation in CMB is the Planck temperature (TT) power spectrum. The CMB TT results provided low values of dark energy density ($\Omega_\Lambda = 0.679(13)$) compatible with our local prediction of $\Omega_\Lambda \approx 0.667$ (Table 3.1). Under the global approach with a three-order contact point, the increase of the distorting parameter

($\alpha > 0.5$) producing an increase of the dark energy $\Omega_\Lambda > 0.7$ and a curvature reduction down to $|\Omega_K| < 0.02$.

These values are comparable with the CMB polarisation power spectrum (EE), because they are non-linear (non-Gaussian) and do not depend on the coordinates (global-like approach) (Figure 6.2.1). Particularly, CMB EE power spectra showed higher values of dark energy $\Omega_\Lambda = 0.711(30)$ with Hubble parameter about $69.9 \pm 2.7\,\mathrm{kms^{-1}Mpc^{-1}}$ and the corresponding value from the linear hyperconical model ($H_0 = 1/t_0$) is $71.69 \pm 0.65\,\mathrm{kms^{-1}Mpc^{-1}}$ (Table 6.1), which are compatible with the values estimated with Large Magellanic Cloud (LMC) Cepheid samples, of about $H_0 = 73 \pm 1\,\mathrm{kms^{-1}Mpc^{-1}}$ (SH0ES [Riess et al. *et al.* 2021, Riess et al. *et al.* 2022, Riess *et al.* 2018b]). In fact, the SH0ES estimation leads to an independent-scale ratio of 1.037 ± 0.036 and a time factor of $F_t = 0.97 \pm 0.05$.

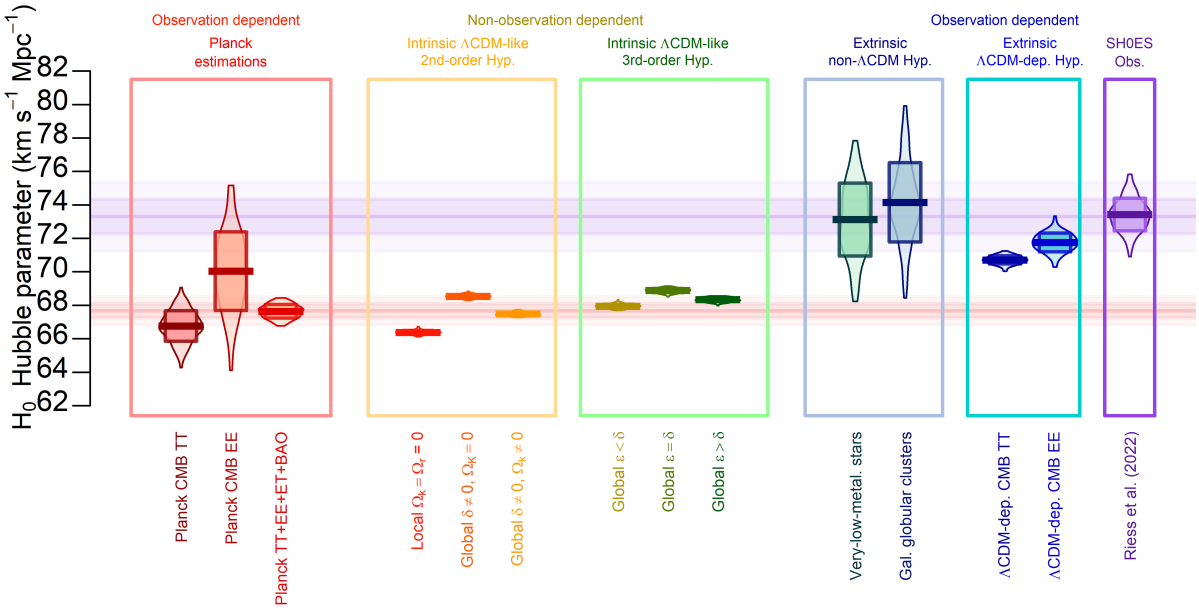

Figure 6.2.1: Hubble parameter estimated under the intrinsic viewpoint, with local (orange box) or global (green box) approaches, and under extrinsic viewpoint (blue boxes) of the Hyperconical model, compared to ΛCDM-dependent Planck legacy (left red box) and SH0ES observations (right purple box), which is obtained by "cosmic distance ladder" (a chain of direct methods).

In summary, our interpretation of the Hubble tension is that cosmology-dependent measurements are strongly influenced by the intrinsic viewpoint of the models used. This is the case of the CMB EE/TT power spectra, most of BAO-based methods and the luminosity distance of SNe Ia among others. In other words, the constraints are applied to a FLRW metric inadequately derived for moving reference frames (see Appendix B). In contrast, cosmology-independent observations such as the purely geometric approaches

such as the SNe distance ladder would be more influenced by extrinsic geometry. Observe that the distance ladder method propagates the 'very local scale' to larger scales through a chain of correlated/overlapped methods, bridging the contrast produced by the distorted stereographic projection (intrinsic viewpoint) and therefore it leads to practically unprojected measurements.

6.2.1.2 Constraints of the projected model with SNe Ia

An estimation of ϵ and α was obtained according to 1048 Type Ia supernovae (SNe Ia) in the range of $0.0101 < z < 2.26$ and collected from the Pantheon sample [Scolnic *et al.* 2018, Zhao *et al.* 2019]. This dataset contains both the heliocentric redshift ($z_{\rm hel}$, direcly observed redshift) and the CMB-frame redshift ($z_{\rm CMB}$) obtainted from standard procedures; that is, the CMB-frame redshift is the redshift after the correction of the Planck-observed CMB dipole caused by the specific velocity of our galaxy plus solar system with respect to the CMB. Taking into account the fact that the standard luminosity distance d_L depends on the combination of both redshifts [Zhao *et al.* 2019, Cao *et al.* 2021], for the KΛCDM model, one can use

$$d_L = (1+z_{\rm hel})\, r' = \sin_K \int_0^{z_{\rm CMB}} \frac{dz}{H_0\sqrt{\Omega_m(1+z)^3+\Omega_K(1+z)^2+\Omega_\Lambda}} \tag{6.2.1}$$

where $\sin_K x := \lim_{\epsilon\to K} \frac{\sin(\sqrt{\epsilon}\, x)}{\sqrt{\epsilon}}$, $K = -\Omega_K H_0^2$; i.e., $\sin_0 x = x$, $\sin_{+1} x = \sin x$, $\sin_{-1} x = \sinh x$.

The hyperconical model predicts a Pearson's chi-squared value of $\chi^2 = 1031.1$ with a cumulative probability of $p_\chi := p(\chi^2 \leq \chi_0^2) = 36.9\%$, which is practically equal to the KΛCDM model fit ($\chi^2 = 1031.7$, $p_\chi = 37.4\%$) and slightly lower than the ΛCDM standard model result ($\chi^2 = 1037.0$, $p_\chi = 42.0\%$). The best-fit parameters of the proposed model are $\alpha = 0.499(13)$ (see Sec. 2.5.5) with a general fit of $\alpha > 0.1$ and $\epsilon = 0.1 \pm 0.2$ (σ levels), which corresponds to $\gamma_0 = 1.6^{+0.4}_{-0.2}$ (Fig. 6.2.2). The distortion exponent is consistent with the theoretical local-value of $\alpha = 0.5$, but the maximum angle deviates from the expected value of $\gamma_0 = \frac{18}{5}\alpha/(1+\epsilon) \approx \frac{2}{3}\pi$, although close to the local value of $\gamma_0 = 2$ (see Eq. 6.1.10).

6.2.1.3 Constraints of the projected model with CC and BAO data

A sample of 34 cosmic chronometers and 7 values from radial BAO size in galaxy distribution (BAO-Gal) was collected in Table 6.2 to model the Hubble parameter (H) as a function of the redshift (z). Omitting the effects of radiation ($\Omega_r \approx 0$) and curvature ($\Omega_K \approx 0$) at $z \leq 1$, one-parameter models were considered in this Section to be adjusted to the measurements. For instance, the Hubble parameter of the standard model (e.g. $\Omega_\Lambda \approx 0.70$, $\Omega_m \approx 0.30$) and the equivalent projection of the hyperconical model (e.g. 3rd-order approach) can be simply represented by

$$H_{proj}(z) \approx H_{stan}(z) :\approx H_{0,stan}\sqrt{\Omega_m(1+z)^3+\Omega_\Lambda}\,. \tag{6.2.2}$$

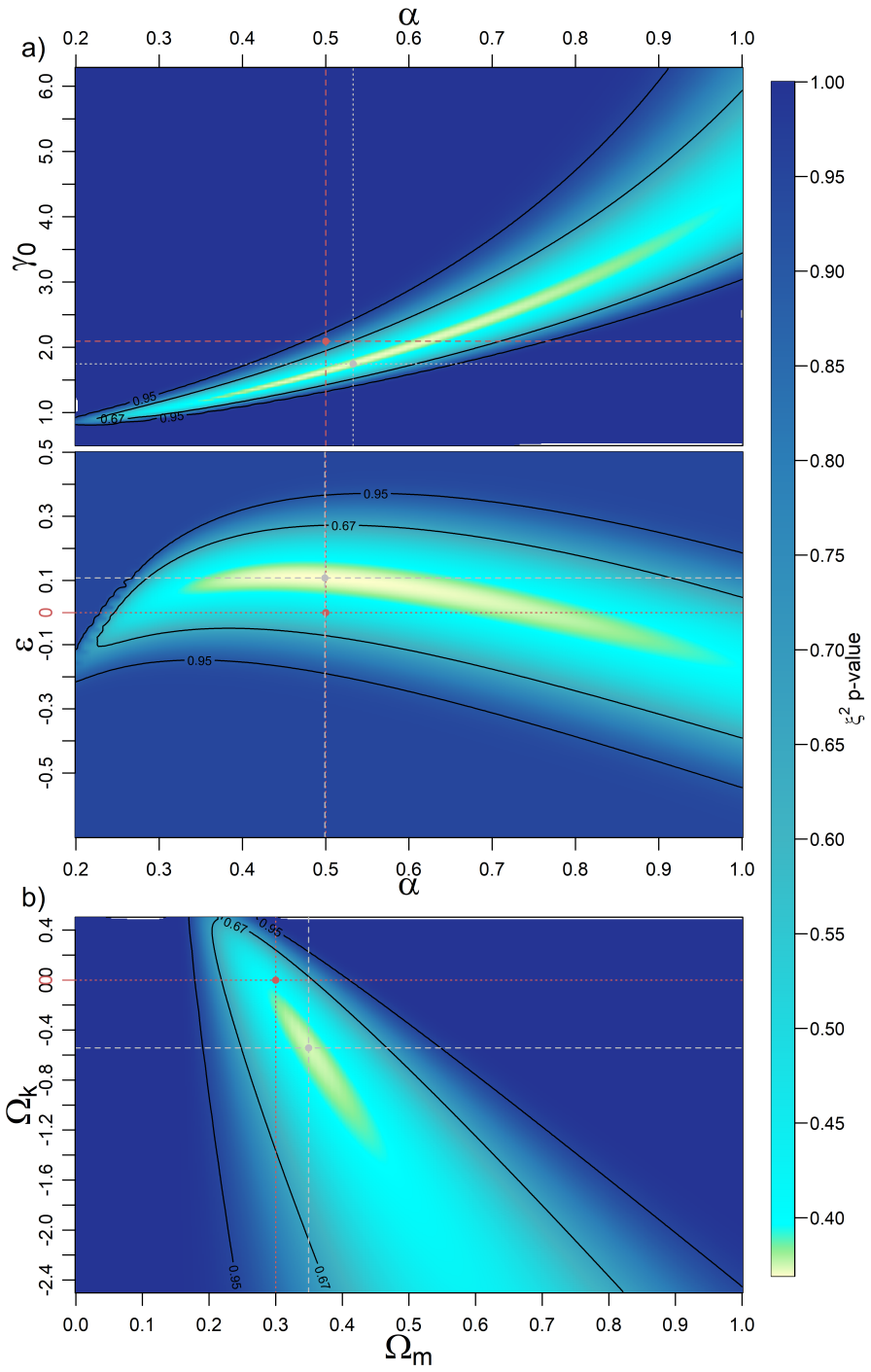

Figure 6.2.2: Observational constraints (chi-square p-value) for (a) the Hyperconical model with parameters (α, γ_0) or (α, ϵ), and (b) the KΛCDM model, according to the Pantheon sample [Scolnic *et al.* 2018, Zhao *et al.* 2019]. The red dots and dotted lines represent theoretical values, while the gray dots and dashed lines marks the best fit in any case. The 95% and 67% confidence levels are highlighted by black continuous contour lines.

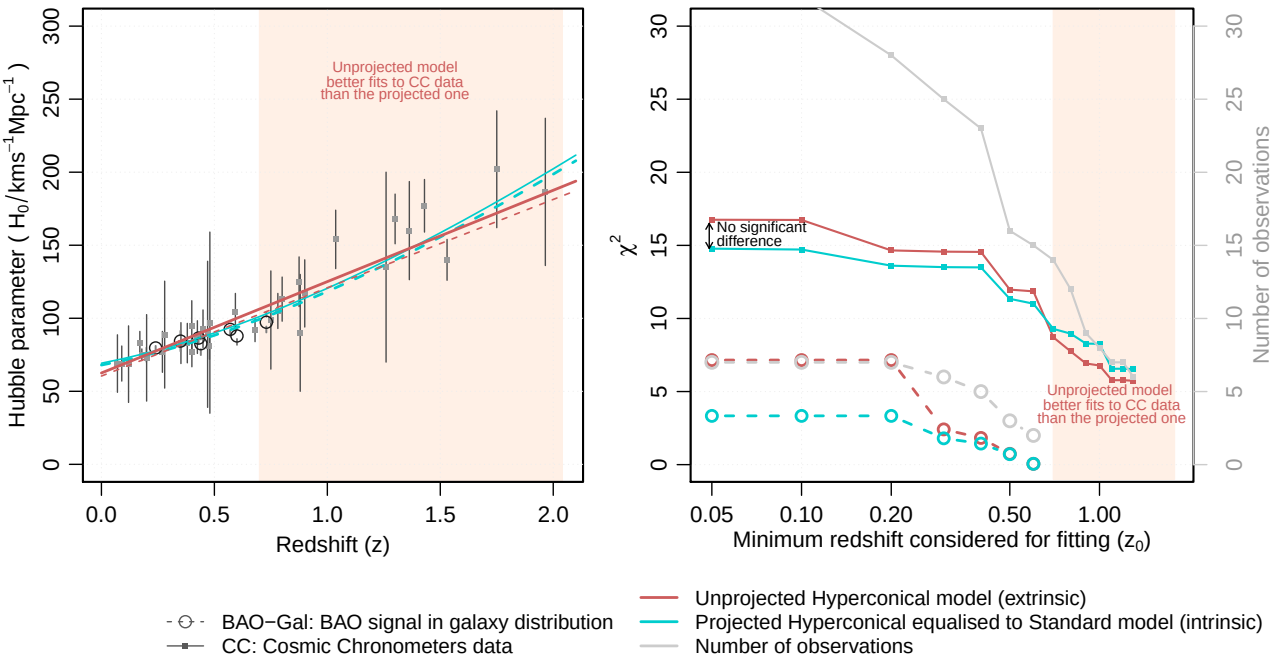

Figure 6.2.3: (Left): Fits of the unprojected and projected hyperconical models to the observations of the Hubble parameter estimated from cosmic chronometers and radial BAO size methods, respectively. (Right): Interpretation of Pearson chi-squared statistics (χ^2) obtained for the fits restricted by $z > z_0$ with respect to a particular threshold z_0.

Although redshift is assumed to be affected by the intrinsic geometry, we also employ the unprojected hypercone to compare. Since it expands linearly, its Hubble parameter is exactly

$$H_{unpr}(z) := H_{0,unpr}(1+z)\ . \tag{6.2.3}$$

Taking the sample of 7 values from the BAO signal in galaxy distribution, the performance of the standard model (and the equivalent projection of the hyperconical model) is clearly better than the unprojected model. Specifically, the standard cosmology obtains $\chi^2 = 3.3$ and $p_\chi = 23\%$ while the unprojected model provides $\chi^2 = 7.2$ and $p_\chi = 69\%$ (Fig. 6.2.3). However, if other methods are considered to constraint the BAO sound horizon scale (e.g. Lyα forest spectra), the new values of H_0 are incompatible with the unprojected model. Specifically, Font-Ribera *et al.* 2014 estimated $H_0 = 226 \pm 8$ at $z = 2.36$ and Delubac *et al.* 2015 found $H_0 = 222 \pm 7$ at $z = 2.36$ under the BAO-Lyα approach. Considering BAO-Gal+BAO-Lyα (9 values), the standard model obtains $\chi^2 = 6.5$ and $p_\chi = 41\%$ while the unprojected model provides $\chi^2 = 17.7$ and $p_\chi = 98\%$, which is rejected at a 0.05 level of significance.

Considering the sample of 34 purely cosmology-independent CC values, projected and unprojected models show closer Pearson Chi-squared statistics, $\chi^2 = 14.8$ and $\chi^2 = 16.8$ respectivaly, that correspond to $p_\chi = 0.3\%$ and $p_\chi = 0.8\%$. For the sub-sample of 8 CC

Table 6.2: Hubble parameter (H) and statistical error (σ) estimated by using Cosmic Chronometers (CC) and radial BAO size from galaxy distribution (BAO-Gal).

z	$H(z)/kms^{-1}Mpc^{-1}$	$\pm 1\sigma(H(z))$	Method	Reference
0.0708	69.0	19.68	CC	Zhang *et al.* 2014
0.09	69.0	12.0	CC	Jimenez *et al.* 2003
0.12	68.6	26.2	CC	Zhang *et al.* 2014
0.17	83.0	8.0	CC	Simon *et al.* 2005
0.179	75.0	4.0	CC	Moresco *et al.* 2012
0.199	75.0	5.0	CC	Moresco *et al.* 2012
0.2	72.9	29.6	CC	Zhang *et al.* 2014
0.240	79.69	2.65	BAO-Gal	Gaztañaga *et al.* 2009
0.27	77.0	14.0	CC	Simon *et al.* 2005
0.28	88.8	36.6	CC	Zhang *et al.* 2014
0.35	84.4	7.0	BAO-Gal	Xu *et al.* 2013
0.352	83.0	14.0	CC	Moresco *et al.* 2012
0.3802	83.0	13.5	CC	Moresco *et al.* 2016
0.4	95.0	17.0	CC	Simon *et al.* 2005
0.4004	77.0	10.2	CC	Moresco *et al.* 2016
0.4247	87.1	11.2	CC	Moresco *et al.* 2016
0.43	86.45	3.68	BAO-Gal	Gaztañaga *et al.* 2009
0.44	82.6	7.8	BAO-Gal	Blake *et al.* 2012
0.4497	92.8	12.9	CC	Moresco *et al.* 2016
0.47	89	50	CC	Ratsimbazafy *et al.* 2017
0.4783	80.9	9.0	CC	Moresco *et al.* 2016
0.48	97.0	62.0	CC	Stern *et al.* 2010
0.57	92.4	4.5	BAO-Gal	Samushia *et al.* 2013
0.593	104.0	13.0	CC	Moresco *et al.* 2012
0.6	87.9	6.1	BAO-Gal	Blake *et al.* 2012
0.68	92.0	8.0	CC	Moresco *et al.* 2012
0.73	97.3	7.0	BAO-Gal	Blake *et al.* 2012
0.75	98.8	33.6	CC	Borghi *et al.* 2022
0.8	113.1	15.1	CC	Jiao *et al.* 2023
0.781	105.0	12.0	CC	Moresco *et al.* 2012
0.875	125.0	17.0	CC	Moresco *et al.* 2012
0.88	90.0	40.0	CC	Stern *et al.* 2010
0.9	117.0	23.0	CC	Simon *et al.* 2005
1.037	154.0	20.0	CC	Moresco *et al.* 2012
1.26	135	65	CC	Tomasetti *et al.* 2023
1.3	168.0	17.0	CC	Simon *et al.* 2005
1.363	160.0	33.6	CC	Moresco 2015
1.43	177.0	18.0	CC	Simon *et al.* 2005
1.53	140.0	14.0	CC	Simon *et al.* 2005
1.75	202.0	40.0	CC	Simon *et al.* 2005
1.965	186.5	50.4	CC	Moresco 2015

points restricted at $z > 1$, it was obtained $\chi^2 = 6.8$ with $p_\chi = 55\%$ for the unprojected model, and $\chi^2 = 8.3$ with $p = 69\%$ for the standard model. In short, the unprojected and projected approaches are statistically indistinguishable for CC data but not for the BAO signal.

Concerning the Hubble parameter constraint, $H_0 = h_0\,\mathrm{km\,s^{-1}Mpc^{-1}}$, the standard model leads to $h_0 = 66.72 \pm 0.65$ for BAO-Gal+BAO-Lyα data (9 points), $h_0 = 68.0 \pm 1.1$ for only BAO-Gal (7 points) and $h_0 = 69.3 \pm 1.3$ for the CC sample (34 points). That is a 2σ-higher expansion rate measured in CC than in BAO-Gal+BAO-Lyα. This tension disappears when Lyα data is dropped. If the CC sample is restricted at $z > 1$, the best fit of the standard model increases the Hubble parameter to $h_0 = 71.3 \pm 3.1$ versus $h_0 = 68.6 \pm 1.1$ for $z < 0.5$. All these small tensions between the local ($z < 0.5$) and larger ($z > 1$) scales are aligned to the results showed in Table 6.2.

6.2.2 Observations of object dynamics

6.2.2.1 Object dynamics

A second practical application of our theoretical framework was deriving a geometrical model for explaining 'object dynamics' within a (1, 3)-Lorentzian manifold [Monjo 2023]. As a paradigmatic candidate of fictitious acceleration, the anomalous dynamics of galaxies have been deeply analyzed by standard and alternative models. For instance, general relativity needs to be complemented by 'dark quantities', as in modern cosmology, to explain the flat curve observed in the orbital velocity of galaxies. However, recent studies claim that 'dark matter' is already falsified since it is not able to explain some phenomena such as the absence of the expected *dynamical friction*[1] in cluster collisions, among other issues [Kroupa 2015, Ardi and Baumgardt 2020]. Combining all the issues of dark matter, the standard model seems to be falsified for more than 7 sigmas [Kroupa 2015, Kroupa *et al.* 2023]. To solve these raising problems, modified Newtonian dynamics satisfactorily describe the same observations by using a 'cosmological acceleration' instead of 'dark matter'.

This section shows results on modelling MDAR data, collected from the SPARC database, which consist of 153 late-type galaxies (spirals and irregulars) with Spitzer photometry and high-quality HI+Halpha rotation curves [McGaugh *et al.* 2007, Lelli *et al.* 2016, Lelli *et al.* 2019]. Similar to the cited studies, and compared to the original set of 175 galaxies of SPARC, 22 objects were excluded due to low inclinations and low quality rotation curves.

To represent the 'flat velocity' of the rotation curves used in the MDAR/BTFR modeling, this Section used the same criterion as in Lelli *et al.* 2019, from which, only 123 objects are used (the remaining 30 galaxies do not satisfy the 5% flatness criteria).

[1] According to Kroupa 2015, dark matter halos should exert a strong breaking force (the *Chandrasekhar dynamical friction*) and dissipate their kinetic energy as they move through each other. This breaking-effect is not seen in the motions of galaxies.

6.2.2.2 Rotation curves

MDAR/BTFR modeling. The rotation curve is immediately obtained from Eq. 4.4.7, which approaches to Eq. 4.3.13 for $a_N \gg c/t$ with $a_N = -v_K^2\,\mathbf{r}/r^2$ and $d^2\mathbf{r}/dt^2 = -v^2\mathbf{r}/r^2$. Another way to express the mass-discrepancy acceleration is the BTFR curve, which is an empirical function $v(M)$ between the baryonic mass (M) and the rotation velocity (v) for a certain radius r, which is an approximate constant value (i.e. a 'flat curve'). In our case, that relationship is immediately found to be:

$$v(r;\gamma_0) \approx \sqrt[4]{\left(\frac{\mathrm{G}M(r)}{r}\right)^2 + \frac{2\mathrm{G}M(r)c}{\gamma_0 t}} \;\Rightarrow\; v(M;\gamma_0) \approx \sqrt[4]{\left(\frac{\mathrm{G}M}{r_M}\right)^2 + \frac{2\mathrm{G}Mc}{\gamma_0 t}}, \quad (6.2.4)$$

where r_M is the galaxy radius as a function of the baryonic mass. Notice that the first term of the root argument is the Newtonian contribution to the rotation curve, while the second term leads to the "flatness" of the rotation curve. To analyze the effect of the Newtonian contribution to the BTFR, we consider a constant angle γ_0 and an averaged radius (for all observed objects) in each galaxy.

γ_M-hypercone-based galaxy rotation curves. The characteristic angle $\gamma_M = \gamma_U$ for empty regions is projected to $\gamma_0(\gamma_U) = \gamma_U/\cos\gamma_U = \frac{2}{3}\pi$. However, nonzero perturbations locally modify the curvature of the spacetime and its causality angles, with additional movements to the expansion of the universe, and therefore $\gamma_0 \neq \frac{2}{3}\pi$ in most of cases. In other words, it is expected that the values of γ_0 depend on the difference between v_E and v_H according to some relationship like Eq. 4.3.4 . Thus, Eq. 4.3.1 becomes

$$\gamma_0(\gamma_M) :\approx \frac{\gamma_M}{\cos\gamma_M} \quad (6.2.5)$$

and, therefore, the orbital speed is now expressed in terms of the unique mean value of the parameter,γ_M as follows

$$v(M;\gamma_M) \approx \sqrt[4]{\left(\frac{\mathrm{G}M}{r_M}\right)^2 + \frac{2\mathrm{G}Mc}{t}\,\frac{\cos\gamma_M}{\gamma_M}} \quad (6.2.6)$$

where the parameter γ_M is assumed to be constant.

γ_{gc}-hypercone-based galaxy rotation curves. Considering all the possible values from the domain of the projective angles, the galactic center is ranged by $\gamma_{gc} \in (\frac{\pi}{3}, \frac{\pi}{2})$; thus, it is possible to model the characteristic angle γ_M of Eq. 4.3.4 as follows:

$$\sin^2\gamma_M(\gamma_{gc}) \approx \sin^2\gamma_U + \left(\sin^2\gamma_{gc} - \sin^2\gamma_U\right)\frac{\frac{2\mathrm{G}M}{r}}{\frac{r^2}{t^2} + \frac{2\mathrm{G}M}{r}}\,. \quad (6.2.7)$$

Thus, replacing γ_M by its function, depending on γ_{gc} in Eq. 6.2.4, we get a BTFR behaviour in terms of that parameter, $v(M;\gamma_M) \Rightarrow v(M,r;\gamma_{gc})$.

$$v(M,r;\gamma_{gc}) \approx \sqrt[4]{\left(\frac{\mathrm{G}M}{r}\right)^2 + \frac{2\mathrm{G}Mc}{t}\,\frac{\cos\gamma_M(r,\gamma_{gc})}{\gamma_M(r,\gamma_{gc})}}\,. \quad (6.2.8)$$

6.2.2.3 Galactic scales

Individually for each galaxy, the parameter γ_M has a large range of values with quartiles about $\gamma_M/\pi = 0.457^{+0.013}_{-0.021}$, and the best fit (Eq. 4.4.7 or equivalently Eq. 6.2.4) to the dataset is found for a constant $\gamma_M/\pi = 0.460 \pm 0.002$ (Fig. 6.2.4). To explain the mass discrepancy, this γ_M-hypercone-based model obtained an Adjusted R-squared of $R^2 = 0.92$, slightly greater than the simple logarithmic model of BTFR ($R^2 = 0.91$). Relative mean absolute error, $RMAE := \text{mean}(|modeled - observed|/observed)$, is also better for the γ_M-hypercone, obtaining $RMAE = 0.108$ versus $RMAE = 0.115$, estimated when the simple empirical BTFR logarithm is used. That is almost $\sim 1\%$ of improvement with only a free parameter.

For a set of 696 objects in 61 high-quality SPARC galaxies [Lelli *et al.* 2019], rotation curves were correctly simulated by the γ_M-hypercone-based model (Eq. 6.2.6; Fig. 6.2.5). The proposed model obtained a relative mean absolute error of $RMAE = 0.070$ and R-squared of $R^2 = 0.955$, that are slightly better ($\sim 1\%$) than the empirical fitting ($RMAE = 0.080$ and $R^2 = 0.953$).

If individual dynamics of the 696 objects are considered, the range of values of $\{\gamma_M/\pi\} \sim (0.44, 0.48)$ is adequately modelled by the γ_{gc}-hypercone-based approach (Eqs. 6.2.7-6.2.8), and the observational constraint yields a constant $\gamma_{gc}/\pi \approx 0.48$. In this case, the R-squared is $R^2 = 0.957$, but the relative error is the same as in the γ_M-hypercone-based model ($RMAE = 0.070$).

The results showed that the hypercone-based galaxy curves have a transitional behaviour between the deep MOND flat curves and the purely Newtonian-Keplerian regime. The γ_M-hyperconical approach is enough to describe adequately the transition between dynamics, but conceptually, the γ_{gc}-hypercone is more adjusted to limit cases of empty spaces and the black hole's environment. However, the difference between the fitted value of $\gamma_{gc}/\pi \approx 0.48$ and the theoretical value of $\gamma_{gc}/\pi = \frac{1}{2}$ is still unexplained by the current version of the model. To confirm this deviation, further work could analyze the range of γ_{gc} in black-hole dynamics.

6.2.2.4 Empty space and solar system scales

The average value of the model parameter $\gamma_M/\pi = 0.457^{+0.013}_{-0.021}$ produces a cosmic acceleration for galaxies in the range of $1.1 \cdot 10^{-11} \leq a_0 \leq 4.5 \cdot 10^{-11}$ ms^{-}2. Is it also observed in our solar system?

The galactic acceleration is lower than 10% compared to the well-known anomaly observed in the Pioneer 10 and 11 spacecrafts. Radio-metric tracking data collected from the Pioneer spacecrafts indicated the presence of an anomalous Doppler frequency drift interpreted as a constant acceleration of $(8.74 \pm 1.33) \cdot 10^{-10} ms^{-2}$ towards the Sun [Turyshev *et al.* 2005]. This anomaly was explained several years later. The model based on thermal radiation pressure (TRP), and the corresponding thermal recoil force (TRF) can explain up to $8 \cdot 10^{-10}$ ms^{-2}. Therefore, no statistically significant anomalous acceleration remains in the data, and it is up to 10% with respect to the original anomaly in the Doppler effect [Rievers and Lammerzahl 2011].

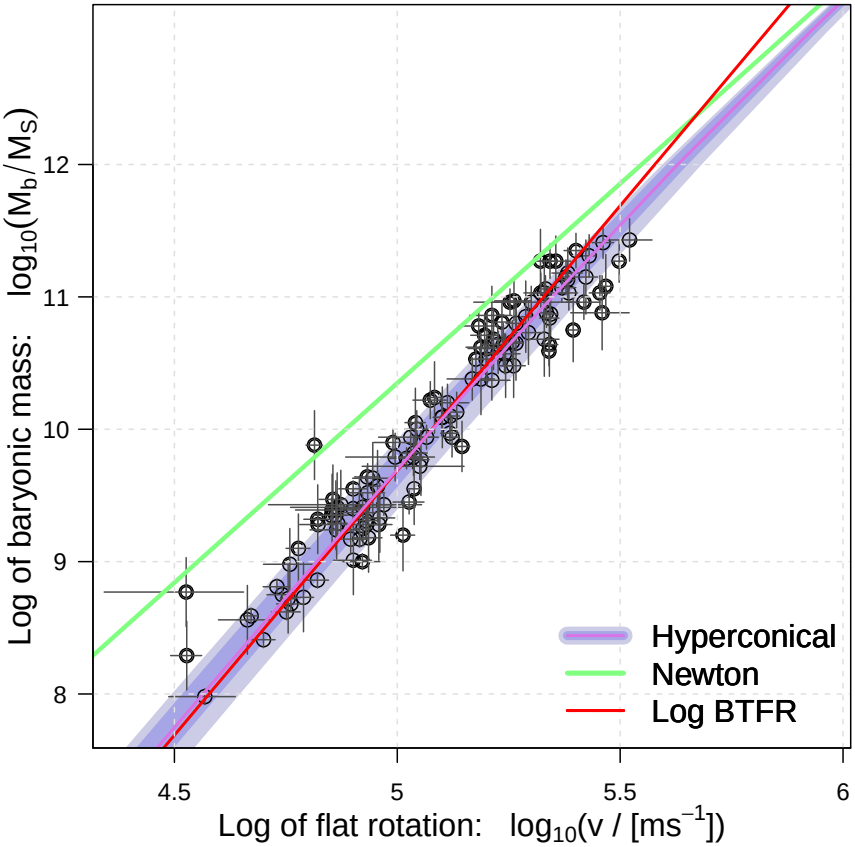

Figure 6.2.4: MDAR/BTFR modeling. Fitting of the hyperconical model (Eq. 6.2.6 with $\gamma_M/\pi = 0.460 \pm 0.002$) to the baryonic Tully–Fisher relation $v(M_b)$ for 123 galaxies with 'flat' velocity (v) and baryonic mass (M_b), expressed in terms of solar mass (M_S). The Newton line represents the Keplerian orbits, while the "Log BTFR" line is the empirical law $M_b \propto v^\epsilon$ with $\epsilon \approx 4$. Finally, the used empirical relationship between the galactic radius r_{M_b} and the baryonic mass M_b is $r_{M_b} \propto M_b^{0.775\pm0.045}$.

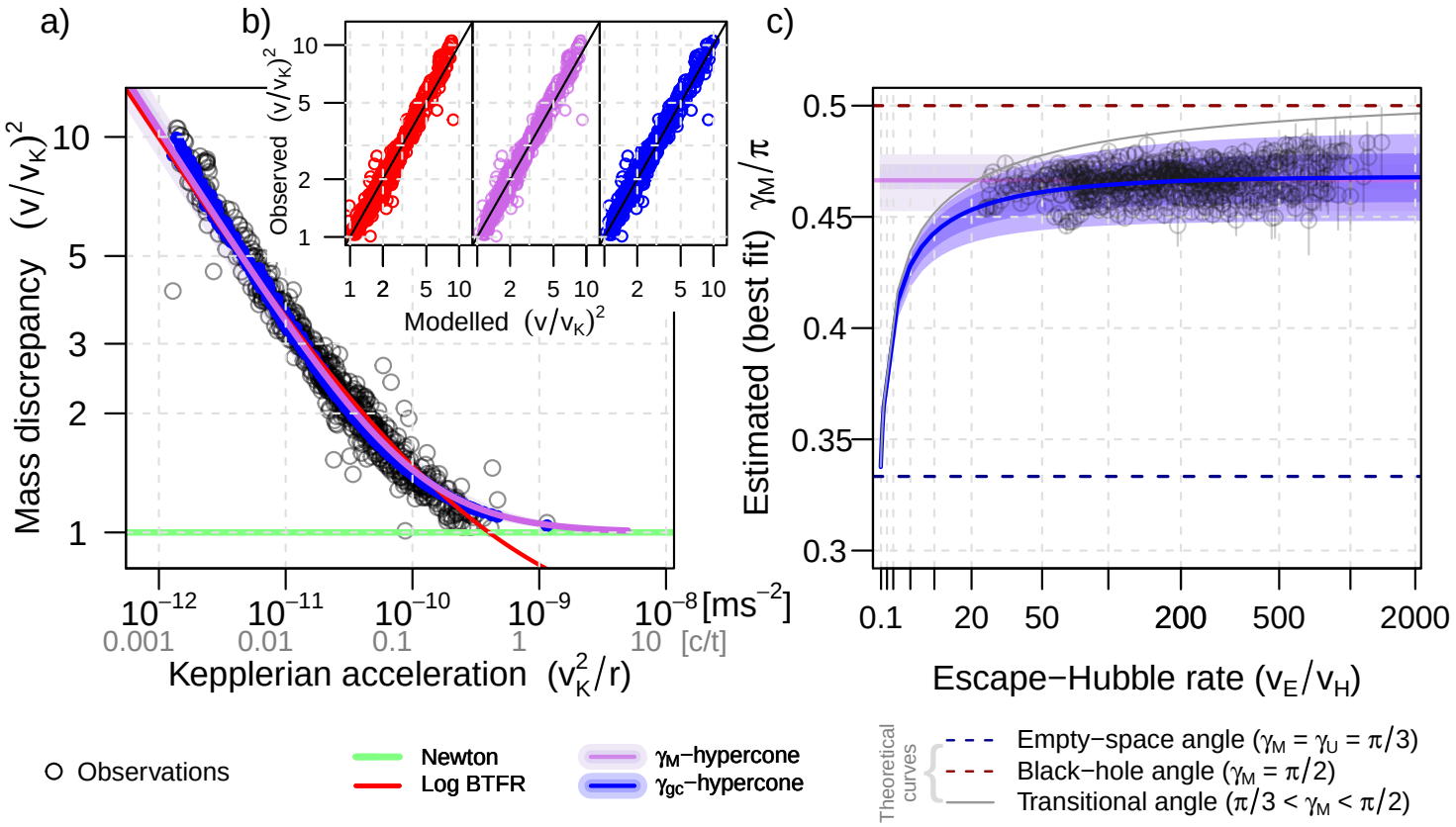

Figure 6.2.5: Modelling of the rotation curve for 61 galaxies collected from SPARC dataset: (a) Fit of Eq. 6.2.6 and 6.2.8 to the observed rotation curves; (b) Scatter plot of observed and modelled velocity according to the empirical "Log BTFR" (Eq. 4.1.1), the γ_M-hypercone-based model (Eq. 6.2.6) and the γ_{gc}-hypercone-based model (Eq. 6.2.8) from 6.2.7); (c) Modelling of the fitted γ_M according to a constant value of $\gamma_M/\pi \approx 0.466^{+0.011}_{-0.013}$ and the γ_{gc}-hypercone, compared to the theoretical curves $\gamma_M = \gamma_U = \pi/3$ and $\gamma_M = \gamma_{gc} = \pi/2$. The 'Newton' line represents the Keplerian orbital curves $v = v_K$, for which $M/M_b = 1 = v^2/v_K^2$.

Specifically, TRF and the Doppler data can be modelled using an exponential decay model in the form $a = a_0 2^{-(t-t_0)/T}$ [Turyshev *et al.* 2011, Turyshev *et al.* 2012]. Setting $t_0 =$ January 1, 1980, Turyshev *et al.* 2011 estimated the parameters $T_{Dopp} = (28.8 \pm 2.0)$ yr, $a_{0,Dopp} = (10.1 \pm 1.0) \cdot 10^{-10}$ m/s^2 fitted to the Doppler data, while the ones for TRF are $T_{TRF} = (36.9 \pm 6.7)$ yr and $a_{0,TRF} = (7.4 \pm 2.5) \cdot 10^{-10}$ m/s^2. Again, the same uncertainty scale is found.

In fact, several studies showed that an acceleration such as that observed in the Pioneer spacecrafts could not have a gravitational origin because when applied as a perturbation to the trajectories of the planets, it leads to much larger anomalies than the observational limit of possible anomalies [Burns 1976, Iorio 2007].

According to Eq. 4.3.13, empty spacetime experiences an acceleration of $a = c/(\gamma_0 t) \approx c/(2t) \approx 3.5 \cdot 10^{-10}$ ms^{-2}. This value is very close to the expected one by a hypothetical Unruh-like radiation, with acceleration

$$a \sim \frac{\frac{4}{5}\pi^2 c^2}{\lambda} \sim \frac{\pi^2 c}{10t} \sim \frac{c}{t}\,, \tag{6.2.9}$$

where $\lambda = 4\Theta = 8ct$ is taken following the Casimir-like effect proposed by McCulloch 2007, obtaining $6.9 \pm 3.5 \cdot 10^{-10} ms^{-2}$ (twice as much as our model).

However, perturbations of (vacuum) energy density cause a local *spatial curvature* larger than the one of empty spacetime, reducing the *fictitious* cosmic acceleration. Considering the Eq. 6.2.7 for the Oort Cloud ($2 \cdot 10^5$ UA) with the most restrictive value for the projective angle ($\gamma_{gc} \leq 0.5\pi$), our model predicts an acceleration anomaly towards the sun of $a_p \geq 3 \cdot 10^{-13}$ m/s^2. Assuming the estimated value of $\gamma_{gc} \geq 0.48\pi$ (fitted from galaxy curves), it corresponds to an anomaly about $a_p \leq 3 \cdot 10^{-11}$ m/s^2 for the inner solar system (5 UA) and $a_p \leq 6 \cdot 10^{-11}$ m/s^2 for the Oort Cloud. This result only provides upper bounds, but it can be compared to the one obtained by Brownstein and Moffat 2006, who predicted an anomaly of about $4 \cdot 10^{-11}$ m/s^2 over the Neptune's orbit (30 UA), and $2 \cdot 10^{-11}$ m/s^2 over the Uranus orbit (19 UA).

According to Iorio 2007, such an effect would be too small to be detected yet, as also it is our lower bound of $a_p \geq 3 \cdot 10^{-13}$ m/s^2 for the Oort Cloud. However, it is necessary to continue analysing the trajectories in the solar system under the perturbation theory to falsify such acceleration or to decide if the prediction is still valid below the detection level of the most recent ephemerides.

In fact, possible disturbances within the solar system were detected in the Kuiper Belt objects (44 UA) from external field effects, and also modelled by MOND [Brown and Mathur 2023]. Similar anomalies are observed in low acceleration orbits of widely separated binary stars, so-called *wide binaries* [Acedo 2020]. Recently, Chae 2024 has confirmed robust evidences for the breakdown of standard gravity from *statistically pure binaries*, that is free of hidden companions. According to these findings, MOND-type modified gravities are favoured to explain the observed anomalies [Zhoolideh-Haghighi and Rahvar 2017, Banik and Zhao 2022, Chae 2023, Hernandez 2023].

6.2.2.5 Physical interpretation

It is possible to draw a conceptual parallel between the apparent acceleration of the expanding universe and the fictitious Coriolis acceleration of a non-inertial system like the Earth. The first one is produced when a reference frame is transformed from the ambient space (with an extrinsic viewpoint) to the tangent Minkowskian spaces where (intrinsic) metric is defined for comoving observers[2]. The second one is the well-known consequence of changing the reference from almost *inertial frames* (e.g., heliocentric coordinates) to the rotating system of the Earth or the observers that live on its surface.[3]

The features of the projected hyperconical (background) metric contribute to the large-scale dynamics of galaxies as the choice of reference frames is the key in non-inertial dynamics. For instance, the Coriolis force experienced by deviated trajectories on the Earth corresponds to the deviated redshifts experienced by Type Ia supernovae stars as a function of the luminosity distance. Similarly, the geostrophic wind defined in large-scale (extratropical) systems is mostly due to the Coriolis acceleration, as the 'flat' speed curve of the spiral galaxies could be due to the apparent acceleration c/t raised from the hypercone-based projection. The black-hole rotation curve would be the analog cyclostrophic wind of tropical cyclones (which are minimally linked to the Coriolis force compared to the extratropical systems). The cyclostrophic flow is the main contribution to the total wind when the centripetal acceleration (from gravity-related pressure gradient) is greater than the Coriolis acceleration, so it is observed in cases of very curved systems (such as a tornado or hurricane).

Therefore, an open question on the fictitious acceleration is its possible evidences at smaller cosmological scales. Specifically, possible anomalous accelerations in the solar system have been analyzed during the last decades, for instance in Kuiper Belt objects [Brown and Mathur 2023][4]. However, no statistically significant differences were yet found with respect to the planetary dynamics. Thus, our results may promote possible experiments to falsify the proposed predictions at a solar-system scale.

Moreover, the hyperconical background metric needs to be further studied since strong links are expected between the extrinsic/intrinsic hyperconical model and the $R_h = ct$ universe of Melia [Melia and Shevchuk 2012, Melia and Maier 2013]. For example, the cosmic timeline of the flat $R_h = ct$ model is exactly the same as in the linear expansion (extrinsic perspective) of the hypercone-based model [Melia 2023], while the curvature is locally and globally compatible under the extrinsic and intrinsic viewpoint, respectively. The fictitious acceleration of the projected hyperconical manifold implies that the values of dark quantities are constant like the 'zero active mass' of the Melia's universe [Melia 2017]. In fact, the linear expansion (e.g. $R_h = ct$ model) better predicts the formation of high-redshift galaxies (so-called 'impossible early galaxies') than the standard ΛCDM [Melia 2023, Melia 2017, Yennapureddy and Melia, Ferreira *et al.* 2022, Gupta 2023].

[2]Since any inertial observer is comoving to the expansion, a (dynamical) transformation is required to obtain the intrinsic perspective of the observer's measurement of *proper time*.

[3]Trajectories traced by Earth's dynamical systems (e.g. the atmosphere) present different lengths due to the coordinate transformation given by the non-inertial change of reference frames.

[4]Moreover, strong evidences have been recently found in *wide binaries* [Chae 2024].

According to our results, paths of both the light and the gravitational interaction in galaxies are drawn on the (intrinsic) manifold in the same way as the atmospheric winds represent flows and interactions of air masses on the Earth's surface. Nonetheless, the cosmic timeline of both systems is defined by the extrinsic reference frames.

6.2.3 Points to be further analyzed

The possible impacts of our theory on smaller objects (e.g. galaxies) are analyzed in the following Sec. 6.2.2, but some scales (e.g. solar system) are not sufficiently explored yet. The problem of constructing embeddings for gravity metrics has been analyzed in many studies [Pavsic and Tapia 2000, Paston and Sheykin 2012]. According to Kasner's theorem, any solution of the Einstein equations needs to be embedded into at least a six-dimensional ambient space [Paston and Sheykin 2012]. However, we have applied a dynamical embedding in only five dimensions to model the universe and provides a procedure to reproduce Schwarzschild effects as a limit case of a more general theory (see Appendix E). Further works could analyze whether it is possible to find a transition way between five-dimensional large-scale effects and six-dimensional local perturbation metrics. For instance, the ADM decomposition allows to compare Kerr-Schild metrics to embed time-constant hypersurfaces, which are spacelike or Cauchy hypersurfaces, into a flat four-dimensional space (plus the temporal dimension) [Bonning *et al.* 2003]. Therefore, Einstein field equations (and their solutions) would actually be an approach that has the same limit case as the linear perturbation of the background metric.

As weaknesses of the theory, the hyperconical model cannot predict the visible matter content or the photon density. In fact, to analyze the first acoustic peak (from the photon-baryon decoupling), it is necessary to introduce baryons and photons into the model. Moreover, linear expansion does not adequately reproduce the CMB BAO spectrum by itself [Tutusaus *et al.* 2016, Fujii 2020]; but the anisotropic temperature distribution in CMB might be produced at $z \sim 10$ instead of the standard $z \sim 1080$ due to dust created in Population III stars; thus avoiding the failure of the linear expansion model [Vavrycuk *et al.* 2017, Melia 2022b]. Linear expansion also presents difficulties to explain the observed abundance of helium about He/H ~ 0.244 in mass, presumably produced by the commonly known as "Big Bang nucleosynthesis" or primordial nucleosynthesis in the early universe [Lewis *et al.* 2016, Chardin *et al.* 2021]. An alternative explanation for that helium mass fraction is the hydrogen fusion in primordial stars, which predicts a black body temperature about $T = 2.76K$, very close to the observed temperature for the Cosmic Microwave background (CMB) radiation [López-Corredoira 2014].

Finally, the proposed model is in its early stage of development, with assumptions in distorted stereographic projections and local-to-global approaches for the time dependence, which are not unique to be compatible with SNe Type-Ia, BAO-Gal and CC observations [Monjo 2017, Monjo and Campoamor-Stursberg 2023]. Therefore, the proposed model needs to be confronted and constrained to more sets of observational data such as galaxy clusters and CMB spectrum.

6.3 Modelling of particle dynamics

6.3.1 Why this?

As the previous section analyzes the perturbation of the metric at classical large scales (e.g. galaxies), this section explores the smallest perturbations possible of the metric, that is, the produced by particle fields (e.g. spinors) [Monjo et al. 2024]. The kind of small perturbations should be similar to the $g \approx \eta - u \otimes u$ obtained (except for the shift term) in Eq. 2.3.10, and similar to the smallest perturbations in a Schwarzschild metric (Eq. 4.2.7), since one can define an escape velocity by $v_E := \sqrt{2\mathrm{G}M/r'}$ and thus radial component of the metric is $g_{rr} = -1 - u_E u_E$; while for the empty spacetime, it was $u_H := r/t$ and $g_{rr} = -1 - u_H u_H$. The similitude is greater for Kerr–Schild coordinates, $g = \eta + \mathfrak{f} U \otimes U$, with vector field U and scalar field $\mathfrak{f}$ [Gurses *et al.* 2018]. Similarly, perturbations for spinors provides a metric like $g \approx \eta + \hat{A} \otimes \hat{A}$ (Eq. 5.3.4).

Therefore, any perturbation on the metric should produce a fictitious acceleration[5]. Thus, our Thesis proposal of *coloured gravity* interprets that Yang-Mills dynamics are also fictitious accelerations as the "force without force" of Wheeler 1961 (see for instance Blum and Furlan 2022). The main difference with GR is that now, the key (unitary) field is not the spacetime metric, but it is a *spacetime-particle* metric, since g depends on quantum numbers (hidden in $\hat{A}$) of each particle field. The motivation for this section is that our model provides explanation for the apparent dark matter and dark energy [Monjo and Campoamor-Stursberg 2023] and for perturbation of ordinary matter in galaxies [Monjo 2023], but radiation is not simulated yet. Therefore, we aimed to explore possible adjustments of our framework to reproduce at least *photons* (i.e. electromagnetic fields) in gravity.[6]

6.3.2 From torsion-free components to a fictitious Lorentz force

As a representative of the geometrization of particle dynamics (*geometrodynamics*), coloured gravity leads to a classical limit of the well-known electromagnetism. Before analysing this classic limit, it is useful to check some properties of the Lorentz connection, since accelerated trajectories of particles can be described by both the TEGR (with torsion) and the GR (without torsion) geodesics.

In fact, the TEGR contorsion can be translated as a Riemann curvature effect [Arcos *et al.* 2004, Krššák *et al.* 2019]. Similarly, electrodynamics can be modelled by torsionless Riemannian geometry because the gauge group is abelian. This means that the subgroup $\mathrm{U}(1) \subset \mathrm{SU}(1,3)$ will be considered in the following sections to describe the gauge potential A (perturbation of the metric). The perturbed co-tetrads lead to a perturbed spin

[5] Remember that, according to the strong equivalence principle (SEP), gravitational acceleration is also a *fictitious acceleration*, since any free-falling particle locally experiences the same measurements as in the flat Minkowskian spacetime.

[6] That is, obtaining *photons* by perturbing the metric.

connection, whose (torsionless) components $\omega_\mu{}^{ab}$ are (Eq. 1.2.4):

$$\begin{aligned}\omega_\mu{}^{ab} &= \hat{e}_\nu{}^a \overset{\circ}{D}\hat{e}^{\nu b} = \hat{e}_\nu{}^a(\partial_\mu \hat{e}^{\nu b} + \overset{\circ}{\Gamma}{}^\nu{}_{\sigma\mu}\hat{e}^{\sigma b}) \\ &= \tfrac{1}{2}(\partial_\mu \hat{e}_\nu{}^b - \partial_\nu \hat{e}_\mu{}^b) - \tfrac{1}{2}\hat{e}^{\nu b}(\partial_\mu \hat{e}_\nu{}^a - \partial_\nu \hat{e}_\mu{}^a) - \tfrac{1}{2}\hat{e}^{\rho a}\hat{e}^{\sigma b}(\partial_\rho \hat{e}_{\sigma c} - \partial_\sigma \hat{e}_{\rho c})\hat{e}_\mu{}^c \\ &\approx \tfrac{1}{2}(\partial_\mu \hat{e}^{ab} - \partial_\mu \hat{e}^{ba} - \partial^a \hat{e}_\mu{}^b + \partial^b \hat{e}_\mu{}^a - \eta^{\rho a}\eta^{\sigma b}\eta_{cd}(\partial^a \hat{e}_\sigma{}^d - \partial^b \hat{e}_\rho{}^d)\delta^c_\mu) \\ &\approx -(\partial^a \phi_\mu{}^b - \partial^b \phi_\mu{}^a) \approx -\tfrac{q}{m}\left(\partial^a(A^b u_\mu) - \partial^b(A^a u_\mu)\right). \end{aligned} \tag{6.3.1}$$

Two interesting properties of the connection are found for application to spinors Ψ and for contraction with γ^μ (useful for vector fields). Taking into account the Lorentz generators for spinors, $S^\Psi_{ab} = i[\gamma_a, \gamma_b]/4$, we obtain

$$\begin{aligned}\omega_\mu{}^{ab} S^\Psi_{ab} &\approx \frac{i}{4}\omega_\mu{}^{ab}[\gamma_a, \gamma_b] \\ &\approx -\frac{i}{4}\tfrac{q}{m}\left(\partial^a(A^b u_\mu) - \partial^b(A^a u_\mu)\right)(\gamma_a\gamma_b - \gamma_b\gamma_a) \approx 0, \end{aligned} \tag{6.3.2}$$

which means that the torsion-free connection does not provide additional terms to the total covariant derivative, and it requires to take into account derivatives of both the spin connection and the gauge covariant derivative, e.g., $\hat{D}_\mu = \hat{\partial}_\mu - i\omega_\mu{}^{ab}S_{ab}/2 = \hat{\partial}_\mu + 0 \simeq \nabla_\mu$. Alternatively, one can incorporate the contorsion part of the Lorentz connection, thus obtaining in a natural way the total covariant derivative $D_\mu \simeq \nabla_\mu$.

On the other hand, the connection form for vector fields is obtained by the contraction with u^μ, and it is also useful to obtain the contraction with dx^μ,

$$\omega_\mu{}^{ab}u^\mu \approx -\frac{q}{m}\left(\partial^a A^b - \partial^b A^a\right) \approx -\frac{q}{m}\mathscr{F}^{ab}, \tag{6.3.3}$$

$$\omega^{ab} := \omega_\mu{}^{ab}dx^\mu \approx \partial^b\phi^a - \partial^a\phi^b = -\frac{q}{m}\mathscr{F}^{ab}d\tau, \tag{6.3.4}$$

where the equality $\gamma_\mu\gamma^\mu = \gamma^\mu\gamma_\mu = 4$ has been used and, in particular, $\gamma^\mu(\partial^a\gamma_\mu) = 0$. Moreover, recall that $\mathscr{F}^{ab} := \partial^a A^b - \partial^b A^a$ are the components of the U(1) field-strength tensor, i.e., the components of the 2-form Faraday curvature $\mathbf{F} := \frac{1}{2}\mathscr{F}_{\mu\nu}\mathrm{d}x^\mu \wedge \mathrm{d}x^\nu = \mathrm{d}A = (\partial_\mu A_\nu)\mathrm{d}x^\mu \wedge \mathrm{d}x^\nu$. Notice that details on possible non-abelian effects of the sources are lost if the contorsion is not added.

For a vector field v^a, the total time derivative $\mathbf{D}_\tau := \hat{\gamma}^\mu D_\mu = \gamma^\mu\partial_\mu$ behaves well. Recall that the equation of motion for a free particle is given by $\mathbf{D}_\tau v^a = 0$ (Eq. 1.3.10), that is,

$$\mathbf{D}_\tau v^a := \hat{\gamma}^\mu D_\mu v^a = \mathbf{d}_\tau v^a + \eta_{bc}\omega_\mu{}^{ac}u^\mu v^b = 0 \quad \Rightarrow \quad \mathbf{d}_\tau v^a \approx \frac{q}{m}\mathscr{F}^{ac}v_c, \tag{6.3.5}$$

which is the equation of a particle subject to a geodesic-like[7] Lorentz force. As mentioned in the previous sections, the acceleration of spinless particles can be modelled by both

[7]Here, geodesics depend on each particle, so they are not features of the spacetime but of the *spacetime-particle*, as an indivisible entity.

the torsion tensor (like an *external* force) and the geodesic equation within the pseudo-Riemannian geometry. That is to say, the description of the movement is provided by the Ricci coefficient of rotation and, therefore, it is also into the Ricci tensor.

In local coordinates, since the components of $\mathrm{d}\mathscr{F}^a{}_b$ are sixteen real functions, the Lorentz curvature 2-form components are

$$R^a{}_b = \mathrm{d}\omega^a{}_b + \omega^a{}_c \wedge \omega^c{}_b \approx -\frac{q}{m}\mathrm{d}\mathscr{F}^a{}_b d\tau + \left(\frac{q}{m}\right)^2 \mathscr{F}^a{}_c \wedge \mathscr{F}^c{}_b d\tau^2. \tag{6.3.6}$$

Similarly, applying $\hat{e}_\mu{}^a = e_\mu{}^a + \phi_\mu{}^a$ adequately to the Ricci curvature, taking into account Eq. 6.3.1, the first-order Ricci scalar for the Hilbert–Einstein action is

$$\begin{aligned} R &:= R_{ab} \wedge \star\hat{e}^{ab} = R_{\mu\nu ab}\hat{e}^{\mu\nu ab} = \frac{1}{2}(\partial_\mu \omega_{\nu ab} + \omega_{\mu a}{}^c \omega_{\nu cb})\left(\hat{e}^{\mu a}\hat{e}^{\nu b} - \hat{e}^{\mu b}\hat{e}^{\nu a}\right) \approx \\ &\approx -\tfrac{1}{2}\tfrac{q}{m}\partial_\mu\left(\partial_a(A_b u_\nu) - \partial_b(A_a u_\nu)\right)\left(\hat{e}^{\mu a}\hat{e}^{\nu b} - \hat{e}^{\mu b}\hat{e}^{\nu a}\right) + 0 \approx \\ &\approx -\tfrac{q}{m}\partial^a\left(\partial_a(A_b u^b) - \partial_b(A_a u^b)\right) \approx -\tfrac{1}{m}\partial^a\partial_a(A_b j^b) \end{aligned} \tag{6.3.7}$$

where $\partial^a\partial_b(A_a u^b) = 0$ and $j^b := qu^b$ are considered. This scalar curvature density is consistent with the electromagnetism prescription, as it is shown in the following subsection.

6.3.3 Physical prescription

According to the above developments, the electrodynamics equations are obtained by the choice of a potential energy origin, which causes curved geodesics of the *spacetime-particle field*.[8] This subsection is focused on the description of that idea and its consequences in a classical way. Of course, electromagnetism is defined by the abelian subalgebra $\mathfrak{u}(1) \subset \mathfrak{su}(1,3)$. Therefore, the metric perturbation $\phi_\mu{}^a = A^a u_\mu$ is now real, isomorphic to the classical linear perturbation in gravity.

Spacetime-particle geodesics. For classical gravitational interactions, the geodesics generated by a *source energy* do not depend on the energy (inertial mass) of the point object in "free fall". However, the metric perturbed by a gauge potential now differs from that situation, since it depends on the mass m and the charge q of every "test particle", forming a new indivisible entity of *spacetime-particle field*. In other words, the interaction energy (qA) is not the same than the inertial energy (m). In order to ensure continuity in the metric tensor field, g, it is required that all the quantities are intertwined fields (constant or not), that is,

$$g_{\mu\nu}(x) \approx \eta_{\mu\nu} + 2\phi_{\mu\nu}(x) \approx \eta_{\mu\nu} + 2\frac{q(x)}{m(x)}A_\mu(x)u_\nu(x). \tag{6.3.8}$$

where the fields m and q are not constant due to the dependence on the position of the particle fields. The potential vector field, $A(x)$, needs to be the sum of all of the potentials

[8]Notice that it is not possible to geometrize electromagnetism in the same way that Einstein did with gravity because it does not satisfy an equivalence principle. The equations of motion of charged particles cannot be geodesics of the same affine connection because the relationship q/m is not the same for all particles, as is the case in the ratio between inertial mass and gravitational mass [Friedman 1983].

evaluated at x, including the gauge field generated by q and any possible external fields. Under a quantum perspective, the classical limit can be obtained by *expectation values*. See for instance the two-particle interaction detailed as follows.

Two-particle interaction. Let us consider a system with only two (almost) point particles, '1' and '2'. For the particle '1', let q_1 be its electric charge, u_1^α be its 4-velocity, $y = (t, \vec{r}_1) \in \mathbb{R}^4$ is location and A_1 be the vector field caused by it. Analogously, for the particle '2', let q_2 be its electric charge, u_2^α be its 4-velocity, m be its mass, $x = (t, \vec{r}_2)$ be its location, and A_2 be the vector field caused by it, which is assumed to be negligible, i.e., $|A_2| \ll |A_1|$. Therefore, the total vector field, $A(x) \approx A_1(x)$, is essentially external and the metric evaluated at x should be interpreted, on a macroscopic scale, in one of the following two ways,

$$g_{\mu\nu}^{(a)} \approx \eta_{\mu\nu} + 2\phi_{\mu\nu}^{(a)} \approx \eta_{\mu\nu} + 2\frac{q_2}{m}A_1^{(2)}u_{2\mu}u_{2\nu}, \tag{6.3.9}$$

$$g_{\mu\nu}^{(b)} \approx \eta_{\mu\nu} + 2\phi_{\mu\nu}^{(b)} \approx \eta_{\mu\nu} + 2\frac{q_2}{m}A_{1(\mu}u_{2\nu)}m, \tag{6.3.10}$$

where $A_1^{(2)} \approx A_{1\gamma}u_2^\gamma$ and $A_{1(\mu}u_{2\nu)} := (A_{1\mu}u_{2\nu} + u_{2\mu}A_{1\nu})/2 = A_1(u_{1\mu}u_{2\nu} + u_{2\mu}u_{1\nu})/2$ are defined by a scalar function $\zeta(r)$ such that $A_{1\gamma}(r) = q_1u_{1\gamma}\zeta(r)$, and the relative distance $r := \max\{|\vec{r}_1 - \vec{r}_2|, r_m\}$ is measured with respect to a minimum value r_m. By defining the four-currents as $J_{1\nu} := q_1u_{1\nu}$ and $J_{1\nu} := q_2u_{2\nu}$, we can identify the semi-classical perturbation $\Phi_{\alpha\beta}$:

$$g_{\mu\nu}^{(a)} \approx \eta_{\mu\nu} + \tfrac{2}{m}\zeta(r)J_1^\gamma J_{2\gamma}u_{2\mu}u_{2\nu} \approx: \eta_{\mu\nu} + \Phi_{\mu\nu}^{(a)} \Rightarrow \Phi_{\mu\nu}^{(a)} = \tfrac{4\mathrm{G}}{r_m}\zeta(r)J_1^\gamma J_{2\gamma}u_{2\mu}u_{2\nu}, \tag{6.3.11}$$

$$g_{\mu\nu}^{(b)} \approx \eta_{\mu\nu} + \tfrac{2}{m}\zeta(r)J_{1(\mu}J_{2\nu)} \approx: \eta_{\mu\nu} + \Phi_{\mu\nu}^{(b)} \Rightarrow \Phi_{\mu\nu}^{(b)} = \tfrac{4\mathrm{G}}{r_m}\zeta(r)J_{(1\mu}J_{2\nu)}, \tag{6.3.12}$$

where the minimum distance (or spatial gauge) has been chosen in the *event horizon* of the test particle '2', i.e., $r_m := 2\mathrm{G}m$ with $w = 1/3$ (see Eqs. H.1.7 and Eq. H.1.12 of Appendix A). If the retarded potential terms are omitted (this can be done because '1' and '2' are considered as point particles), the scalar function is $\zeta(r) = \mathrm{k}/r$, where $\mathrm{k} = 1/(4\pi)$ is the Coulomb constant with permittivity $\epsilon_0 \equiv 1$ in natural units. Now, one can identify, for instance, Eq. 6.3.12 with

$$\begin{aligned}\Phi_{\mu\nu}^{(b)} &\approx 4\frac{\mathrm{G}}{\mathrm{k}}\zeta_m A_{(1\mu}J_{2\nu)} \approx 4\mathrm{G}\,\zeta_m\frac{J_{(1\mu}J_{2\nu)}}{r} \approx 4\frac{\mathrm{G}}{\mathrm{k}}\frac{\mathrm{k}q_2}{r_m}\frac{kq_1}{r}u_{(1\mu}u_{2\nu)} \\ &\approx 4\frac{\mathrm{G}}{\mathrm{k}}\,A_{(1\mu}\,A_{2\nu)},\end{aligned} \tag{6.3.13}$$

where $\zeta_m := \zeta(r_m) = \mathrm{k}/(2\mathrm{G}m) = 1/(8\pi\mathrm{G}m) = 1/(\kappa m)$, while $A_1 := A_1(r)$ and $A_2 := A_2(r_m) := J_2\zeta_m$, as the reference is at the particle '2'.

6.3.4 Lorentz force and Maxwell equations

Lorentz force. The electric energy perturbation leads to the Lorentz force. To prove this, it is enough to use the linearized gravity (Eq. H.1.9 of Appendix H) and the metric of

Eq. 6.3.9 or Eq. 6.3.10. For both metrics, the Lagrangian functional for a test particle '2' is the same:

$$L \;=\; \frac{m}{2} g_{\alpha\beta} u_2^\alpha u_2^\beta \;\approx\; \frac{m}{2}\eta_{\alpha\beta} u_2^\alpha u_2^\beta + A_1^\gamma q_2 u_{2\gamma}. \tag{6.3.14}$$

The second-order term of the metric is omitted because its effects are negligible for point particles (see Appendix B). By defining the Faraday tensor as $F_{\gamma\alpha} := \partial_\gamma A_{1\alpha} - \partial_\alpha A_{1\gamma}$, the Euler–Lagrange equations (Eq. H.1.10 in Appendix A) are

$$\begin{aligned} \frac{d}{d\tau}\left(m u_{2\alpha} + q_2 A_{1\alpha}\right) - q_2 u_2^\gamma \frac{\partial A_{1\gamma}}{\partial x_2^\alpha} =& \frac{d}{d\tau}\left(m u_{2\alpha}\right) + q_2 u_2^\gamma \frac{\partial A_{1\alpha}}{\partial x_2^\gamma} - q_2 u_2^\gamma \frac{\partial A_{1\gamma}}{\partial x_2^\alpha} \\ =& \frac{d}{d\tau}\left(m u_{2\alpha}\right) + q_2 u_2^\gamma \mathscr{F}_{\gamma\alpha} = 0, \end{aligned} \tag{6.3.15}$$

which is the Lorentz force.

Perturbation sources. The *Source Analysis* (SA) is defined by considering that the total potential field $A(x)$ is generated only by the source '1' at $x = x_1$, i.e., $q(x) = q_1(x)$, $J(x) = J_1(x)$ and $A(x) = A_1(x)$. Nevertheless, classically it may be more interesting to consider the *Interaction Analysis* (IA), with a test particle '2' with $q_2 \ll q_1$ that is moving parallel to '1' (i.e., $u := u_1 = u_2$) to reproduce a stationary frame. For both cases, the metric of Eq. 6.3.11 is equal to Eq. 6.3.12, and the IA recovers the SA when q_2 is replaced by q_1. For instance, let

$$\Phi_{\mu\nu} \equiv \Phi_{\mu\nu}^{(b)} \approx 4\frac{\mathrm{G}}{\mathrm{k}}\zeta_m A_{1\mu} J_{2\nu} = 4\frac{\mathrm{G}}{\mathrm{k}}\zeta_m A_{1\mu} q_2 u_\nu.$$

By using the first-order Einstein field equations (Eq. H.1.3 of Appendix A), we find that

$$\begin{aligned} R_{\mu\nu}^{(1)} \approx 8\pi\left(P_{\mu\nu} - \frac{P}{2} g_{\mu\nu}\right) \;\Longrightarrow\; & -\frac{1}{2}\partial^\gamma\partial_\gamma \Phi_{\mu\nu} \approx 8\pi \mathrm{G}\hat{\rho}_q u_\mu u_\nu \\ \;\Longrightarrow\; & -2\frac{\mathrm{G}}{\mathrm{k}}\zeta_m q_2 \partial^\gamma\partial_\gamma(A_{1\mu} u_\nu) \approx 8\pi\mathrm{G}\hat{\rho}_q u_\mu u_\nu, \end{aligned} \tag{6.3.16}$$

where $w = 1/3$ is required, which corresponds to a perfect fluid, and the total energy density (including pressure effects and omitting retarded terms) equals to

$$\hat{\rho}_q \approx -\frac{\mathrm{d}(J_1^\gamma J_{2\gamma}\zeta_m)}{\mathrm{d}V} \approx -q_2 Q\,\zeta_m, \tag{6.3.17}$$

where the (rest) charge density is given by

$$Q(y) \;:=\; \frac{\mathrm{d}q_1}{\mathrm{d}V} :\approx q_1 \int \frac{\delta^4(y-x)}{\sqrt{-g}}\mathrm{d}\tau.$$

Because the test particle appears in both sides of Eq. 6.3.16, the dependence on $\zeta_m q_2$ vanishes. As expected, by considering the SA instead of the IA, it also vanishes. With this, the Maxwell equations are obtained in Lorentz gauge formulation,:

$$\partial^\gamma\partial_\gamma A_{1\mu} \approx 4\pi k j_\mu, \tag{6.3.18}$$

with $j_\mu := Q\,u_\mu$. Similar results were found first by Monjo 2010 and then by Noskov 2016. Note that the harmonic coordinate condition $\partial^\alpha\Phi_{\alpha\beta} = \frac{1}{2}\eta^{\alpha\gamma}\partial_\beta\Phi_{\alpha\gamma}$ for $\Phi_{\alpha\beta} \approx q_2\zeta_m A u_\alpha u_\beta$ is equivalent to the Lorentz gauge ($\partial^\gamma A_\gamma = 0$) when the four-velocity u^β is applied to both sides of the Eq. 6.3.16, as A is an electrostatic field ($u^\beta\partial_\beta A = 0$) and $0 = \partial^\gamma(u^\beta u_\beta) = 2u^\beta\partial^\gamma u_\beta$. To complete this result, the homogeneous equation $\nabla_{[\alpha}\mathscr{F}_{\beta\gamma]} = \nabla_{[\alpha}\nabla A_{[\beta\gamma]]} = 0$ is easily obtained from the first Bianchi identity, $R^\sigma{}_{[\beta\gamma\delta]} = 0$, by applying the identity $A_\sigma R^\sigma{}_{\beta\gamma\delta} = \nabla_{[\gamma}\nabla_{\delta]}A_\beta$. This is also trivially found by using the 2-form representation of the Faraday tensor ($\mathbf{F} = \frac{1}{2}\mathscr{F}_{\mu\nu}dx^\mu\wedge dx^\nu = \mathrm{d}A$), i.e., $\mathrm{d}\mathbf{F} = 0$, because the second exterior derivative is zero ($\mathrm{d}^2 \equiv 0$).

6.3.5 First-order Lagrangian density

The matter Lagrangian [Harko 2010], $\mathscr{L}_M = -\rho\sqrt{-g}$, where $\rho = I_w^{-1}\hat{\rho}$ is the proper energy, which is related to the effective total energy density. For electromagnetism, one has $\hat{\rho} \approx \hat{\rho}_q = -j_{1\mu}J_2^\mu\zeta_m$, where $j_{1\mu} := Qu_{1\mu}$ is the density of source four-current and $J_{2\mu} := q_2u_{2\mu}$ is a test-particle 4-current. With the first-order Ricci tensor, $R^{(1)}_{\mu\nu} = -\frac{1}{2}\partial_\gamma\partial^\gamma\Phi_{\mu\nu}$, and Eq. 6.3.13, the Einstein–Hilbert Lagrangian density is

$$\begin{aligned}\mathscr{L}[g^{\mu\nu}] =& \sqrt{-g}\left(\frac{g^{\mu\nu}R_{\mu\nu}}{16\pi\mathrm{G}} - \rho\right)\\ \approx& \sqrt{-g}\,g^{\mu\nu}\left(\frac{-1}{8\pi\mathrm{k}}\partial_\gamma\partial^\gamma(\zeta_m A_{(1\mu}J_{2\nu)}) + \frac{1}{2}j_{(1\mu}J_{2\nu)}\zeta_m\right).\end{aligned} \tag{6.3.19}$$

The Euler–Lagrange equations only depend on the fields $g^{\mu\nu}$. Setting the latter equal to zero and contracting with respect to the velocity of the test particle u_2^ν, we conclude that

$$\frac{1}{4\pi\mathrm{k}}\partial_\gamma\partial^\gamma(A_{(1\mu}J_{2\nu)}) = j_{(1\mu}J_{2\nu)} \implies \partial_\gamma\partial^\gamma A_{1\mu} = 4\pi\mathrm{k}j_{1\mu},$$

as expected. Observe that the electromagnetism is formulated as a particular case of Coloured Gravity.

6.3.6 Charge-energy and source-gravity relationships

The integration of Eq. 6.3.17 leads to an electrical energy potential with the origin in r_m, which is calculated by the displacement of a test particle '2' between r_m and r, both in a stationary reference system. In other words, the electrical energy suffered by '2' (since we take r_m in '2') is

$$m_q(r) :\approx J_1^\alpha J_{2\alpha}\Delta\zeta(r) + O(\partial\zeta^2) = J_1^\alpha\Delta A_{2\alpha}(r) + O((\partial A_2)^2), \tag{6.3.20}$$

where $\Delta A_2^\alpha(r) := J_2^\alpha(\zeta(r) - \zeta(r_m))$ is the hypothetical electromagnetic 4-potential of '2'. The possible second order term, $O((\partial A_2)^2)$, is an electromagnetic self-energy of the particle '2' (e.g., from the Faraday tensor, $F^{\mu\alpha}F^\nu{}_\alpha - \frac{1}{4}\eta^{\mu\nu}F_{\alpha\beta}F^{\alpha\beta}$). By comparing to the

limit case of the semi-classical gravity perturbation with $w = 1/3$, $\Phi^{(a)}_{\alpha\beta} = 4\phi(r)u_\alpha u_\alpha$, it is easy to identify an approach for the gravitational potential:

$$\phi(r) \approx \frac{\mathrm{G}J_1^\gamma J_{2\gamma}\zeta_m}{r} = \frac{\mathrm{G}}{\mathrm{k}}A_{1\mu}J_2^\mu\zeta_m = \frac{\mathrm{G}}{\mathrm{k}}A_\mu(r)J^\mu(r)\zeta_m, \tag{6.3.21}$$

where $A_\mu(r)$ and $J^\mu(r)$ are the total potential field vector and the 4-current, respectively, evaluated at r. In the SA case, it is found that $\phi(r) = r_q^2/(r_m r)$, where $r_q^2 := \mathrm{G}\,\mathrm{k}q^2$ is the characteristic length scale of the Reissner–Nordström metric, whose electromagnetic term is $\phi(r) = r_q^2/r^2$ [Giorgi 2019]. To make compatible both metrics, it is necessary to use the (Kerr–Schild) double-copy solution, i.e.,

$$\Phi_{\mu\nu}(r) = 4\phi(r)u_\mu u_\nu \sim -2\frac{\mathrm{G}}{\mathrm{k}}\hat{A}_\mu\hat{A}_\nu = -\kappa\hat{A}_\mu\hat{A}_\nu,$$

where $\hat{A}_\mu := \Delta A_\mu = A_\mu(r) - A_\mu(r_m)$. Note that the residual constant is omitted.

Consistently with the linearized gravity (Eq. H.1.12 of Appendix H), the electric-based perturbation energy suffered by '2' is also $m_q \approx mI_w\Delta\phi(r) = mI_w(\phi(r) - \phi(r_m))$ when $\phi(r)$ is predominantly of electrical origin (Eq. 6.3.21 and Eq H.1.12 of Appendix H). Setting it equal to Eq. 6.3.20, one can easily check that

$$m_q(r) \;\approx\; J_1^\alpha\Delta A_{2\alpha}(r) \;\approx\; mI_w(\phi(r) - \phi(r_m)). \tag{6.3.22}$$

Because the origin is at the test particle ($r_m = 2\mathrm{G}m$), the total potential energy ($r \to \infty$) of Eq. 6.3.22 represents the total *source energy* with $w = 1/3$, i.e., $m_q(\infty) = -J_1^\alpha J_{2\alpha}\zeta_m = -q_1q_2\zeta_m = -q_1q_2/(\kappa m) < 0$. For instance, supposing that the self energy of a q-charged particle is $m_q(\infty) = m$, it follows that

$$\kappa\, m^2 = -q^2\,. \tag{6.3.23}$$

Therefore, in order to translate some semi-classical results between gravity and electromagnetism, it is useful to define the application:

$$\begin{aligned} \mathcal{T} :&\mathbb{R}\cdot\mathscr{Q} \;\to i\mathbb{R} \\ &C\cdot q \;\mapsto \mathcal{T}(C\cdot q) := C\cdot\mathcal{T}(q) := C\cdot i\sqrt{\frac{2\mathrm{G}}{\mathrm{k}}}\,m = C\cdot i\sqrt{\kappa}\,m, \end{aligned} \tag{6.3.24}$$

where $\mathscr{Q}$ is the space of the coupling constants, $\mathrm{k} = 1/4\pi$ and $\kappa = 8\pi\mathrm{G}$, while q and m are the charge and the mass, respectively, of a point particle in natural units ($1 = c = \hbar = \epsilon_0$). Thanks to this transformation, Eq. 6.3.21 recovers the classical gravitational field, $\phi(r) = -\mathrm{G}m/r < 0$, which is a (simple) *gravity spacetime* perturbation. In fact, the equivalent energy perturbation for the SA case (with $J^\gamma := J_1^\gamma = J_2^\gamma$) is the equivalence $\mathcal{T}(m_q(\infty)) = \mathcal{T}(-q^2\zeta_m) = m$, and Eq. 6.3.11 leads to the linearized gravity with $w = 1/3$.

An important outcome is that the *source energy* is negative when the total integral is taken into account ($m_q(\infty) = -J^\gamma J_\gamma\zeta_m = -q^2\zeta_m < 0$ for the SA). To obtain positive

energy (mass) it is necessary to combine electric charges with different signs and make quantum-electrodynamic corrections. The (effective) electrical neutrality of the matter (sources) is key to understand the obtaining of an effective positive energy.

The classical gravity interaction can be understood as a sum of the effects provided by the (effective) energy interactions of the *coloured gravity*, which could include all the other interactions (source effects). As a drawback, the proposed semi-classical theory cannot predict fundamental parameters, e.g., the Coulomb or the fine-structure constants. However, the double-copy solution of the perturbed metric could provide relevant information on fundamental interaction, and higher-order corrections can be analyzed in future works.

To extend the spacetime algebra to a cosmological scale, the proposed methodology can be applied to the hyperconical model of Monjo (e.g. Monjo 2017, Monjo 2018, Monjo and Campoamor-Stursberg 2020) by using either nonlocal or asymptotic symmetries [Krasnikov 2021, Fabbrichesi *et al.* 2021]. This is a key at cosmological scales because the hyperconical model explains *dark quantities* but it does not produce photons by itself, since it establishes a 'zero active' energy [Monjo 2023, Monjo and Campoamor-Stursberg 2023].

Chapter 7

Conclusions

7.1 On the hypotheses

This Thesis was developed on the basis of three hypotheses: I) Spacetime manifold is inertial; II) Spacetime manifold is responsible for its dynamics, and III) the dynamics of nature is metrically determined.

According to the first hypothesis ('on inertia'), this dissertation proved that our natural spacetime manifold presents inertial (linear) dynamics in the absence of external fields, as it is inherited from an ambient manifold.

Therefore, the second hypothesis ('on natural dynamics') was automatically satisfied, because the ambient spacetime determines the dynamics of observers (moving frames) that live inside. Moreover, Hamiltonian/Lagrangian equations, showed that the hyperconical manifold produces consistent dynamics if the curvature is $k = 1$, which is also consistent with the local (spatial) flatness condition. From this finding, adequate Lagrangian equations also determine that the manifold curvature is independent of the matter content.

Regarding the third hypothesis ('on metric-based nature'), the work proved that local perturbations of the metric can be generalized to squared $SU(1,3)$ generators. This implies that gauge-based interactions of the nature (electromagnetism, weak and strong forces) could be expressed in terms of an extension of the geodesic lines in a spacetime-particle field. Our ambitious objective has been only partially addressed in the last Chapter, focused on the electromagnetic acceleration (Lorentz force).

7.2 On manifold dynamics

7.2.1 Curvature of the universe

A dynamical embedding technique is used in this Thesis to derive a spacetime manifold in a natural way under a flat five-dimensional Minkowskian space. The most simple case is based on inertial or linear expansion (hypercone) of a manifold, with a priori positive, null or negative curvature k, where observer frames are comoving to the inertial expansion of the spacetime.

Thus, the hyperconical metric tensor is obtained by assuming that the spacetime expands independently of its matter content. For instance, one can suppose that any observer is placed on either a 3-spheroid or 3-hyperboloid with radial expansion (4-hypercone). The key idea is that the proper time of each observer is preserved, and thus fixes an initial reference time, even though its position varies in time due to the expansion.

A remarkable feature of the hyperconical model is that reference transformation leads to a radial inhomogeneity assimilable (i.e. projected) to a fictitious acceleration (i.e., it predicts an apparent dark energy). For the particular case of $k = 1$, the hyperconical universe has a (Ricci) scalar curvature that is locally equivalent to a flat-space FLRW case, and dark energy is very close to the standard estimation.

The Lagrangian analysis for the proposed model is in agreement with the observations. The comoving trajectories are solutions of the Euler-Lagrange equations, corresponding

to the trivial case with stationary linear expansion. Moreover, the Hamiltonian ADM equations showed that the Lagrangian density of the model needs a vacuum energy term and a positive curvature of ($k = 1$) to ensure that the evolution of the metric is consistent at a local scale. This is coherent with the best prediction of dark energy density, also found for $k = 1$.

In other words, the symplectic geometry of Lorentzian manifolds shows that it is not possible to consistently build an infinite spacetime with finite time by keeping the basic principle of unprivileged places (e.g. Big Bang point). As a result, the model fits the observations better than the standard model and it explains current problems such as the Hubble tension, the origin of dark energy, galaxy dynamics and evolution, among others. Therefore, as a consequence of this natural manner of deriving a cosmology, we found that spacetime is closed (finite). Under minimally singular dynamics of manifolds, the finite light speed determines a finite space as time is finite too.

7.2.2 Local symmetries

This Thesis also explored symmetry properties of the inhomogeneous hyperconical universes according to affine transformations such as displacements and rotations.

By using Killing vectors, it is shown that the angular rotations are global symmetries, while spatial translations are merely local symmetries. The corresponding preserved linear momentum presents a scaling factor $a(t)$, as expected. Finally, the three Lorentz boosts are also local symmetries (for the ordinary orthogonal frame).

For the most of the analyzed cases, the symmetric properties refer to the local case and assuming that the parameter k is globally homogeneous (leading to a radial inhomogeneous metric). That is, the proposed model should be understood as an alternative model to be analyzed in greater depth, adding corrections from higher order terms or other approximations.

It is observed that gauge Noether symmetries are potentially relevant in the analysis of the field equations in the linearly expanding system. Whether the related conservation currents derived from this approach provide an additional insight into the interpretation of the Hubble parameter compatible with observational data is still an open question. For instance, radial inhomogeneity of the metric can be interpreted as a fictitious acceleration, which breaks all the non-rotational local symmetries at large distances.

7.2.3 Fictitious acceleration

From the hypothesis of a linearly expanding hypersphere (hypercone), 'lapse' and 'shift' terms of the metric are produced by the comoving frames, which equals an effective radial inhomogeneity that approaches to the flat FLRW metric at a local scale (Section 2.3.3). Notice that radial inhomogeneity is similar to a fictitious acceleration, but only as the accelerated spacetime is considered a constant picture.

Specifically, there exists a unique local projection that transforms the extrinsic hypercone to the ΛCDM model showing the same acceleration for all times, independently of

the age t of the universe (Section 2.5), since it is the unique possibility to obtain a Hubble $H = 1/t$. To show the viability of this idea, we found third-order approximate solutions, where these values of dark energy and dark matter are predicted.

The (intrinsic) proper distance obtained from the standard model could be interpreted as a locally conformal projection of the comoving distance of the (extrinsic) hyperconical universe. This projection causes a distortion that would provide the origin of the dark energy linked to the cosmological constant. Particularly, imposing equality up to third order, dark energy and matter densities are about $\Omega_\Lambda \approx 0.7$ and $\Omega_m \approx 0.3$, respectively. At least locally, this is equivalent to a hypothetical compensation of the matter effect (deceleration) by a dark energy effect (acceleration), like a zero-active gravitational mass. Consistently, there is a mathematically compatibility between the expansion explained under the standard model and the view of the hyperconical model.

The stronger competitor of the standard model is a linearly expanding model, the so-called $R_h = ct$ model. Apparently, the flat standard accelerated and linear-expanding $R_h = ct$ universes are incompatible. However, the hyperconical model provides a bridge to connect both perspectives: i) the extrinsically homogeneous linearly expanding hypercone equivalent to the $R_h = ct$ model at every point and ii) the intrinsically apparently accelerated flat ΛCDM. These perspectives explain the Hubble tension found when model-independent (purely geometrical) measurements are compared with model-dependent observations. Schematically, the two different perspectives can be summarized as follows:

$$\text{Hyperconical model (closed, linear \& homogeneous)} \Rightarrow \begin{cases} \text{Local extrinsic viewpoint} \equiv R_h = ct \text{ metric (flat, linear \& homogeneous)} \\ \text{Local intrinsic viewpoint} \equiv \text{Radial inhom. metric (closed, linear \& inhomogeneous)} \equiv \text{Apparent ΛCDM model (flat, “accelerated” \& homogeneous) + MOND} \end{cases}$$

In sum, the hyperconical universe is extrinsically closed (curvature $k \equiv k_{hyp} = 1$), with a radius equal to the age t of the universe, expanding as light speed (i.e., $a = t/t_0$) and with a locally flat spatial curvature ($k_{hyp} = 1 \Leftrightarrow K_{FLRW} = 0$), as required in the $R_h = ct$ model. More specifically, the Ricci scalar curvature is equal to that obtained for a flat FLRW metric with linear expansion.

7.2.4 Practical applicability

Currently, standard cosmology presents a list of problems that are difficult to solve without the addition of new parameters that could lead to overfitting effects. Among others, the list includes incompatible estimations of the Hubble parameter ('Hubble tension'), a universe density that is practically equal to the critical density ('flatness problem') and a dark matter estimated in CMB Planck mission that is excessive and/or inconsistent with estimations from galaxies. This subsection summarizes the fact that most of the issues raised can be solved by modifying the initial hypothesis to derive the universe (FLRW) metric.

Particularly, we developed a mathematical prescription to derive the spacetime manifold $(\mathbb{R}^4, g)$ by dynamical embedding of it into a higher-dimensional space $(\mathbb{R}^5, \eta)$ with the Minkowskian metric η. To determine possible solutions at an early stage, we first assumed the most simple case, which was sufficient: a **homogeneous finite object with linear expansion**. For instance, a hypersphere S^3_t was considered with a radius equal to the age $t \in \mathbb{R}_{\geq 0}$ of the universe, embedded into the Cartesian product of its time $(\mathbb{R}_{\geq 0})$ and its purely four-dimensional space $\mathbb{R}^4$, that is a hyperconical object $\mathcal{H}^4 := S^3_{\mathbb{R}_{\geq 0}} \subset \mathbb{R}_{\geq 0} \times \mathbb{R}^5$. By applying a time transformation of the moving frames, a radially inhomogeneous and closed universe $(\mathcal{H}^4)$ is obtained for a given observer, it is possible to model the above-mentioned cosmological problems.

To attain our goal, two remarks were considered: a) the spatial section (shape) of our universe manifold does not depend on matter content, and b) there exists a locally conformal projection that assimilates the curvature as an acceleration. This equivalence was tested by parametric families of stereographic projections according to local and global approaches. The result is a Hubble expansion law compatible with the SH0ES estimations, under the extrinsic viewpoint; and another Hubble parameter compatible with the ΛCDM model up to third order of series expansion, under an intrinsic viewpoint. Therefore, it is proposed that Hubble tension can be explained as an effect of both geometrical perspectives: On the one hand, compared to the Plank Legacy estimation of $h_0 = 67.4 \pm 0.5$ [Aghanim *et al.* 2020b], our intrinsic ΛCDM-based compatibility leads to a Hubble parameter between 66.38 and 68.87 by using the universe age estimate $(13.80 \cdot 10^9$ years) as a necessary parameter. On the other hand, with ΛCDM-independent observations (e.g. very-low-metallicity stars and galactic globular clusters), the extrinsic viewpoint of our model predicts a Hubble parameter between 73 and 74, which is compatible with the value of $h_0 = 73.30 \pm 1.04$, estimated with the distance ladder method applied to the Cepheid-SNe sample. The explanation of why the distance ladder is extrinsic is that the technique propagates the 'local scale' to larger scales through a chain of correlated and overlapped methods, bridging the contrast produced by the distorted stereographic projection (intrinsic viewpoint) and therefore leading to practically unprojected measurements.

If galaxies are taken into account (e.g. cosmic chronometers and radial BAO size methods), the extrinsic viewpoint underestimates the Hubble parameter at local scales ($h_0 < 65$ at $z < 0.5$) but it is compatible with the intrinsic modelling at larger scales

($h_0 \approx 70$ at $z > 1$).

Collaterally, the fitted values of cosmological parameters are interpreted as apparent density values, different to the real matter contents (baryons and radiation). That is, apparent dark quantities (energy and matter) emerged from the proposed model without considering any kind of matter content. Particularly, dark energy densities (Ω_Λ) between $\frac{2}{3} \approx 0.667$ and $\frac{13}{18} \approx 0.722$ emerge when curvature is set to zero ($\Omega_K = 0$) or is freely nonzero ($\Omega_K = -1/18 \approx -0.055$), while third-order model-compatibility leads to the following values: $\Omega_\Lambda = 0.708 \pm 0.005$ and $\Omega_K = -0.012 \pm 0.003$.

7.3 On object dynamics

7.3.1 Fictitious accelerations

As dark energy can be interpreted as a geometrical consequence of the distorting stereographic projection, dark matter can also be modelled by the same projection, and it is enough to use the first-order perturbation approach. To build the proposed model, two additional ingredients are required: (1) massive objects are defined as perturbations of the vacuum energy density, and (2) centrifugal force has an extra orthogonal contribution due to the curvature radius t of the Universe. This corresponds to a time-like component in the total centrifugal force, whose squared modulus is proportional to fourth power of the speed (v^4), and the term $r/(\gamma_0 ct)$ of the distorted projection contributed to it, where r is the radial spatial distance, γ_0 is a distorting parameter and c is the speed of light. Thus, the distorting stereographic projection contributes to deep MOND behaviour with the acceleration c/t divided into the projected angle γ_0.

7.3.2 Practical applicability

Using SPARC data, the proposed fictitious force explains the mass discrepancy (M/M_b) slightly better ($\sim 1\%$) than the BTFR empirical fitting ($RMAE = 0.115$ and $R^2 = 0.91$ versus $RMAE = 0.108$ and $R^2 = 0.92$, respectively) and also better for galaxy rotation curves ($RMAE = 0.080$ and $R^2 = 0.953$ versus $RMAE = 0.070$ and $R^2 = 0.957$, respectively), even considering a unique parameter. Furthermore, the new model explains the transition between the Newtonian and cosmological scales in a natural way. Therefore, the proposed theoretical framework is a candidate for the relativistic formulation of MOND behaviour [Banik and Zhao 2022, Monjo 2023].

It is remarkable that our goal is achieved by employing two key points (the mass of perturbations and the centrifugal force) but with a minimal change of the Lagrangian density of the GR. The proposal is adapting the background metric to the hyperconical universe, since its scalar curvature is equal to the vacuum energy density. Specifically, under the first-order perturbation approach, our proposal of linearized modified gravity is given by $h_{\mu\nu} :\approx g_{\mu\nu} - g^{back}_{\mu\nu}$ where $g_{\mu\nu}$ is the perturbed hyperconical metric and $g^{back}_{\mu\nu}$ is the background metric of the universe, which replaces the usual flat 4D Minkowskian metric $\eta = \mathrm{diag}(1, -1, -1, -1)$. This linearisation is equivalent to saying that the matter content

does not affect the shape of the universe but locally perturbs the metric. That is the Lagrangian density of the matter (e.g. $\mathscr{L}_m = \rho$) is linked to the difference $\Delta R = R - R_u$ between total Ricci scalar and the universe's Ricci scalar $R_u \approx -6/t^2$. On the other hand, the distorted stereographic projection is a key to recovers deep MOND regimes under the hyperconical model. Particularly, the resulting new coordinates experience a fictitious acceleration like the one modelled by MOND theories.

Further work could analyze possible observations related to the predicted anomalous accelerations in the solar system of about $10^{-11}\mathrm{m/s^2}$, according to the theoretical framework developed in this Thesis. Particularly, it is possible that residual unexplained accelerations (about 10%) of the Pioneer 10 and 11 spacecrafts (or of other objects) are due to the time-like contribution of centrifugal force in the hyperconical universe. Thus, the present work is a candidate for a more precise theory of GR, and it would be useful to better estimate the Newtonian constant of gravity. Finally, connections between the proposed model and Melia's $R_h = ct$ universe could be deeply explored, especially concerning the role of 'zero active mass' in the theory developed [Melia 2018].

7.4 On particle dynamics

7.4.1 Recipe for a quantum gravity

The 'moving frame theory' developed for particle fields (spinors) was based on perturbed tetrads and spacetime generators with a covariant Wilson-line term (in the Lorentz gauge) representing the modified ground state of the spacetime generators according to the observer's frame of reference.

The introduction of that small perturbation to the local coordinates formulates gauge interaction phenomena for SU(1, 3) Yang–Mills dynamics. In particular, unitary (gauge) transformations of local phases are equivalent to the change of reference system from local coordinates to the observer's reference frame. In fact, the translation-gauge covariant derivative is set to coincide with the SU(1, 3)-gauge covariant derivative, and the transformation can be simplified as a change of the reference frame (like a choice of the gauge potential origin).

As a general output for SU(1, 3) interactions, the metric depends on the field features (coupling factors) at each position. To ensure continuity in the metric tensor field, the coupling factors should also be fields, and it is forbidden that two different features, e.g., two masses, are at the same 4-position (this is similar to the Pauli exclusion principle in fermionic statistics). In fact, SU(1, 3) can be formulated from the complexified perturbations of the Clifford–Dirac algebra and, therefore, the results of this Thesis could provide basic ideas for a future *quantum coloured gravity*.

7.4.2 Fictitious acceleration

From Eq. 5.3.1 and applying *geodesic equations*[1], the zero covariant acceleration provides a 'fictitious' force that, for electromagnetism (Eq. 6.3.5 and 6.3.15), coincides with the Lorentz force (see Section 6.3.4). We expect that it is possible to generalize very similar results for SU(1, 3)-Yang-Mills fields, with the difference that non-abelian fields should produce interactions for shorter distances, as it is observed and modelled by quantum chromodinamics and quantum electroweak interactions. Further works will explore these interesting possibilities.

7.4.3 Practical applicability

As a particular limit, the classical electromagnetism with Lorentz force and Maxwell equations is recovered from the Einstein Field Equations by using the perturbed tetrad. On a macroscopic scale, it is equivalent to set a spatial gauge, r_m, for the energy origin in the electric 4-potential field. This origin is set in the event horizon of each test particle with energy m and the equation of state $w = 1/3$, i.e., $r_m = 2\mathrm{G}m$.

In this context, spacetime would present continuous rough fields given by the small gauge-based perturbations (linked to the coupling constants and the particle quantum numbers). Moreover, the torsion of the developed metric ($g \sim \eta + A \otimes A$) can be interpreted with the picture of a spacetime with a double-helix-like structure based on pairs $A \otimes A$ of entangled virtual $\mathfrak{su}(1, 3)$ bosons (e.g. photons). These potential fields are the connection (force carrier or virtual-particle exchange) of a double-copy gauge transformation, generated by an extended Poincaré algebra, $\mathbb{R}^{1,3} \oplus \mathfrak{u}(1, 3)$.

[1] Of course, they are not classical geodesic equations of spacetime metric, but they are geodesics of *spacetime-particle* fields.

References

Bibliography

[Abedi and Salti 2015] *Gen. Rel. Grav.* **47** 93 https://doi.org/10.1007/s10714-015-1935-z

[Acedo 2020] *J. High Energy Phys.* **6** 209.https://doi.org/10.3390/universe6110209

[Achour *et al.* 2016] *J. High Energy Phys.* **2016** 100. https://doi.org/10.1007/JHEP12%282016%29100

[Akbar 2017] *Phys. Rev. D* **2017** 95, 064058 https://doi/10.1103/PhysRevD.95.064058

[Adam *et al.* 2015] *Astron. Astrophys* **594** A8 https://doi.org/10.1051/0004-6361/201525820

[Adamek *et al.* 2020] *Class. Quantum Grav.* **37** 154001 https://doi.org/10.1088/1361-6382/ab939b

[Ade *et al.* 2016] Planck 2015 results. XIII. Cosmological parameters *Astron. Astrophys.* **596** A13 https://doi.org/10.1051/0004-6361/201525830

[Aghanim *et al.* 2020a] Planck 2018 results. V. CMB power *Astron. Astrophys.* **641** A5 https://doi.org/10.1051/0004-6361/201936386

[Aghanim *et al.* 2020b] Planck 2018 results. VI. Cosmological parameters *Astron. Astrophys.* **641** A6 https://doi.org/10.1051/0004-6361/201833910

[Aguirre *et al.* 2001] *Astrophys. J.* **561** 550–558 https://doi.org/10.1086/323376

[Aldrovandi *et al.* 2006] *AIP Conference Proceedings* **810** 217 https://doi.org/10.1063/1.2158724

[Alfonsi *et al.* 2020] *J. High Energ. Phys.* **2020** 91 https://doi.org/10.1007/JHEP07(2020)091

[Almeida 2003] *arXiv:math/***0307165** https://doi.org/10.48550/arXiv.math/0307165

[Anastasiou *et al.* 2017] *Phys. Rev. D* **96** 026013 https://doi.org/10.1103/physrevd.96.026013

[Anderson *et al.* 2006] Anderson L B, and Wheeler J T 2006 Yang–Mills gravity in biconformal space. *Class. Quantum Grav.* **24**, 475-495 https://doi.org/10.1088/0264-9381/24/2/012

[Angus *et al.* 2006] *Mon. Not. R. Astron. Soc.* **371** 138–146 https://doi.org/10.1111/j.1365-2966.2006.10668.x

[Arcos *et al.* 2004] Arcos H I, de Andrade VC and Pereira JG 2004 Torsion and gravitation: a new view. *Int. J. Mod. Phys. D* **13** 807 https://doi.org/10.1142/S0218271804003858

[Ardi and Baumgardt 2020] *J. Phys.: Conf. Ser.* **1503** 012023 https://doi.org/10.1088/1742-6596/1503/1/012023

[Arnowitt *et al.* 1959] *Physical Review.* **116** (1959) 1322–1330 https://doi.org/10.1103/PhysRev.116.1322

[Arnowitt *et al.* 2008] *Gen. Relelativ. Gravit.* **40** (2008) 1997–2027

[Asencio *et al.* 2022] matter *Mon. Not. R. Astron. Soc.* **515** 2981–3013 https://doi.org/10.1093/mnras/stac1765

[Asgari *et al.* 2021] *Astron. Astrophys.* **645** A104, https://doi.org/10.1051/0004-6361/202039070

[Ashtekar *et al.* 2014] *ArXiv*:**1408.4336** https://doi.org/10.48550/arXiv.1408.4336

[Avelino and Kirshner 2016] *Astrophys. J.* **828** 35 https://doi.org/10.3847/0004-637X/828/1/35

[Badía-Majós *et al.* 2006] *J. Phys. A: Math. Gen.* **39** 14699-14726 https://doi.org/10.1088/0305-4470/39/47/013

[Bahamonde *et al.* 2023] *Rep. Prog. Phys.* **86**, 026901 https://doi.org/10.1088/1361-6633/ac9cef

[Bakopoulos and Kanti 2014] *Gen. Relativ. Gravit.* **46** 1742 https://doi.org/10.1007/s10714-014-1742-y

[Banik and Zhao 2022] *Symmetry* **14** 1331 https://doi.org/10.3390/sym14071331

[Barbieri and Tesi 2018] *Eur. Phys. J. C***78** 193 https://doi.org/10.1140/epjc/s10052-018-5680-9

[Barkana 2018] *Nature* **555** 71–74 https://doi.org/10.1038/nature25791

[Beck and Sarkis 2023] *Phys. Rev. D* **107**, 023006 https://doi.org/10.1103/PhysRevD.107.023006

[Becker *et al.* 2007] *String theory and M-theory: A modern introduction.* Cambridge University Press. ISBN 978-0-521-86069-7. https://nucleares.unam.mx/~alberto/apuntes/bbs.pdf

[Bekenstein 2004] *Phys. Rev. D* **70** 083509 https://doi.org/10.1103/PhysRevD.70.083509

[Bekenstein and Milgrom 1984] *Astrophys. J.* **286** 7 https://ui.adsabs.harvard.edu/abs/1984ApJ...286....7B/abstract

[Beltracchi and Gondolo 2019] *Phys. Rev. D* **99** 084021

[Benisty and Staicova 2021] *Astron. Atrophys.* **647** A38 https://doi.org/10.1051/0004-6361/202039502

[Benoit-Lévy and Chardin 2012] *Astron. Astrophys.* **537** id.A78 https://doi.org/10.1051/0004-6361/201016103

[Bern *et al.* 2010a] *Phys. Rev. D* **82** 065003 https://doi.org/10.1103/physrevd.82.065003

[Bern *et al.* 2010b] *Phys. Rev. Lett.* **105** 061602 https://doi.org/10.1103/PhysRevLett.105.061602

[Bhattacharya *et al.* 2013] *Astrophysical J* **766** 32 https://doi.org/10.1088/0004-637X/766/1/32

[Blake *et al.* 2012] *Mon. Not. R. Astron. Soc.* **425** 405–414 https://doi.org/10.1111/j.1365-2966.2012.21473.x

[Blanchet 2007] *Class. Quantum Grav.* **24** 3529 https://doi.org/10.1088/0264-9381/24/14/001

[Blum and Furlan 2022] *How John Wheeler Lost His Faith in the Law.* In: Ben-Menahem, Y. (eds) Rethinking the Concept of Law of Nature. Jerusalem Studies in Philosophy and History of Science. Springer, Cham. https://doi.org/10.1007/978-3-030-96775-8_11 Arxiv: https://arxiv.org/abs/2206.14664

[Bonning *et al.* 2003] *Phys. Rev. D* **68** 044019 https://doi.org/10.1103/PhysRevD.68.044019

[Borghi *et al.* 2022] *Astrophys. J. Lett.* **928** L4 https://doi.org/10.3847/2041-8213/ac3fb2

[Borsten 2020] *La Rivista del Nuovo Cimento* **43** 97-186 https://doi.org/10.1007/s40766-020-00003-6

[Borsten and Duff 2015] *Physica Scripta* **90** 108012 https://doi.org/10.1088/0031-8949/90/10/108012

[Brax 2013] *Class. Quantum Grav.* **30** 214005 https://doi.org/10.1088/0264-9381/30/21/214005

[Brown 1993] *Class. Quantum Grav.* **10** 1579-1606 https://doi.org/10.1088/0264-9381/10/8/017

[Brown and Mathur 2023] *Astrophys. J.* **166** 168 https://doi.org/10.3847/1538-3881/acef1e

[Brownstein and Moffat 2006] *Class. Quantum Grav.* **23** 3427 https://doi.org/10.1088/0264-9381/23/10/013

[Buchert *et al.* 2006] *Class. Quantum Grav.* **23** 6379–6408. https://doi.org/10.1088/0264-9381/23/22/018

[Buchert *et al.* 2020] *Gen. Relativ. Gravit.* **52** https://doi.org/10.1007/s10714-020-02670-6

[Burns 1976] *Am. J. Phys.* **44**, 944-949 https://doi.org/10.1119/1.10237 https://doi.org/10.1119/1.10237

[Cai *et al.* 2016] *Rept. Prog. Phys.* **79**, 106901 https://doi.org/10.1088/0034-4885/79/10/106901

[Camarena *et al.* 2022] Camarena D. et al 2022. A void in the Hubble tension? The end of the line for the Hubble bubble.*Class. Quantum Grav.* **39** 184001 https://doi.org/10.1088/1361-6382/ac8635

[Cao *et al.* 2021] *Mon. Not. Roy. Astron. Soc.* **504** 300–310 https://doi.org/10.1093/mnras/stab942

[Capozziello *et al.* 2009] *Physica Scripta* **79** 025901 https://doi.org/10.1088/0031-8949/79/02/025901

[Capistrano *et al.* 2022] *arXiv:2009.02167* https://doi.org/10.48550/arXiv.2009.0216

[Capozziello *et al.* 2022] *Eur. Phys. J. C* **82**865 https://doi.org/10.1140/epjc/s10052-022-10823-x

[Cembranos and Diez-Valle 2019] *arXiv*:**1903.03209** https://doi.org/https://doi.org/10.48550/arXiv.1903.03209

[Chae *et al.* 2020] textitAstrophys. J. **904** 51 https://doi.org/10.3847/1538-4357/abbb96

[Chae 2022] *Astrophys. J.* **941** 55 https://doi.org/10.3847/1538-4357/ac93fc

[Chae 2023] *Astrophys. J.* **952** 128 https://doi.org/10.3847/1538-4357/ace101

[Chae 2024] *Astrophys. J.* **960** 114 https://doi.org/10.3847/1538-4357/ad0ed5

[Chardin *et al.* 2021] *Astron. Astrophys.* **652** A91 https://doi.org/10.1051/0004-6361/202140575

[Chatterjee *et al.* 2017] *J Cosmol. Astropart. Phys.* **2017** 062-062 https://doi.org/10.1088/1475-7516/2017/01/062

[Chen *et al.* 2015] *Commun. Math. Phys.* **338** 31–80 https://doi.org/10.1007/s00220-015-2381-1

[Ciufolini *et al.* 2019] *Sci Rep* **9** 15881 https://doi.org/10.1038/s41598-019-52183-9

[Clifford 1876] *Proceedings of the Cambridge Philosophical Society* **2** 157–158 https://archive.org/details/proceedingscamb06socigoog/page/n175/mode/2up?view=theater

[Clifton et al. 2012] Clifton T *et al.* 2012, Phys. Rep. **513**, 1-189 https://doi.org/10.1016/j.physrep.2012.01.001

[Clowe *et al.* 2006] *Astrophys. J, Lett* **648** L109-L113 https://doi.org/10.1086/508162

[Comeron *et al.* 2023] *Astrophys. Astron.* **675** A143 https://doi.org/10.1051/0004-6361/202346291

[Cossu *et al.* 2019] *Eur. Phys. J. C* **79** 638. https://doi.org/10.1140/epjc/s10052-019-7137-1

[Courant and Hilbert 1989] *Methods of Mathematical Physics* **Vol. I** (First English ed.). New York: Interscience Publishers and Wiley ISBN 978-0471504474. https://doi.org/10.1002/9783527617210 (pdf available)

[Crater *et al.* 2011] *Eur. Phys. J. Plus* **126** 16 https://doi.org/10.1140/epjp/i2011-11016-x

[Cuceu *et al.* 2019] *J Cosmol. Astropart. Phys.* **10** 044 https://10.1088/1475-7516/2019/10/044

[Dam *et al.* 2017] *Mon. Not. R. Astron Soc.* **472** 835–851 https://doi.org/10.1093/mnras/stx1858

[de Andrade and Pereira 1997] *Phys.Rev.D* **56** 4689-4695

[de Andrade *et al.* 2000] arXiv:gr-qc/0011087 https://doi.org/10.48550/arXiv.gr-qc/0011087

[deBlok *et al.* 2008] *Atrophys. J.* **136** https://doi.org/10.1088/0004-6256/136/6/2648

[Delubac *et al.* 2015] *Astron. Astrophys* **574** A59 https://doi.org/10.1051/0004-6361/201423969

[Deruelle *et al.* 2010] *Prog. Theor. Phys.* **123** 169-185 https://doi.org/10.1143/PTP.123.169

[Di Cintio and Lelli 2016] *Mon. Not. R. Astron. Soc. Lett.* **456** L127-L131 https://doi.org/10.1093/mnrasl/slv185

[Di Valentino *et al.* 2021] *Class. Quantum Grav.* **38** 153001 https://doi.org/10.1088/1361-6382/ac086d

[Dittus and Lämmerzahl 2007] *Advances in Space Research* **39** 244-248 https://doi.org/10.1016/j.asr.2004.09.027

[DiValentino *et al.* 2020] *Nat. Astron.* **4** 196–203. https://doi.org/10.1038/s41550-019-0906-9

[Dressel *et al.* 2015] *Physics Reports* **589** 1-71 https://doi.org/10.1016/j.physrep.2015.06.001

[Eardley 1986] *Commun. Math. Phys.* **106** 137–158 https://doi.org/10.1007/BF01210929

[Eddington 1921] *Nature* **106** 802-804 https://doi.org/10.1038/106802a0

[Eddington 1933] *The Expanding Universe*. Cambridge University Press, London https://doi.org/10.1017/CBO9780511564208

[Ehlers *et al.* 2005] *Nonholonomic systems via moving frames: Cartan equivalence and Chaplygin Hamiltonization*. In: Marsden, J.E., Ratiu, T.S. (eds) *The Breadth of Symplectic and Poisson Geometry*. Progress in Mathematics, **vol 232**. Birkhäuser Boston. Cambridge University Press, London https://doi.org/10.1007/0-8176-4419-9_4

[Einstein 1905] "Zur Elektrodynamik bewegter Körper." *Annalen der Physik.* **17** 891 https://doi.org/10.1002/andp.19053221004 English translation: "On Electrodynamics of Moving Bodies". http://hermes.ffn.ub.es/luisnavarro/nuevo_maletin/Einstein_1905_relativity.pdf

[Einstein and Grossmann 1913] "Entwurf einer verallgemeinerten Relativitätstheorie und einer Theorie der Gravitation." *Zeitschrift für Mathematik und Physik* **62** 225–261 https://link.springer.com/content/pdf/10.1007/BF01999515.pdf English translation: "Outline of a Generalized Theory of Relativity and of a Theory of Gravitation." http://www.icra.it/MG/doc/Einstein_Entwurf_1913.pdf

[Einstein 1928] "Riemann-Geometrie mit Aufrechterhaltung des Begriffes des Fernparallelismus" *Preussische Akademie der Wissenschaften, Phys.math. Klasse, Sitzungsberichte*, 217–221. https://doi.org/10.1016/j.hm.2005.11.005

[Ellis 2011] *Class. Quantum Grav.*, **28** 164001 https://doi.org/10.1088/0264-9381/28/16/164001

[Füzfa 2015] *Phys. Rev. D* **93** 024014 https://doi.org/10.1103/PhysRevD.93.024014

[Fabbrichesi *et al.* 2021] *Phys. Rev. D* **103** 095026 https://doi.org/10.1103/PhysRevD.103.095026

[Famaey and McGaugh 2012] *Living Rev. Relativ.* **15** 10 https://doi.org/10.12942/lrr-2012-10

[Favale *et al.* 2023] *Mon. Not. Roy. Astron. Soc.* **2023** stad1621 https://doi.org/10.1093/mnras/stad1621

[Ferrari *et al.* 1989] *Gen. Relativ. Gravit.* **21** 69-78 https://doi.org/10.1007/BF00756185

[Ferreira *et al.* 2022] *Astrophys. J. Lett.* **938** L2 https://doi.org/10.3847/2041-8213/ac947c

[Ferreti 2014] *J. High Energ. Phys.* **2014** 142 https://doi.org/10.1007/JHEP06(2014)142

[Fontanini *et al.* 2019] *Phys. Rev. D* **99** 064006. https://doi.org/10.1103/PhysRevD.99.064006

[Font-Ribera *et al.* 2014] *J. Cosmol. Astropart. Phys.* **2014** 027 https://doi.org/10.1088/1475-7516/2014/05/027

[Fröhlich and Werner 2013] *Europhys. Let.* **101** 47007. https://doi.org/10.1209/0295-5075/101/47007

[Freedman *et al.* 2019] *Astrophys. J.* **882** ab2f73 https://doi.org/10.3847/1538-4357/ab2f73

[Friedrich 2000] *Dirac Operators in Riemannian Geometry*. Graduate Studies in Mathematics, American Mathematical Society, ISBN: 082182055 https://doi.org/10.1007/s10714-015-1935-z

[Friedman 1983] *Foundations of Space-Time Theories: Relativistic Physics and Philosophy of Science.* Princeton University Press. https://doi.org/10.1126/science.222.4627.1007.b http://www.jstor.org/stable/j.ctt7ztj02

[Fujii 2020] *Res. Notes AAS* **4** 72 https://doi.org/10.3847/2515-5172/ab9537

[Galloway 2000] *Annales de l'Institut Henri Poincaré A* **1** 543–567 https://doi.org/10.1007/s000230050006

[Gaztañaga *et al.* 2009] *Mon. Not. R. Astron. Soc.* **399** 1663–1680 https://doi.org/10.1111/j.1365-2966.2009.15405.x

[Gentile 2008] *Astrophys. J.* **684** 1018 https://doi.org/10.1086/590048

[Gertov *et al.* 2019] *J. High Energ. Phys.* **2019** 181 https://doi.org//10.1007/JHEP02(2019)181

[Giorgi 2019] *Class. Quantum Grav.* **36** 205001

[Goddy *et al.* 2023] *Mon. Not. R. Astron. Soc.* **520** 3895-3908 https://doi.org/10.1093/mnras/stad298

[Gotay *et al.* 2004] *arXiv:math-ph/***0411032** https://doi.org/10.48550/arXiv.math-ph/0411032

[Gomis *et al.* 2021] *J. High Energ. Phys.* **2021** 47 https://doi.org/10.1007/JHEP08(2021)047

[Goto *et al.* 2010] *Class. Quantum Grav.* **27** 025005 https://doi.org/10.1088/0264-9381/27/2/025005

[Gryb 2015] *Gen. Relativ. Gravit.* **47** 37 https://doi.org/10.1007/s10714-015-1875-7

[Gu 2018a] *Adv. Appl. Clifford Algebras* **28** 79 https://doi.org/10.1007/s00006-018-0896-1

[Gu 2018b] *Adv. Appl. Clifford Algebras* **28** 37 https://doi.org/10.1007/s00006-018-0852-0

[Guo *et al.* 2020] *Class. Quantum Grav.* **37** 085016 https://doi.org/10.1088/1361-6382/ab77ec

[Gupta 2023] *Mon. Not. Roy. Astron. Soc.* **stad2032** https://doi.org/10.1093/mnras/stad2032

[Gurses *et al.* 2018] *Phys. Rev. D* **98** 126017 https://doi.org/10.1103/PhysRevD.98.126017

[Gurzadyan and Stepanian 2021] *Astron. Astrophys.* **653** A145 https://doi.org/10.1051/0004-6361/202141736

[Gwak *et al.* 2016] *J. High Energ. Phys.* **2016** 55 https://doi.org/10.1140/epjc/s10052-022-10204-4

[Harikumar *et al.* 2022] *Eur. Phys. J. C* **82** 241 https://doi.org/10.1140/epjc/s10052-022-10204-4

[Harko 2010] *Phys. Rev. D* **81** 044021 https://doi.org/10.1103/physrevd.81.044021

[Herfray *et al.* 2016] *Class. Quantum Grav.* **33** 235001 https://doi.org/10.1088/0264-9381/33/23/235001

[Hernandez 2023] *Mon. Not. Roy. Astron.* **525** 1401-1415 https://doi.org/10.1093/mnras/stad2306

[Herold *et al.* 2022] *Astrophys. J. Lett.* **929** L16 https://doi.org/10.3847/2041-8213/ac63a3

[Hollands and Wald 2002] *Gen. Relativ. Gravit.* **34**, 2043-2055. https://doi.org/10.1023/A:1021175216055.

[Husemoller 1994] *Fibre Bundles.* New York: Springer. ISBN 978-0-387-94087-8.(pdf available)

[Iorio 2007] *Found. Phys.* **37** 897-918 https://doi.org/10.1007/s10701-007-9132-x

[Izaurieta *et al.* 2019] *Eur. Phys. J. C* **79** 337 https://doi.org/10.1140/epjc/s10052-019-6852-y

[Jiao *et al.* 2023] *Astrophys. J. Supl.* **265** 48 https://doi.org/10.3847/1538-4365/acbc77

[Jimenez *et al.* 2009] *Phys. Rev. D* **80** 023004 https://doi.org/10.1103/PhysRevD.80.023004

[Jimenez *et al.* 2003] *Astrophys. J.* **593** 622–629 https://doi.org/10.1086/376595

[Jimenez *et al.* 2019] *J. Cosmol. Astropart. Phys.* **2019** 043 https://doi.org/10.1088/1475-7516/2019/03/043

[Jimenez and Loeb 2002] *Astrophys. J.* **573** 37–42 https://doi.org/10.1086/340549

[John 2019] *Mon. Not. Roy. Astron. Soc. Lett.* **484** L35–L37 https://doi.org/10.1093/mnrasl/sly243

[Jost 2011] *Riemannian Geometry and Geometric Analysis* Springer https://doi.org/10.1007/978-3-642-21298-7

[Kamionkowski and Knox 2003] *Phys. Rev. D*, **67** 063001 https://doi.org/10.1103/PhysRevD.67.063001, https://www.arxiv.org/abs/astro-ph/0210165

[Křížek and Somer 2023] *Friedmann Equation.* In: *Mathematical Aspects of Paradoxes in Cosmology.* Springer, Cham. https://doi.org/10.1007/978-3-031-31768-2_6

[Kamionkowski and Riess 2022] arXiv:2211.04492, https://doi.org/10.48550/arXiv.2211.04492

[Kasner 1921a] *Amer. J. Mathem.*, **43** 126-129

[Kasner 1921b] *Amer. J. Mathem.*, **43** 126-129

[Katz 2016] *Physics of the Dark Universe* **12** 24-36 https://doi.org/10.1016/j.dark.2016.01.002

[Khruschev 2004] *arXiv:hep-ph/0311346* https://doi.org/10.48550/arXiv.hep-ph/0311346

[Knox and Millea 2020] *Phys. Rev. D* **101** 043533 https://doi.org/10.1103/PhysRevD.101.043533 arXiv:1908.03663

[Kobayashi 2009] *Foundations of Differential Geometry* **Vol. 1** Wiley Classics Library. Vol. 1. Wiley. ISBN 978-0-471-15733-5. (Theory of connections) [1963]

[Kogan *et al.* 2003] *Int. J. Mod. Phys.* **A18** 1827 https://doi.org/10.1142/s0217751x03013715

[Koiller *et al.* 2001] *Anais da Academia Brasileira de Ciência* **73** 165-190 https://www.redalyc.org/pdf/327/32773203.pdf

[Kovács *et al.* 2020] *Mon. Not. Roy. Astron. Soc.* **499** 320-333 https://doi.org/10.1093/mnras/staa2631

[Krasnikov 2021] *Modern Physics Letters A*, **36**, 2150104. https://doi.org/10.1142/S0217732321501042 arXiv:2012.10161 [hep-ph]

[Krasnov and Percacci 2018] *Class. Quantum Grav.* **35** 143001 https://doi.org/10.1088/1361-6382/aac58d

[Kroupa 2015] *Canadian J. Phys.* **93** 169-202 https://doi.org/10.1139/cjp-2014-0179

[Kroupa *et al.* 2023] *arXiv.2309.11552* https://doi.org/10.48550/arXiv.2309.11552

[Krššák *et al.* 2019] *Class. Quantum Grav.* **36** 183001 https://doi.org/10.1088/1361-6382/ab2e1f

[Lanczos 1970] *Space Through the Ages: The Evolution of Geometrical Ideas from Pythagoras to Hilbert and Einstein*. Academic Press. p. 222. https://archive.org/details/spacethroughages0000lanc

[Lelli *et al.* 2016] *Astrophys J.* **816** L14 https://doi.org/10.3847/2041-8205/816/1/L14

[Lelli *et al.* 2019] *Mon. Not. R. Astron. Soc.* **484** 2367 https://doi.org/10.1093/mnras/stz205

[Lewis *et al.* 2016] *Mon. Noti. Roy. Astron. Soc.* **460** 291-296 https://doi.org/10.1093/mnras/stw1003

[Liddle 2003] *An Introduction to Modern Cosmology*, Wiley, Chichester ISBN 978-1-118-50209-9

[Liddle 2004] *Mon. Not. Roy. Astron. Soc.* **351** L49–L53 https://doi.org/10.1111/j.1365-2966.2004.08033.x

[Lindley D 1987] *Nature* **328** 289, https://doi.org/10.1038/328289a0

[Lima 2007] *arXiv*:0708.3414 https://doi.org/10.48550/arXiv.0708.3414

[Lin *et al.* 2019] *Phys. Rev. D* **100** 6, 063542 https://doi.org/10.1103/PhysRevD.100.063542

[Liu *et al.* 2022] *Astrophys. J.* **927** 28 https://doi.org/10.3847/1538-4357/ac4c3b

[López-Corredoira 2014] *Found. Phys.* **47** 711–768 https://doi.org/10.1007/s10701-017-0073-8

[Maddox 2005] Chapter 2 Beginner-Level Proofs. Equivalence Relations: The Idea of Equality. Equivalence classes. In: *Mathematical Thinking and Writing*, Harcourt/Academic Press, ISBN 0-12-464976-9. https://srirejeki345.files.wordpress.com/2012/10/maddox-randall-b-mathematical-thinking-and-writing_2.pdf

[Maia et al. 2005] *Class. Quan. Grav.* **22** 1623-1636 https://doi.org/10.1088/0264-9381/22/9/010

[Mannheim 2006] *Prog. Part. Nucl. Phys.* **56**, 340-445 https://doi.org/10.1016/j.ppnp.2005.08.001

[Mannheim 2007] arXiv:0707.2283 [hep-th] https://doi.org/10.48550/arXiv.0707.2283

[Marsch and Narita 2015] *Front. Phys.* **13** 82. https://doi.org/10.3389/fphy.2015.00082

[Mavromatos *et al.* 2009] *Phys. Rev. D* **79** 081301 https://doi.org/10.1103/PhysRevD.79.081301

[McCulloch 2007] McCulloch M E 2007 Modelling the Pioneer anomaly as modified inertia *Mon. Not. R. Astron. Soc.* 376 338–342 https://doi.org/10.1111/j.1365-2966.2007.11433.x

[McFeron and Székelyhidi 2012] *Commun. Math. Phys.* **313** 425–443 https://doi.org/10.1007/s00220-012-1498-8

[McGaugh *et al.* 2007] *Astrophys. J.* **659** 149 https://doi.org/10.1086/511807

[McGaugh 2004] *Astrophys. J.* **609** 652 https://doi.org/10.1086/421338

[Melia 2007] *Mon. Not. R. Astron. Soc.* **382** 1917-1921 https://doi.org/10.1111/j.1365-2966.2007.12499.x

[Melia 2017] *Front. Phys.* **12** 129802. https://doi.org/10.1007/s11467-016-0611-4

[Melia 2018] *Mon. Not. R. Astron. Soc.* **481** 4855–4862 https://doi.org/10.1093/mnras/sty2596

[Melia 2022] *Mod. Phys. Let. A* **37** 2250016 https://doi.org/10.1142/S021773232250016X

[Melia 2022b] *Astrophys. J.* **941** 178 https://doi.org/10.3847/1538-4357/aca412

[Melia 2023] *Mon. Not. Roy. Astron. Soc. Lett.* **521** L85–L89 https://doi.org/10.1093/mnrasl/slad025

[Melia and Abdelqader 2009] *Int. J. Mod. Phys. D* **18** 1889 https://doi.org/10.1142/S0218271809015746

[Melia and Maier 2013] *Mon. Not. Roy. Astron. Soc.* **432** 2669–2675 https://doi.org/10.1093/mnras/stt59

[Melia and Shevchuk 2012] *Mon. Not. R. Astron Soc.* **419** 2579 *https://doi.org/10.1111/j.1365-2966.2011.19906.x*

[Meneghetti *et al.* 2020] *Science* **369** 6509 https://doi.org/10.1126/science.aax5164

[Merritt 2017] *Stud. Hist. Philos. Sci. B* **57**, 41-52, ISSN 1355-2198 https://doi.org/10.1016/j.shpsb.2016.12.002

[Milgrom 1983] *Astrophys. J.* **270** 365-370 https://ui.adsabs.harvard.edu/abs/1983ApJ...270..365M/abstract

[Minkowski 1915] *Annalen der Physik.* **352** 927–938 https://doi.org/10.1002/andp.19153521505

[Misner and Wheeler 1957] *Annals Phys.* **2** 525-603 https://doi.org/10.1016/0003-4916(57)90049-0

[Mitra 2013] *Gravit. Cosmol.* **19** 134–137 https://doi.org/10.1134/S0202289313020072

[Moerdijk and Mrčun 2003] *Introduction to foliations and Lie groupoids.* Cambridge Studies in Advanced Mathematics, vol. 91, Cambridge University Press, ISBN 978-0-521-83197-0, MR 2012261 https://catdir.loc.gov/catdir/samples/cam041/2003046172.pdf

[Moffat et al. 2014] *Astrophys. J.* **270** 365-370 https://ui.adsabs.harvard.edu/abs/1983ApJ...270..365M/abstract

[Moffat and Toth 2018] *https://doi.org/10.1093/mnrasl/sly176* **482** L1-L3. https://doi.org/10.1093/mnrasl/sly176

[Monjo 2010] arXiv:1012.4730v1

[Monjo 2017] *Phys. Rev. D* **96** 103505. https://doi.org/10.1103/PhysRevD.96.103505 arXiv:1710.09697

[Monjo 2018] *Phys. Rev. D* **98** 043508 (LS16206D). https://doi.org/10.1103/PhysRevD.98.043508 arXiv:1808.09793

[Monjo 2023] *Class. Quantum Grav.* **40** 235002 https://doi.org/10.1088/1361-6382/ad0422

[Monjo 2024] *Phys. Rev. D* **XL10857** (Under review)

[Monjo and Campoamor-Stursberg 2020] *Class. Quantum Grav.* **37** 205015 https://doi.org/10.1088/1361-6382/abadaf

[Monjo and Campoamor-Stursberg 2023] *Class. Quantum Grav.* **40** 195006 https://doi.org/10.1088/1361-6382/aceacc

[Monjo et al. 2024] *Class. Quantum Grav.* **41** (Under review)

[Monteiro *et al.* 2021] *J. High Energy Phys.* **2021** 268-268 https://doi.org/10.1007/jhep05(2021)268

[Moresco *et al.* 2012] *J. Cosmol. Astropart. Phys.* **2012** 053 https://doi.org/10.1088/1475-7516/2012/07/053

[Moresco 2015] *Mon. Not. R. Astron. Soc. Lett.* **450** L16–L20 https://doi.org/10.1093/mnrasl/slv037

[Moresco *et al.* 2016] *J. Cosmol. Astropart. Phys.* **5** 014 https://doi.org/10.1088/1475-7516/2016/05/014

[Mosterín 1999] *Philosophy of Science* **66**, 1-49 https://doi.org/10.1086/392675

[Nash 1956] *Ann. of Math.* **63** 20–635 https://doi.org/10.2307/1969989

[Nojiri and Odintsov 2007] *Int. J. Geom. Methods Mod. Phys.* **04** 115–145 https://doi.org/10.1142/s0219887807001928

[Noskov 2013] *Gravit. Cosmol.* **19** 257–264 https://doi.org/10.1134/S0202289313040129

[Noskov 2016] *Gravit. Cosmol.* **22** 199-207 https://doi.org/10.1134/S0202289316020134

[Olmo 2011] *Int. J. Modern Phys. D* **20** 413-462 https://doi.org/10.1142/S0218271811018925

[OMalley *et al.* 2017] *Astrophys. J.* **838** 162 https://doi.org/10.3847/1538-4357/aa6574

[O'Neill 1983] *Semi-Riemannian Geometry With Applications to Relativity, Pure and Applied Mathematics* **103** 488p. Academic Press. ISBN 9780080570570 https://doi.org/10.1137/1028086

[Paliathanasis 2016] *Class. Quantum Grav.* **33** 075012 https://doi.org/10.1088/0264-9381/33/7/075012

[Paston and Sheykin 2012] *Class. Quantum Grav.* **29** 095022 https://doi.org/10.1088/0264-9381/29/9/095022

[Pavsic and Tapia 2000] arXiv:gr-qc/0010045, https://doi.org/10.48550/arXiv.gr-qc/0010045

[Penrose 2004] *The Road to Reality: A Complete Guide to the Laws of the Universe.* Vintage Books, London ISBN 978-0679454434.

[Pereira 2012] *AIP Conference Proceedings* **1483** 239. https://doi.org/10.1063/1.4756972

[Pérez *et al.* 2019] *Class. Quantum Grav.* **36** 055002 https://doi.org/10.1088/1361-6382/ab0189

[Perlmutter *et al.* 1999] *Astrophys. J.* **517** 565 https://doi.org/10.1086/307221

[Peskin and Schroeder 2018] *An Introduction to Quantum Field Theory.* CRC Press, New York.

[Poulin *et al.* 2018] *Phys. Rev. D* **98** 083525 https://doi.org/10.1103/PhysRevD.98.083525

[Poulin *et al.* 2019] *Phys. Rev. Lett.* **122** 221301 https://doi.org/10.1103/PhysRevLett.122.221301

[Preston and Morris 2014] *J. Cosmol. Astropart. Phys.*, **2014** 017–017 https://doi.org/10.1088/1475-7516/2014/09/017

[Ratsimbazafy *et al.* 2017] Ratsimbazafy A L, Loubser S I, Crawford S M et al. 2017 Age-dating luminous red galaxies observed with the Southern African Large Telescope *Mon. Not. R. Astron. Soc.* 467 3239–3254. https://doi.org/10.1093/mnras/stx301

[Red'Kov *et al.* 2008] *Symmetry, Integrability and Geometry: Methods and Applications* **4** 021 https://doi.org/10.3842/SIGMA.2008.021

[Riess *et al.* 2018a] *Astrophys. J.* **853** 126 https://doi.org/10.3847/1538-4357/aaa5a9

[Riess *et al.* 2018b] *Astrophys. J.* **855** 136 https://doi.org/10.3847/1538-4357/aaadb7

[Riess *et al.* 2019] *Astrophys. J.* **876** 85 https://doi.org/10.3847/1538-4357/ab1422

[Riess et al. *et al.* 2021] *Astrophys. J. Lett.* **908** L6 https://doi.org/10.3847/2041-8213/abdbaf

[Riess et al. *et al.* 2022] *Astrophys. J. Lett.* **934** L7 https://doi.org/10.3847/2041-8213/ac5c5b

[Rievers and Lammerzahl 2011] *Ann. Phys. (Berlin)* **523** 439-449 https://doi.org/10.1002/andp.201100081

[Sachs 1968] *Il Nuovo Cimento B Series 10*, **55** 199-219 https://doi.org/10.1007/bf02711556

[Şafarík 2003] Heavy Ions (High-Energy Physics) In Meyers RA: Encyclopedia of Physical Science and Technology (Third Edition), Academic Press, 293-307, ISBN 9780122274107. https://doi.org/10.1016/B0-12-227410-5/00313-6

[Sahin2016] *Eur J. Phys.* **37** 065404 https://doi.org/10.1088/0143-0807/37/6/065404

[Samushia *et al.* 2013] *Mon. Not. R. Astron. Soc.* **429** 1514–1528 https://doi.org/10.1093/mnras/sts443

[Saridakis *et al.* 2021] *arXiv:2105.12582* **[gr-qc]** https://doi.org/10.48550/arXiv.2105.12582

[Sauer 2005] *Historia Mathematica* **33** 399-439 https://doi.org/10.1016/j.hm.2005.11.005

[Schlaufman *et al.* 2018] *Astrophys. J.* **867** 98 https://doi.org/10.3847/1538-4357/aadd97

[Schmeikal 2001] *Adv. Appl. Clifford Algebras* **11** 63-80 https://doi.org/10.1007/BF03042039

[Schmeikal 2004] Transposition in Clifford Algebra: SU(3) from Reorientation Invariance. In: Ablamowicz R. (eds) Clifford Algebras. *Progress in Mathematical Physics* **34**, Birkhäuser Boston https://doi.org/10.1007/978-1-4612-2044-2_23

[Schwartz 2023] *Class. Quantum Grav.* **40** 105008 https://doi.org/10.1088/1361-6382/accc02

[Sharpe 1997] *Differential Geometry: Cartan's Generalization of Klein's Erlangen Program.* New York: Springer. ISBN 0-387-94732-9.

[Scolnic *et al.* 2018] *Astrophys. J.* **859** 101 https://10.3847/1538-4357/aab9bb

[Seifert 2007] *Phys. Rev. D* **76** 064002 https://doi.org/10.1103/PhysRevD.76.064002

[Simon *et al.* 2005] *Phys. Rev. D Part. Fields, Gravit. Cosmol.* **71** 123001 https://doi.org/10.1103/PhysRevD.71.123001

[Skagerstam *et al.* 2018] *Class. Quantum Grav.* **36** 015011 https://doi.org/10.1088/1361-6382/aaf113

[Skordis and Złośnik 2021] *Phys. Rev. Lett.* **127** 161302 https://doi.org/10.1103/PhysRevLett.127.161302

[Speck 2018] *Commun. Math. Phys.* **364** 879–979.

[Spergel *et al.* 2007] (WMAP collaboration) *Astrophys. J. Suppl.* **170** 377-408 https://doi.org/10.1086/513700

[Steinhardt 2011] *Scientific Americ*an **304** 36-43 https://doi.org/10.1038/scientificamerican0411-36

[Stern *et al.* 2010] *J. Cosmol. Astropart. Phys.* **2010** 8 https://doi.org/10.1088/1475-7516/2010/02/008

[Sylvester 1852] *Philosophical Magazine* **4** 138–142 https://doi.org/10.1080/14786445208647087

[Tamang *et al.* 2015] *Class. Quantum Grav.* **32** 235028 https://doi.org/10.1088/0264-9381/32/23/235028

[Tomasetti *et al.* 2023] arXiv:2305.16387 https://doi.org/10.48550/arXiv.2305.16387

[Touboul *et al.* 2022] *Class. Quantum Grav.* **39** 204009 https://doi.org/10.1088/1361-6382/ac84be

[Trautman 2008] *J. Geometry and Physics* **58** 238-252 https://doi.org/10.1016/j.geomphys.2007.11.001

[Trippe 2014] *Zeitschrift für Naturforschung A* **69** 173-187 https://doi.org/10.5560/zna.2014-0003

[Tseytlin 2000] Born–Infeld Action, Supersymmetry and String Theory. in Shifman M. (Ed.) *The Many Faces of the Superworld* 417-452 University of Minnesota https://doi.org/10.1142/9789812793850_0025

[Turyshev *et al.* 2005] *Amer. J. Phys.* **73** 1033–1044 https://doi.org/10.1119/1.2008300

[Turyshev *et al.* 2011] *Phys. Rev. Lett.* **107** 081103 https://doi.org/10.1103/PhysRevLett.107.081103

[Turyshev *et al.* 2012] *Phys. Rev. Lett.* **108** 241101 https://doi.org/10.1103/PhysRevLett.108.241101

[Tutusaus *et al.* 2016] *Phys. Rev. D* **94** 103511 https://doi.org/10.1103/PhysRevD.94.103511

[van Dongen 2010] *Einstein's Unification.* In Pekonen, O. Cambridge University Press. ISBN: 9780521883467. https://www.math.ru.nl/~landsman/Jeroen.pdf.

[van Dongen 2021] *Stud. Hist. Philos. Sci. Part A* **89** 164-176. https://doi.org/10.1103/RevModPhys.33.63

[Vavrycuk *et al.* 2017] *Mon. Not. Roy. Astron. Soc.: Let.* **470** L44 https://doi.org/10.1103/PhysRevD.94.103511,

[Vaz and Rocha 2016] An Introduction to Clifford Algebras and Spinors, Oxford University Press. https://doi.org/10.1093/acprof:oso/9780198782926.001.0001

[Wheeler 1961] "Geometrodynamics and the Problem of Motion." *Rev. Mod. Phys.* **33** 63-78. https://doi.org/10.1103/RevModPhys.33.63,

[Wheeler 1966] *Curved empty space as the building material of the physical world: an assessmentIn* Logic, Methodology, and Philosophy of Science, edited by E. Nagel. Stanford University Press. 1263723 https://www.sciencedirect.com/science/article/abs/pii/S0049237X09706044

[Will 2014] *Living Rev. Relativ.* **17** 4 https://doi.org/10.12942/lrr-2014-4

[Williams 2020] *Adv. Math. Physics.* **2020** 1263723 https://doi.org/10.1155/2020/1263723

[Wiltshire 2007] *Phys. Rev. Let.* **99** 251101. https://doi.org/10.1103/physrevlett.99.251101

[Wise 2015] *Theor. Math. Phys.* **19** 1017-1041 https://doi.org/10.4310/ATMP.2015.v19.n5.a3

[Xu *et al.* 2013] *Mon. Not. R. Astron. Soc.* **431** 2834–2860 https://doi.org/10.1093/mnras/stt379

[Yan *et al.* 2015] *Phys. Lett. B* **742** 149–159.

[Yennapureddy and Melia] *Phys. Dark Universe* **20** 65-71 https://doi.org/10.1016/j.dark.2018.03.00

[Yoo and Watanabe 2012] *Int. J. Modern Phys. D* **21** 1230002 https://doi.org/10.1142/s021827181230002

[Yu *et al.* 2018] *Astrophys. J.* **856** 3 https://doi.org/10.3847/1538-4357/aab0a2

[Zhang *et al.* 2014] *Res. Astron. Astrophys.* **14** 1221–1233 https://doi.org/10.1088/1674-4527/14/10/002

[Zhao *et al.* 2019] *Mon. Not. Roy. Astron. Soc.* **486** 5679–5689 https://doi.org/10.1093/mnras/stz1259

[Zinn-Justin 2019] *Quantum chromodynamics: A non-Abelian gauge theory*, From Random Walks to Random Matrices. Oxford Academic https://doi.org/10.1093/oso/9780198787754.003.0013

[Zhoolideh-Haghighi and Rahvar 2017] *Mon. Not. Roy. Astron. Soc.* **468** 4048-4055 https://doi.org/10.1093/mnras/stx692

Appendices

Appendix A

Standard spacetime

A.1 ΛCDM model

Spacetime is the common term used to refer to Lorentzian manifolds in mathematical physics. The simplest spacetime is given by the (flat) four-dimensional Minkowskian metric $\eta_{1,3} = \text{diag}(1, -1, -1, -1)$, or equivalently $\eta_{3,1} = \text{diag}(-1, 1, 1, 1)$, which extends the classical (flat) Euclidean space with metric $I = \text{diag}(1, 1, 1)$. Extensive generalizations are the Riemannian and pseudo-Riemannian metrics, describing metric tensor fields with usually nonzero spatial curvature (i.e. different to the flat Euclidean and Minkowskian metrics). Thus, four-dimensional Lorentzian spacetimes are pseudo-Riemannian metrics with signature $(1, 3)$ or $(3, 1)$ and, therefore, it only has one time coordinate that has different sign in the metric (we prefer the $\eta_{1,3}$ case, that is 1 positive and 3 negative signs). In cosmological theories, the standard spacetime is given by the Friedman-Lemaître-Robertson-Walker (FLRW) metric, and matter is assumed to determine its dynamics according to the *general relativity*.

A reminder of the standard model (known as ΛCDM) of cosmology is required in this Thesis to facilitate a comparison with the new results. The FLRW metric is obtained by combining a manifold with constant spatial curvature K and a scale factor $a(t)$, which expands with time t. One can suppose the spatial section of the universe is a 3-sphere S^3 of curvature $K = 1/R^2$, or a 3-hyperboloid H^3 of curvature $K = -1/R^2$, where R is the radius of curvature (i.e., a general curvature is $K = \pm 1/R^2$), or an Euclidean space (flat universe) obtained from the limit as K approaches zero. With this, the metric in comoving spherical coordinates (t, r', θ ,ϕ) is given by

$$ds^2 = dt^2 - a(t)^2 \left(\frac{dr'^2}{1 - Kr'^2} + r'^2 d\Sigma^2 \right) \tag{A.1.1}$$

where $d\Sigma^2 := d\theta^2 + \sin^2\theta d\phi^2$. The scale factor $a(t)$ represents the expansion of the universe, and hence the Hubble parameter is defined as $H := \dot{a}/a$. The Ricci tensor $R_{\alpha\beta}$ is calculated using the metric $g_{\alpha\beta}$ deduced from Eq. 1.1.3, and thus, Einstein field

equations are obtained according to:

$$R_{\alpha\beta} - \frac{1}{2} g_{\alpha\beta} R = 8\pi \mathrm{G} P_{\alpha\beta} + \Lambda g_{\alpha\beta} \tag{A.1.2}$$

where R is the scalar curvature, G is the gravitational constant, Λ is the cosmological constant and $P_{\alpha\beta}$ is the stress-energy tensor. If one assumes that the universe is a homogeneous perfect fluid at rest (of density ρ and pressure p) and calculates the Ricci tensor, the following Friedmann equations are obtained [Křížek and Somer 2023]:

$$\left(\frac{\dot{a}}{a}\right)^2 = \frac{8\pi \mathrm{G}\rho}{3} + \frac{\Lambda}{3} - \frac{K}{a^2} \tag{A.1.3}$$

$$\left(\frac{\ddot{a}}{a}\right) = -\frac{4\pi \mathrm{G}}{3}(\rho + 3p) + \frac{\Lambda}{3} \tag{A.1.4}$$

If the critical density is defined as $\rho_{crit} := 3{H_0}^2/8\pi G$, where H_0 is the current value for the Hubble parameter, Eq. A.1.3 is usually rewritten as:

$$\frac{H^2}{{H_0}^2} = \frac{\rho}{\rho_{crit}} + \frac{\rho_\Lambda}{\rho_{crit}} - \frac{K}{{H_0}^2 a^2} \tag{A.1.5}$$

where ρ_Λ is the dark energy density, defined as $\rho_\Lambda := \Lambda/8\pi\mathrm{G}$. Assuming that the matter density ρ is cold (non ultra-relativistic), its equation of state $w := p/\rho$ is approximately $w \approx 0$, and it varies by the expansion as a^{-3}. If the universe is dominated by radiation or ultra-relativistic particles, $w \approx 1/3$ and ρ varies as a^{-4}. Therefore, Eq. A.1.5 can be rewritten as:

$$\frac{H_\Lambda^2}{{H_0}^2} = \Omega_r \left(\frac{a_o}{a}\right)^4 + \Omega_m \left(\frac{a_o}{a}\right)^3 + \Omega_K \left(\frac{a_o}{a}\right)^2 + \Omega_\Lambda \tag{A.1.6}$$

where $\Omega_i := \rho_i/\rho_{crit}$ are the ΛCDM parameters for radiation (ρ_r), matter (ρ_m), dark energy (ρ_Λ) and curvature ($\Omega_K := -K/H_0^2 a_o^2$). Since the redshift z depends on the scale factor as $1 + z = a_o/a$, trivially, the parameter Hubble $H = \dot{a}/a$ depends on the redshift z too [Liddle 2003]. International projects assuming the ΛCDM model, such as the Wilkinson Microwave Anisotropy Probe (WMAP) and the Planck Mission, have estimated that $\Omega_r \approx 8.4 \cdot 10^{-5}$, $\Omega_m = 0.3089 \pm 0.0062$, $\Omega_\Lambda = 0.6911 \pm 0.0062$ and $\Omega_K \approx 0$.

A.2 Measurement of cosmological distances

Some definitions are also required, especially to distinguish among the main cosmological distances: the light-travel distance (or universe age), the comoving distance, the angular distance, the luminosity distance and the distance modulus.

Definition A.2.1 (**Global time** or **light-travel distance**)**.** If the Hubble time is defined as $t_H = 1/H$, the **global time**, *age of the universe*, *light-travel distance* or *lookback time* dt is linked with the scale factor $1+z$ as $dt/t_H = -dz/(1+z)$. Therefore, the **global time** can be obtained from the total light-travel distance:

$$t_0 = \int_0^\infty \frac{dz}{(1+z)H(z)} = \frac{1}{H_0} F_T \tag{A.2.1}$$

where F_T is the time correction factor, i.e., the quotient between the Hubble time (H_0^{-1}) and the age of the universe (t_0). For the ΛCDM model, it is:

$$F_T = \int_0^\infty \frac{dz}{(1+z)\sqrt{\Omega_m(1+z)^3 + \Omega_K(1+z)^2 + \Omega_\Lambda}} \tag{A.2.2}$$

For example, for a flat universe without any cosmological constant ($\Omega_\Lambda = 0$) one finds $F_T = 2/3$.

Definition A.2.2 (**Comoving distance**)**.** Another interesting measurement is the comoving distance r'. This is given by the null geodesic with no angular variations ($d\Sigma = 0$) in the considered metric. This distance can be written using the redshift z and the Hubble parameter, $H = \dot{a}/a$, with the scale factor expressed as $a/a_0 = 1/(1+z)$ where $a_{\hat{o}} \equiv 1$ is the current value of a. For example, using spherical coordinates (t, r', θ, ϕ) in a diagonal metric $g = (1, g_{r'r'}, g_{\theta\theta}, g_{\phi\phi})$, the **comoving distance**[1] is given by isolating the radial coordinate r' from:

$$\int_0^{r'} \frac{\sqrt{g_{r'r'}}dr'}{a} = -\int_{t_{\hat{o}}}^{t} \frac{dt}{a} = \int_0^z \frac{dz}{H_\Lambda(z)} =: \hat{r}'_\Lambda(z) \tag{A.2.3}$$

For the ΛCDM model, the comoving distance is given by:

$$r' = \sin_K \int_0^z \frac{dz}{H_o\sqrt{\Omega_m(1+z)^3 + \Omega_K(1+z)^2 + \Omega_\Lambda}} \tag{A.2.4}$$

where $\sin_K x := \lim_{\epsilon\to K} \epsilon^{-1/2}\sin(\epsilon^{1/2}x)$, i.e., $\sin_0(x) = x$, $\sin_{+1} x = \sin x$, $\sin_{-1} x = \sinh x$, and recall that $K = -\Omega_K H_o^2$.

Definition A.2.3 (**Angular diameter distance**)**.** Angular distance or angular diameter distance, r_A, is given by the proper area of an infinitesimal surface dA with t and r' constant, i.e.:

$$dA := \sqrt{g_{\theta\theta}g_{\phi\phi}}d\phi d\theta := r_A^2 \sin\theta d\phi d\theta \tag{A.2.5}$$

[1] In some references, r' is called "comoving radial coordinate" or "transverse comoving distance", while the "(simply) comoving distance" is reserved for the measurement $\hat{r}'_\Lambda(z) := \int_0^z \frac{dz}{H_\Lambda(z)}$, and the "proper distance" is usually defined by $\hat{r}_\Lambda(z) := a(z)\hat{r}'_\Lambda(z)$. For a flat FLRW metric ($K = 0$), "comoving distances and "transverse comoving distances" are equivalent $r' = \hat{r}'_\Lambda$.

For metrics with $g_{\phi\phi} = -a^2 r'^2 \sin^2\theta$ and $g_{\theta\theta} = -a^2 r'^2$, the angular distance r_A is related to the comoving distance by

$$r_A = ar' = \frac{r'}{1+z}\,. \tag{A.2.6}$$

Definition A.2.4 (**Luminosity distance**)**.** Using the above result, the luminosity distance is $r_L := r_A/a^2 = r'/a$, according to Etherington's reciprocity relation.

A.3 Spherical limit case

Notice that FLRW metrics can have positive, null or negative curvature K. However, any unbounded homogeneous perfect fluid can be modelled as a limit case of a spherical perfect fluid, which has only positive curvature.

Remark A.3.1 (**Spherical prefect fluid**)**.** Let $r_s := 2\mathrm{G}\rho\frac{4}{3}\pi R^3$ be the Schwarzschild radius of a static spherical perfect fluid with homogeneous density ρ and radius R. Defining the parameter $\mathscr{R}^2 := R^3/r_s = 3/(8\pi G\rho)$, the interior Schwarzschild metric is [Beltracchi and Gondolo 2019]

$$ds^2 = \left(\frac{3}{2}\sqrt{1-\frac{R^2}{\mathscr{R}^2}} - \frac{1}{2}\sqrt{1-\frac{r^2}{\mathscr{R}^2}}\right)^2 dt^2 - \left(1-\frac{r^2}{\mathscr{R}^2}\right)^{-1} dr^2 - r^2 d\Sigma^2$$

where $d\Sigma^2 := d\theta^2 + \sin^2\theta\, d\varphi^2$. For an isotropic and homogeneous universe, each observer is located at the center ($r = 0$) of some spherical perfect fluid of radius R and density equal to the critical density ρ_{crit}, thus $\mathscr{R}^2 = 3/(8\pi G\rho_{crit}) = t_H^2$, where $t_H = 1/H_0$ is the Hubble time. On the other hand, the radius $R > r$ is arbitrarily large or small, since the outside of the sphere does not matter. Choosing constant r and $R = r + \varepsilon$ for some $\varepsilon > 0$, the limit of the metric when $\varepsilon \to 0$ is

$$ds^2 = \left(1-\frac{r^2}{t_H^2}\right) dt^2 - \left(1-\frac{r^2}{t_H^2}\right)^{-1} dr^2 - r^2 d\Sigma^2$$

and, if $R \to t_H$ is chosen, the result is the same but replacing dt by $dt/2$. On the other hand, for $\rho \neq \rho_{crit}$, only the inner content of the sphere contributes to the metric. For example, if empty spheres ($\rho = 0$) are considered, the parameter $\mathscr{R}^{-2} \to 0$ and the metric is the flat Minkowskian case.

Appendix B

Derivation of the hyperconical metric

B.1 The hyperconical metric

This annex aims to show two fundamental and related points of the present Thesis: (a) the Friedmann–Lemaître–Robertson–Walker (FLRW) metric is derived by combining an static manifold and a time dimension, which is not adequate since it omits the effects of an observer living in a moving reference frame. (b) The derivation of the hyperconical model in a similar way to the FLRW metric but without setting a static reference frame, chosen as a more suitable alternative to solve some open issues in cosmology.

To facilitate the reading, a three-dimensional case is considered first. Let q_{t_0} be a map from spherical coordinates $p = (\gamma, \phi, \theta) \in U = (0, \pi) \times (0, \pi) \times (-\pi, \pi) \subset \mathbb{R}^3$ to a hypersphere $S^3_{t_0} \subset \mathbb{R}^4$ of radius t_0 given by

$$\begin{array}{rccl} q_{t_0}: & U \subset \mathbb{R}^3 & \to & S^3_{t_0} \subset \mathbb{R}^4 \\ & p & \mapsto & q_{t_0}(p) = (x, y, z, u) = (\vec{r}, u) \\ & \| & & \| \\ & (\gamma, \phi, \theta) & \mapsto & (t_0 \sin\gamma \sin\phi \sin\theta,\ t_0 \sin\gamma \sin\phi \cos\theta,\ t_0 \sin\gamma \cos\phi,\ t_0 \cos\gamma) \end{array} \tag{B.1.1}$$

where $\vec{r} := (x, y, z) := (r \sin\phi \sin\theta, r \sin\phi \cos\theta, r \cos\phi)$ is the ordinary three-dimensional spatial vector, $r := |\vec{r}| = t_0 \sin\gamma$, and $u := t_0 \cos\gamma = t_0 \sqrt{1 - \sin^2\gamma}$ is the extra spatial dimension of the ambient or embedding space $\mathbb{R}^4$ where $S^3_{t_0}$ lives. It is also possible to define a two-dimensional vector $\vec{\ell} := (x, y) \in S^1_\ell \subset \mathbb{R}^2$ such that $\ell := |\vec{\ell}| = r \sin\phi$. Therefore, the three-component vector is now $\vec{r} = (\vec{\ell}, z) \in S^2_r \subset \mathbb{R}^3$ and $z = r \cos\phi$ is the (third) extra dimension. Using these definitions, the first fundamental form g_{S^2} of the sphere parameteriation $s_r : (\phi, \theta) \in V = (0, \pi) \times (-\pi, \pi) \subset \mathbb{R}^2 \mapsto (r \sin\phi \sin\theta,\ r \sin\phi \cos\theta,\ r \cos\phi) \in S^2_r$ represents an infinitesimal distance over S^2_r as follows:

$$\begin{array}{rcl} g_{S^2} & = & (\partial_i \vec{r} \cdot \partial_j \vec{r})_{i,j \in \{\theta,\phi\}} = \begin{pmatrix} r^2 \sin^2\phi & 0 \\ 0 & r^2 \end{pmatrix} \\ \| & & \\ ds^2_r & = & (g_{S^2})_{\theta\theta} d\theta^2 + (g_{S^2})_{\phi\phi}\, d\phi^2 = r^2 \sin^2\phi d\theta^2 + r^2 d\phi^2 \end{array} \tag{B.1.2}$$

Since $\ell = r\sin\phi$ and $\phi = \arcsin(\ell/r)$,

$$ds_r^2 = (g_{S^2})_{\theta\theta}\, d\theta^2 + (g_{S^2})_{\phi\phi}\, d\phi^2 = \ell^2 d\theta^2 + \frac{d\ell^2}{1-\frac{\ell^2}{r^2}} \tag{B.1.3}$$

Repeating the same process but with $\gamma = \arcsin(r/t_0)$, the distances over the hypersphere $S^3_{t_0} \subset \mathbb{R}^4$ are given by the derivation of the parameterization $q_{t_0} : U \subset \mathbb{R}^3 \to S^3_{t_0}$ as displayed in Eq. B.1.1; that is,

$$dq_{t_0}^2 = r^2\sin^2\phi d\theta^2 + r^2 d\phi^2 + \frac{dr^2}{1-\frac{r^2}{t_0^2}} \quad =: \quad r^2 d\Sigma^2 + \frac{dr^2}{1-\frac{r^2}{t_0^2}} \tag{B.1.4}$$

This is the metric for a **static hypersphere**[1]. This metric can be directly obtained by taking the differential of Eq.B.1.1, for instance by taking the measurements performed by an observer located at $o_{t_0} := (\vec{0}, t_0) \in S^3_{t_0} \subset \mathbb{R}^4$, that is:

$$d(q_{t_0} - o_{t_0})^2 \;=\; (d\vec{r}, du)^2 \;=\; \left(d\left(r\vec{e}_r\right), d\left(t_0\sqrt{1-\sin^2\gamma} - t_0\right)\right)^2 \tag{B.1.5}$$

where $\vec{e}_r := \vec{r}/r$ is the unitary spatial vector. Using the angle $\gamma = \arcsin(r/t_0) \in [0, \pi/2)$, the last term contributes to:

$$du \;=\; d\left(t_0\cos\gamma\right) = -t_0\sin\gamma d\gamma = -\frac{dr}{\sqrt{1-\frac{r^2}{t_0^2}}}\frac{r}{t_0} \tag{B.1.6}$$

$$du^2 + dr^2 + r^2 \;=\; \frac{dr^2}{1-\frac{r^2}{t_0^2}}\frac{r^2}{t_0^2} + dr^2 = \frac{dr^2}{1-\frac{r^2}{t_0^2}} \tag{B.1.7}$$

while $r d\vec{e}_r$ contributes to $r^2 d\Sigma^2$. Now, the FLRW metric for a linearly expanding hypersphere is easily obtained replacing the distance $r \to r' := (t_0/t)r$, that is $r'/t_0 = r/t$ and adding a scale factor $a(t) = t/t_0$ to the spatial distance, as well as adding the contribution of dt^2:

$$ds^2_{FLRW} := dt^2 - a(t)^2 dq_{t_0}^2 \quad = \quad dt^2 - \left(\frac{t}{t_0}\right)^2\left(r'^2 d\Sigma^2 + \frac{dr'^2}{1-\frac{r'^2}{t_0^2}}\right) \tag{B.1.8}$$

However, the spatial term on the right is only valid assuming a static hypersphere. Therefore, one needs to repeat the calculus of Eq. B.1.5, replacing $t_0 \to t$ and considering the contributions of dt within both dr and du to obtain the distances over the hyperconical universe with coordinates $s_{\hat{\mathcal{H}}^4} = (t, r, \theta, \phi)$,

$$ds^2_{\hat{\mathcal{H}}^4} := dt^2 - d(q_t - o_t)^2 = dt^2\left(2\sqrt{1-\frac{r'^2}{t_0^2}} - 1\right) - \frac{t^2}{t_0^2}\left(\frac{dr'^2}{1-\frac{r'^2}{t_0^2}} + r'^2 d\Sigma^2\right) - \frac{2r't}{t_0^2}\frac{dr'dt}{\sqrt{1-\frac{r'^2}{t_0^2}}} \tag{B.1.9}$$

[1]Static hypersphere is simply defined by the usual hypersphere, of constant radius, in contrast to dynamical radius (e.g. a hypersphere with the linear expanding radius.

where it has been used that $r = (t/t_0)r'$ to separate the contributions from dr^2 to comoving spatial dr'^2 and temporal dt^2 terms. Now, by identifying the metric g in the distance $ds^2_{Hyp} = g_{tt}\,dt^2 - g_{r'r'}\,dr'^2 - 2g_{r't}\,dr'dt$, lapse $g_{tt} \neq 1$ and shift $g_{r't} \neq 0$ components emerge compared to the FLRW metric. Observe that the differential line $d(s_{\hat{\mathcal{H}}^4} - O_t)$ leads to an embedding for the observers' path $O_t := (t, o_t) = (t, \vec{0}, t)$ because they measure distances from a set reference time, $O'_t := (t_0, \vec{0}, t)$ [Monjo 2017].

Nevertheless, the expansion terms of the metric g can be absorbed by a radial inhomogeneity in the purely spatial component, by changing the coordinate $t \to t' := t\sqrt{g_{tt}}$. Thus, the metric expressed in the new coordinates slightly differs from the FLRW metric for $r' \ll t$. For instance, taking $\nu \equiv 1$, one finds

$$
\begin{aligned}
g'_{tt} &= 1 && \text{(B.1.10)}\\
g'_{\phi\phi} &= -a(t', r')^2 r'^2 sin^2\theta && \text{(B.1.11)}\\
g'_{\theta\theta} &= -a(t', r')^2 r'^2 && \text{(B.1.12)}\\
g'_{r'r'} &= g_{r'r'} - \frac{g_{0r}^2}{g_{00}} = -a(t', r')^2 \frac{2 - \sqrt{1 - \frac{r'^2}{t_0^2}}}{2\left(1 - \frac{r'^2}{t_0^2}\right) - \sqrt{1 - \frac{r'^2}{t_0^2}}} \approx \\
&\approx -a(t', r')^2 \frac{1 + \frac{r'^2}{2t_0^2}}{1 - \frac{3r'^2}{2t_0^2}} \approx -a(t', r')^2 \left(1 + \frac{2r'^2}{t_0^2}\right) + ... && \text{(B.1.13)}
\end{aligned}
$$

with scale factor

$$
a(t', r') = \frac{t'}{t_0\sqrt{2\left(\sqrt{1 - \frac{r'^2}{t_0^2}} - 1\right) + 1}} \approx \frac{t'}{t_0\sqrt{1 - \frac{r'^2}{t_0^2}}} \approx \frac{t'}{t_0}\left(1 + \frac{r'^2}{2t_0^2}\right) \qquad \text{(B.1.14)}
$$

B.2 Example of coordinate change

In spite of the resemblance with a FLRW metric, the radial inhomogeneity leads to two remarkable features: (1) At each point ($r' \equiv 0$), Ricci curvature of g is equivalent to a flat FLRW universe with almost linear acceleration C.2 . (2) Moreover, if g is projected over a plane, the inhomogeneity can be assimilated to a ΛCDM-like acceleration [Monjo 2018]. For instance, a family of coordinate changes could be the following:

Let $\gamma(r') = \sin^{-1}(r'/t_0)$ be the coordinate angle, $\gamma_0 := \pi/3$ a constant corresponding to the real domain for the comoving distance r', and $\alpha \in \mathbb{R}_{\geq 0}$ be a fitting parameter. Now, we can define the family ${}_\sigma f^\alpha : U \subset \mathcal{H}^4 \to \mathbb{R}^4$ of locally-conformal transformations such that

$$
\begin{aligned}
{}_\sigma f^\alpha(t',\ r',\ \phi,\ \theta) &= (t', f^\alpha_{\hat{r}}(r'), \phi, \theta) && \text{(B.2.1)}\\
{}_\sigma f^\alpha_{\hat{r}}(r') &:= \sigma_0 t_0\, \mathbf{trig}^{-1} \frac{\gamma(r')}{\sigma_0\left(1 - \frac{\gamma(r')}{\gamma'_0}\right)^\alpha} && \text{(B.2.2)}
\end{aligned}
$$

where **trig** is any trigonometric function such that the first derivative is $\mathrm{trig}'(0) = 1$, mainly **sin**, **tan**, **sinh** and **tanh**, while $\sigma_0 \in \mathbb{C}$. For instance, Monjo 2018 used **trig** = **tan** with two limit cases, ${}_{\infty}F_{\gamma} = \lim_{\sigma_0 \to \pm\infty} {}_{\sigma}f_{\hat{r}}^{\alpha}$, and ${}_{2}f_{\hat{r}}^{\alpha} := \lim_{\sigma_0 \to \pm 2} {}_{\sigma}f_{\hat{r}}^{\alpha}$. Considering $k \equiv 1$ and $\Omega_r = 9.0 \pm 0.5 \cdot 10^{-5}$, their numerical solutions correspond to complex values:

$$\alpha = 0.2830219501(1) \pm c_{\alpha}\mathrm{i} \tag{B.2.3}$$

$$\Omega_{\Lambda} = 0.6937181(17) \pm c_{\omega} \tag{B.2.4}$$

where the constants $c_{\alpha}, c_{\omega} \in \mathbb{R}$ become zero for $\sigma_0 = \pm 2.416113322(1)\,\mathrm{i}$. Nevertheless, as discussed in this Thesis, the choice of locally-conformal transformations is not globally unique but the local limit logically does.

Appendix C

Ricci curvature of the extrinsic model

C.1 Ricci curvature tensor

The Ricci curvature tensor can be calculated from the Riemann curvature tensor defined for signature (1,3) as:

$$R_{\alpha\beta} := R^{\mu}_{\alpha\mu\beta} = \partial_\mu \Gamma^{\mu}_{\alpha\beta} - \partial_\beta \Gamma^{\mu}_{\mu\alpha} + \Gamma^{\mu}_{\rho\mu}\Gamma^{\rho}_{\alpha\beta} - \Gamma^{\mu}_{\rho\beta}\Gamma^{\rho}_{\alpha\mu} \tag{C.1.1}$$

where $\Gamma^{\mu}_{\alpha\beta}$ are the Christoffel symbols, which for the affine connection Levi-Chivita it is satisfied that $\nabla g = 0$ and g is symmetric (without torsion). Therefore:

$$\Gamma^{\mu}_{\alpha\beta} = \frac{1}{2} g^{\mu\nu} \left(\partial_\alpha g_{\nu\beta} + \partial_\beta g_{\alpha\nu} - \partial_\nu g_{\alpha\beta}\right) \tag{C.1.2}$$

To obtain shorter expressions, we have worked with $g_{\mu\nu}$ instead of $g'_{\mu\nu}$, which locally coincide. After performing the calculations, we can see that the time component of the Ricci tensor is $R_{00} \equiv 0$ for all positions. This contrasts with the FRW metric, for which the result is $R^{FRW}_{00} = -3\ddot{a}/a$. The spatial elements are:

$$R_{r'r'} = -\left(\frac{\dot{a}}{a}\right)^2 \frac{2k^2}{2b - b^2 + k - 1} g_{r'r'} \tag{C.1.3}$$

$$R_{\theta\theta} = -\left(\frac{\dot{a}}{a}\right)^2 \frac{(4b - b^2 + 2k - 3)k^2}{(2b - b^2 + k - 1)^2} g_{\theta\theta} \tag{C.1.4}$$

$$R_{\phi\phi} = -\left(\frac{\dot{a}}{a}\right)^2 \frac{(4b - b^2 + 2k - 3)k^2}{(2b - b^2 + k - 1)^2} g_{\phi\phi} \tag{C.1.5}$$

Therefore, the manifold is only maximally symmetric in the spatial components ($R_{ij} = 1/3 \cdot R g_{ij}$) at local scale ($r' = 0$, i.e. $b = 1$). In this case, the spatial part of the Ricci tensor is $R_{ij} = -2k(\dot{a}/a)^2 g_{ij}$. This contrasts with the FRW result:

$$R^{FRW}_{ij} = -\frac{\ddot{a}}{a} g^{FRW}_{ij} - 2\left(\frac{\dot{a}}{a}\right)^2 g^{FRW}_{ij} - \frac{2K}{a^2} g^{FRW}_{ij} \tag{C.1.6}$$

C.2 Ricci scalar curvature

Finally, the Ricci scalar curvature is obtained from the trace $R := R^{\alpha}_{\alpha}$ as:

$$R = -\frac{6k^2}{t^2}\frac{2b - \frac{1}{3}(2b^2+1) + k - 1}{(2b - b^2 + k - 1)^2} \tag{C.2.1}$$

For each point ($r' = 0$), the scalar curvature can be simplified to

$$R = -\frac{6k}{t^2} = -\frac{6}{\nu^2 t^2} \tag{C.2.2}$$

that corresponds to a 3-sphere (of radius νt) embedded into $\mathrm{R}^{1,4}$. If $k = 1$, the Ricci scalar is equivalent to the case of FRW metric with linear scale factor $a = t/t_0$ and curvature $K = 0$, i.e., this is apparently flat under the FRW view.

Appendix D

Einstein-Hilbert Lagrangian density

D.1 Perturbed vacuum Lagrangian density

Assuming that GR is valid at local scales, the total Lagrangian density is obtained by modifying the standard Einstein-Hilbert term [Monjo and Campoamor-Stursberg 2020],

$$\mathscr{L} = \frac{1}{16\pi \mathrm{G}} \Delta R + \mathscr{L}_M \;\approx\; \frac{1}{16\pi \mathrm{G}} \left(R + \frac{6}{\nu^2 t^2} \right) - \rho_M \;\approx\; \frac{c^2}{16\pi \mathrm{G}} R - \Delta\rho \,, \qquad \text{(D.1.1)}$$

where $\Delta R := R - R_u$ is the curvature perturbation with respect to the local limit of the Ricci curvature of the (empty) hyperconical universe, $R_u = -6/(\nu^2 t^2)$, with $\nu = 1$ for the unpertubed spacetime, while $\mathscr{L}_M = -\rho_M$ is the Lagrangian of mass-energy, and $\Delta\rho = \rho_M - \rho_0$ is the density perturbation compared to the "vacuum energy" $\rho_0 := 3/(8\pi \mathrm{G} t^2)$ and its mass-related event radius is $r_{\mathfrak{M}} := 2\mathrm{G}\mathfrak{M} := 2\mathrm{G}\rho_0 \frac{4}{3}\pi t^3 = t$, where $\mathfrak{M}$ is a "total mass" linked to ρ_0. Moreover, the squared escape velocity linked to ρ_0 at r is $v_E^2(\rho_0) = 2\mathrm{G}\rho_0 \frac{4}{3}\pi r^3 = r^2/t^2 = v_H^2$. Therefore, the total density ρ_M leads to a total squared escape velocity $v_E^2(\rho_M)$ as follows

$$v_E^2(\rho_M) = 2\mathrm{G}\rho_M \frac{4}{3}\pi r^3 = 2\mathrm{G}\left(\rho_0 + \Delta\rho\right) \frac{4}{3}\pi r^3 = \frac{r^2}{t^2} + \frac{2\mathrm{G}M}{r} = v_E^2(\rho_0) + v_E^2(\Delta\rho) \,, \quad \text{(D.1.2)}$$

where it has been used that $M := \Delta\rho \frac{4}{3}\pi r^3 \;\propto\; \rho_0 t^3 \;\propto\; t$.

Now, let $\theta_M := M/\mathfrak{M} \ll 1$ be a (small) constant fraction of energy corresponding to the perturbation $\Delta\rho$, and $r_M := 2\mathrm{G}M = \theta_M t$ be the mass-related event radius. Thus,

$$\frac{2\mathrm{G}M}{r} = \frac{\theta_M t}{r' \frac{t}{t_0}} = \frac{\theta_M t_0}{r'} =: \frac{2\mathrm{G}M_0}{r'} \,. \qquad \text{(D.1.3)}$$

Therefore, the relationship of $M/r = M_0/r'$ is satisfied since $r/t = r'/t_0$.

D.2 New Einstein field equations

The background metric of the universe leads to $R^u_{00} = 0$ and $R^u_{ij} = \frac{1}{3} R_u \, g_{ij}$ (see Appendix C). Since $R_u = -\frac{6}{t^2}$, Einstein field equations turn locally into

$$\begin{cases} \kappa P_{00} & = \Delta R_{00} - \frac{1}{2}\Delta R g_{00} & \approx & R_{00} - \frac{1}{2} R g_{ij} - \frac{3}{t^2} g_{ij} \\ \kappa P_{ij} & = \Delta R_{ij} - \frac{1}{2}\Delta R g_{ij} & \approx & R_{ij} - \frac{1}{2} R g_{ij} - \frac{1}{t^2} g_{ij} \end{cases} \tag{D.2.1}$$

where $\kappa = 8\pi \mathrm{G}$ and $P_{\mu\nu}$ are the stress-energy tensor components. Notice that the new terms $-\frac{3}{t^2}$ and $-\frac{1}{t^2}$ behave like the effects of a dynamical dark energy with equation of state $w = -1/3$ (i.e. varying as a^{-2}).

Appendix E

Embedding local gravity

E.1 Exact solutions embedded in six dimensions

A well-known solution to the Einstein field equations is the Schwarzschild metric, that is an exact solution for the vacuum case ($R_{ij} - \frac{1}{2}Rg_{ij} = 0$) corresponding to an external gravitational field of an uncharged, non-rotating, spherically symmetric body of mass M. The Schwarzschild solution yields

$$ds^2 = \left(1 - \frac{2\mathrm{G}M}{r}\right) dt^2 - \left[\left(1 - \frac{2\mathrm{G}M}{r}\right)^{-1} dr^2 + r^2 d\Sigma^2\right] , \tag{E.1.1}$$

which cannot be immersed into a five flat spacetime. More specifically, Kasner's theorem ensures that any solution of the Einstein equations needs to be embedded into at least a six-dimensional ambient space [Kasner 1921a, Paston and Sheykin 2012]. An example of six-dimensional embedding was firstly proposed by Kasner 1921b. Kasner defined an auxiliar variable,

$$dR := \sqrt{\frac{\eta}{2}\mathrm{G}Mr} - 2\mathrm{G}M\, dr \;\Rightarrow\; R = 2\sqrt{2\mathrm{G}M(r - 2\mathrm{G}M)}\,, \tag{E.1.2}$$

to rewrite Eq. E.1.1 in Cartesian coordinates (x, y, z) plus two more terms:

$$ds^2 = -dx^2 - dy^2 - dz^2 - dR^2 + \frac{R^2}{R^2 + 16\mathrm{G}^2M^2} dt^2\,, \tag{E.1.3}$$

in which, last term is not an exact differential. Thus, Kasner defined a surface

$$dS^2 = dR^2 + \frac{R^2}{R^2 + 16\mathrm{G}^2M^2} dt^2 =: dX^2 + dY^2 + dZ^2$$

to find an explicit expression of the 6-dimensional embedding.

E.2 Approximated embedding in five dimensions

In spite of the above limitation, an approximation to the Schwarzschild solution can be obtained into a flat five-dimensional ambient space. For instance, let $(t, \vec{r}, u) := (t, x, y, z, u) \in \mathbb{R}^{1,4}_{\eta}$ be Cartesian coordinates, including an extra spatial dimension u in the five-dimensional Minkowski plane. As used in the hyperconical embedding (Appendix B), $u := t\cos\gamma - t$ is chosen to mix space and time. Now, it includes a gravity field with central mass M observed at a distance $\hat{r}$ such that $\sin^2\gamma := \frac{r^2}{t^2} := \frac{r'^2}{t_0^2} := \frac{\hat{r}^2}{t_0^2} + \frac{2\mathrm{G}M}{\hat{r}}$ is defined for some small constant $t_0 \in \mathbb{R}$ and comoving distance $r' := \frac{t}{t_0}r$. Notice that r and r' are coordinates linked to the mass M, in contrast to the observed radial distance $\hat{r}$. Thus, the line element is

$$ds^2 \;=\; (dt, d\vec{r}, du)^2 \;=\; dt^2 - d\left(r\vec{e}_r\right)^2 - du^2 \;=\; dt^2 - dr^2 - r^2 d\Sigma^2 - d\left(t\cos\gamma - t\right)^2 \,,$$

where $\vec{e}_r := \vec{r}/r := \vec{r}'/r' =: \vec{\hat{r}}/\hat{r}$ is the unitary spatial vector. The extra spatial dimension du contributes to:

$$\begin{aligned} du &= d\left(t\cos\gamma - t\right) = dt\left(\cos\gamma - 1\right) - t\sin\gamma d\gamma \\ du^2 &= dt^2\left(\cos^2\gamma - 1\right)^2 + t^2\sin^2\gamma\, d\gamma^2 - 2t\left(\cos\gamma - 1\right)\sin\gamma\, d\gamma dt \end{aligned}$$

and adding the differential of the radial coordinate,

$$\begin{aligned} dr &= d\left(t\sin\gamma\right) = \sin\gamma dt + t\cos\gamma d\gamma \\ &\Rightarrow \quad du^2 + dr^2 = dt^2\left(2 - 2\cos\gamma\right) + t^2 d\gamma^2 + 2t\sin\gamma\, d\gamma dt \end{aligned}$$

Finally, the total differential for $x^\mu = (t, r', \theta, \varphi) \in \mathbb{R}^{1,4}_{\hat{g}}$ is given by

$$ds^2 \;=\; dt^2 - d\vec{r}'^2 - du^2 = \hat{g}_{tt}dt^2 + \hat{g}_{r'r'}dr'^2 + \hat{\hat{g}}_{\theta\theta}d\theta^2 + \hat{g}_{\varphi\varphi}d\varphi^2 + 2\hat{g}_{r't}dr'dt$$

Thus, using that $t_0 d\gamma = dr'/\cos\gamma$,

$$\begin{aligned} \hat{g}_{tt} &= 2\cos\gamma - 1 \;\approx\; 1 - \frac{\hat{r}^2}{t_0^2} - \frac{2\mathrm{G}M}{\hat{r}} \\ \hat{g}_{r'r'} &= -\frac{t^2}{t_0^2}\frac{1}{\cos^2\gamma} \;=\; -\frac{t^2}{t_0^2}\left(1 - \frac{\hat{r}^2}{t_0^2} - \frac{2\mathrm{G}M}{\hat{r}}\right)^{-1} \approx -\frac{t^2}{t_0^2}\left(1 + \frac{\hat{r}^2}{t_0^2} + \frac{2\mathrm{G}M}{\hat{r}}\right) \\ \hat{g}_{r't} &= \frac{t}{t_0}\tan\gamma \;=\; \frac{t}{t_0}\frac{r'}{t_0}\left(1 - \frac{\hat{r}^2}{t_0^2} - \frac{2\mathrm{G}M}{\hat{r}}\right)^{-1/2} \;\approx\; \frac{t}{t_0}\frac{r'}{t_0} + O\left(\frac{\hat{r}^3}{2t^3}\right) \approx \\ &\approx \frac{t}{t_0}\left(\frac{\hat{r}^2}{t_0^2} + \frac{2\mathrm{G}M}{\hat{r}}\right)^{1/2} + O\left(\frac{\hat{r}^3}{2t^3}\right) \\ \hat{g}_{\theta\theta} &= -\frac{t^2}{t_0^2}r'^2 \\ \hat{g}_{\varphi\varphi} &= -\frac{t^2}{t_0^2}r'^2\sin^2\theta\,. \end{aligned}$$

Therefore, assuming linearized perturbations of the metric $\hat{g}_{\mu\nu} = \hat{g}^{back}_{\mu\nu} + h_{\mu\nu}$ with $\hat{g}^{back}_{\mu\nu} := \hat{g}_{\mu\nu}|_{M=0}$, we can find a local approach to the Schwarzschild metric perturbation $h|_{Schw}$ as follows

$$\begin{aligned} h_{\mu\nu}\big|_{Schw} &:= \hat{g}_{\mu\nu} - \hat{g}_{\mu\nu}\big|_{M\to 0} \\ g_{Schw} &= \left(\eta_{\mu\nu} + h_{\mu\nu}\big|_{Schw}\right) dx^\mu dx^\nu \\ g_{Schw} &= \left(1 - \frac{2\mathrm{G}M}{r}\right) dt^2 - \frac{t^2}{t_0^2}\left[\left(1 + \frac{2\mathrm{G}M}{\hat{r}}\right) dr'^2 + r'^2 d\Sigma^2\right] + \text{shift}\,. \end{aligned} \quad \text{(E.2.1)}$$

where the shift term $g_{r't}$ is omitted. A similar result is also obtained for $\hat{g}_{\mu\nu}$ when $\hat{r}/t_0 \ll 1$, that is $\lim_{(\hat{r}/t_0)\to 0}[\hat{g}_{\mu\nu}] \approx g_{Schw}$. Finally, removing the shift term, and using Kerr-Schild coordinate time, $t \mapsto t' = t + \phi(r)$, with $\phi'(r) := 2\mathrm{G}M/(1 - 2\mathrm{G}M)$, the Kerr-Schild perturbation is obtained for $t = t_0$ as follows:

$$h_{\mu\nu}\big|_{Schw} = \eta_{\mu\nu} - \frac{2\mathrm{G}M}{\hat{r}} k_\mu k_\nu \quad \text{(E.2.2)}$$

where k_μ is a null four-vector, for instance $k_\mu = (1, 1, 0, 0)$ [Gurses *et al.* 2018].

Remark E.2.1 (**Metric components and speeds relation**)**.** Notice that the Schwarzschild metric (Eq. E.2.2) is similar to the $g \approx \eta + u \otimes u$, since one can define an escape velocity by $v_E := \sqrt{2\mathrm{G}M/\hat{r}'}$ and thus $g_{rr} = -1 - u_E u_E$; while for the empty spacetime, it is $u_H := r/t$ and $g_{rr} = -1 - u_H u_H$.

In summary, the first-order approach from the 5-dimensional embedded hyperconical metric (Eq. E.2.1) differs with respect to the Schwarzschild vacuum solution by the scale factor t^2/t_0^2. Therefore, the classical Newtonian limit of the GR is also recovered in the hyperconical model, because the largest contribution to the gravity dynamics is given by the time component of the metric perturbation $\tilde{h}_{tt}$. That is, the Schwarzschild geodesics are linearized by

$$\frac{d^2 x^\mu}{d\tau^2} \approx \frac{1}{2}\eta^{\mu\nu}\frac{\partial}{\partial x^\nu} h_{tt}\left(\frac{dt}{d\tau}\right)^2 \,, \quad \text{(E.2.3)}$$

where $h_{tt} \approx -2\mathrm{G}M/\hat{r}$.

Appendix F

Distorted projection with global time

F.1 Example of global solution

Applying the global relationship $t(\gamma)$ proposed in 2.5.4.2, it is found that $u(t,\gamma) = t\cos\gamma$ is given by:

$$\begin{aligned}
\gamma = 0 \quad &\Rightarrow \quad t = t_0\lambda^{-1} \quad \Rightarrow \quad u(t,0) = u(t_0,0)\lambda^{-1} \\
\gamma = \gamma_{\max} \quad &\Rightarrow \quad \frac{t_0\lambda^{-1} - t(\gamma_{\max})}{t_0} \leq 1 \quad \Rightarrow \quad \frac{u(t_0,\gamma_{\max})\lambda^{-1} - u(t,\gamma_{\max})}{u(t_0,\gamma_{\max})} \leq 1 \\
\gamma \in [0,\gamma_{\max}) \quad &\Rightarrow \quad \frac{u(t_0,\gamma)\lambda^{-1} - u(t,\gamma)}{u(t_0,\gamma_{\max})} \in [0,1)\,,
\end{aligned} \tag{F.1.1}$$

where the maximum angle $\gamma_{\max} \sim \gamma_U = \pi/3$ is chosen to be the domain limit for an empty space, and $t_0\lambda^{-1} - t \leq t_0$ is the maximum difference allowed. Linearly with γ, the $t(\gamma)$ relationship of Eq. F.1.1 is approximately given by

$$(t_0\lambda^{-1} - t)\cos\gamma \approx t_0\cos\gamma_U\,\frac{\gamma}{\gamma_U} \approx: t_0\,\frac{\gamma}{\gamma_0}\,. \tag{F.1.2}$$

with projected angle $\gamma_0 := \frac{\gamma_U}{\cos\gamma_U} = \frac{2}{3}\pi \sim 2$ for empty spaces. Isolating t from the above expression, Eq. 2.5.7 is now:

$$t_0 \approx -t_0 + \left(t_0\left(\frac{1}{\lambda_s} - \frac{\gamma}{\gamma_0\cos\gamma}\right)\cos\gamma + t_0\right)\lambda_s \quad \Rightarrow \quad \lambda_s \approx \frac{2-\cos\gamma}{1-\frac{\gamma}{\gamma_0}} \sim \frac{1}{1-\frac{\gamma}{\gamma_0}}\,. \tag{F.1.3}$$

Similar results to Eq. F.1.3 are found if the local projection is used instead of the global approach, with a theoretical value of $\gamma_0 = 2$ and an observational constraint of $\gamma_0 = 1.6^{+0.4}_{-0.3}$ fitted to Type Ia Supernovae redshift [Monjo and Campoamor-Stursberg 2023].

Appendix G

Example for estimating parameters with Maple

G.1 Basic definitions

Uploading Maple tools:

> $with(SolveTools)$

$[AbstractRootOfSolution, Basis, CancelInverses, Combine, Complexity, Engine, GreaterComplexity, Identity, Inequality, Linear, Parametric, Polynomial, PolynomialSystem, RationalCoefficients, SemiAlgebraic, SortByComplexity]$

Angle γ of an object with respect to an observer located at a spatial distance of r, assuming unitary age of the Universe, $t = 1$; and maximum value $\gamma_{\max}$ for which the (unprojected) hyperconical metric exists [Monjo 2017, Monjo 2018, Monjo and Campoamor-Stursberg 2020]:

> $\gamma := r \to \arcsin(r)$

$\gamma := r \mapsto \arcsin(r)$

> $\gamma_{\max} := \frac{2}{3}\pi$

$\gamma_{\max} = 2.094395103$

The auxiliary function $\xi(r)$ used in Monjo 2017 to obtain the relationship between comoving distance and redshift:

> $\xi := r \to \mathrm{sqrt}(1-(1-\cos(\gamma(r)))^2)/(\cos(\gamma(r))*(2*(\cos(\gamma(r))-1)+1))$

$\xi = x \mapsto \frac{\sqrt{1-(1-\cos(\gamma(r)))^2}}{\cos(\gamma(r))\cdot(2\cdot\cos(\gamma(r))-1)}$

> $\xi_{tayl} := r \to taylor(\xi(r), r = 0, 10)$

$\xi_{tayl} := r \mapsto taylor(\xi(r), r = 0, 10)$

Solving the comoving coordinate r_z as a function of redshift (z):

> $r_z := solve(\int \xi_{tayl}(r)dx = \log(1+z), x)$

$r_z := z - \frac{1}{2}z^2 - \frac{1}{6}z^3 + \frac{1}{2}z^4 - \frac{13}{40}z^5 + \mathrm{O}(z^6)$

G.2 Definition projection families

The global approach with two parameters $\alpha \in (0,1]$ ***and*** $\gamma_0 \in \mathbb{R}$***:***

> $f_{glob} := r \to r \cdot (\dfrac{2-\cos(\gamma(r))}{1-\frac{\gamma(r)}{\gamma_0}})^{\alpha}$

$$f_{glob} := r \mapsto r \cdot \left(\frac{2-\cos(\gamma(x))}{1-\frac{g(r)}{\gamma_0}}\right)^{\alpha}$$

Local approach, with three or more parameters $(\alpha, b_1, b_2, ...)$***,***$\alpha \in (0,1]$***,*** $b_i \in (0,1)$***:***

> $f_{loc} := r \to r \cdot (\dfrac{2}{1+(1-b_1 \cdot x + b_2 \cdot r^2)\cdot\cos(\gamma(r))})^{a}$

Although the set of three parameters (α, b_1, b_2) is enough to find the local solution, two more terms (b_3 and b_4) are considered to check consistency of the higher-order equations:

> $f_{loc} := r \to x \cdot (\dfrac{2}{1+(1-b_1 \cdot x + b_2 \cdot r^2 + b_3 \cdot x^3 + b_4 \cdot x^4)\cdot\cos(\gamma(r))})^{a}$

$$f_{loc} := r \mapsto r \cdot \left(\frac{2}{1+(1-b_1\cdot x+b_2\cdot x^2+b_3\cdot r^3+b_4\cdot x^4)\cdot\cos(\gamma(x))}\right)^{a}$$

To ensure local consistency (Eq. 6.1.8), it is necessary to set that

> $b_1 := 1$

$$b_1 := 1$$

G.3 Hubble parameter of the hyperconical model

Under the global approach:

> $H_{glob} := simplify(series((\dfrac{d}{d\,z} f_{glob}(r_z))^{-1}, z = 0,5))$

$$H_{glob} = 1 + \frac{-2a+\gamma_0}{\gamma_0} z + \frac{1}{2}\frac{(-3a+3)\gamma_0{}^2-2a\gamma_0+5\alpha^2-3a}{\gamma_0{}^2} z^2 - \frac{1}{3}\frac{a\left(-12\alpha\,\gamma_0{}^2+8\alpha^2+7\gamma_0{}^2-12a+4\right)}{\gamma_0{}^3} z^3 +$$
$$+ \frac{1}{24}\frac{65\alpha^4+\left(-162\gamma_0{}^2+32\gamma_0-162\right)\alpha^3+\left(39\gamma_0{}^4-48\gamma_0{}^3+147\gamma_0{}^2-48\gamma_0+127\right)\alpha^2+\left(-15\gamma_0{}^4+28\gamma_0{}^3-35\gamma_0{}^2+16\gamma_0-30\right)\alpha+9\gamma_0{}^4}{\gamma_0{}^4} z^4 + \mathrm{O}(z^5)$$

> $H_{glob}^j := eval\left(\frac{1}{j!}\frac{d^j}{d\,z^j}\,H_{glob}, z=0\right)$

Under the local approach:

> $H_{loc} := simplify(series((\frac{d}{d\,z} f_{loc}(r_z))^{-1}, z=0,5))$

$$H_{loc} := 1 + (-\alpha+1)\,z + \left(\frac{3}{2} + \frac{5\alpha^2}{8} + \frac{(12b_2-13)\alpha}{8}\right) z^2 - \frac{1}{6}\alpha\,(2\alpha^2 + 12\alpha\,b_2 - 9\alpha - 6b_2 - 12b_3 + 3)\,z^3 +$$
$$+ \left(\frac{3}{8} + \frac{65\alpha^4}{384} + \frac{(648b_2-422)\alpha^3}{384} + \frac{\left(624b_2{}^2-1080b_2-1056b_3-13\right)\alpha^2}{384} + \frac{\left(-240b_2{}^2+48b_2+96b_3+960b_4-174\right)\alpha}{384}\right) z^4 + \mathrm{O}(z^5)$$

> $H_{loc}^j := eval\left(\frac{1}{j!}\frac{d^j}{d\,z^j}\,H_{loc}, z=0\right)$

G.4 Standard Hubble parameter and its Taylor-Maclaurin expansion:

$H := z \to \mathrm{sqrt}(\Omega_r \cdot (1+z)^4 + \Omega_m \cdot (1+z)^3 + \Omega_K \cdot (1+z)^2 + \Omega_\Lambda)$

$$H = z \mapsto \sqrt{\Omega_r \cdot (z+1)^4 + \Omega_m \cdot (z+1)^3 + \Omega_K \cdot (z+1)^2 + \Omega_\Lambda}$$

> $H_{stan} := simplify(taylor(H(z), z=0,5))$

$$H_{stan} := \sqrt{\Omega_r + \Omega_m + \Omega_K + \Omega_\Lambda} + \frac{1}{2}\frac{4\Omega_r+3\Omega_m+2\Omega_K}{\sqrt{\Omega_r+\Omega_m+\Omega_K+\Omega_\Lambda}} z + \frac{1}{2}\frac{\frac{3\Omega_m{}^2}{4}+(\Omega_K+3\Omega_\Lambda+3\Omega_r)\Omega_m+2\Omega_r{}^2+(3\Omega_K+6\Omega_\Lambda)\Omega_r+\Omega_K\Omega_\Lambda}{(\Omega_r+\Omega_m+\Omega_K+\Omega_\Lambda)^{\frac{3}{2}}} z^2 +$$
$$+ \frac{-\Omega_m{}^3+(-2\Omega_K-20\Omega_\Lambda)\Omega_m{}^2+((-20\Omega_\Lambda+4\Omega_r)\Omega_K+8\Omega_\Lambda(\Omega_\Lambda-5\Omega_r))\Omega_m-8(\Omega_\Lambda-\Omega_r)\left(\Omega_K{}^2-4\Omega_\Lambda\Omega_r\right)}{16(\Omega_r+\Omega_m+\Omega_K+\Omega_\Lambda)^{\frac{5}{2}}} z^3 + \frac{64\Omega_\Lambda{}^3\Omega_r-\left(240\Omega_m{}^2+(160\Omega_K+896\Omega_r)\Omega_m+16\Omega_K{}^2+256\Omega_r\Omega_K+896\Omega_r{}^2\right)\Omega_\Lambda{}^2}{128(\Omega_r+\Omega_m+\Omega_K+\Omega_\Lambda)^{\frac{7}{2}}} z^4 +$$

$$+\frac{\left(168{\Omega_m}^3+(280\Omega_K+560\Omega_r){\Omega_m}^2+\left(224{\Omega_K}^2+448\Omega_r\Omega_K+640{\Omega_r}^2\right)\Omega_m+64{\Omega_K}^3+224{\Omega_K}^2\Omega_r+320{\Omega_r}^3\right)\Omega_\Lambda}{128(\Omega_r+\Omega_m+\Omega_K+\Omega_\Lambda)^{\frac{7}{2}}}z^4-\frac{32\left(\frac{3{\Omega_m}^2}{8}+(\Omega_K+\Omega_r)\Omega_m+\frac{5\Omega_r\Omega_K}{2}\right)\left(\Omega_r\Omega_K-\frac{{\Omega_m}^2}{4}\right)}{128(\Omega_r+\Omega_m+\Omega_K+\Omega_\Lambda)^{\frac{7}{2}}}z^4+\mathrm{O}(z^5)$$

> $H^j_{stan} := eval\left(\frac{1}{j!}\frac{d^j}{d\,z^j}\,H_{stan}, z=0\right)$

G.5 Equalising for each approach order of the Hubble parameter

Systems of the 2nd-, 3rd- and 4th-order equations for $H_{glob} = H_{stan}$:

> $GSys2 := \{H^0_{stan}=H^0_{glob}, H^1_{stan}=H^1_{glob}, H^2_{stan}=H^2_{glob}\}$

$$GSys2=\left\{\sqrt{\Omega_r+\Omega_m+\Omega_K+\Omega_\Lambda}=1, \frac{4\Omega_r+3\Omega_m+2\Omega_K}{2\sqrt{\Omega_r+\Omega_m+\Omega_K+\Omega_\Lambda}}=\frac{-2\alpha+\gamma_0}{\gamma_0}, \frac{\frac{3{\Omega_m}^2}{4}+(\Omega_K+3\Omega_\Lambda+3\Omega_r)\Omega_m+2{\Omega_r}^2+(3\Omega_K+6\Omega_\Lambda)\Omega_r+\Omega_K\Omega_\Lambda}{2(\Omega_r+\Omega_m+\Omega_K+\Omega_\Lambda)^{\frac{3}{2}}}=\frac{(-3\alpha+3){\gamma_0}^2-2\alpha\gamma_0+5\alpha^2-3a}{2{\gamma_0}^2}\right\}$$

> $GSys3 := \{H^0_{stan}=H^0_{glob}, H^1_{stan}=H^1_{glob}, H^2_{stan}=H^2_{glob}, H^3_{stan}=H^3_{glob}\}$

$$GSys3 := \left\{\sqrt{\Omega_r+\Omega_m+\Omega_K+\Omega_\Lambda}=1, \frac{4\Omega_r+3\Omega_m+2\Omega_K}{2\sqrt{\Omega_r+\Omega_m+\Omega_K+\Omega_\Lambda}}=\frac{-2\alpha+\gamma_0}{\gamma_0},\right.$$
$$\frac{-{\Omega_m}^3+(-2\Omega_K-20\Omega_\Lambda){\Omega_m}^2+((-20\Omega_\Lambda+4\Omega_r)\Omega_K+8\Omega_\Lambda(\Omega_\Lambda-5\Omega_r))\Omega_m-8(\Omega_\Lambda-\Omega_r)\left({\Omega_K}^2-4\Omega_\Lambda\Omega_r\right)}{16(\Omega_r+\Omega_m+\Omega_K+\Omega_\Lambda)^{\frac{5}{2}}}=-\frac{a\left(-12\alpha{\gamma_0}^2+8\alpha^2+7{\gamma_0}^2-12\alpha+4\right)}{3{\gamma_0}^3},$$
$$\left.\frac{\frac{3{\Omega_m}^2}{4}+(\Omega_K+3\Omega_\Lambda+3\Omega_r)\Omega_m+2{\Omega_r}^2+(3\Omega_K+6\Omega_\Lambda)\Omega_r+\Omega_K\Omega_\Lambda}{2(\Omega_r+\Omega_m+\Omega_K+\Omega_\Lambda)^{\frac{3}{2}}}=\frac{(-3\alpha+3){\gamma_0}^2-2\alpha\gamma_0+5\alpha^2-3a}{2{\gamma_0}^2}\right\}$$

> $GSys4 := \{H^0_{stan}=1, H^1_{stan}=H^1_{glob}, H^2_{stan}=H^2_{glob}, H^3_{stan}=H^3_{glob}, H^4_{stan}=H^4_{glob}\}$

$$GSys4 := \left\{\sqrt{\Omega_r+\Omega_m+\Omega_K+\Omega_\Lambda}=1, \frac{4\Omega_r+3\Omega_m+2\Omega_K}{2\sqrt{\Omega_r+\Omega_m+\Omega_K+\Omega_\Lambda}}=\frac{-2\alpha+\gamma_0}{\gamma_0},\right.$$
$$\left.\frac{-{\Omega_m}^3+(-2\Omega_K-20\Omega_\Lambda){\Omega_m}^2+((-20\Omega_\Lambda+4\Omega_r)\Omega_K+8\Omega_\Lambda(\Omega_\Lambda-5\Omega_r))\Omega_m-8(\Omega_\Lambda-\Omega_r)\left({\Omega_K}^2-4\Omega_\Lambda\Omega_r\right)}{16(\Omega_r+\Omega_m+\Omega_K+\Omega_\Lambda)^{\frac{5}{2}}}=-\frac{a\left(-12\alpha{\gamma_0}^2+8\alpha^2+7{\gamma_0}^2-12\alpha+4\right)}{3{\gamma_0}^3},\right.$$

$$\frac{1}{128}\frac{64{\Omega_\Lambda}^3\Omega_r+\left(-240{\Omega_m}^2+(-160\Omega_K-896\Omega_r)\Omega_m-16{\Omega_K}^2-256\Omega_r\Omega_K-896{\Omega_r}^2\right){\Omega_\Lambda}^2}{(\Omega_r+\Omega_m+\Omega_K+\Omega_\Lambda)^{\frac{7}{2}}}z^4+$$
$$+\frac{1}{128}\frac{\left(168{\Omega_m}^3+(280\Omega_K+560\Omega_r){\Omega_m}^2+\left(224{\Omega_K}^2+448\Omega_r\Omega_K+640{\Omega_r}^2\right)\Omega_m+64{\Omega_K}^3+224{\Omega_K}^2\Omega_r+320{\Omega_r}^3\right)\Omega_\Lambda}{(\Omega_r+\Omega_m+\Omega_K+\Omega_\Lambda)^{\frac{7}{2}}}z^4-$$
$$-\frac{1}{128}\frac{32\left(\frac{3{\Omega_m}^2}{8}+(\Omega_K+\Omega_r)\Omega_m+\frac{5\Omega_r\Omega_K}{2}\right)\left(\Omega_r\Omega_K-\frac{{\Omega_m}^2}{4}\right)}{(\Omega_r+\Omega_m+\Omega_K+\Omega_\Lambda)^{\frac{7}{2}}}=\frac{65\alpha^4+\left(-162{\gamma_0}^2+32\gamma_0-162\right)\alpha^3+\left(39{\gamma_0}^4-48{\gamma_0}^3+147{\gamma_0}^2-48\gamma_0+127\right)\alpha^2+\left(-15{\gamma_0}^4+28{\gamma_0}^3-35{\gamma_0}^2+16\gamma_0-30\right)\alpha+9{\gamma_0}^4}{24{\gamma_0}^4},$$
$$\left.\frac{\frac{3{\Omega_m}^2}{4}+(\Omega_K+3\Omega_\Lambda+3\Omega_r)\Omega_m+2{\Omega_r}^2+(3\Omega_K+6\Omega_\Lambda)\Omega_r+\Omega_K\Omega_\Lambda}{2(\Omega_r+\Omega_m+\Omega_K+\Omega_\Lambda)^{\frac{3}{2}}}=\frac{(-3\alpha+3){\gamma_0}^2-2\alpha\gamma_0+5\alpha^2-3a}{2{\gamma_0}^2}\right\}$$

Systems of the 2nd-, 3rd- and 4th-order equations for $H_{loc}=H_{stan}$:

> $LSys1:=\{H^0_{stan}=H^0_{loc},H^1_{stan}=H^1_{loc}\}$

$$LSys1:=\left\{\sqrt{\Omega_r+\Omega_m+\Omega_K+\Omega_\Lambda}=1,\frac{4\Omega_r+3\Omega_m+2\Omega_K}{2\sqrt{\Omega_r+\Omega_m+\Omega_K+\Omega_\Lambda}}=-a+1\right\}$$

> $LSys2:=\{H^0_{stan}=H^0_{loc},H^1_{stan}=H^1_{loc},H^2_{stan}=H^2_{loc}\}$

$$LSys2:=\left\{\sqrt{\Omega_r+\Omega_m+\Omega_K+\Omega_\Lambda}=1,\frac{\frac{3{\Omega_m}^2}{4}+(\Omega_K+3\Omega_\Lambda+3\Omega_r)\Omega_m+2{\Omega_r}^2+(3\Omega_K+6\Omega_\Lambda)\Omega_r+\Omega_K\Omega_\Lambda}{2(\Omega_r+\Omega_m+\Omega_K+\Omega_\Lambda)^{\frac{3}{2}}}=\frac{3}{2}+\frac{5\alpha^2}{8}+\frac{(12b_2-13)a}{8},\frac{4\Omega_r+3\Omega_m+2\Omega_K}{2\sqrt{\Omega_r+\Omega_m+\Omega_K+\Omega_\Lambda}}=-a+1\right\}$$

> $LSysN:=\{H^0_{stan}=H^0_{loc},H^1_{stan}=H^1_{loc},H^2_{stan}=H^2_{loc},...,H^N_{stan}=H^N_{loc}\}$

$$LSysN:=\left\{\sqrt{\Omega_r+\Omega_m+\Omega_K+\Omega_\Lambda}=1,\frac{\frac{3{\Omega_m}^2}{4}+(\Omega_K+3\Omega_\Lambda+3\Omega_r)\Omega_m+2{\Omega_r}^2+(3\Omega_K+6\Omega_\Lambda)\Omega_r+\Omega_K\Omega_\Lambda}{2(\Omega_r+\Omega_m+\Omega_K+\Omega_\Lambda)^{\frac{3}{2}}}=\frac{3}{2}+\frac{5\alpha^2}{8}+\frac{(12b_2-13)a}{8},\frac{4\Omega_r+3\Omega_m+2\Omega_K}{2\sqrt{\Omega_r+\Omega_m+\Omega_K+\Omega_\Lambda}}=-a+1,...\right\}$$

G.6 Some explicit solutions

Under the global approach with $\Omega_r=0$:

> $SolGSys2a:=solve(eval(GSys2,\Omega_r=0),\{\Omega_K,\Omega_m,\Omega_\Lambda\})$

$$SolGSys2a := \left\{ \Omega_K = -\frac{-3\alpha\gamma_0{}^2+9\alpha^2-2\alpha\gamma_0+2\gamma_0{}^2-3a}{\gamma_0{}^2}, \Omega_\Lambda = \frac{-3\alpha\gamma_0{}^2+9\alpha^2+2\alpha\gamma_0+3\gamma_0{}^2-3a}{3\gamma_0{}^2}, \Omega_m = \frac{2\left(-3\alpha\gamma_0{}^2+9\alpha^2-4\alpha\gamma_0+3\gamma_0{}^2-3\alpha\right)}{3\gamma_0{}^2} \right\}$$

Under the global approach with $\Omega_r = 0$ and $\epsilon = 0$:

$$> SolGSys2b := solve(eval(eval(eval(GSys2, \Omega_r = 0), \alpha = \frac{\gamma_0 \cdot 5}{18} \cdot (1+0)), \gamma_0 = 2 \cdot (1+\delta)), \{\Omega_K, \Omega_m, \Omega_\Lambda\})$$

$$SolGSys2b := \left\{ \Omega_K = \frac{60\delta^2+43\delta-2}{36(1+\delta)}, \Omega_\Lambda = -\frac{20\delta^2-11\delta-26}{36(1+\delta)}, \Omega_m = -\frac{20\delta^2+9\delta-6}{18(1+\delta)} \right\}$$

Under the global approach with $\epsilon = 0$:

$$> SolGSys2c := solve(eval(eval(GSys2, \alpha = \frac{\gamma_0 \cdot 5}{18} \cdot (1+0)), \gamma_0 = 2 \cdot (1+\delta)), \{\Omega_K, \Omega_m, \Omega_\Lambda\})$$

$$SolGSys2c := \left\{ \Omega_K = \frac{72\Omega_r\delta+60\delta^2+72\Omega_r+43\delta-2}{36(1+\delta)}, \Omega_\Lambda = -\frac{12\Omega_r\delta+20\delta^2+12\Omega_r-11\delta-26}{36(1+\delta)}, \Omega_m = -\frac{48\Omega_r\delta+20\delta^2+48\Omega_r+9\delta-6}{18(1+\delta)} \right\}$$

Under the local approach with $\Omega_r = 0$:

$$> SolLSys2 := eval(eval(eval(solve(Sys2, \{\Omega_r, \Omega_m, \Omega_\Lambda\}), \Omega_r = 0), \Omega_K = 0), b_2 = -0.6250000000)$$

$$SolLSys2 := \left\{ 0 = \frac{9}{8}\alpha^2 - 2.562500000\alpha + 1, \Omega_\Lambda = \frac{2}{3} + \frac{3}{8}\alpha^2 - 0.1875000000\alpha, \Omega_m = -\frac{2}{3} - \frac{3}{2}\alpha^2 + 2.750000000\alpha \right\}$$

G.7 Some numerical solutions

Under the 2rd-order global approach with $\Omega_K := 0$, $\Omega_r \approx 0$ and $\delta := \frac{\pi}{3} - 1$:

$$> Glob2a := solve(eval(eval(eval(GSys2, \Omega_K = 0), \gamma_0 = \gamma_{\max}), \Omega_r = 0), \{\alpha, \Omega_m, \Omega_\Lambda\})$$

$$Glob2a := \big(\{\Omega_\Lambda = 0.7024821736, \Omega_m = 0.2975178264, \alpha = 0.5798576424\},$$
$$\{\Omega_\Lambda = 1.403529648, \Omega_m = -0.4035296479, \alpha = 1.681060440\}\big) \quad \% \textit{ Rejected by } |\epsilon| > 0.05 \textit{ against the hypothesized}$$

Under the 2rd-order global approach with $\Omega_K \approx 0$, $\Omega_r \neq 0$ and $\delta := \frac{\pi}{3} - 1$:

> $Glob2b := solve(eval(eval(eval(eval(GSys2, \alpha = \frac{\gamma_{\max} \cdot 5}{18} \cdot (1+\epsilon)), \Omega_K = 0), \gamma_0 = \gamma_{\max}), \Omega_r = (9.0 \pm 0.5) \cdot 10^{-5}), \{\epsilon, \Omega_m, \Omega_\Lambda\})$

$Glob2b := \big(\{\Omega_\Lambda{=}0.7024603068, \Omega_m{=}0.2974446832, \epsilon{=}-0.003442680711\}$,
$\{\Omega_\Lambda{=}1.403614854, \Omega_m{=}-0.4037098636, \epsilon{=}1.889674596\}\big)$ % *Rejected by* $|\epsilon| > 0.05$ *against the hypothesized*

Under the 2nd-order global approach with $\epsilon = 0 = \delta$:

> $Glob2c := solve(eval(eval(eval(GSys2, \alpha = \frac{2 \cdot 5}{18}), \gamma_0 = 2), \Omega_r < 10^{-6}, \{\Omega_K, \Omega_m, \Omega_\Lambda\})$

$Glob2c := \big(\{\Omega_K{=}-0.05555365536, \Omega_\Lambda{=}0.7222219055, \Omega_m{=}0.3333307997\}\big)$

Under the 3rd-order global approach with $\delta := \frac{\pi}{3} - 1$:

> $Glob3a := solve(eval(eval(eval(GSys3, \alpha = \frac{\gamma_{\max} \cdot 5}{18} \cdot (1+\epsilon)), \Omega_r = (9.0 \pm 0.5) \cdot 10^{-5}), \gamma_0 = \gamma_{\max}), \{\Omega_m, \Omega_\Lambda, \epsilon, \Omega_K\})$

$Glob3a := \big(\{\Omega_K{=}-0.01506989666, \Omega_\Lambda{=}0.7032645994, \Omega_m{=}0.3117152973, \epsilon{=}-0.01482948873\}$,
$\{\Omega_K{=}-1.037499098, \Omega_\Lambda{=}0.8262953330, \Omega_m{=}1.211113765, \epsilon{=}-0.602832789\}$, % *Rejected by* $|\epsilon| > 0.05$ *against the hypothesized*
$\{\Omega_K{=}-23.00134246, \Omega_\Lambda{=}10.88033003, \Omega_m{=}13.12092243, \epsilon{=}6.775601874\}\big)$ % *Rejected by* $|\epsilon| > 0.05$ *against the hypothesized*

Under the 3rd-order global approach with $\delta := 0$:

> $Glob3b := solve(eval(eval(eval(GSys3, \gamma_0 = 2 \cdot (1+\epsilon)), \alpha = \frac{5}{18} \cdot 2 \cdot (1+\epsilon), \Omega_r = (9.0 \pm 0.5) \cdot 10^{-5}), \{\Omega_m, \Omega_\Lambda, \epsilon, \Omega_K\})$

$Glob3b := \big(\{\Omega_K{=}-0.01180432187, \Omega_\Lambda{=}0.7076701777, \Omega_m{=}0.3040390442, \epsilon{=}0.03446605021\}$,
$\{\Omega_K{=}-1.777163130 - 0.6769511395\,\mathrm{I}, \Omega_\Lambda{=}1.296123114 + 0.2256503798\,\mathrm{I}, \Omega_m{=}1.480944916 + 0.4513007597\,\mathrm{I}$,
$\epsilon{=}-0.9330767129 + 0.3272025928\,\mathrm{I}\}$, % *Rejected by* $|\epsilon| > 0.05$ *against the hypothesized*
$\{\Omega_K{=}-1.777163130 + 0.6769511395\,\mathrm{I}, \Omega_\Lambda{=}1.296123114 - 0.2256503798\,\mathrm{I}, \Omega_m{=}1.480944916 - 0.4513007597\,\mathrm{I}$,
$\epsilon{=}-0.9330767129 - 0.3272025928\,\mathrm{I}\}\big)$ % *Rejected by* $|\epsilon| > 0.05$ *against the hypothesized*

> $\alpha_0 := \frac{5}{18} \cdot 2 \cdot (1 + 0.0344660502)$

$\alpha_0 := 0.5747033611$

Under the 3rd-order global approach with $\delta \approx \epsilon$:

> $Glob3c := solve(eval(eval(eval(GSys3, \gamma_0 = 2 \cdot (1+\epsilon)), \alpha = \frac{5}{18} \cdot 2 \cdot (1+\epsilon)^2), \Omega_r = (9.0 \pm 0.5) \cdot 10^{-5}), \{\Omega_m, \Omega_\Lambda, \epsilon, \Omega_K\})$

$Glob3c := (\{\Omega_K = -0.008224618587, \Omega_\Lambda = 0.7134102773, \Omega_m = 0.2947193413, \epsilon = 0.01872009185\},$
$\{\Omega_K = -0.8314306745, \Omega_\Lambda = 0.1622564948, \Omega_m = 1.669079180, \epsilon = -2.21028057\},$ % *Rejected by* $|\epsilon| > 0.05$ *against the hypothesized*
$\{\Omega_K = -1.494505474 + 0.2003060777\,\mathrm{I}, \Omega_\Lambda = 0.8997689646 + 0.01441767501\,\mathrm{I}, \Omega_m = 1.594641509 - 0.2147237527\,\mathrm{I},$
$\epsilon = -0.8157642221 + 0.2192031925\,\mathrm{I}\},$ % *Rejected by* $|\epsilon| > 0.05$ *against the hypothesized*
$\{\Omega_K = -1.494505474 - 0.2003060777\,\mathrm{I}, \Omega_\Lambda = 0.8997689646 - 0.01441767501\,\mathrm{I}, \Omega_m = 1.594641509 + 0.2147237527\,\mathrm{I},$
$\epsilon = -0.8157642221 - 0.2192031925\,\mathrm{I}\})$ % *Rejected by* $|\epsilon| > 0.05$ *against the hypothesized*

Under local approach with $\Omega_K := 0$ for 2nd-, 3rd- and 4th-order expansions:

> $Loc2 := solve(eval(eval(eval(eval(LSys2, j = 0), \Omega_K = 0), \alpha = 0.5), \Omega_r = 0.0), \{b_2, \Omega_m, \Omega_\Lambda\})$

$Loc2 := \{\Omega_\Lambda = 0.6666663333, \Omega_m = 0.3333326667, b_2 = -0.6250006667\}$

> $Loc3 := solve(eval(eval(eval(LSys3, \Omega_r = 0.0), \alpha = 0.5), \Omega_K = 0), \{b_2, \Omega_\Lambda, \Omega_m, b_3\})$

$Loc3 := \{\Omega_\Lambda = 0.6666666667, \Omega_m = 0.3333333333, b_2 = -0.6250000000, b_3 = -0.1041666667\}$

> $Loc4 := solve(eval(eval(eval(LSys4, \Omega_r = 0.0), \alpha = 0.5), \Omega_K = 0), \{b_2, \Omega_\Lambda, \Omega_m, b_3, b_4\})$

$Loc4 := \{\Omega_\Lambda = 0.6666666667, \Omega_m = 0.3333333333, b_2 = -0.6250000000, b_3 = -0.1041666667, b_4 = -0.3494791666\}$

Appendix H

Linearized gravity and gravitomagnetism

H.1 Linearized gravity for a point particle

To support the analysis of the classical limit at a macroscopic scale, in this Appendix we recall some results of Classical Relativity, especially from the linearized formalism and the gravitomagnetism solution [Capozziello *et al.* 2009, Skagerstam *et al.* 2018]. Using local coordinates with an affine connection, the Ricci curvature tensor components ($R_{\alpha\beta}$) are computed from the Riemann curvature tensor components ($R^{\mu}_{\alpha\beta\gamma}$), i.e.,

$$R_{\alpha\beta} := R^{\mu}_{\alpha\mu\beta} = \partial_{\mu}\Gamma^{\mu}_{\alpha\beta} - \partial_{\beta}\Gamma^{\mu}_{\mu\alpha} + \Gamma^{\mu}_{\rho\mu}\Gamma^{\rho}_{\alpha\beta} - \Gamma^{\mu}_{\rho\beta}\Gamma^{\rho}_{\alpha\mu}, \tag{H.1.1}$$

where $\Gamma^{\mu}_{\alpha\beta}$ are the Christoffel symbols of the second kind, which for the Levi–Civita connection $\hat{\nabla}$ satisfy $\hat{\nabla}g = 0$, such that g is free of torsion. Therefore, for a perturbed metric, $g_{\alpha\beta} \approx \eta_{\alpha\beta} + \Phi_{\alpha\beta}$, the first order Christoffel symbols are

$$\Gamma^{\mu}_{\alpha\beta} = \frac{1}{2}g^{\mu\nu}\left(\partial_{\alpha}g_{\nu\beta} + \partial_{\beta}g_{\alpha\nu} - \partial_{\nu}g_{\alpha\beta}\right) \approx \frac{1}{2}\eta^{\mu\nu}\left(\partial_{\alpha}\Phi_{\nu\beta} + \partial_{\beta}\Phi_{\alpha\nu} - \partial_{\nu}\Phi_{\alpha\beta}\right). \tag{H.1.2}$$

By using the harmonic coordinates condition, i.e., $\eta^{\beta\gamma}\partial_{\gamma}\Phi_{\alpha\beta} = \frac{1}{2}\eta^{\beta\gamma}\partial_{\alpha}A_{\beta\gamma}$, the Einstein field equations with the first order of Ricci tensor read

$$R^{(1)}_{\alpha\beta} \approx -\frac{1}{2}\partial_{\gamma}\partial^{\gamma}\Phi_{\alpha\beta} \approx 8\pi\mathrm{G}\left(P_{\alpha\beta} - \frac{P}{2}g_{\alpha\beta}\right), \tag{H.1.3}$$

where G is the Newtonian gravitational constant and $P_{\alpha\beta}$ is the stress-energy tensor. For a point particle 'i' located at $x_i = (t, \vec{r}_i)$ with energy m and 4-velocity $u^{\alpha} := dx^{\alpha}_i/d\tau$ (with respect to the proper time $d\tau$), the 4-momentum is $P^{\alpha} := mu^{\alpha}$. If we take $N(r)$ particles at a distance $r = |\vec{r} - \vec{r}_i|$ from the particle 'i', then the stress-energy corresponds to that of a perfect fluid [Brown 1993], that is,

$$\begin{aligned} P^{\alpha\beta} &:= \sum_{i=1}^{N(r)} \int \frac{\delta^4(x - x_i)}{\sqrt{|g(x)|}}(mu^{\alpha}u^{\beta}d\tau)_i \\ &= \hat{\rho}(r)u^{\alpha}u^{\beta} - \sigma(r)g^{\alpha\beta} = \rho(r)((1+w)u^{\alpha}u^{\beta} - wg^{\alpha\beta}), \end{aligned} \tag{H.1.4}$$

where $w := \sigma/\rho$ is the equation of state, and $\hat{\rho} := \rho(r) + \sigma(r) = \rho(r)(1+w)$ is the *total energy density*, which consists of the *rest energy density*, $\rho(r)$, and the *pressure*, $\sigma(r) := n\partial\rho(r)/\partial n - \rho(r)$, being $n := \mathrm{d}\rho/\mathrm{d}V$ the particle number density. The solution of the Einstein equations for this case is

$$\Phi_{\alpha\beta} \approx 4\phi(r)\left(u_\alpha u_\beta - \frac{1}{2}\left(\frac{1-3w}{1+w}\right)\eta_{\alpha\beta}\right) + K_{\alpha\beta}, \tag{H.1.5}$$

where $\phi(r) := -\mathrm{G}\hat{m}/r$, $\hat{m} := (1+w)m$, and $K_{\alpha\beta}$ are constants of integration. For purely static dust ($w = 0$, $u_0 = 1$, $u_i = 0$ for $i \in \{1,2,3\}$), and by recalling that $\eta_{\alpha\beta} = \mathrm{diag}(1,-1,-1,-1)$, we have

$$\Phi_{00} = \Phi_{ii} = 2\phi(r) + K = -\frac{2\mathrm{Gm}}{r} + K, \tag{H.1.6}$$

where $K := K_{00} = K_{ii}$. Therefore, the Newtonian gravitational field is recovered, and the perturbation $\Phi_{\alpha\beta}$ equals the first order of the Schwarzchild metric. Any double-copy perturbation requires that $w = 1/3$, as a photonic perfect fluid, whence

$$\Phi_{\alpha\beta} \approx 4\phi(r)u_\alpha u_\beta + K_{\alpha\beta}. \tag{H.1.7}$$

Derivation from the Lagrangian formulation. The classical Newtonian gravity can be obtained by using the extremal theory for the first order perturbation of the metric g. Let m and x^α be the mass and the position, respectively, of a test point particle (with state w_m) living in a spacetime perturbed by a (source) mass M (with state w). The action functional for this particle is

$$S = \int m d\tau = \int m d\lambda \sqrt{g_{\mu\nu}\frac{dx^\mu}{d\lambda}\frac{dx^\nu}{d\lambda}} \approxeq \int \frac{m}{2} g_{\mu\nu} u^\mu u^\nu d\tau, \tag{H.1.8}$$

where $u^\mu := dx^\nu/d\lambda$ and the homomorphism between $\delta\sqrt{\Box} = 0$ and $\frac{1}{2}\delta\Box = 0$ has been used (see Def. 1.3.2). Now, the gravitational field is $\phi := -\mathrm{G}\hat{M}/r < 0$, with $|g_{\alpha\alpha}| \leq 1$ (classical spacetime gravity), and the Lagrangian functional is

$$\begin{aligned} L &= \frac{m}{2} g_{\alpha\beta} u^\alpha u^\beta \approx \frac{m}{2}\left(\eta_{\alpha\beta} + 4\phi(r)\left(u_\alpha u_\beta - \left(\frac{1-3w}{1+w}\right)\frac{\eta_{\alpha\beta}}{2}\right)\right) u^\alpha u^\beta \\ &= \frac{m}{2}\eta_{\alpha\beta}u^\alpha u^\beta + m\left(\frac{1+5w}{1+w}\right)\phi(r) = \frac{m}{2}\eta_{\alpha\beta}u^\alpha u^\beta + mI_w\phi(r), \end{aligned} \tag{H.1.9}$$

where $I_w := (1+5w)/(1+w)$. The corresponding Euler–Lagrange equations are the geodesic equations, $du^\mu/d\tau = -\Gamma^\mu_{\alpha\beta}u^\alpha u^\beta$, but this approach leads to

$$\frac{d}{d\tau}\frac{\partial L}{\partial u^\alpha} - \frac{\partial L}{\partial x^\alpha} = 0 \quad \Rightarrow \quad f := m\frac{du_\alpha}{d\tau} = mI_w\frac{\partial\phi(r)}{\partial x^\alpha}. \tag{H.1.10}$$

which corresponds to the classical Newtonian force at the limit $w = 0$ (purely dust particles). By taking spherical coordinates with radius r, the classical gravitational energy is defined by the work,

$$m'(r) := \int_{r_m}^{r} f(r')dr' = mI_w \int_{r_m}^{r} \frac{\partial\phi(r')}{\partial r'}dr' = mI_w\Delta\phi(r), \tag{H.1.11}$$

where r_m is the origin of the energy potential and $\Delta\phi(r) := \phi(r) - \phi(r_m)$. It is usual to choose $r_m \to \infty$ as the energy origin, but we purposely set $r_m = \mathrm{G}I_w m$ or $r_m = \mathrm{G}I_w\hat{M}$, were w depends on the source M. Therefore, the (semi-)classical gravitational-energy perturbation is

$$m'(r) = mI_w\left(-\frac{\mathrm{G}\hat{M}}{r} + \frac{\mathrm{G}\hat{M}}{r_m}\right). \tag{H.1.12}$$

The total potential energy for a test point particle depends on the origin chosen. If $r_m = \mathrm{G}I_w\hat{M}$ is set as the source origin, then the semi-classical potential energy, $m'(r) = m + m\phi(r)$, approaches $\lim_{r\to\infty} m'(r) = m$, i.e., the test particle self-energy. By changing the origin to the test particle position, $r_m = \mathrm{G}I_w m$, the total energy, $m'(r) = M + m\phi(r)$, represents the total *source energy* when $\lim_{r\to\infty} m'(r) = M$. Therefore, for both cases the total contribution of gravity is zero. In any way, the kinetic and gravitational energies in GR depend on the reference system or the connection. For instance, in teleparallel gravities it is found that the total energy of the coupled matter and gravity is proportional to the 3-space Ricci scalar up to first-order perturbation [Abedi and Salti 2015].

H.2 Linearized gravitomagnetism

Separable perturbation. Let $\Phi_{\alpha\beta}(t, r)$ be a two-particle metric perturbation that depends on the time, t, and on the relative position of the point particles, r. By assuming that the only dependence in t is given by the 4-velocity, $u_\alpha = u_\alpha(t)$, the solution to the first order Einstein field equations for perfect fluids is quasi-stationary, i.e., it is similar to the Eq. H.1.5. This implies that, like the stress-energy source tensor $P_{\alpha\beta} = \hat{\rho}u_\alpha u_\beta - \frac{w}{1+w}\hat{\rho}\eta_{\alpha\beta}$ and the source tensor $P_{\alpha\beta} - \frac{1}{2}P\eta_{\alpha\beta} = \hat{\rho}u_\alpha u_\beta - \frac{1-3w}{2(1+w)}\hat{\rho}\eta_{\alpha\beta}$, the metric perturbation can be decomposed into two terms: a term $\bar{A}_{\alpha\beta}$ proportional to the 4-velocity tensor, $u_\alpha u_\beta$ (for instance, using a 4-potential, $\bar{A}_\beta := \bar{A}u_\beta$ with static field $\bar{A} := 2\sqrt{-\phi}$), and another term $\bar{B}_{\alpha\beta}$ proportional to the flat metric tensor, $\eta_{\alpha\beta}$, and to another static field, $\bar{B}$ (see, for instance, Eq. H.1.5). Therefore,

$$\Phi_{\alpha\beta} \approx \bar{A}_{\alpha\beta} + \bar{B}_{\alpha\beta}, \quad \bar{A}_{\alpha\beta} := \bar{A}_\alpha\bar{A}_\beta, \quad \bar{B}_{\alpha\beta} := -\bar{B}^2\eta_{\alpha\beta}, \tag{H.2.1}$$

where one can identify the perturbation $\bar{A}_{\alpha\beta}$ as in the Kaluza–Kein metric, but in four dimensions, that is, as a double-copy linearized gravity [Gurses *et al.* 2018].

Maxwell-like equations. The first order Einstein field equations (Eq. H.1.3) for quasi-stationary perfect fluids can be split into two parts:

$$\partial_\gamma \partial^\gamma \bar{A}_{\alpha\beta} \approx \quad -16\pi \mathrm{G} \hat{\rho} u_\alpha u_\beta, \tag{H.2.2}$$

$$\partial_\gamma \partial^\gamma \bar{B}_{\alpha\beta} \approx \quad 16\pi \mathrm{G} \tfrac{1-3w}{2(w+1)} \hat{\rho} \eta_{\alpha\beta}, \tag{H.2.3}$$

where the harmonic coordinate condition has been chosen. By taking $w = 1/3$, Eq. H.2.2 is very similar to Maxwell equation in the Lorentz gauge when replacing the electric 4-current, $j^\mu := \hat{\rho} u^\mu$, by a tensor, $J^{\mu\nu} := \hat{\rho} u^\mu u^\nu$. Qualitatively, a gravitational analog of the *electromagnetic induction* is the frame-dragging derived by the *Lense-Thirring effect.*[1]

Lorentz-like force. Similar dynamics to the Lorentz force can be obtained from the geodesic equations at first order:

$$\frac{du^\gamma}{d\tau} \approx -\Gamma^\gamma_{\alpha\beta}{}^{(1)} u^\alpha u^\beta \approx -(\Gamma^\gamma_{\alpha\beta}{}^{(A)} + \Gamma^\gamma_{\alpha\beta}{}^{(B)}) u^\alpha u^\beta, \tag{H.2.4}$$

where $\Gamma^\gamma_{\alpha\beta}{}^{(A)}$ and $\Gamma^\gamma_{\alpha\beta}{}^{(B)}$ are the first order Christoffel symbols for the the metric perturbations $\bar{A}_{\alpha\beta}$ and $\bar{B}_{\alpha\beta}$, respectively.

By multiplying $u^\alpha u^\beta$ on both sides of the equations, and by recalling that $u_\gamma \partial_\nu u^\gamma = 0$ and $u^\alpha \partial_\alpha \bar{A} = u^\alpha \partial_\alpha \bar{B} = 0$, where $\bar{A}$ and $\bar{B}$ are static fields, the following equation is obtained:

$$\frac{du^\gamma}{d\tau} \approx \bar{A}^\mu \bar{F}_\mu{}^\gamma + \bar{B} \partial^\gamma \bar{B}, \tag{H.2.5}$$

where $\bar{F}_{\beta\nu} := \partial_\beta \bar{A}_\nu - \partial_\nu \bar{A}_\beta$. The case $\bar{B} = 0$ is equivalent to the Lorentz force law. The gravitational Lorentz force can also be obtained by using a Lagrangian functional with $B = 0$, that is, $\phi = -\bar{A}^2/2 = -\eta_{\alpha\beta} \bar{A}^\alpha \bar{A}^\beta / 2$. In this case, we have

$$L \approx \frac{m}{2} g_{\alpha\beta} u^\alpha \beta \approx \frac{m}{2} (1 - \bar{A}^2) \eta_{\alpha\beta} u^\alpha u^\beta. \tag{H.2.6}$$

The corresponding Euler–Lagrange equations (Eq. H.1.10) are

$$\begin{aligned} \frac{d}{d\tau} \left(m u_\alpha - m \bar{A} \bar{A}_\alpha \right) + m \bar{A}^\gamma \frac{\partial \bar{A}_\gamma}{\partial x^\alpha} &= 0, \\ \frac{d}{d\tau} \left(m u_\alpha \right) - m \bar{A}^\gamma \frac{\partial A_\alpha}{\partial x^\gamma} + m \bar{A}^\gamma \frac{\partial \bar{A}_\gamma}{\partial x^\alpha} = \frac{d}{d\tau} \left(m u_\alpha \right) - m \bar{A}^\gamma \bar{F}_{\gamma\alpha} &= 0, \end{aligned} \tag{H.2.7}$$

where the conditions $d\bar{A}/d\tau = 0$ and $d/d\tau = u^\gamma \partial_\gamma$ have been used.

[1] The *Lense-Thirring effect* is a correction of GR to the precession of a gyroscope near a large rotating mass.

Appendix I

Second-order of point Lorentz force

From the exact solution of the metric (Eq. 5.3.3), the Lagrangian reads

$$L = \frac{m}{2} g_{\alpha\beta} u_2^\alpha u_2^\beta \quad = \quad \frac{m}{2} \eta_{\alpha\beta} u_2^\alpha u_2^\beta + A_1^\gamma q_2 u_{2\gamma} - \frac{4\pi \mathrm{G}}{\mathrm{k}} m A_1^\gamma A_{2\gamma} \tag{I.0.1}$$

The corresponding Euler–Lagrange equations are

$$\begin{aligned} &\frac{d}{d\tau}\left(m u_{2\alpha}\right) + q_2 u_2^\gamma \frac{\partial A_{1\alpha}}{\partial x_2^\gamma} - q_2 u_2^\gamma \frac{\partial A_{1\gamma}}{\partial x_2^\alpha} + \frac{4\pi \mathrm{G}}{\mathrm{k}} m \frac{\partial}{\partial x_2^\alpha}\left(A_1^\gamma A_{2\gamma}\right) \\ &\qquad = \frac{d}{d\tau}\left(m u_{2\alpha}\right) + q_2 u_2^\gamma \mathscr{F}_{\gamma\alpha} + \frac{4\pi \mathrm{G}}{\mathrm{k}} m \frac{\partial}{\partial x_2^\alpha}\left(A_1^\gamma A_{2\gamma}\right) = 0, \end{aligned} \tag{I.0.2}$$

which correspond to the second-order correction of the Lorentz force. For instance, let $A_{2\gamma} = \mathrm{k} q_2 / r$ be constant when the distance is $r = 1\mathrm{m}$ with respect to a proton ($m_p = 938\mathrm{MeV}$, $q = 1\mathrm{e}$) where a Synchrotron is placed. Therefore

$$\Delta\left(m_p u_{2\alpha}\right) \quad = \quad -q_2 u_2^\gamma \mathscr{F}_{\gamma\alpha}\, \Delta\tau + 4\pi \mathrm{G} \frac{m_p}{r c^4} q_2 u_{2\gamma} \frac{\partial A_1^\gamma}{\partial x_2^\alpha}\, \Delta\tau. \tag{I.0.3}$$

Notice that the speed of light $c \equiv 1$ is highlighted only to conveniently remind the units, although natural units are chosen in this work. To estimate the order of magnitude of the correction, one can take for instance a proton accelerated by a Synchrotron up to $m_p\, u_{2\alpha} = 469\mathrm{GeV} = 500\, m_p$, that is, a relativistic 4-velocity of $u_{2\alpha} = \gamma v_\alpha = 500$, where $v_\alpha = 0.999998$ and $\gamma = 1/\sqrt{1 - v_\alpha^2}$. Therefore, $-q_2 u_{2\gamma} \mathscr{F}_{\gamma\alpha}\, \Delta\tau \sim q_2 u_{2\gamma} \partial A_1^\gamma / \partial x_2^\alpha\, \Delta\tau \sim 500\mathrm{GeV}$, and the final order of magnitude is

$$\Delta\left(m_p u_{2\alpha}\right) \quad \sim \quad -q_2 u_2^\gamma \mathscr{F}_{\gamma\alpha}\, \Delta\tau \left(1 - 4\pi \mathrm{G} \frac{m_p}{r c^4}\right), \tag{I.0.4}$$

which is a correction by gravity absolutely negligible for the proton.